



UNIVERSITY OF NAIROBI

**FABRICATION AND OPTIMIZATION OF AN EFFECTIVE
ANAEROBIC DIGESTER FOR BIOGAS PRODUCTION USING
VEGETABLE WASTES FROM WAKULIMA AND KANGEMI
MARKETS IN NAIROBI COUNTY, KENYA**

BY

JAMES KAMAU MBUGUA

I80/50383/2016

**A Research Thesis Submitted in Fulfillment of the Requirements for the
Award of Degree of Doctor of Philosophy in Chemistry of the University
of Nairobi**

November 2021

DECLARATION

DECLARATION

I declare that this proposal is my original work and has not been submitted elsewhere for examination, the award of degree of publication. Where other people's work or my work has been used, this has properly been acknowledged and referenced in accordance with the University of Nairobi's requirements.

Sign: 

Date: 25/11/2021

JAMES KAMAU MBUGUA

Reg. No. 180/50383/2016

Department of Chemistry

University of Nairobi

This thesis is submitted for examination with our approval as the research supervisors:

Signature

Date

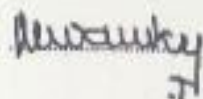
Dr. Joseph Mwaniki

Department of Chemistry

University of Nairobi

P.O box 30197-00100 Nairobi, Kenya

jmwaniki@uonbi.ac.ke



25/11/2021

Dr. Damaris Mbui

Department of Chemistry

University of Nairobi

P.O box 30197-00100 Nairobi, Kenya

dmbui@uonbi.ac.ke



25/11/2021

DEDICATION

To the families of my late friends and mentors, Prof G.N. Kamau and Prof. F.B Mwaura.

ACKNOWLEDGEMENT

I wish to sincerely thank Dr. J. Mwaniki for his suggestions, critical thought, motivation, and guidance, which laid the groundwork for this study. I gratefully acknowledge Dr. D. Mbui for her regarded supervision, unremitting support, motivation and useful feedback throughout my research work.

My deepest gratitude's to the technicians and support staff from University of Nairobi, department of chemistry, Veterinary Pathology, Microbiology & Parasitology and department of nutrition and food science, for their technical advice throughout this course.

I acknowledge grants from the National Research Fund to carry out the doctoral thesis study.

I really appreciate the assistance and timely disbursement of research funds from the University of Nairobi grant and DVC-RIE offices.

PUBLICATIONS AND PATENTS

1. **Mbugua James K**, Gabriel A. Waswa, Damaris M. Nduta and Joseph M. Mwaniki (2021) Characterization and Application of Eburru Zeolite Rocks in Upgrading Biogas to Bio-Methane, *J Environ Anal Chem* 8: 335.
2. **Kamau J. M***, Mbui D. N, Mwaniki J. M, Waswa G. A. (2021) Effect of Thermo-Chemical Pretreatment of Kenyan Market Waste on Mesophilic Biogas Production, *International Journal of Scientific Research in Science, Engineering and Technology*,**8**(3),22-31
3. **James K. Mbugua**, Joseph M. Mwaniki, Damaris M. Nduta and Francis B. Mwaura (2021), Upgrading Biogas Using Eburru Zeolitic Rocks and Other Adsorbent Materials to Remove Carbon Dioxide and Hydrogen Sulphide, *Tanzania Journal of Science* **47**(2): 421-431.
4. **Mbugua J. K¹**, Mbui D. N¹, Mwaniki J. M¹, Mwaura F. B (2021), A Micro-Controller Based Biogas Leakage and Fire Detection System, *International Journal of Scientific Research in Science, Engineering and Technology*, **8**(2), 216-221
5. **Mbugua J. K**, Mbui D. N, Mwaniki J. M, Mwaura F. B (2020), Biochemical Methane Potential (BMP) of Market Wastes from Nairobi Inoculated with Dagoretti Slaughterhouse Waste, *International Journal of Scientific Research in Science, Engineering and Technology (IJSRSET)* **7**(4), pp. 81-90.
6. **Kamau J. M**, Mbui D. N, Mwaniki J. M, Mwaura F. B (2020) Lab Scale Biogas Production from Market Wastes and Dagoretti Slaughterhouse Waste in Kenya, *International Journal of Energy and Environmental Research*, **8**(1), pp.12-21
7. **Kamau J. M**, Mbui D. N, Mwaniki J. M, Mwaura F. B (2020) Influence of Substrate Proximate Properties On Voltage Production in Microbial Fuel Cells, *International Journal of Energy and Environmental Research* **8**(1), pp.12-21
8. **Kamau, J. M.**, Mbui, D. N., Mwaniki J. M., & Mwaura, F. B. (2020), Proximate analysis of fruits and vegetables wastes from Nairobi County, Kenya. *Research Journal of Food Science and Nutrition*, **5**(1), 9-15.

9. **Kamau J.M**, Mbui D.N, Mwaniki J.M, Mwaura F.B (2019), Application of microbial fuel cells in the degradation of 2,4,5,6-tetrachloroisophthalonitrile (chlorothalonil), *Journal of Bioscience and Biotechnology Discovery*, **4**(2), pp 28-35
10. **Kamau J.M**, Mbui D.N, Mwaniki J.M, Mwaura F.B (2018) Utilization of rumen fluid in production of bio–energy from market waste using microbial fuel cells technology. *Journal of Applied Biotechnology & Bioengineering*, **5**(4)
11. **Kamau JM**, Mbui DN, Mwaniki JM, Mwaura FB (2018), Characterization of voltage from food market waste: microbial fuel cells. *Int J Biotech & Bioeng.* **4**:3

12. **Kamau J.M**, Mbui D.N, Mwaniki J.M, Mwaura F.B, Kamau G.N (2017) Microbial Fuel Cells: Influence of External Resistors on Power, Current and Power Density. *J Thermodyn Catal* **8**: 182. doi: 10.4179/2160-7544.1000182.

LIST OF PATENTS

1. Patent Application No. **KE/P/2020/3707**: Biogas Digester Automation, filed on August, 2020.
2. A Micro-Controller Based Biogas Leakage and Fire Detection System with KIPI, under review.

ABSTRACT

This work focuses on generation of biogas and voltage from market wastes inoculated with abattoir wastes. The market wastes were analyzed for proximate and ultimate composition using standard techniques. Bacterial studies of the inoculum involved microbial counts, isolation in anaerobic conditions and bio-chemical analysis. Biogas production was done at psychrophilic, mesophilic and thermophilic conditions using market wastes. The influence of acidic and alkaline waste pretreatments, pH, temperature, C: N ratio, inoculum to substrate ratio and proximate properties was also investigated. Biogas upgrade was studied using zeolite rocks, desulphurizer, maize cobs, steel wire and worn out tyres cartridges. A portable digester was fabricated which incorporated agitation, pH monitoring and temperature regulation mechanism with an *Arduino*-based automatic biogas leakage detection and mitigation measures. A 1450 L Ferro-cement and a 14000 L bricks pilot scale digesters were constructed. Bio-slurry was employed in vegetable and maize farming. Finally, waste conversion to electricity was studied using microbial fuel cell technology at optimized conditions.

The results obtained in this research show that the microbial counts in rumen fluid and cow dung were $3.15 \pm 0.01 * 10^{10}$ cfu/mL and $1.50 \pm 0.02 * 10^{10}$ cfu/mL respectively. The volatile solids were found to be 81.69 ± 1.52 and $73.50 \pm 2.20\%$ of the total solids while the C: N ratio was 29.62 ± 0.51 and 17.06 ± 0.50 in rumen fluid and cow dung respectively.

Thermophilic biogas production was highest in waste mixtures at 4700 mL for the 1.5 L reactor capacity. The thermochemical pretreatment results in more cumulative biogas production at 6200 mL, followed by thermal at 4900 mL and then chemical pretreatments at 3750 mL for 500 g mixed fruits and vegetable market wastes for 500 mL -1500 mL digester capacity. The optimal pH observed in this study was 6.70 – 7.23. Biogas production was highly dependent on proximate properties like moisture, carbohydrates, fat and protein levels. The best working range for C: N ratio was 19 – 30, with higher levels significantly reducing biogas production.

The biochemical methane potential studies revealed that generated biogas was 1000 to 3500 mL/g.VS with CH₄ levels of 56 – 60%. The measured level of raw biogas was

227ppm H₂S, >20% CO₂ and 52-56% CH₄. The most efficient upgrade material was zeolite rocks with upgrade levels of 89 – 93% methane. The total removal for zeolite was observed to be 75% for CO₂ and 95.34% for H₂S. A re-engineered digester with automatic loading, agitation and pH and temperature regulation mechanisms was fabricated and biogas yields studied from the pilot scale studied. A portable biogas safety device was designed and developed using *Arduino* micro-controller. The device alerts the user in the event of excess smoke or fire breakout via a call or SMS using the SIM900 GSM module.

Microbial fuel cell technology was employed in direct conversion of market wastes to electricity. The results obtained from the MFC indicated that voltage recovered increased with time. On average, avocado and watermelon produced 0.357V and 0.009V, respectively. The power density generated was 0.060856 to 22.53043 $\mu\text{W}/\text{M}^2$, while the current density was 0.751315 to 63.11044 mA/m². *Clostridium Spp.*, *Proteus* and rumen fluid generated 0.622 V, 0.465 V and 0.759V, respectively. The data obtained from varying MFC operating parameters indicate that $6.6668 * 10^{-3} \text{ m}^2$ electrode S/A produced 0.00399 m² and 0.01331 m² voltage and power, respectively. Tomato wastes generated 0.385 V, 0.038 mA and 0.01463 Mw, voltage, current and power, respectively across 45 K Ω resistor. Anaerobic digestion and microbial fuel cells technologies are recommended for market and abattoir wastes management.

Keywords: *Arduino, Biogas, Bio-methane, Market wastes, Microbial fuel cells.*

TABLE OF CONTENTS

DECLARATION ii

DEDICATION iii

PUBLICATIONS AND PATENTS v

ABSTRACT vii

TABLE OF CONTENTS ix

LIST OF TABLES xvi

LIST OF FIGURES xvii

LIST OF APPENDICES xxiii

LIST OF ABBREVIATIONS AND SYMBOLS xxiv

CHAPTER 1: 1

 1.1 INTRODUCTION 1

 1.2 Background 1

 1.3 Food Waste 2

 1.4 Biogas 3

 1.4.1 Benefits of Biogas Technology 3

 1.5 Biogas Digesters 4

 1.5.1 Digester Construction Materials 4

 1.5.2 Effect of Temperature 4

 1.5.3 Substrate Consumption 5

 1.5.4 Biogas Yield and Loading Rate 5

 1.5.5 Biogas Storage 6

 1.5.6 Biogas digesters types and designs 6

 1.6 Air Quality Index (AQI) 11

 1.6.1 Gas leakage detection tools in Arduino 11

1.7 Bio-slurry	13
1.8 Fuel Cells.....	14
1.8.1 Microbial Fuel Cells	14
1.9 Statement of the Problem	20
1.10 Objectives.....	22
1.10.1 General Objective	22
1.10.2 Specific Objectives	22
1.11 Justification and Significance of the Study	23
CHAPTER 2:	25
2.1 LITERATURE REVIEW	25
2.2 Food wastage.....	25
2.2.1 Energy Potential of Food Waste Digestion	26
2.3 Anaerobic Digestion.....	27
2.3.1 Substrates in Anaerobic Digestion	27
2.3.2 Methane Potential of Various Substrates.....	28
2.4 Biochemical Anaerobic Digestion Process	29
2.4.1 Hydrolysis.....	29
2.4.2 Acidogenesis.....	30
2.4.3 Acetogenesis.....	30
2.4.4 Methanogenesis	30
2.5 Methanogenic Bacteria.....	31
2.5.1 Bacteria Extraction, Isolation, Identification and Culturing.....	32
2.6 Biogas Upgrading.....	32
2.7 Co-Digestion	33
2.8 Macro and Micro-Nutrients and Toxic Compounds	33

2.9 Continuous and Batch-Type Digesters.....	33
2.10 Digestate Resource Recovery Options	34
2.11 Biogas Calculations.....	34
2.11.1 Domestic Gas Demand.....	34
2.11.2 Size and Site for Biogas Digesters	34
2.11.3 Size of the Digester.....	35
2.11.4 Daily Gas Production.....	35
2.11.5 Specific Gas Production	36
2.11.6 Loading Rate.....	36
2.12 Models for Calculating Biogas Production	36
2.12.1 Artificial Neural Network.....	38
2.12.2 The theoretical methane potential.....	38
2.13 Online Biogas Application	40
2.14 Digester Design System	40
2.15 Arduino.....	41
2.15.1 Arduino Desktop IDE.....	41
2.15.2 Arduino Libraries	44
2.15.3 Arduino Sketch Structure	45
2.15.4 Arduino Motors	46
2.15.5 Type-K Thermocouple MAX775	46
2.15.6 pH sensor in Arduino.....	47
2.15.7 SIM900 GSM GPRS Shield	47
2.15.8 Gas detection in the environment	48
49	
2.15.9 Flame Sensor	52

2.16 Microbial fuel cells.....	53
2.17 Bio-slurry Application.....	53
CHAPTER 3:	54
3.1 MATERIALS AND METHODS	54
3.2 Materials and Reagents	54
3.3 Sampling Area.....	55
3.4 Procedure.....	56
3.4.1 Sample Collection.....	56
3.4.2 Pre-Treatment	56
3.4.3 Bacteria Total Count, Culture, Isolation and Identification	56
3.4.4 Waste Analysis	57
3.5 Biogas Production	61
3.5.1 Digester Pressure Tests.....	61
3.5.2 Biogas Measurement	63
3.5.3 Biogas production at psychrophilic conditions	64
3.5.4 Biogas production optimization.....	69
3.6 Modelling Studies	72
3.7 Biogas Upgrade.....	73
3.7.1 Natural zeolite rock analysis.....	75
3.8 Fabrication of a Digester	77
3.9 Digester Automation Design.....	79
3.9.1 Loading rate	79
3.9.2 Temperature Monitoring using Arduino.....	80
3.9.3 Agitation mechanism	81
3.9.4 pH Regulation Using pH Probe and Arduino.....	81

3.9.5 Re-engineered Digester Biogas Production.....	83
3.9.6 Automated Digester Biogas Production	84
3.9.7 Safety Measures in Biogas Production.....	87
3.10 Pilot Scale Set-Up	89
3.10.1 Solids Retention Time	91
3.10.2 Hydraulic Retention Time (HRT).....	91
3.10.3 Organic Loading Rate.....	91
3.11 Fabrication of a Ferro-cement digester	91
3.12 Construction of a 14000 liters' digester	92
3.13 Microbial Fuel Cells.....	93
3.13.1 Microbial Fuel Cells Construction	93
3.13.2 Circuit Assembly	94
3.13.3 Resistance Variations	94
3.13.4 Microbial Fuel Cells Parameter Optimization.....	95
3.13.5 The Pilot Scale of Microbial Fuel cells	97
3.13.6 Degradation of chlorothalonil in microbial fuel cells.....	97
3.14 Digestate application in the container garden	97
CHAPTER 4:	99
4.1 RESULTS AND DISCUSSIONS	99
4.2 Food wastes	99
4.2.1 Macro and micro-nutrient and heavy metals analysis	99
4.2.2 Pesticide levels	103
4.2.3 Proximate analysis	105
4.2.4 Ultimate composition analysis.....	109
4.3 Inoculum studies	112

4.3.1 Inoculum analysis	113
4.4 Biogas production	117
4.4.1 Pressure Tests	117
4.4.2 Biogas Measurement	118
4.4.3 Influence of different inoculum on biogas production	124
4.4.4 Optimization Studies	133
4.5 Biogas upgrade	156
4.14.1 Characterization of Eburru Zeolite Rocks	157
4.14.2 Biogas from cow dung upgrade	162
4.15 Simulation and modeling	169
4.15.1 Anaerobic Digestion Kinetic Study	169
4.15.2 Bio-methane Potential studies	176
4.15.3 Anaerobic Biodegradability	177
4.16 Pilot Scale Experiments	179
4.7.1 Operation of Ferro-Cement and 14 m ³ Digesters	184
4.7.2 Temperature Regulation in the digester	186
4.8 Biogas digester Automation	187
4.9 Biogas Safety	192
4.10 Microbial Fuel Cells	193
4.10.1 Pure culture voltage modelling	199
4.10.2 Influence of External Resistance	202
4.10.3 Rumen fluid	207
4.10.4 Influence of substrate proximate analysis of voltage production	213
4.10.5 Pilot-scale study	216
4.10.6 Chlorothalonil degradation studies	217

4.10.7 Concentration Variation	222
4.11 Bio-slurry application.....	224
CHAPTER 5	231
5.1 CONCLUSIONS AND RECOMMENDATIONS	231
5.2 Conclusions	231
5.3 Recommendations	233
5.4 Recommendations for Further Work.....	234
5.5 Beneficiaries of The Work	234
5.6 References	236

LIST OF TABLES

Table 2.1: Typical methane yields for biochemical components	27
Table 4.1: Proximate analysis on dry weight fruit and vegetable wastes	106
Table 4.2: Proximate properties on wet weight fruit and vegetable wastes.....	107
Table 4.3: The ultimate analysis properties of fruits and vegetable waste	110
Table 4.4: Physical properties of various market wastes	111
Table 4.5: Total microbes count from dung and rumen fluid samples.	113
Table 4.6: Cow dung and slaughterhouse waste biochemical properties	114
Table 4.7: Trace elements in the inoculums	116
Table 4.8: The C: N ratio of market wastes	144
Table 4.9: The pH of the substrate before and after loading to the digester.	152
Table 4.10: Diffraction parameter data for Eburru zeolite rocks sample	158
Table 4.11: Formulation of Eburru zeolite rocks sample	159
Table 4.12: The EDX content of Eburru zeolite rocks	159
Table 4.13: The Infrared band location of Eburru zeolite materials.....	160
Table 4.14: Composition properties of zeolite rocks	162
Table 4.15: The methane energy values	175
Table 4.16: Table of Experimental and theoretical BMPs.....	176
Table 4.17: Table of of different feedstock's biodegradability	178
Table 4.18: Proximate analysis properties for different wastes	213
Table 4.19: Proximate properties of tomatoes	218
Table 4.20: Loam soil properties	224
Table 4.21: General observation for crops with different manure.....	227

LIST OF FIGURES

Figure 1.1: Projected world energy.....	1
Figure 1.2: Fixed dome biogas reactor	7
Figure 1.3: Floating-Drum Biogas digester	8
Figure 1.4: Ballon digester (a) schematic and (b) balloon type digester	8
Figure 1.5: Schematic diagram of horizontal biogas plants.....	9
Figure 1.6: Earth bag biogas plant (a) schematic and (b) ferro-cement tank.....	10
Figure 1.7: Portable digester from Biotech Company in India.....	10
Figure 1.8: An (a) Arduino Uno R3 board, (b) MQ2 sensor and (c) GSM SIM 900.	13
Figure 1.9: MFC working principle illustration.....	14
Figure 1.10: The electron transport chain.	16
Figure 1.11: Microbial fuel cell	20
Figure 1.12: Photo of vegetable waste in Kangemi market (10 th December 2019).....	21
Figure 1.13: Open-air slaughterhouse waste treatment in Kiambu.....	21
Figure 2.1: Food supply and wastage hierarchy	26
Figure 2.2: Methane yield for various feedstocks.....	28
Figure 2.3: Schematic flow diagram of the AD process.....	29
Figure 2.4: Anaerobic digestion microbes.	31
Figure 2.5: A screenshot of distinct parts of the Arduino IDE	42
Figure 2.6: A Screenshot showing the 2 parts of Arduino sketch	43
Figure 2.7: A K-type MAX775 thermocouple.....	46
Figure 2.8: Various parts of the pH probe	47
Figure 2.9: A SIM900 GSM/GPRS Shield (a) front side and (b) back side.....	48
Figure 2.10: MQ2 gas sensor pins	49
Figure 2.11: MQ2 gas sensor calibration.....	50
Figure 2.12: A flame sensor.....	52
Figure 3.1: A map of the sampling points.....	55
Figure 3.2: Pressure test setup for 1 liter bottle.	62
Figure 3.3: Pressure tests setup for 120l digester.....	62
Figure 3.4: Schematics of gravimetric biogas methods (Sasha et al., 2015)	63
Figure 3.5: Volumetric biogas methods (Mbugua et al., 2020).....	63
Figure 3.6 : Biogas production set up at psychrophilic conditions.....	64
Figure 3.7: Biogas production measuring with a (a) glass syringe and (b) biogas analyzer.	65
Figure 3.8: A set-up of biogas production at the mesophilic condition.....	66
Figure 3.9: Biogas production at room temperature (a) 1 l reactor (b)5 l reactor	67
Figure 3.10: GP810 multi-gas detector from Henan, China	68
Figure 3.11: Biogas analyzer measuring biogas quality from potato waste	68
Figure 3.12: A setup of fruits and vegetable market wastes pretreatment process.....	70
Figure 3.13: Large scale biogas production from pretreated market wastes	71

Figure 3.14: Setup for (a) psychrophilic and (b) mesophilic and thermophilic batch setup	71
Figure 3.15: Screenshots of online biogas application	73
Figure 3.16: The biogas upgrading cartridges; rubber tires, natural zeolite rocks, commercial desulphurizer, maize cobs and steel wire.....	74
Figure 3.17: Biogas upgrade setups at (a) psychrophilic and (b) mesophilic conditions.	75
Figure 3.18 (a) Biogas composition analysis setup (b) Commercial desulphurizer (c) combined upgrade material.....	75
Figure 3.19: Natural zeolite rock	76
Figure 3.20: The biogas upgrading set-up	77
Figure 3.21: The (a) plastic drum (b) plumbing items (c) cutting material used for digester design	78
Figure 3.22: Substrate loading gate valve set up.	79
Figure 3.23: A schematic of thermocouple with an LCD.	80
Figure 3.24: Arduino controlled servo for warm water circulation	80
Figure 3.25: An Arduino servo-controlled agitator.	81
Figure 3.26: pH probe calibration using a multi-meter.....	82
Figure 3.27: pH probe calibration using an offset code.....	82
Figure 3.28: Digester pH monitoring with (a) Arduino and (b) portable pH meter	83
Figure 3.29: The biogas digesters	84
Figure 3.30: Block diagram of the automated digester.....	85
Figure 3.31: A schematic diagram of automation biogas production design	86
Figure 3.32: Automated biogas digester	87
Figure 3.33: A block diagram of Arduino Based methane, Smoke & Fire Detection.....	88
Figure 3.34. Prototype schematic diagram	89
Figure 3.35: The pilot-scale biogas production setup (a) 120 – 240 liters (b) 5 – 20 liters	90
Figure 3.36: Pilot-scale biogas upgrade setup (a) using a desulphurizer (b) using zeolite.....	90
Figure 3.37: Set-up of H-shaped microbial fuel cells with a multi-meter	94
Figure 3.38: Set-up of H-shaped microbial fuel cells.....	94
Figure 3.39: Carbon rods electrodes compartments A-0.01331 m ² , B-0.00666 m ² and C-0.00399 m ²	96
Figure 3.40: A picture of a container garden (a) bio-slurry, (b) cow dung, (c) dry manure (d) is the blank set (e) avocado	98
Figure 4.1: The XRF- spectrum for fresh wastes.....	100
Figure 4.2: XRF- spectrum for digested wastes.....	100
Figure 4.3: The elemental composition of fresh and digested wastes.	102
Figure 4.4: The % composition of fresh and digested wastes.....	103
Figure 4.5: GC-MS chromatogram	104
Figure 4.6: Pressure tests line plots.....	118
Figure 4.7: Plot of volumetric and gravimetric measured biogas	119
Figure 4.8: Biogas produced from fruit wastes at psychrophilic conditions	120

Figure 4.9: Biogas produced from vegetable wastes at psychrophilic conditions	121
Figure 4.10: Biogas produced from wastes at psychrophilic conditions	122
Figure 4.11: Biogas produced from market wastes mixtures at psychrophilic conditions	123
Figure 4.12: Biogas produced from market wastes inoculated with dung and rumen at psychrophilic conditions.	124
Figure 4.13: Biogas produced from fruit wastes inoculated with cow dung at psychrophilic conditions.	125
Figure 4.14: Biogas produced from market wastes inoculated with rumen fluid at psychrophilic conditions	126
Figure 4.15: Biogas production from un-inoculated market waste at mesophilic conditions	127
Figure 4.16: Surface plot of biogas production from market waste at psychrophilic temperatures.....	128
Figure 4.17: Surface plot of biogas production from market waste at mesophilic temperatures.....	129
Figure 4.18: Surface plot of biogas production from market waste at thermophilic temperatures.....	129
Figure 4.19: Mesophilic(37 ⁰ C) biogas production from un-inoculated market wastes ..	130
Figure 4.20: Mesophilic (37 ⁰ C) biogas production from inoculated market wastes	131
Figure 4.21: Thermophilic(55 ⁰ C) biogas production from inoculated market wastes...	132
Figure 4.22: Cumulative biogas produced from F.V.M.W. with varying pretreatment methods	134
Figure 4.23 : Cumulative biogas generated from alkaline and acidic pretreated F.V.M.W.	135
Figure 4.24 : Biogas generated from NaOH pretreated market wastes	136
Figure 4.25: Biogas generated from HCl pretreated market wastes	137
Figure 4.26: Biogas generated from NaOH and HCl pretreated avocado, mango and banana wastes.....	138
Figure 4.27: Cumulative biogas produced from pretreated F.V.M.W. at pilot scale.....	139
Figure 4.28: Plot of biogas produced for wastes to fluid rumen ratios.....	140
Figure 4.29: Plot of biogas produced for wastes to cow dung ratios	141
Figure 4.30: Plot of biogas produced for wastes to different inoculum ratios.....	141
Figure 4.31: Biogas production at temperature ranges of 14 ⁰ C – 19 ⁰ C and 24 ⁰ C – 27 ⁰ C	142
Figure 4.32: Plot of biogas generation at different temperatures.....	143
Figure 4.33: Biogas production from market wastes with different C: N ratios at mesophilic condition.....	145
Figure 4.34: Biogas production at thermophilic condition with distinct C: N ratios.....	146
Figure 4.35: Influence of moisture content on biogas production.	147
Figure 4.36: Influence of carbohydrates content on biogas production.....	148
Figure 4.37: Influence of fat content on biogas production.....	149

Figure 4.38: Influence of protein content on biogas production.....	150
Figure 4.39: Daily pH changes per waste.	151
Figure 4.40: Plot of influence of pH on biogas production	153
Figure 4.41: Biogas generation from co-digested substrates	154
Figure 4.42: Plot of biogas production from agitated and un-agitated digesters.....	156
Figure 4.43: XRD spectra of commercial zeolite rocks sample	157
Figure 4.44: Eburru zeolite rocks XRD spectrum	158
Figure 4.45: FT-IR spectra of Eburru zeolite rocks sample.....	160
Figure 4.46: The SEM images of Eburru zeolitic rock.....	161
Figure 4.47: Biogas upgrade levels using steel wire and tyres	163
Figure 4.48: Biogas upgrade using maize cobs and desulphurizer.....	164
Figure 4.49: Biogas upgrade using zeolite rocks	164
Figure 4.50: Plot of carbon dioxide levels after upgrade.....	165
Figure 4.51: Plot of hydrogen sulfide levels after upgrade.....	166
Figure 4.52: The % methane after raw biogas upgrade	167
Figure 4.53: Plot of % methane and carbon dioxide after upgrade	168
Figure 4.54: Pilot-scale CO ₂ and CH ₄ levels after clean up	168
Figure 4.55: Plot of the linear model for market wastes biogas production	170
Figure 4.56: The exponential plot for FVMW mixture biogas production.....	171
Figure 4.57: Exponential plot for banana wastes biogas production	172
Figure 4.58: The normal distribution curves for biogas production.	173
Figure 4.59: The Gompertz plot for FVMW plus rumen biogas production.....	174
Figure 4.60: Bar graphs of pilot-scale biogas production at thermophilic and psychrophilic temperatures	179
Figure 4.61: Time graph of cumulative biogas produced in a 5l large-scale digester	180
Figure 4.62: Plot of cow dung psychrophilic biogas generation	181
Figure 4.63: Plot of psychrophilic biogas production from FVMW mixture + cow dung	181
Figure 4.64: A plot of mesophilic biogas production from FVMW + rumen.....	182
Figure 4.65: A 60l portable digester with a stirrer and hot water circulation pipe	183
Figure 4.66: A 120 liter digester biogas production	183
Figure 4.67: A (a)1.45 m ³ Ferro-cement digesters and (b) 14 m ³ brick digesters	184
Figure 4.68: Plot of temperature changes in water	186
Figure 4.69: DC-motor anaerobic digester agitator	187
Figure 4.70: Digester temperature at night	188
Figure 4.71: Digester temperature at night	189
Figure 4.72: Plot of digester pH.....	189
Figure 4.73: Final biogas digester automation connections.....	190
Figure 4.74: Cumulative biogas for different digesters	191
Figure 4.75: Biogas leakage and flame detector alarm system.....	192
Figure 4.76: LED display when (a) all is running well (b) in the event of smoke, fire or methane leak	193

Figure 4.77: Anodic chamber sample stained plate	194
Figure 4.78: Plates of microbes in the anodic chamber of MFC (a) and (b) in blood agar and (c) in McKonkey agar	194
Figure 4.79: Electron microscope images of (a) Proteus and (b) Clostridium spp. bacteria	195
Figure 4.80: Plot of daily voltage using different culture	196
Figure 4.81: Plot of current daily production for different cultures.	197
Figure 4.82: Plot of daily power production for different microbes.	197
Figure 4.83: Plot of daily current density for different cultures.	198
Figure 4.84: Surface plots of daily power and current densities.....	199
Figure 4.85: Fitted plots for voltage generation by Proteus a) linear b) Gompertz	200
Figure 4.86: Fitted plots for voltage generation by Clostridium spp a) linear b) Gompertz	201
Figure 4.87: Gompertz fitted plots for voltage generation by rumen fluid microbes	201
Figure 4.88: Linear fitted plots for voltage generation by Clostridium spp+ proteus cultures	202
Figure 4.89: Plot of voltage across different resistors and open circuit.....	203
Figure 4.90: Plot of daily voltage for different fruit wastes using cow dung	204
Figure 4.91: Plot of power against time generated by other fruits wastes.	204
Figure 4.92: Plot of current density against time.	205
Figure 4.93: Plot of power density against time.	206
Figure 4.94: Plot of power density versus current density for fruits waste in cow dung	206
Figure 4.95: Plot of voltage versus days of tomato and avocado inoculated with rumen waste	207
Figure 4.96: Bar graphs of power generated from tomato and avocado wastes	208
Figure 4.97: Plot of voltage produced by varying amount of rumen matter.....	208
Figure 4.98: Power generated by 1:1 avocado, mango mixture to rumen fluid.....	209
Figure 4.99: Bar graphs showing effect of A1-0.00399m ² , A2-0.00666m ² and A3-0.01331m ² electrode S/A.	210
Figure 4.100: Current density plots for different electrode surface area	211
Figure 4.101: Different electrodes surface area Power density	211
Figure 4.102: Voltage across different resistor	212
Figure 4.103: Different fruits wastes current and voltage	214
Figure 4.104: Bar graph of fruit energy levels versus voltage output	216
Figure 4.105: Pilot-scale voltage in OCV and across different resistors	217
Figure 4.106: Daily voltage production from various glucose levels.....	219
Figure 4.107: Plots of daily current for various glucose levels	219
Figure 4.108: Daily power production at different glucose levels.....	220
Figure 4.109: Surface plots of daily power density and current density	221
Figure 4.110: Percentage chlorothalonil degraded at different glucose levels	222
Figure 4.111: Daily voltage and current generated for varying amount of chlorothalonil	223

Figure 4.112: Daily power generated for a varying amount of chlorothalonil	223
Figure 4.113: A photo of (a) mixed market waste and (b) the digestate.	225
Figure 4.114: Container gardens with (a) bio-slurry, (b) cow dung (c) dried manure and (d) blank	225
Figure 4.115: Bar graphs of crop lengths per manure applied.....	226
Figure 4.116: Crop production in container garden (week 1).....	228
Figure 4.117: Crop production in container garden (week 3).....	228
Figure 4.118: Crop production in container garden (week 6).....	229
Figure 4.119: Crop production in container garden (week 9).....	229
Figure 4.120: The avocado tree where digestate application was done. (a)week 3 (b) week 6 (c) week 9.....	230
Figure 5.1: Schematic of the 60 L digester.	289
Figure 5.2: A schematic of the metallic stirrer	290
Figure 5.3: Schematic of the 60 l digester	291
Figure 5.4: A schematic of the agitator.....	292
Figure 5.5: Fabrication of plastic drum digester steps	293
Figure 5.6: A schematic of the 1400 liters Ferro-cement digester.....	294
Figure 5.7: A schematic of the manual stirrer.....	295
Figure 5.8: The steps followed in fabrication of Ferro-cement reactor	296
Figure 5.9: A schematic of the 14000-liter digester	297
Figure 5.10: The steps followed in fabrication of 14 m ³ reactor.....	298
Figure 5.11: Picture demonstration of how to use biogas digesters	299

LIST OF APPENDICES

5.7.1	Appendix A: NACOSTI Research Permit.....	286
5.7.2	Appendix B: Macro and micro nutrient composition in market wastes	288
5.7.3	Appendix C: The 60 Liters' Digester Description.....	289
5.7.4	Appendix D: The 120 Liters' Digester Description	291
5.7.5	Appendix E: The 1450 Liters' Ferro-cement Digester Description	294
5.7.6	Appendix F: The 14000 Liters' Digester Description	297
5.7.7	Appendix G: Digester Temperature regulation	300
5.7.8	Appendix H: pH monitoring and regulation.....	302
5.7.9	Appendix I: Biogas leaks, smoke and fire detection code.....	305
5.7.10	Appendix J: 14m ³ and 1.45 m ³ Biogas Digesters Costing	309
5.7.11	Appendix K: OBA macro-nutrient biogas prediction.....	310

LIST OF ABBREVIATIONS AND SYMBOLS

AD	-	Anaerobic Digestion
ADM1	-	Anaerobic digestion model number one
AOAC	-	Association of Official Agricultural Chemists
ASM1	-	Anaerobic sludge model number 1
BS	-	Bio-slurry
BMP	-	Bio methane potential
CD	-	Current Density
C: N	-	Carbon to Nitrogen ratio
CRAN	-	Comprehensive R Archive Network
CSTR	-	Continuous flow stirred-tank reactor
CT	-	Chlorothalonil
DEC	-	Dedicated Energy Crop
DET	-	Direct Electron Transfer
DM	-	Dry Matter
DS	-	Digested Slurry
EET	-	Extracellular Electron Transfer
FAO	-	Food and Agriculture Organization
FF	-	Fresh Feedstock
FS	-	Fixed Solids
FVMW	-	Fruit and Vegetable Market Wastes
FYM	-	Farmyard manure
GHG	-	Green House Gases
GND	-	Ground

GPRS	–	Global Pocket Radio Service
GSM	–	Global Systems of Mobile communications
HRT	-	Hydraulic Retention Time
IDE	–	Integrated Development Environmental
IET	-	Indirect Electron Transfer
LCD	–	Liquid Crystal Display
MET	-	Mediated Electron Transfer
MFC	-	Microbial Fuel Cells
MGRT	-	Minimum Guaranteed Retention Time
MM	-	Mineral Matter
MQ	-	<i>‘Mǐngǎn’ ‘Qǐ lai’</i>
NACOSTI	-	National Commission for Science and Technology
NADH	-	Nicotinamide adenine dinucleotide
NFE	-	Nitrogen Free Extract
NPG	-	Natural Petroleum Gas
oDM	-	Organic Fraction of Dry Matter
PD	-	Power Density
rRNA	-	Ribosomal Ribonucleic Acid
RS	-	Raw Slurry
SEM	-	Standard error-of-mean
SIM	–	Subscriber Identity Module
SMS	–	Short Message Service
SOFC	-	Solid Oxide Fuel Cell
SOP	-	Standard Operating Procedures
SRT	-	Solid retention time

SSE	-	Sum of squared errors
STP	-	Standard Temperature and Pressure
TPN	-	Total Protein Content
TS	-	Total Solids
TSS	-	Total suspended solids
USB	-	Universal Serial Bus
VFA	-	Volatile Fatty Acids
VM	-	Volatile Matter
VS	-	Volatile Solid
VSS	-	Volatile suspended solids
XF	-	Crude Fiber
XL	-	Crude fat
XP	-	Crude protein
Ω	-	Ohms

CHAPTER 1:

1.1 INTRODUCTION

1.2 Background

Hydropower and fossil fuels are the main energy source in Kenya. Charcoal and firewood serve many rural and some urban dwellers, which have drastically reduced the forest cover. From the GTZ, 2007 reports, wood fuel and biomass contribute 65.3% Kenya energy consumption, while petroleum, electricity and other sources intake is 32% (PAC, 2010). Since 2014, new electricity connections have gone up by 46% with primary school's connections rising from 8, 203 in 2013 to 22, 175 schools in 2016 (African Development Fund, 2014). Reduction of electricity connection fee to KShs. fifteen thousand targeted at increasing connectivity by 70% by 2017. In the last decade, Kenya's Liquefied Petroleum Gas (LPG) intake has increased by 59 percent, from 40000 to 80000 metric tons per year (GTZ, 2009; Githiomi, 2012).

The United States energy information administration (EIA) predicts that the energy intake in the world will increase by 28% by 2040. Figure 1.1 shows the EIA's chart on energy source (EIA, 2017). The projected increased demand for energy supply is caused by population growth as well as economic development (EIA, 2019; BP, 2019).

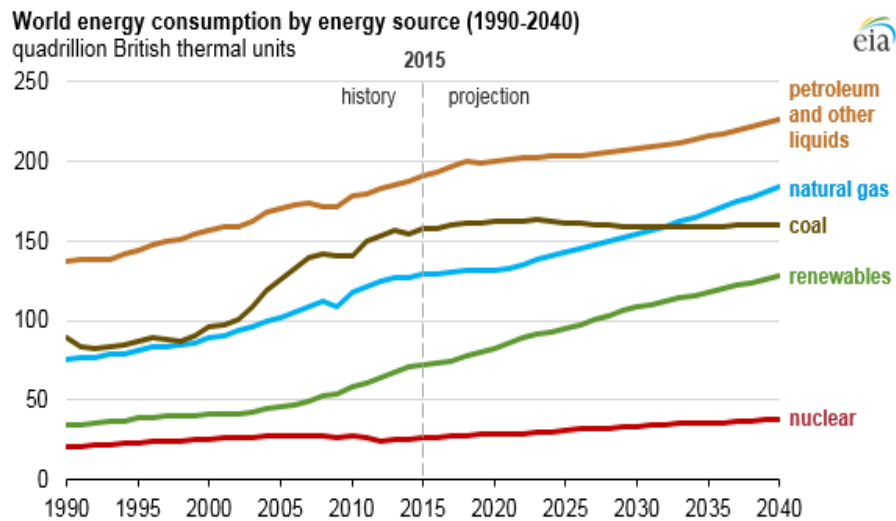


Figure 1.1: Projected world energy

1.3 Food Waste

With persistent increment in world population, food waste and accumulation are becoming big issues all over the world (Kunwar *et al.*, 2017; Gustavsson *et al.*, 2011; Anonymous., 2018). Food wastage is increasing at an exponential rate, posing serious challenges to our society such as pollution, health risks, and a lack of disposal space. The term food loss refers to the reduction of safe to eat food mass in the entire section of the supply chain resulting to scarcity of consumable food (Gustavsson *et al.*, 2011). Food waste (FW) refers to the removal of foodstuff from the supply chain resulting from spoilage or expiry caused by weak economic behavior (Beede *et al.*, 1995; FAO, 2012). Agricultural produce wastes originate during harvest, transport, storing, processing and marketing. FAO reports that almost 1.3b tons of food comprising of vegetables, meat, wheat, fruits, and milk products are wasted (FAO, 2012). Food wastage (FW) is projected to increase with technological and population increase. For instance, in Asian countries, the annual quantity of city FW might rise from 278 to 416 million tonnes from 2005 to 2025 (Melikoglu *et al.*, 2013). Approximately 1.4b hectares of fertile land (28% of the world's agricultural area) are utilized yearly in production of food that is wasted (Melikoglu *et al.*, 2013). Further, food waste contributes to greenhouse gas (GHG) pollution through an accumulation of about 3.3b tonnes of CO₂ into the atmosphere annually. Incineration and open air dumping are the conventional ways of managing food waste (Agarwal *et al.*, 2005; Kumar and Goel., 2009; Kumar *et al.*, 2010; Talyan *et al.*, 2008). Dioxins are a significant issue resulting from FW burning due to excess moisture (Katami *et al.*, 2004). Incineration further destroys nutrients and constituent elements in waste, thus reducing the economic fee of a substrate. Therefore, alternative techniques are needed for the administration of FW (Ma *et al.*, 2009). Anaerobic digestion (AD) is an attractive alternative to the world's renewable energy by utilizing food waste to generate biogas. Due to their high bio-digestibility and high-water levels (75–90%), watery fresh fruit and vegetable wastes would be a suitable feedstock for renewable energy recovery via the anaerobic digestion (Forster *et al.*, 2008).

1.4 Biogas

Biogas refers to a natural gas produced from the digestion of biodegradable organic matter by microbes in the anaerobic degradation (AD) process. Biogas components include; CH₄, CO₂ and traces of H₂S, other gases, moisture and siloxane (EnDev, 2012, Githiomi *et al.*, 2009). An effective and efficient performance, especially in terms of volume and organic waste stabilization resulting in biogas production, makes anaerobic digestion widely employable in organic wastes disposal (Amon *et al.*, 2007). Anaerobic digestion reduces the mass of wastes, generate fertilizer and renewable energy. The AD usually takes place under psychrophilic conditions (12-17°C), mesophilic (35-37°C) and thermophilic conditions at 55-60°C (Gene, 1986). At mesophilic anaerobic digestion conditions, the solubility properties of carbon dioxide are reduced, resulting in increased pH. This leads to increased levels of ammonia from proteins or urea degradation (Dieter *et al.*, 2008). Mesophilic AD is the most common for organic degradation. It is estimated that the breakdown of volatile solids under mesophilic conditions is 40% at a solid retention time of 30 to 40 days (Dieter *et al.*, 2008). pH, temperature, C: N ratios, loading rates, ammonia inhibitors, among others, are some of the physical and chemical parameters which highly influence the success of sludge degradation in anaerobic digestion. Temperature is the most critical parameter influencing biogas production. A slight fluctuation in temperature significantly affects the AD bacteria. The AD process takes place at a mesophilic range of 35 °C and a thermophilic temperature of 55°C. Maintaining the temperature constant is essential as the methane forming bacteria has optimum growth at a particular temperature. Methane-forming bacteria are divided into two categories based on the temperature at which bacteria growth is optimum (Soetaert, 2008). The anaerobic breakdown range at mesophilic and thermophilic conditions is still a subject under investigation (Gene, 1986; Deiter *et al.*, 2008).

1.4.1 Benefits of Biogas Technology

Anaerobic fermentation has evolved from a relatively simple biomass conversion technique; well-functioning biogas plants can offer a variety of merits to consumers, society and the environment (Reza *et al.*, 2016). Among these advantages are:

- a. Generation of carbon neutral green energy (heat, light, electricity).
- b. Generation of bio-slurry from organic matter.
- c. Reduction of harmful pathogens.
- d. Improve livelihood for women by reducing cooking time and the time they use to fetch cooking fuel.

1.5 Biogas Digesters

A biogas digester is a compartment where anaerobic digestion of organic wastes takes place. The process requires an oxygen-free environment and therefore, the compartment should be airtight. The following parameters are considered in digesters operation and design;

1.5.1 Digester Construction Materials

The reactor fabrication materials depend on the geography of the location, water drainage and raw material available (Shian *et al.*, 1979). With technological advancement, low cost material has been utilized in biogas digester construction. For example, In India, stones and bricks have been used in the construction of household digesters (Anand and Singh, 1993). The material selected for reactor construction should be locally available and cheap (Garfi *et al.*, 2011).

1.5.2 Effect of Temperature

The most critical biogas reactor operation parameter is temperature. Methanogens are very sensitive to changes in temperatures (Singh *et al.*, 1995; Maurya *et al.*, 1993; Steven & Schulte., 1979; Ferrer *et al.*, 2009). With temperature change from 10 to 25 °C, biogas generated increases tenfold. The capacity of biogas generated at high temperatures (mesophilic) and low HRT is the same as the marsh gas recovered at low temperatures (psychrophilic) and high hydraulic retention time (HRT) (Ferrer *et al.*, 2009). During winter, low digestion rates are experienced in digesters when the temperature decreases below 15 °C (Anand & Singh, 1993). Temperature regulations in the digesters have led to discoveries of maintenance techniques. Solar panels have been used for heating the

reactors (Shian, *et al.*, 1979). Misra *et al.*, 1992 designed and fabricated a solar device whose reactor heating efficiency decreased during winter. Temperature maintenance is the primary reason why most digesters are built underground (Sibisi and Green, 2005). Geothermal power has been employed in heating underground reactors (Ramana and Singh, 2000). Singh, 1993, suggested covering the reactor top with charcoal, which raised the reactor temperature by 3°C and gas generation by 7%–15%, though it is done frequently. The digester temperature is maintained by covering it with certain insulation materials (Misra *et al.*, 1992).

1.5.3 Substrate Consumption

In theory, most organic matter is degradable to biogas (Bond & Templeton., 2011). However, the feedstock used is highly influenced by raw material, reactor type, and its operating conditions (Mohammad, 1991). Traditionally, cow dung was the primary substrate for biogas generation. The CH₄ in cow dung was 50%, while pig waste generated 60% (Xavier & Nand, 1990). The utilization of crop and kitchen solid matter as the substrate in AD is underexploited. The high levels of fat in kitchen wastes enhance biogas production (Lansing *et al.*, 2010; Bond & Templeton., 2011). Digestion of combined biomass has a synergistic effect on biogas recoveries (Shah, 1997; Mata-Alvarez *et al.*, 2000). Multi-substrate digestion improves the nutrient need, maintains pH, and may result in good synergisms (Yen & Brune., 2007; Murto *et al.*, 2004; Gegelenis *et al.*, 2007). Besides, several research show that co-digestion yields more CH₄ than single substrate degradation (Lansing *et al.*, 2010; Llabrés-Luengo & Mata., 1988; Li *et al.*, 2009; Garfí *et al.*, 2011; Levi & Dorothy *et al.*, 2009).

1.5.4 Biogas Yield and Loading Rate

The optimal total solids (TS) in biogas generation feedstock's ranges from 5% to 10% (Bouallagui *et al.*, 2003; Bond & Tempoleton, 2011). Increasing the TS to 19% lowers biogas generation (Shyam & Sharma., 1994). At mesophilic conditions, the OLR of 2–3 kgVS/m³/day is appropriate. However, OLRs for high biomass content is over 10% (Subramanian, 1977). The highest biogas yield achieved with the Janta model and the

updated plug flow reactor is 10.4–10.6 kgVS/m³ /day (Anjan., 1988) though 0.26–0.55m³/kgVS/day have been reported for domestic reactors (Singh & Gupta., 1990; Safley., 1992; Xavier & Nand., 1990). For mesophilic digesters, the hydraulic retention times (HRT) is 20 to 100 days (Ferrer *et al.*, 2009; Garfi *et al.*, 2011; Lansing *et al.*, 2008; Bond & Templeton., 2011). When HRT is lowered from 90 days to 60 days and the OLR subsequently increased, biogas generation is increased (Ferrer *et al.*, 2011). The microbes are often washed out in household reactors in case of unstirred digesters (Jash, & Ghosh., 1990; Martí-Herrero., 2011; Hamad *et al.*, 1981)

1.5.5 Biogas Storage

Biogas storage is a major concern. For this reason, onsite use of biogas is most common though it can be upgraded and packed in gas cylinders and gasbags. Current digesters have gas space in their design for storage. Biogas storage is vital during high production time for further use. Gasbags are widely employed in biogas transportation (Shain *et al.*, 1979; Zhang., 1989; Rodriguez *et al.*, 1997; Ezekoye & Okeke., 2006; Moulik *et al.*, 1978; Aguilar., 2001). A pressure release valve is used when gas containers are full (Rodriguez *et al.*, 1997; Rodriguez & Preston., 2001).

1.5.6 Biogas digesters types and designs

A bioreactor is a physical structure whose primary function is to provide an anaerobic condition for bacteria, which upon the breakdown of organic matter, releases biogas (Hoerz *et al.*, 2008). The fixed-dome and floating-drum biogas plants are the most common in developing countries (Hoerz *et al.* 2008). Some digester reactors' design is highlighted.

1.5.6.1 Fixed-Dome Biogas Plant

A fixed-dome reactor has a fixed gas holder at the upper part of the digester. The reactor has a compensation tank to store the displaced substrate when gas formation starts (Seadi *et al.* 2013). On releasing the pressure, the substrate flows back to the digestion (Rajendran *et al.*, 2012). Figure 1.2 shows a fixed-dome digester (Hoerz *et al.*, 2008).

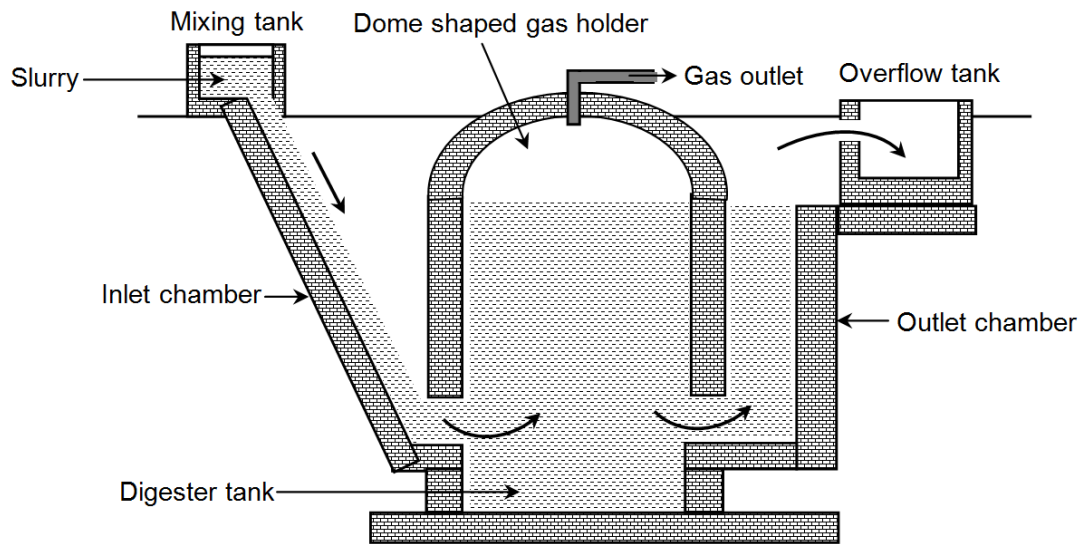


Figure 1.2: Fixed dome biogas reactor

The substrate is mixed in the mixing chamber and allowed into the digester via the inlet channel. When gas forms, it fills the gas holder and starts pushing the bio-slurry to the overflow tank. The primary type of fixed dome digesters includes Chinese Fixed dome, Janata Model, Deenbandhu, and Carmatec model (Hoerz *et al.*, 2008).

1.5.6.2 Floating-Drum Biogas digester

This reactor has metallic gas storage, circular chamber, an inlet and outlet ports. The metallic gas holder fits into the circular chamber and floats on pressure build up in the reactor (Istok 2013). The gas holder looks like inverted pot and floats on the feedstock (Mostajir *et al.*, 2013). On accumulation of gas generated, the cover rises and fall with pressure (Hagegard 2008). The cost of construction depends on factors, like temperature, the size of biogas digester and the substrate (Biogas, 2007). The floating drum digeseter is shown in figure 1.3 (Hoerz *et al.*, 2008).

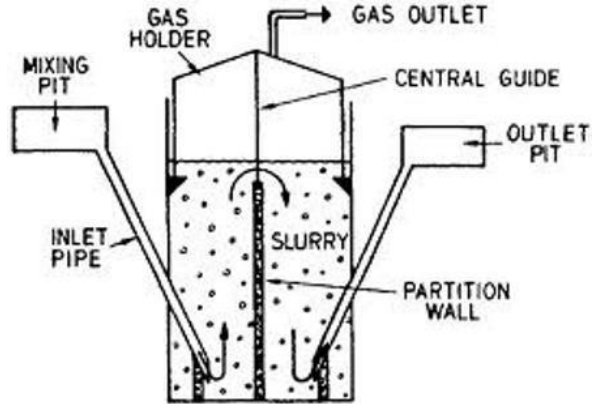


Figure 1.3: Floating-Drum Biogas digester

1.5.6.3 Balloon Biogas Plants

The reactor and the gas space are combined in a balloon like bag. The gas holder is at the upper part of the digester. During AD, to increase the pressure of the gas at the outlet pipe, a heavy metal or stone is placed at the top of the balloon (Biogas, 2007). A pressure release valve is installed to expel excess gas. The balloon is made of UV resistant reinforced plastic or synthetic caoutchouc (Sharma and Kar, 2015). This digester can last for 2–5 years (Hoerz *et al.*, 2008) and is shown in figure 1.4 (Vogeli, 2014; *FAO,1996*).

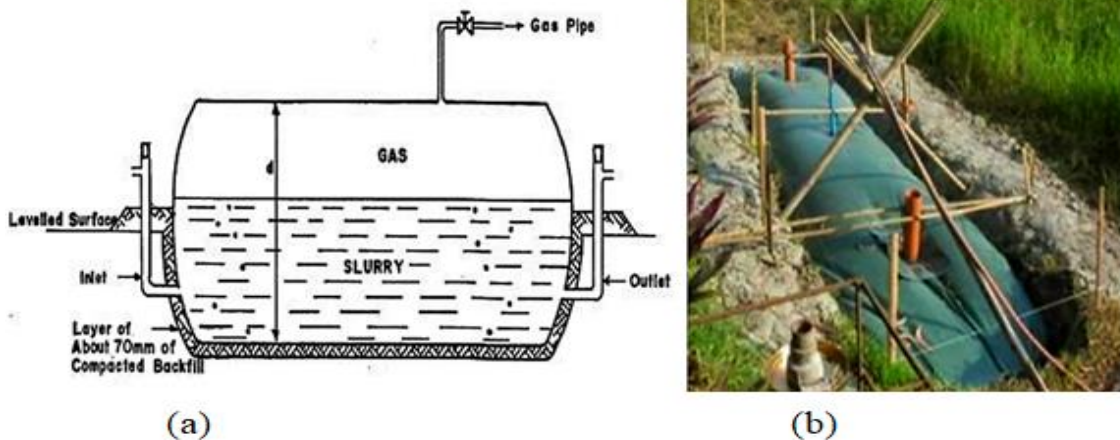


Figure 1.4: Balloon digester (a) schematic and (b) balloon type digester

1.5.6.4 Horizontal Biogas Plants

This type of digester is installed in places where digging is not possible due to rocks or water. The reactor is made up of a chamber, gas holder and an upgrade unit (Forst, 2002). The reactor is usually made of concrete (Hoerz *et al.*, 2008) as shown in figure 1.5 (Forst 2002).

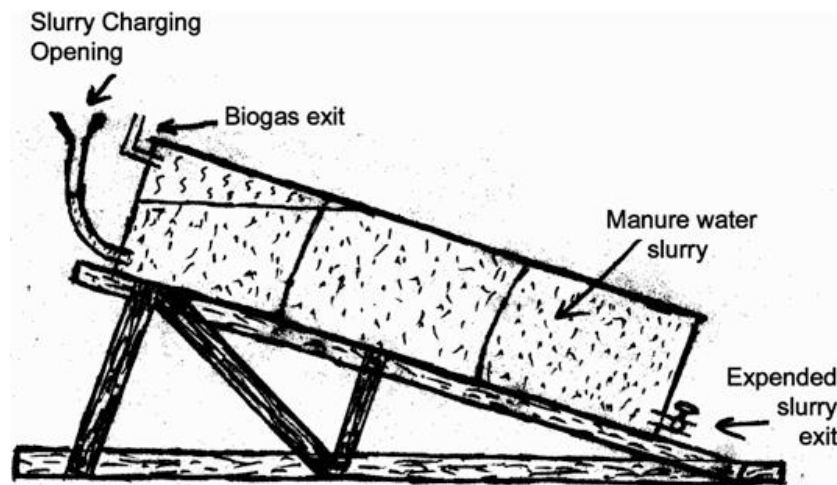


Figure 1.5: Schematic diagram of horizontal biogas plants

1.5.6.5 Earth-Pit Biogas Plants

In earth-pit plants shown in figure 1.6 (Geiger, 2010), the gasholder is made of plastic or metallic sheet. It is made up of chamber, substrate inflow and outflow pipes. A heavy object is placed on the gas space to achieve high pressure with a discharge pipe placed on the wall (Hoerz *et al.*, 2008). The feedstock mixing is done at the inlet tank and allowed to flow into the reactor. During AD, the gas generated pushes the feedstock out through the outlet pipe and is employed in fertilizer (Geiger 2010).

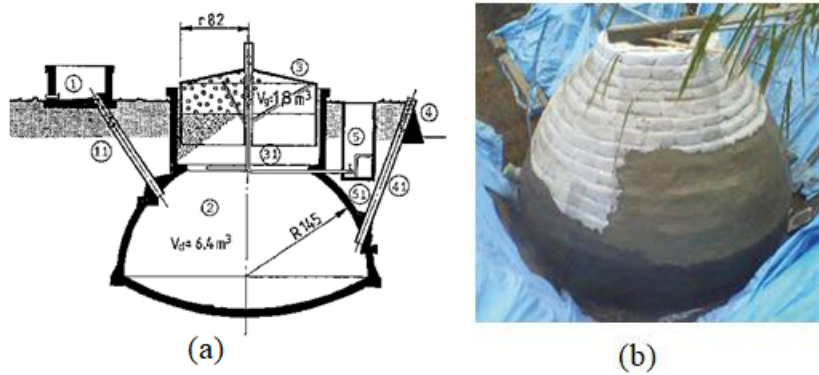


Figure 1.6: Earth bag biogas plant (a) schematic and (b) ferro-cement tank

1.5.6.6 Portable digesters

Biotech Company from India has designed and developed a portable digester that can treat household wastes hygienically at the kitchen level. This helps to overcome the fuel crisis to a great extent. Among the significant merits and demerits of biotech digester include; It is easy to install and the fact that it requires a small space (1m^2). However, the initial cost to buy is high. A portable digester from Biotech India is shown in figure 1.7. This digester operates by feeding with kitchen wastes. When the gas is formed, it lifts the top cover while an outlet channel allows bio-slurry overflow. A gas outlet valve is used to regulate gas outflow when cooking.



Figure 1.7: Portable digester from Biotech Company in India

1.5.6.7 Smart Biogas Digesters

Application of Internet of Things in biogas system has become an area of research. This has always involved making smart reactors using micro-controllers like *Arduino*. In 2019, Daniyan et al, worked on the design, fabrication and performance evaluation of a smart system for the production of biogas. The plant was designed using Autodesk Inventor and fabricated with stainless steel due to its high resistance to biological corrosion. An Arduino Uno Microcontroller was also connected to a pressure, pH and temperature sensors to monitor the process parameters of the developed biogas plant. The system detected any malfunction of the continuous stirred tank using micro-controllers. In other works, Daniyan *et al.*, 2019 developed a smart biogas system capable of operating on animal wastes to generate electrical energy. They designed a smart biogas system, fabricate the designed system, evaluated and optimized the performance of the developed biogas system (Daniyan *et al.*, 2019). While a low cost, efficient, portable biogas plant for the generation of energy from discarded kitchen wastes and food waste was developed by Sunil et al, 2013.

1.6 Air Quality Index (AQI)

The Air Quality Index (AQI) shows the daily air pollution levels. The AQI is determined based on CO, N₂O, SO₂, particulate matter and ozone level. Based on the ranks of the five pollutants, air quality is categorized into six groups which state how harmful it is for people to breathe. These categories are color-coded from 0 to 500 (EAP, 2014).

Airborne particles and ground-level ozone are the most dangerous air pollutants (EAP, 2015_b) since they threaten human health. EAP, 2015_b reports that particulate matter (P.M 2.5) is a threat to human life in both short- and long-term exposure. The suggested mitigation methods to air pollutants exposure is the use of clean fuel like biogas and installation of air purifiers.

1.6.1 Gas leakage detection tools in Arduino

Gas detection systems employ the internet of things policy in their development. The smart systems are designed with sensors, quantification and control elements that make reasonable decisions based on the signal data which supports the system's flexibility and adaptability. In most situations, autonomous operations, such as networking capabilities, closed-loop control, and energy efficiency, are attributed to a system's smartness (Akhras, 2000). With an intelligent operational management system, a smart system should have a high level of reliability, performance and consistency (Akhras, 2000). The designs are made up of:

1.6.1.1 Arduino UNO R3

The *Arduino UNO R3* shown in figure 1.8 is a free and open-source low cost embedded systems development platform. It consists of an ATMEL ATMEGA328-P PV microcontroller, an 8-bit device from the AVR family with advanced RISC architecture and DIP28 encapsulation, which has 32KB of Flash, being 512Bytes for the bootloader, having a low power consumption.

1.6.1.2 Module GSM/GPRS SIM 900

SimCom's GSM / GPRS SIM900 module (figure 1.8) has GSM and GPRS technology, which can make calls, send and receive text messages and even use the internet from a phone chip, with all these features functions coupled to an Arduino microcontroller; we can get various functionality.

1.6.1.3 MQ Series Sensors

The MQ-2 gas sensor is employed in the detection of CO, H₂, CH₄ and combustible gases (LPG) in the levels of 100ppm to 3000ppm. The working principle is the ionization of the gas on interaction with the sensor, followed by absorption by the sensor element. This creates a potential difference which is relayed to the processor unit in form of current

1.6.1.4 Arduino IDE

This is the Arduino code writing environment. The programs are called sketches and have two parts. The gas detection devices are shown in figures 1.8.

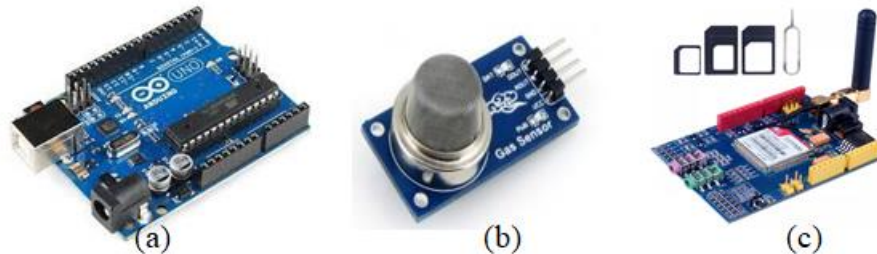


Figure 1.8: An (a) *Arduino Uno* R3 board, (b) MQ2 sensor and (c) GSM SIM 900.

1.7 Bio-slurry

Crop residues, animal (pig, poultry, and cattle) and human waste, such as urine and dung, can all be fed into a biogas reactor. About 25-30% of the TS is digested into biogas, and while 70-75% results to bio-slurry (Gurung, 1998). Biogas and bio-slurry improve fertilizer quality, reduce odors and diseases, and provide renewable energy and fuel, among other things (Holm – Niesen *et al.*, 2009). Bio-slurry can be used to fertilize crops directly or added to the composting of other organic materials. Bio-slurry is an already-digested source of animal waste. If urine (animal and/or human) is added, more nitrogen is added to the bio-slurry, which can speed up the compost-making process. This improves the carbon/nitrogen (C/N) ratio in the compost (SNV, 2011). Depending on the reactor type, bio-slurry is composed of 93% water and 7% dry matter. The bio-slurry has N, P, K, Zn, Mn, Cu and Fe (Gurung, 1998). Bio-slurry is a suitable alternative to chemical fertilizers (Serge, 2012) and can be applied in liquid form, compost or dry form. Bio-slurry raises crop production by 25%, according to Warnars (2012). When compared to ordinary manure, bio-slurry can increase cereal crop production by 10% to 30%. (Gurung, 1998). Vegetables, fruit trees and root crops are the most receptive crops to bio-slurry and bio-slurry compost in terms of increased yields (Gurung, 1998; Ullah *et al.*, 2008).

1.8 Fuel Cells

Fuel cells are electrochemical devices that convert chemical energy into electrical energy efficiently and with minimal environmental pollutions (Stauffer *et al.*, 2004). Fuel cells are continually fed with fresh reactants to maintain electron supply. Many different types of fuels have been used in fuel cell technology, e.g. hydrogen, natural gas, methanol, organic matter, etc. In a typical fuel cell, fuel is fed continuously to the anode and an oxidant is fed continuously to the cathode. The electrochemical reactions take place at the electrodes to produce an electric current through the electrolyte while driving a complimentary electric current that performs work on the load (Stauffer *et al.*, 2004).

1.8.1 Microbial Fuel Cells

An MFC is a bio-system which changes chemical energy to electricity using microbes as catalyst (Logan, 2008). The MFC has four major parts; anode, cathode, an ion exchange membrane, and a microbial fuel. At the anode, the biomass or organic waste is oxidized, releasing electrons and protons. Electrons enters the cathodic compartment via an external electric circuit, while protons move via the membrane. Electrons and protons are consumed in the cathodic cell, combining with oxygen to form water. Figure 1.9 illustrates the working principle of the microbial fuel cell (Rabaey and Verstraete., 2005).

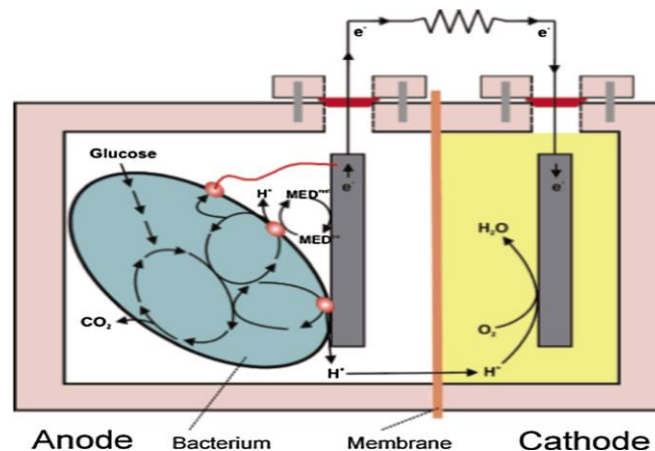


Figure 1.9: MFC working principle illustration

Potter M.C (1911) observed the utilization of microbes to produce electricity in 1911. He generated electricity using platinum electrodes from *Escherichia Coli* and *Saccharomyces* cultures. In the 1980s, MFC advanced by the use of electron mediators to enhance the current density and power output, which accelerated the electron transfer process (Davis and Higson, 2007). The mediators then cross the membrane, releasing the electrons to the anode, where they are oxidized in the bulk solution in the anodic chamber. The electron transfer rate is increased as a result of this cyclic process, which boosts the power production. Examples of synthetic exogenous mediators are dyes and metal organics like neutral red, methylene blue and Fe (III) EDTA. Synthetic mediators have limited applications in MFCs due to their toxicity and instability. Microbial metabolites (Endogenous mediators) are one form of naturally occurring compound that certain microbes can use as mediators. Humic acids, anthraquinone, and sulphur oxyanions (sulphate and thiosulphate) can all transport electrons from the cell membrane to the anode (Park and Zeikus, 2000; Bennetto, 1990).

An advancement in MFC came with the discovery of microbes which could directly transfer electrons to the anode. (Kim *et al.*, 1999; Chaudhuri and Lovley, 2003). These microbes are operationally stable and yield a high Coulombic efficiency and are all electrochemically active and can form a biofilm on the anode surface and transfer electrons directly by conductance through the membrane anode (Kim *et al.*, 1999, Chaudhuri and Lovley, 2003). The anode serves as the final electron acceptor in the dissimilatory respiratory chain of the microbes in the biofilm when they are used. Biofilms that grow on a cathode surface can also aid electron transfer between microbes and electrodes. For an MFC system that contains microbes in both chambers, cathodes may serve as electron donors for *Thiobacillus ferrooxidans* suspended in a catholyte (Prasad *et al.*, 2006).

1.8.1.1 Electron transfer mechanism

An electron movement chain is used by microbes to generate electricity in MFC s shown in figure 1.10 (Reece *et al.*, 2014). A mediator disrupts the electron movement and shuttles it to the anode. An MFC is like an expansion of electron movement chain with the last

phase (interaction of electron, oxygen and hydrogen to water) taking place out of microbe cell (Justin., 2012).

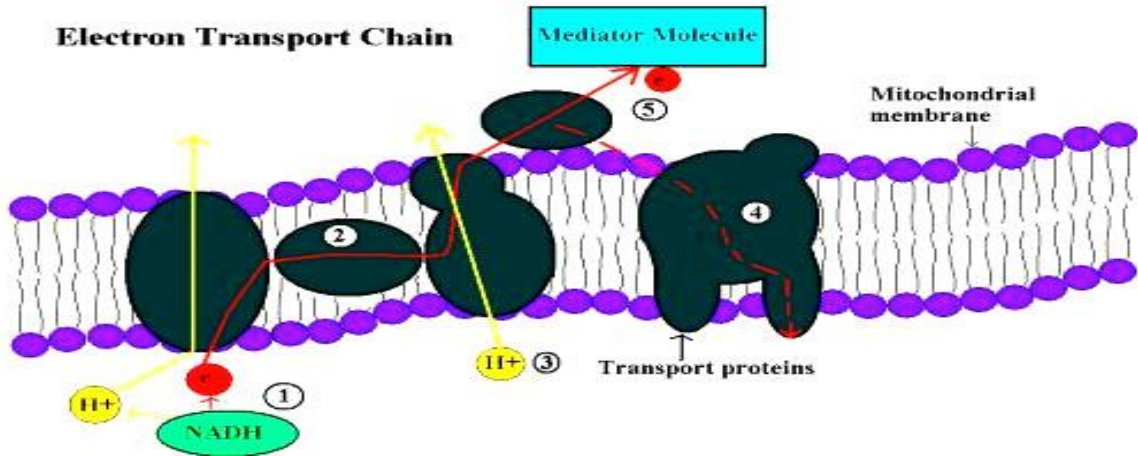


Figure 1.10: The electron transport chain.

The electron movement path starts with NADH, which is a natural movement molecule which discharge an electron and a proton (H^+). As indicated in figure 1.10, the electron goes via the red path through the protein in the mitochondrial membrane. This results in the pumping of hydrogen ions (H^+) through the membrane. Typically, for bacterial cells, the electron moves along the red dotted path and meet oxygen to form water. In MFC, the electron follows the red path to the anode with the help of a mediator. It is this knowledge in electron movement chain that Allen and Bennetto (2013) used to design the MFC cell. Technological advancement has been made with the patenting of the first MFC technology taking place in the 2000s (Biffinger & Ringeisen, 2008). Since then, research is focused on maximizing electrode materials, microbe's types and electron movement for power output optimization.

1.8.1.2 Voltage Generation in MFC Fundamentals

Only if the overall reaction is thermodynamically favorable generates electricity in an MFC. The response can be measured in terms of Gibbs free energy, which is a measure

of the maximum work that can be obtained from the reaction and is expressed in Joules (J) (Brad et al., 1985; Newman., 1973), calculated as

$$\Delta G_r = \Delta G_r^0 + RT \ln(\pi) \dots \dots \dots (1.1)$$

where ΔG_r (J) is the Gibbs free energy for the specific conditions, ΔG_r^0 is the Gibbs free energy under standard conditions usually defined as 298.15 K, 1 bar pressure, and 1 M concentration for all species, R (8.31447 J mol⁻¹ K⁻¹) is the universal gas constant, T (K) is the absolute temperature, and π is the reaction quotient calculated as the activities of the products divided by those of the reactants (Alberty., 2003, Amend *et al.*, 2001, Thauer *et al.*, 1977).

For MFC calculations, it is more convenient to evaluate the reaction in terms of the overall cell electromotive force (emf), E_{emf} (V), defined as the potential difference between the cathode and anode. This is related to the work, W (J), produced by the cell, or

$$W = E_{emf} Q = -\Delta G_r \dots \dots \dots (1.2)$$

Where $Q = nF$ is the charge, n is the number of electrons, and F is Faraday's constant (9.64853 * 10⁴C/mol). Combining these two equations, we have

$$E_{emf} = \frac{-\Delta G_r}{nF} \dots \dots \dots (1.3)$$

At standard operation conditions, $\Pi = 1$ and therefore we obtain equation 1.4

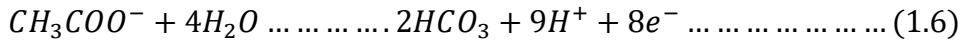
$$E_{emf}^0 = \frac{-\Delta G_r^0}{nF} \dots \dots \dots (1.4)$$

E_{emf}^0 (V) is the standard emf. Therefore, equation 1.4 can be converted to equation 1.5 for the overall reaction potential. Equation 1.5 is positive for a favorable reaction.

$$E_{emf} = E_{emf}^0 - \frac{RT}{nF} \ln(\pi) \dots \dots \dots (1.5)$$

1.8.1.3 Standard Electrode Potentials

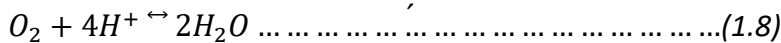
The half-cell reactions can be employed in the analysis of MFC description or individual responses at the anode and cathode (Bard *et al.*, 1985). For example, if bacteria oxidize acetate at the anode, we write the reaction as



The standard potentials are reported relative to the normal hydrogen electrode (NHE), which has a potential of zero at standard conditions (298 K, pH2) 1 bar, [H+] 1 M). To obtain the theoretical anode potential, E_{an} , under specific needs, we use equation 1.7, with the activities of the different species assumed to be equal to their concentrations. For acetate oxidation, we therefore have

$$E_{an} = E_{an}^0 - \frac{RT}{8F} \ln \dots\dots\dots (1.7)$$

For the theoretical cathode potential, E_{cat} , if we consider the case where oxygen is used as the electron acceptor for the reaction, we can write



$$E_{an} = E_{an}^0 - \frac{RT}{4F} \ln \dots\dots\dots (1.9)$$

The cell voltage depends on the catholyte used. For instance, MnO₂ and Fe (CN)₆ have been used instead of oxygen. The overall performance is also influenced by the pH. Using the standard emf data, cell potential can be determined using equation 1.10.

$$E_{emf} = E_{cath} - E_{an} \dots\dots\dots (1.10)$$

E_{emf} determined using equation 1.10 equals that of equation 1.3 and equation 1.5 if the pH at the anode and the cathode are equal. This shows that using different anode and cathode, different cell voltage is obtained.

1.8.1.4 Resistance in MFC

Resistance refers to a measure of how hard it is for an electrical current to pass in a conducting material. For a uniform material of electrical resistivity ρ (Ωm) surface S (m^2) and distance L (m) it is given by the following equation:

$$R = \rho \frac{L}{S} \dots \dots \dots (1.11)$$

Typical values of the electrical resistivity ρ for common materials at 20°C range from $1.59 \times 10^{-8} \Omega \text{ m}$ for silver to $7.5 \times 10^{17} \Omega \text{ m}$ for quartz and even more for engineered materials like polytetrafluoroethylene (PTFE). The main aim of a fuel cell is to generate current and not pass it through. However, there exist internal current blockage in MFC as discussed.

1.8.1.5 Internal Resistance of an MFC

In MFC, the voltage generated must overcome the electrolytic, anodic and cathodic internal resistance (Sharbrough *et al.*, 2008). Other ways have to be used to determine the internal resistance. According to equation 1.12

$$E_{cell} = E_{emf} - R_f I_{cell} \dots \dots \dots (1.12)$$

The slope of the linear section of the polarization curve represents the internal resistance of an MFC. MFC generates its maximum power (P_{max} , W) when $R_{int} = R_{ext}$ (Hoboken, 2005) where R_{int} can be determined as:

$$R_f = (E_{emf} - E_{max}) / I_{max} \dots \dots \dots (1.13)$$

Where E_{max} (V) and I_{max} (A) are the cell voltage and current that give the maximum power.

At the same time, following Ohm’s law

$$R_{ext} = \frac{E_{max}}{I_{max}} \dots \dots \dots (1.14)$$

Hence, when $R_f = R_{ext}$,

$$E_{max} \frac{E_{emf}}{2} \dots \dots \dots (1.15)$$

A schematic representation of MFC with an attached external resistor is shown in figure 1.11 (Lovley, 2006).

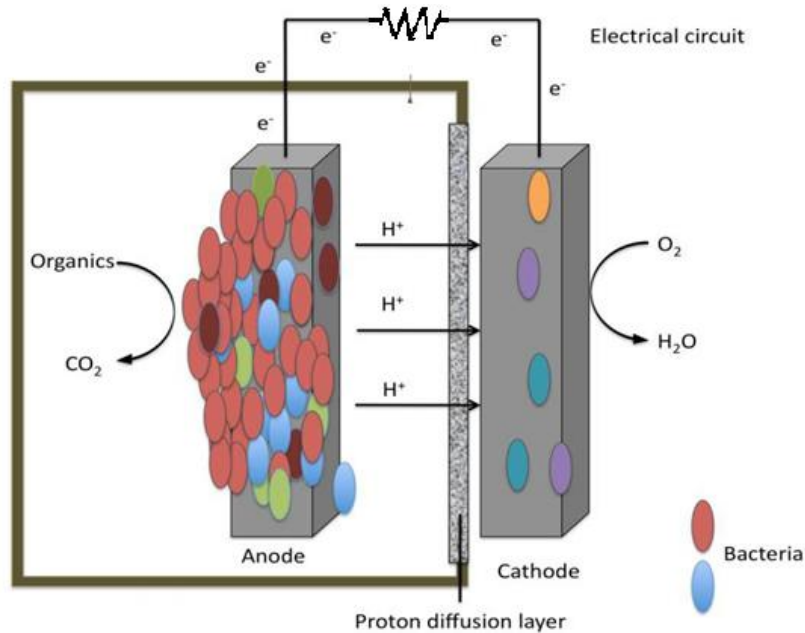


Figure 1.11: Microbial fuel cell

1.9 Statement of the Problem

Figure 1.12 represents a photo of *Kangemi* market in Nairobi. This is a case representation of most market places in Kenya and major towns in particular. Most County markets have market wastes disposal problems leading to landfill pile up of wastes. Landfills are breeding places for rodents as well as sources of green house gases emissions.



Figure 1.12: Photo of vegetable waste in Kangemi market (10th December 2019)

Dagoretti abattoir discharges thousands of liters of rumen wastes per day. The rumen is made up of methanogenic bacteria, employable in biogas generation. The waste from the slaughterhouse is drained into the Nairobi River. Since the water is used for domestic purposes, this has pollution consequences. Instead of draining the fluid to the drainage system, the fluid can be used in biogas systems during the AD digestion. In most slaughterhouses in Kenya, rumen waste is treated in the open air, as shown in figure 1.13 releasing methane and carbon dioxide to the atmosphere.



Figure 1.13: Open-air slaughterhouse waste treatment in Kiambu

Biogas digester failure arising from improper design, environmental changes, poor management in terms of operation conditions, toxic materials, loading rate concerns, among others, is relatively common.

Optimized AD process leads to high biogas production. Upgrading and storage are not only costly but also require heavy machinery. Achieving a critical pressure and temperature of 25 kPa (4psi) and -162°C would not be achievable in households. It is, therefore, essential to use biogas as it is produced in fuel cells to convert excess produced biogas to electricity. This solves the problem of storage and the risk of air pollution during high biogas production times. Therefore, there is a need for proper domestic and market waste management systems aimed at recycling and energy generation. Moreover, organic wastes are hazardous to human life.

1.10 Objectives

1.10.1 General Objective

The primary goal was to fabricate a biogas reactor and assess the potential of application of market vegetable and fruits wastes from Kenyan markets in energy production.

1.10.2 Specific Objectives

The specific objectives were to:

- i. Assess the biochemical properties of cow dung and rumen fluid for use as inoculum in AD of market wastes from Wakulima and Kangemi markets.
- ii. Assess the carbohydrate, fat and protein content of collected vegetable wastes from Kangemi and Wakulima markets for biogas production at optimal conditions under mesophilic (37°C) and thermophilic (55°C) laboratory scale.
- iii. Optimize C: N ratios, pH, temperature and substrate mixtures of vegetable wastes using co-digestion with locally available fruit wastes.
- iv. Develop an effective portable biogas digester which incorporates temperature regulation and agitation mechanism.

- v. Develop a biogas upgrading and purification method for the reduction of CO₂, H₂S, and other impurities.
- vi. Investigate the potential of conversion of market waste to electricity via microbial fuel cells technology.

1.11 Justification and Significance of the Study

Generation of renewable energy using vegetable wastes from Nairobi markets will not only provide a solution to the energy crisis in the country but also offer waste management solutions in the market. The waste is disposed to decay, yet it can be digested to provide cooking gas and more environmentally friendly and cheap fertilizer to local farmers. Recent literature (Leta *et al.*, 2015; Graunke, 2007) shows the use of pure substrates at normal operating conditions with little work being done on complex substrates from Kenyan markets. The anaerobic digestion of sterile wastes has been focused on two substrates only, i.e. pure substrates and two substrates mixture. Further, no work has been done on the identification and isolation of methanogens from slaughterhouses in Kenya for anaerobic digestion of different combinations of carbohydrates, protein and fat in various wastes from Kangemi and Wakulima markets. Previous studies on AD have focused on psychrophilic (non-heated) conditions with the substrate being livestock and human wastes. Little work has been done on mesophilic and thermophilic conditions in Kenya due to digester failure emanating from both design and operation conditions of AD reactors. There is a need to research ways to reduce the market and slaughterhouse pollution. Utilization of rumen fluid as AD inoculum solves river water pollution problems by ensuring bacteria are not released to the water body. The utilization of rumen fluid in the AD of vegetable wastes will solve the slaughterhouses waste disposal problem for slaughterhouses in Nairobi County and Kiambu County. Currently, the fluid goes to waste. This fluid is rich in methanogens, which increase anaerobic digestion biogas production significantly (Mwaniki *et al.*, 2016).

The study also focuses on optimization of market waste anaerobic digestion as a mean of utilizing persistent market waste to propose better use of organic waste in various markets to solve the problems of energy shortage and waste disposal in Kenya. Mobile digesters designed and constructed using readily available material will also be done. The design is aimed at incorporating temperature and agitation mechanisms, which have contributed mainly to digesters' failure over the years. Isolation, identification and culturing of microbes from rumen fluid are necessary because pre-treated and homogenized vegetable wastes can be digested by introducing the cultured bacteria to the substrate anaerobically. This is important since most urban dwellers do not have cattle though they have vegetable wastes in bulk. Therefore, this work was focused on isolation, identification of methanogens applicable to degradation of market wastes at optimized conditions for maximum biogas production. AD process is susceptible to changes in pH, temperature, C: N ratio, heavy metals and pesticide residues and therefore, it is vital to study how they affect anaerobic biogas production. As a microbiological process, biogas recovery is influenced by these variables and feedstock's chemical and physical properties. The microbial fuel cell will be developed to understand how best the produced methane can be put to other uses. Is it possible for every home to recycle its domestic wastes, particularly concerning energy generation for lighting houses and cooking purposes?

CHAPTER 2:

2.1 LITERATURE REVIEW

This section describes documented research works on biogas production from organic wastes and MFC related to this work.

2.2 Food wastage

Food losses are reported during production, processing, distribution, retailing and consumption and are estimated to be around 1.3 billion tonnes (Banks *et al.*, 2018). The two types of food wastes are: avoidable and inevitable. The inevitable portion primarily compose of an edible fraction of food, e.g. peels. Food wastage has necessitated for food waste hierarchies shown in figure 2.1 (based on JRC, 2017) with prevention being the primary option. The hierarchy proposes wastage of only unsuitable food material (Banks *et al.*, 2018).

The best option to consider in food waste management is conversion to energy via AD or bio-refineries. The European Parliament to the Commission and the Member countries recommend that the definition of food loss and waste include both edible and inedible food material. Food waste refers to edible or inedible food that has been removed from the production or supply chain to be disposed, from main production, processing, manufacturing, transportation, storage, retail to customer levels, except for immediate use (EU Parliament, 2017).

An estimated 36-56% of fruits supplied in the world is wasted during post-harvest and during consumption because they do not meet the set quality standards. Fruit wastage in developing countries emanate primarily from after-harvest and transportation because of the perishable nature of fruits (Gustavsson *et al.*, 2011). Fruits wastage during processing results in solid (peel, seed, and stones) and liquid (juice and wastewater) wastes.

FOOD SUPPLY CHAIN

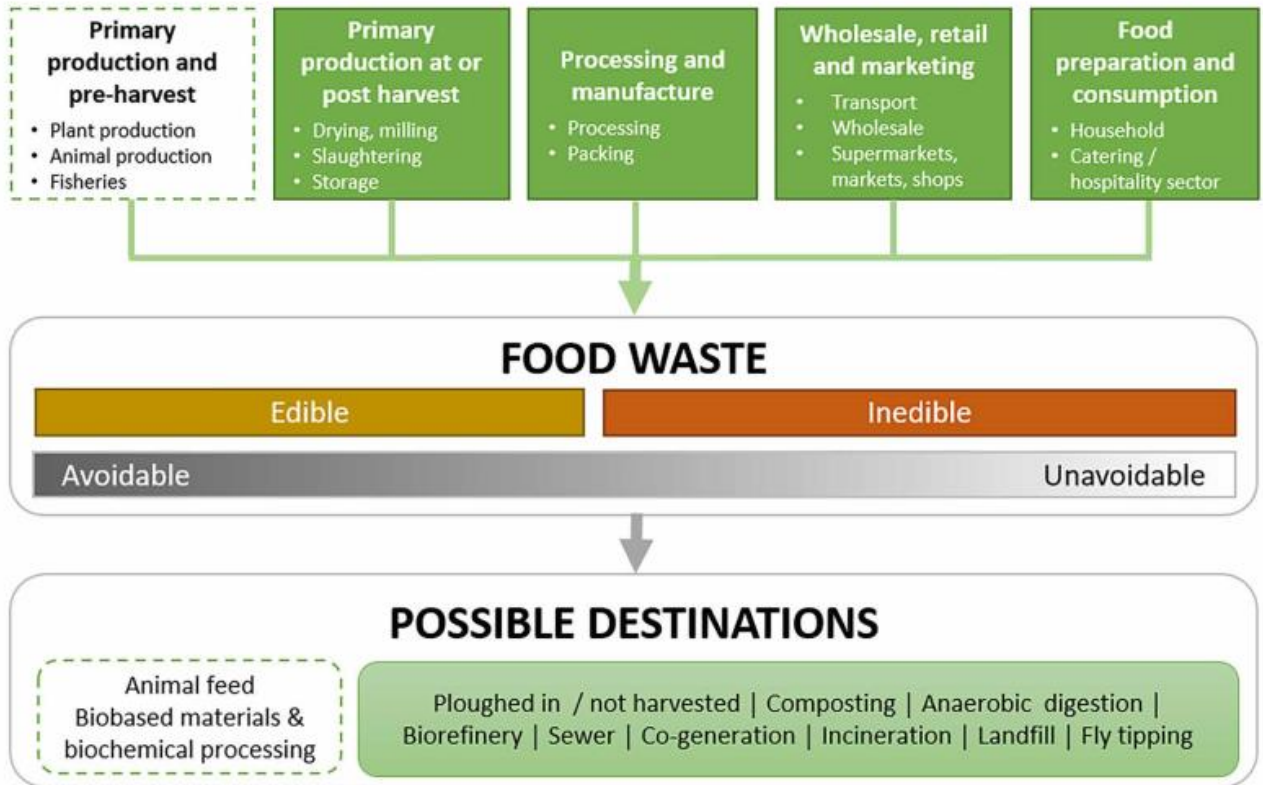


Figure 2.1: Food supply and wastage hierarchy

2.2.1 Energy Potential of Food Waste Digestion

The theoretical and experimental methane recovery capacity of waste can be determined from the biochemical and elemental compositions of a sample. This is discussed exhaustively in the IEA Bioenergy Report (Weinrich *et al.*, 2018). The Biochemical Methane Potential (BMP) and biogas content of waste can be predicted from the proximate property's analysis. Cellulose and hemicellulose are complex carbohydrates which are convertible to biogas, but lignin digestibility is unachievable in AD process. The BMP of an organic matter can be obtained from its elemental composition, assuming total degradability (Symons and Buswell, 1933). The BMP values show the maximum methane, which can be recovered from a sample (Angelidaki and Sanders, 2004). The experimental and theoretical BMP value of food is close due to high degradability. Table 2.1 (adapted from Angelidaki and Sanders, 2004) shows the methane yields which is recoverable from various proximate properties of food waste.

Table 2.1: Typical methane yields for biochemical components

Substrate	Typical composition	Methane yield ^a [L CH ₄ g ⁻¹ VS]	CH ₄ [% Vol]
Simple sugars – e.g. glucose	C ₆ H ₁₂ O ₆	0.373	50
Carbohydrate – complex	C ₆ H ₁₀ O ₅	0.415	50
Protein	C ₅ H ₇ NO ₂	0.495	50
Lipid	C ₅₇ H ₁₀₄ O ₆	1.013	70
Cellulose	C ₆ H ₁₀ O ₅	0.415 ^b	50
Hemicellulose	Variable	0.424 ^c	50

2.3 Anaerobic Digestion

Anaerobic digestion (AD) is a microbial process whereby microbes digest multiplexes degradable matters in the absence of atmospheric oxygen. This process is familiar to ruminant animals and natural systems like marine water sediments. Co-digestion is also very common in AD, which is degradation of multiple substrates (Al Seadi and Nielsen, 2004).

2.3.1 Substrates in Anaerobic Digestion

The availability of anaerobic microbes, high water content, its low cost and availability make animal waste and effluent highly usable for AD process (Olah *et al.*, 2006). Water in the sludge act as a solvent that facilitates the proper flow of substrate in the digester and thorough mixing. Usage of dedicated energy crops (DEC) in biogas generation, together with animal waste, has increased in popularity. DEC used in AD must be easily digestible, e.g., pre-mature maize, fodder and other grassy crops. De-lignification is vital to increase the digestibility of woody crops before loading to the AD reactor. Substrates for AD are classified in terms of origin, dry matter content, methane production potential, pre-treatment, etc. (Abotzoglou *et al.*, 2009). Anaerobic degradation of market organic waste for renewable energy has interested many scientists in the recent past (Kamm *et al.*, 2006). The main component of household and market waste is biodegradable organic matter. For example, according to Voelegi *et al.*, (2009) in Dar es Salaam, 67% of the total solid waste was AD degradable matter.

Inappropriate disposal of market waste in market places and street paths pollute the environment by making a breeding environment for vectors and rodents. Besides, poor waste management contaminates surface and groundwater (Gerardi, 2003). Organic waste from various sources can effectively be treated by anaerobic digestion process as compared to composting. This has the advantage of generating biogas before the trash can be used for agricultural purposes. For example, biogas digesters that digest organic market wastes have been implemented in India (FAO, 2011).

2.3.2 Methane Potential of Various Substrates

The total methane potential for various substrates is shown in figure 2.2 (Norma McDonald, 2007). From the model, it is evident that residual fats and rapeseed cake have the highest methane potentials, while cattle manure has the least.

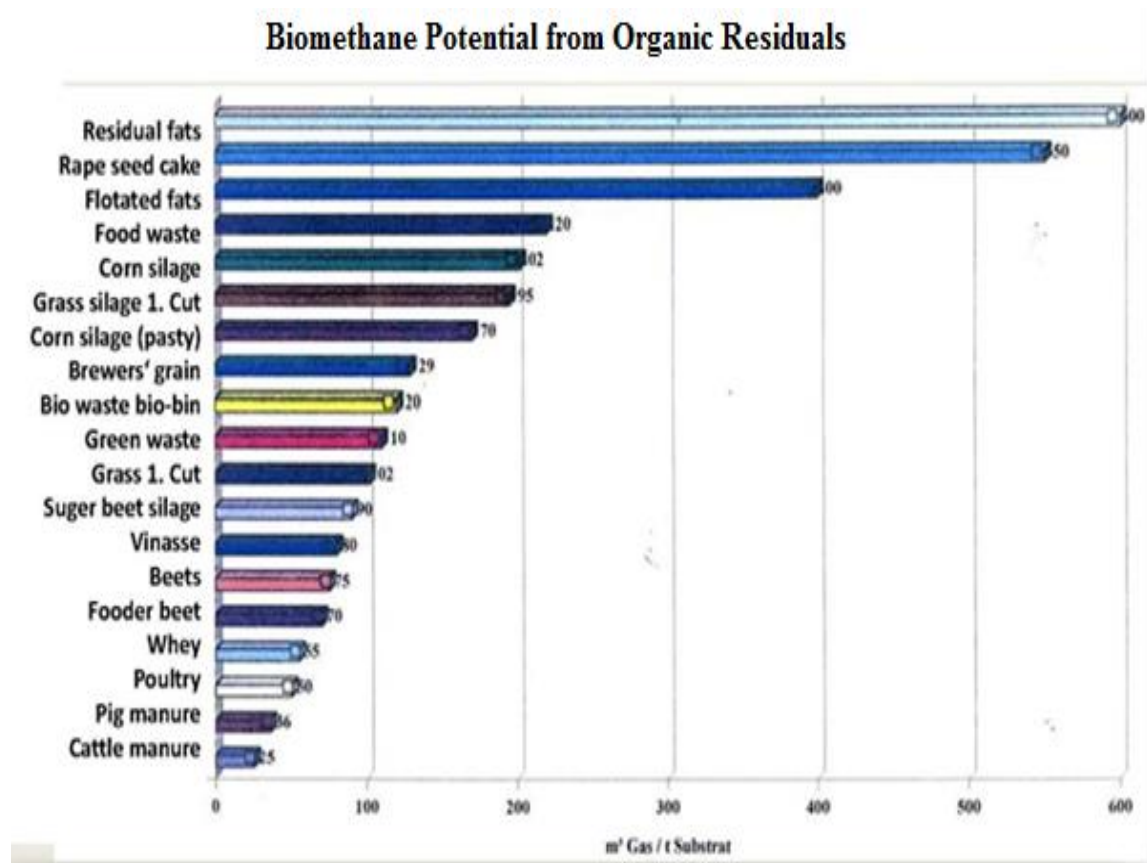


Figure 2.2: Methane yield for various feedstocks

2.4 Biochemical Anaerobic Digestion Process

Methane (60%) and carbon (IV) dioxide are the main components of biogas while the digestate consists of the decomposed substrate. The gas produced during AD is primarily in the form of methane. The process takes place in four steps in which microorganisms break down the substrate into small pieces. These steps are hydrolysis, acidogenesis, acetogenesis and methanogenesis. In figure 2.3 the AD process flow is shown (Teodorita, 2008). The processes take place simultaneously in an AD digester (Olah *et al.*, 2006; Kamm *et al.*, 2006 and Al Seadi and Nielsen, 2004).

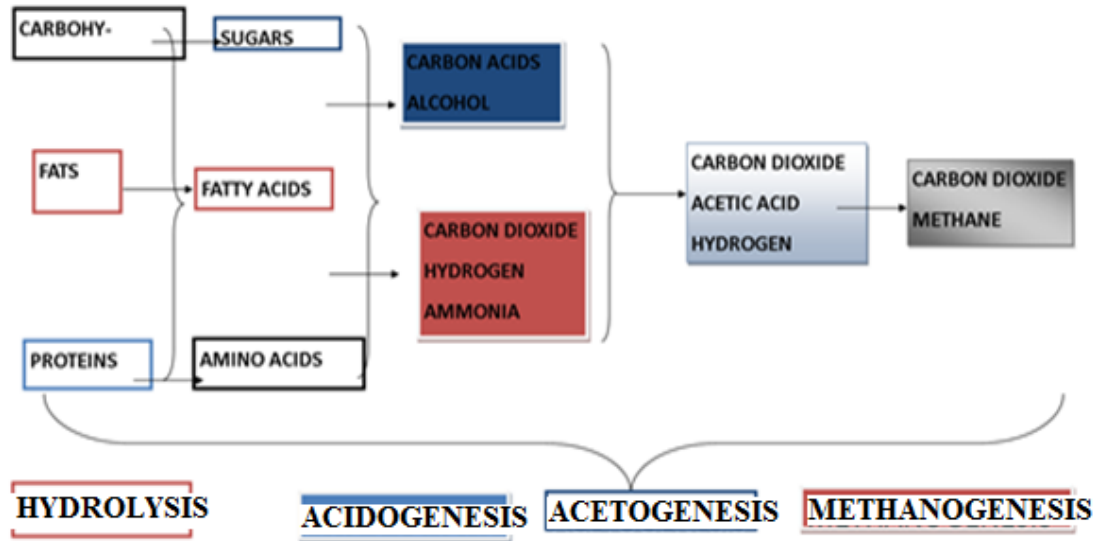
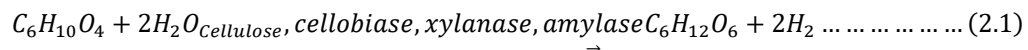


Figure 2.3: Schematic flow diagram of the AD process

The rate of substrate decomposition to produce biogas is dictated by the slowest of the four significant steps, e.g. in the digestion of cellulose, lignin and hemicellulose; hydrolysis is the rate-determining step (Teodorita, 2008).

2.4.1 Hydrolysis

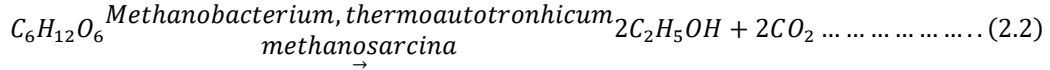
This is the first step whereby complex organic molecules are degraded to smaller units, as indicated in figure 2.3 above.



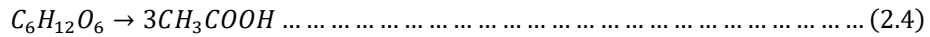
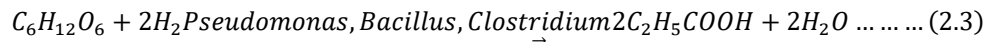
Hydrolytic enzymes further process the by-products (bi-polymers) to simple soluble compounds (Ostrem, 2004).

2.4.2 Acidogenesis

Methanogenic microbes process simple sugars, amino acids and fatty acids to acetate, CO₂, H₂, VFA and alcohols (Bilitewski *et al.*, 1997).

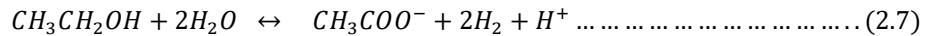
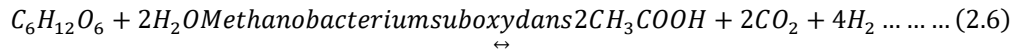
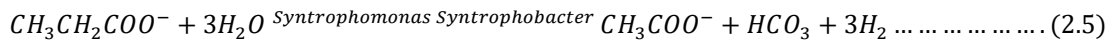


In equation 2.2, the products of hydrolysis are converted to carbon dioxide and alcohols by acidogenic bacteria. Further, the ethanoic acid is formed which proceeds to acetogenesis phase (equation 2.3 and 2.4).



2.4.3 Acetogenesis

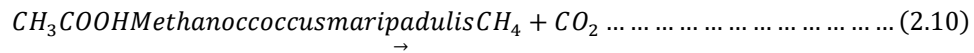
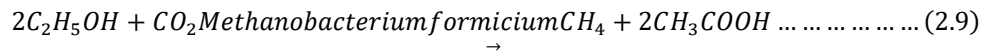
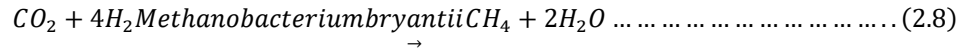
The acidogenesis products are further transformed to CH₃COO⁻, CO₂ and H₂ by methanogens.



Production of hydrogen is essential as it increases the partial pressure of hydrogen (Ostrem, 2004; Lopes *et al.*, 2004). Acetogenesis and methanogenesis are symbiotic processes that run simultaneously.

2.4.4 Methanogenesis

In this process, CH₄ and CO₂ are produced by methanogenic bacteria, e.g., *Methanobacterium bryantii*, *Thermoautotronhicum* and *Methanosarcina*. Methane is derived from acetate and reaction of CO₂ and H₂.



Methanogenesis is the rate-determining step. This is a very critical process influenced by the operation conditions (FAO, 2011; Al Seadi and Nielsen 2004; Keenan *et al.*, 1993; Verma, 2002).

2.5 Methanogenic Bacteria

AD processes involve the decay of organic substrates resulting in formation of methane, CO₂, and other gases as well as bio-slurry (Lopes *et al.*, 2004). The process is driven by a series of bacteria that degrade and return organic matter to the environment as the reaction yields renewable energy (Kossman, 2000). Bacteria multiply at a very high rate, and the growth rate is affected by pH, temperature, among other factors. Figure 2.4 (Gerardi, 2003) below summarizes the microbes responsible for methane production in an AD process

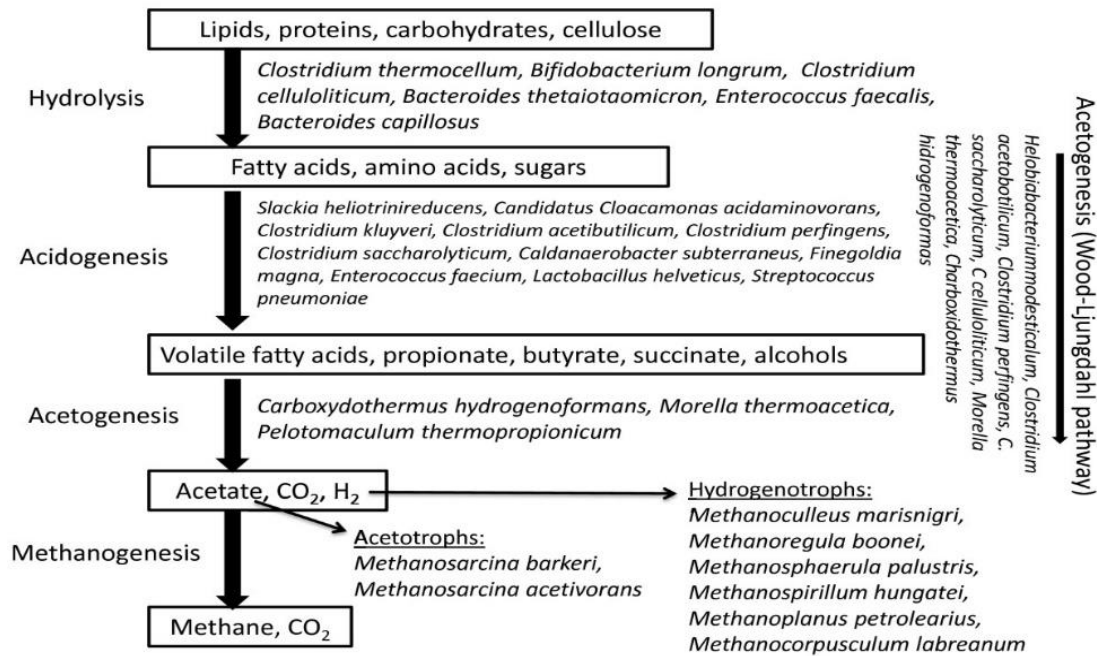


Figure 2.4: Anaerobic digestion microbes.

2.5.1 Bacteria Extraction, Isolation, Identification and Culturing

Methanogenic microbes degrade organic wastes in the rumen to give methane as a by-product. A cow's rumen can be visualized as a compartmentalized bioreactor that contains bacteria, archaea, protozoa, fungi and phage (Frey *et al.*, 2009). These organisms degrade ingested organic matter into fermentation products like hydrogen, acetate, propionate and butyrate. Methanogens are responsible for the fermentation process by continuous removal of hydrogen during carbon dioxide reduction to methane (Janssen, 2010). Cow dung is made up of 80% water and undigested plant matter, which is not only rich in nutrients but also micro-organisms. A recent study by Bharti shows that the lower part of the gut contains *Lactobacillus*, *Acidophilus*, *B. Sutilis*, *Enterococcus Diacetylactis*, *Bifido* bacterium and yeast (Bharti *et al.*, 2015). Methanogenic bacteria isolation and culturing from cow dung has been described by Hungate (1950). This method explains how to grow bacteria in anaerobic conditions. The technique was modified by Bryant and Robinson (1968) and was improved by Holdenman and Moore (1972). The method involves the preparation and inoculation of the media in an oxygen-free environment. This is done by sealing the set up with a butyl rubber stopper after placing the petri dish plates with the spread nutrient agar in the compartment. This method has the demerit of allowing oxygen into the system. Bacteria are cultured in a media described by Bryant *et al.*, (1968). The media e.g. nutrient agar allows the growth of all the bacteria present. In contrast, selective media like thiosulfate citrate bile agar for vibrios and glutamate starch phenol agar for *Aeromonads* and *Pseudomonads* allow the growth of specific genera.

2.6 Biogas Upgrading

Biogas upgrading involves the separation of minor impurities like water, hydrogen sulphide and carbon dioxide. Methods primarily used for CO₂ separation are practical, not only in removing it but also in eliminating other minor compounds. The amount of CO₂ and H₂S removed can be reduced from the produced biogas via adsorption and absorption

processes using readily available material like worn-out tires, activated charcoal, etc. (Al Seadia *et al.*, 2004).

2.7 Co-Digestion

This is a method for increasing CH₄ formation from low-yielding or hard to digest feedstock. It is applied to rectify various factors affecting the AD process, like carbon-nitrogen content and substantial retention time. It involves the mixing of a substrate having superior C: N with that of a low rate to obtain a compromising median value that favors the process of AD (Gerardi, 2003; Cook, 1986; Vesilind, 1998). By so doing, the process of AD can be optimized hence yielding a higher volume of biogas.

2.8 Macro and Micro-Nutrients and Toxic Compounds

Survival and growth of microorganisms in anaerobic digestion are highly dependent on micro-nutrients like iron, nickel, cobalt, molybdenum, tungsten, etc. and macronutrients like C, N, P and S. Anaerobic digestion is inhibited by an insufficient supply of nutrients and trace elements in addition to highly digestible substrates. Toxic materials like mercury and pesticides, which are added to the reactor during the input of feedstock into the AD process, inhibit microbial activities leading to digester failure (Al Seadi and Nielsen, 2004; Keenan *et al.*, 1993; Cook, 1986).

2.9 Continuous and Batch-Type Digesters

A batch reactor is widely employed for feedstock with high total solid content. In this context, the digester is loaded and the reactor sealed completely for the AD process till digestion is complete. Eventually, the content of the reactor is removed and used as fertilizer. Among the merits of a batch mode of digestion include ease in operation, no mixing and that contaminants are removed efficiently (Cook, 1986). In a continuous stirred tank reactor, the digester is continuously and mechanically fed with the slurry, with biogas production having minimal or no interruption. This is the most common AD digestion digester type.

2.10 Digestate Resource Recovery Options

Technological advancement has improved digestate resource recovery options. Bio-solids and digestate have agricultural applications to utilize nutrients and micronutrients in improving soil structure and fertility. Beyond agricultural use, the need for renewable fuel sources, reduction of greenhouse gasses and reducing transportation cost to the suitable application sites have led to the evolution of new digestate recovery options. Use of digestate for agricultural activities like the application as fertilizer has the following disadvantages: high nitrogen content leading to ammonia and nitrate pollution, high dilution requirements and need for supplementary nutrient addition to create a balanced fertilizing need.

2.11 Biogas Calculations

In biogas production, there are essential calculations involved. These calculations are briefly discussed in brief below:

2.11.1 Domestic Gas Demand

This is defined as the daily gas consumption for domestic usage. In determining domestic gas demand, previous consumptions are essential. e.g. the energy derived from 1kg of firewood is equivalent upto 200 liters of biogas while 1 kg of cow dung can produce to 100 liters of biogas (Adiotomre and Ukrakpor, 2015).

2.11.2 Size and Site for Biogas Digesters

The daily feed, retention time and digester volume are the primary consideration in determining the reactor size and location. The dependency of biogas plant size on daily feedstock and hydraulic retention time cannot be ignored. The substrate available dictates the design and the size of the reactor, which in turn reflects the capacity of biogas produced daily. For example, one cow produces an average of 10 kg of dung daily. In most households in Kenya, there are three cows. This means an average of 30 kg of manure daily. 1 kg can produce up to 0.1 m³ of biogas. This means that 30kg of manure produces 1.2 m³ of biogas (Alemayehu and Abile, 2014).

2.11.3 Size of the Digester

The amount of slurry available daily and the duration of retention time dictates the capacity of the reactor. In a given case, biogas digester consists of feedstock and water. This means that the digester volume is calculated by multiplying the daily feed by retention time (Alemayehu and Abile, 2014). This can be represented mathematically as

$$V_d = S_d * R_T \dots \dots \dots (2.11)$$

Where V_d is digester volume, S_d is the daily substrate input and R_T equals to the retention time. R_T is highly dependent on the temperature at which the digester is set. Typically, 40 days is the average retention time. The daily substrate loading is highly influenced by the water added in the reactor to attain a solid level of 4-8%. This can be represented as follows;

$$S_d = B + W_d \dots \dots \dots (2.12)$$

Where B is the feedstock and W_d is water added daily

Ratios of 1:3, 1:2, and 1:1 biomass to water (weight by weight) have been used widely in agricultural biogas plants (Hobson *et al.*, 1981).

2.11.4 Daily Gas Production

The gas produced daily in a given biogas production system can be calculated based on daily substrate input (S_d) and volatile solids (VS) content (Wall and Schneeberger, 2008).

$$G = VSxG_y \dots \dots \dots (2.13)$$

Where G is gas produced daily. Based on the wet sample weight (B)

$$G = B * G_y(\text{moist mass}) \dots \dots \dots (2.14)$$

Introducing the standard gas-yield values per livestock unit (LSU) we can use equation 2.15 to calculate the gas produced daily;

$$G = \text{number of LSU} * G_y \dots \dots \dots (2.15)$$

Where B is biomass weight and G_y is the volume of gas produced per wet biomass and LSU is livestock unit.

2.11.5 Specific Gas Production

Daily gas generation rate, G_p , subject to digester volume is calculated as follows;

$$G_p = \frac{G}{V_d} \dots \dots \dots (2.16)$$

Where G_p is the volume of gas generated daily and V_d is the daily digester volume

2.11.6 Loading Rate

The digester feeding rate L_{dT} is given by:

$$L_{dT} = \frac{TS}{\frac{d}{V_d}} \dots \dots \dots (2.17)$$

And in terms of volatile solids, the loading rate is given by equation 2.18

$$L_{dV} = \frac{VS}{\frac{d}{V_d}} \dots \dots \dots (2.18)$$

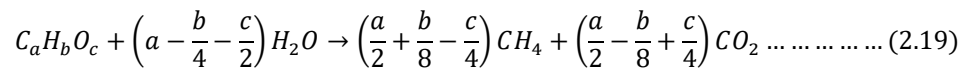
Where L_{dT} is daily loading, VS is volatile solids; TS is total solids, V_d is the volume of the digester per day, VS is volatile solids, d is the number of days and L_{dV} is digester loading volume.

2.12 Models for Calculating Biogas Production

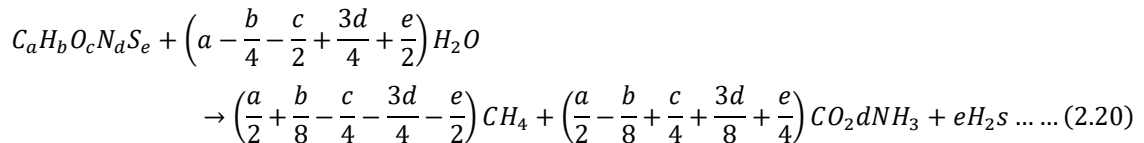
Biogas production models can be classified as dynamic or static based on the retention time factor. Anaerobic digestion models can also be classified as 0-, 1-, 2- or 3-dimensional concerning space dependency and finally, a model can be theoretical or experimental (Angelidaki *et al.*, 1999). In any given anaerobic digestion of wastes, an experimental simulation can be designed based on correlation between operating

variables. The predictions from any developed designs are validated against with real data (Sanders *et al.*, 2003).

The simplest way to predict biogas production from a sample of organic matter is by employing models which are based on the organic content of a substrate. The overall yield is carbon dioxide, and methane produced predictions. Buswell and Mueller (1952) indicate that if the elemental composition of the feedstock is known, the amount of CO₂ and CH₄ yield is given by equation 2.19, which does not include organic matter used for bacteria metabolism.



In 1976, Boyle did a modification of Buswell and Mueller equation to incorporate the amount of ammonia and hydrogen sulphide compositions in biogas. The modification is shown in equation 2.20. a, b, c, d, and e represents the mole ratios of the respective elements.



Baserga (1998) classified the degradable matter of substrates into carbohydrates, proteins and fat and predicted the amount of biogas produced for these components when not co-digested. He indicated that the co-substrates are added to the animal waste to enhance gas production. In 2003, Keymer and Schilcher improved Baserga's model by upgrading the rate of organic matter breakdown based on the nutrient content of a given substrate.

Amon *et al.* (2007) boosted the Keymer and Schilcher (2003) model by classifying the organic matter into four essential components, that is crude protein, fat, natural fiber and NFE.

Anaerobic Digestion Model No. 1 (ADM1) is another model from the International Water Association Task Force in 1998. This model incorporates the biochemical processes, including hydrolysis, acidogenesis, acetogenesis and methanogenesis and

Physico-chemical processes like liquid-gas transfer and liquid-liquid processes (Batstone *et al.*, 2002). The model received criticism from Kleerebezem & Loosdrecht (2006) indicating that the model is inaccurate in the stoichiometry, retention time-based issues as well as lack of clear thermodynamic boundaries mostly when ΔG -values greater were than 0.

2.12.1 Artificial Neural Network

Artificial Neural Network (ANN) models were developed by Abu Qdais *et al.*, (2010). The model aimed at optimizing temperature, total solids, total volatile solids and pH with the main output as methane. The model showed a good relationship between model data and the actual data gathered from an existing biogas reactor (Abu Qdais *et al.*, 2010). ANN model was developed by Kanat and Saral (2008), which studies biogas generation in a thermophilic digester. The inputs investigated were loading rate, total volatile fatty acids of the effluent with biogas as the main digester output.

2.12.2 The theoretical methane potential

In estimating a feedstock's capacity to generate methane, the theoretical CH₄ potential is commonly employed. The units are milliliters of CH₄ /VS or COD at STP. However, it can also be expressed in terms of the volume of organic material extracted. The chosen CH₄ potential units are primarily mL CH₄g⁻¹VS added. This parameter can be calculated in a variety of ways:

(i) Based on the atomic (AtC) or organic fraction compositions (OFC), the BMP_{Th} has been measured (Angelidaki and Sanders, 2004)

• **BMP_{ThAtC} or B_{o-ThAtC}**. Experimental elemental analysis determination may be used to construct empirical formulae (C_aH_bO_cN_dS_e). The CH₄ generated can be determined by Buswell's equation and the complete stoichiometric reaction of degradable matter to CH₄ and CO₂ (Buswell and Mueller, 1952).

$$B_{(O-ThAtC)} = \frac{\left(\left(\frac{a}{2} \right) + \left(\frac{b}{8} \right) - \left(\frac{c}{4} \right) \right) * 22400}{12a + b + 16c} \dots \dots \dots (2.21)$$

When proteins are present, however, NH₃ and H₂S are generated, which must be factored into Boyle's equation (Boyle, 1976).

$$B_{(O-ThAtc)} = \frac{22400 * \left(\frac{a}{2} + \frac{b}{8} - \frac{c}{4} - \frac{3d}{8} - \frac{e}{4}\right)}{12a + b + 16c + 14d + 32e} \dots \dots \dots (2.22)$$

BMP_{ThOFC} or B_{o-ThOFC}: If the proximate matter is known, the CH₄ yield can be calculated using equation 2.23.

$$BMP_{CHNO(OFC)} = 415 * \%carbohydrates + 496 * \%proteins + 1014 * \%lipids \dots \dots \dots (2.23)$$

The coefficients in this equation are derived from the stoichiometric conversion of model compounds representing average formulae for carbohydrates (C₆H₁₀O₅), proteins (C₅H₇O₂N), and lipids (C₅₇H₁₀₄O₆). These properties are pre-determined using analytical procedures (Angelidaki and Sanders, 2004). Amon *et al.*, (2007); Gunaseelan, (2007) and Schievano *et al.*, (2008) have proposed complex multi-regression models to predict biogas yields based on chemical composition of a substrate.

(ii) The COD method.

In theory, 0.350 L of CH₄ at STP or 0.395 L at 35°C and 1atm can be obtained from 1 g COD removed (COD_{rem}).

• **BMP_{ThCOD} or B_{o-ThCOD}**. Direct determination of COD oftently results in inaccurate results (Raposo *et al.*, 2009, Raposo *et al.*, 2019).

Moreover, COD is necessary for real reactor design, helping to normalize the results independently of VS fraction composition (Batstone *et al.*, 2002). Based on the COD, equation 2.24 is employed.

$$B_{o-ThCOD} = VS_{added} \cdot \left(g \frac{COD}{g} VS\right) \cdot 350 \dots \dots \dots (2.24)$$

The Th_{OD} based on elemental matter is a simple method for determining the substrate methane capacity. The following equation, defined in VDI 4630 method in 2006, is employed in measurement of organic content of substrate using the empirical formula.

$$Th_{oD}(gO_2 \cdot g^{-1}VS) = \frac{16 \left((2a) + \left(\frac{b}{2}\right) - c - \left(\frac{3d}{2}\right) \right)}{12a + b + 16c + 14d} \dots \dots \dots (2.25)$$

The ThOD is calculated as per equation 2.26:

$$B_{(0-ThOD)} = VS_{added} \cdot \left(g \frac{ThOD}{g} VS \right) \cdot 350 \dots \dots \dots (2.26)$$

2.13 Online Biogas Application

Anaerobic degradation of organic matter to renewable energy entails lab and pilot scale investigations and theoretical computation, and process simulation and modelling (Sasha *et al.*, 2018). Sasha *et al.* (2018) have developed biogas software tools that measure and predict methane production for a given substrate. Laboratory scale involves biochemical methane potential studies to predict maximum methane production from a substrate. The relationship between BMP and experimental data employs modelling and simulation calculations (Owen *et al.*, 1976). Proximate composition of vegetable and fruit wastes can be used to predict methane production (Rittmann and McCarty, 2001).

Sasha *et al.* (2018) describe a model made in the R programming environment used for the prediction of methane production potential using biogas package (Hafner *et al.*, 2015, R Core Team., 2017). Methane production can be predicted based on three primary substrates characteristics, namely; chemical oxygen demand, empirical (chemical) formula and macromolecular composition.

2.14 Digester Design System

Ononogbo *et al.*, 2016 observed that fixed dome, plastic and floating drum to be the most preferred reactor designs. ARTI – appropriate rural technology of India, Pune (2003) has established a compact biogas plant that supplies biogas for cooking using waste food rather than cow dung as a feedstock. The plant is close enough for urban households to use it, and about 2000 units are currently in use in Maharashtra, both in urban and rural areas. Karve built a compact biogas system in 2003 that uses starchy or sugary feedstock and was 800 times more efficient than other reactors (Karve, 2007 and Shalini, 2000). Lack of consideration of a mechanism for the mixing of organic slurry during construction and insufficient knowledge of the importance of some process parameters

during the operation of biodigesters leads to their malfunctioning and causes them to be economically unfeasible (Ononogbo *et al.*, 2016).

The criteria considered in the design of the digester included airtightness of the system, mesophilic and thermophilic temperature, nature and type of substrate used, substrate retention period, several cranks turn per minute, and volumetric capacity of the digestion tank (Adesoji *et al.*, 2014). Sunil *et al.* (2013) fabricated a smart biogas digester by incorporating a micro-controller, an SMS module, LCD and an MPX4115 pressure sensor. The digester operations were controlled using software implementation, which included; Microcontroller Programming with Embedded C, Proteus Simulator and PIC Kit 2 Programmer (Sunil *et al.*, 2013).

2.15 Arduino

Arduino is a basic hardware and software electronics platform that is free and open-source. Arduino boards can read inputs and convert them to outputs like turning on an LED, starting a motor, or publishing something to the internet. The *Arduino* programming language (based on Wiring) and the Arduino Software (IDE) (based on Processing) are used to achieve microcontroller functionality. *Arduino* is made up of two parts: a physical programmable circuit board (microcontroller) and software (IDE) that runs on a device and is used to write and upload computer code to the physical board. *Arduino* is an open source programmable circuit board that can be used in a range of makerspace projects, both simple and complex. This board has a microcontroller that can be programmed to detect and manipulate real-world objects. By responding to sensors and inputs, the Arduino can interact with a broad range of outputs, including LEDs, motors, and displays (Maker Space, 2020).

2.15.1 Arduino Desktop IDE

Arduino codes are written and uploaded using an open source which is available for Windows, Linux 32-bit and 64-bit, ARM, ARM64, and Mac OS X platforms. The *Arduino* IDE is a software that allows users to design *Arduino* projects. The *Arduino* IDE's main features are as follows:

- Create a sketch / script
- Download and include external libraries for some devices like sensors
- Flash a microcontroller board and handle errors
- Analyze the running script via the serial plotter and serial monitor

All boards which are compatible to Arduino can use the IDE in the same way. Figure 2.5 illustrate the main parts of the Arduino IDE.

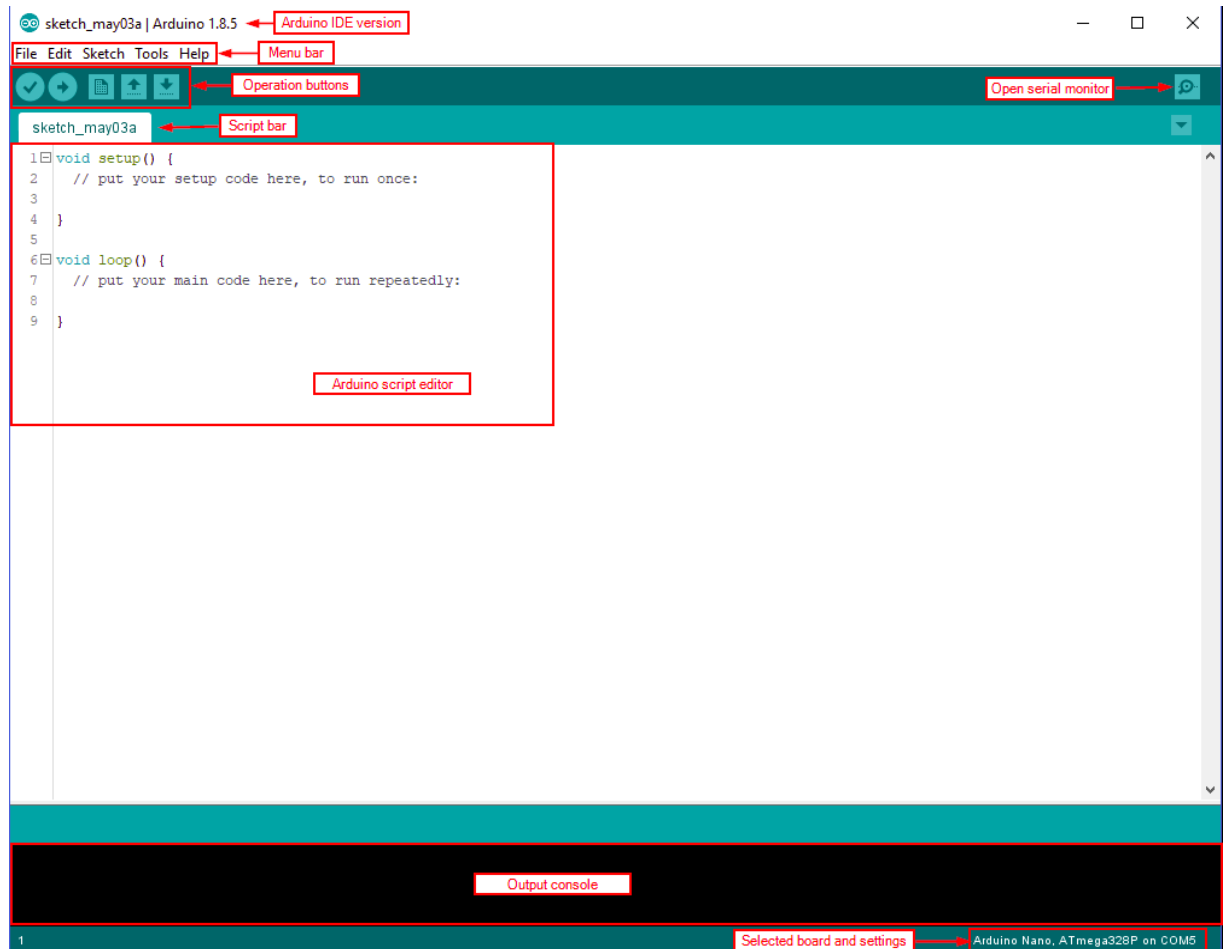


Figure 2.5: A screenshot of distinct parts of the Arduino IDE

The parts are described as follows;

- Arduino IDE version: shows the current version of the Arduino Desktop IDE.
- Menu bar: The menu bar is the main place controlling the IDE.
- Operation buttons:
 - Verify: Check if written code has right syntax

- Upload: Uploads the script to the microcontroller. Code verification is done before uploading the script.
- New: Opens a new script.
- Open: Open a window to select a script from working directory and open the selected script.
- Save: Saves the actual script in the selected folder in working directory.
- Open serial monitor: Opens the serial monitor to view the script output. Use “Serial.print(“This is the serial output”);” to print one line as output.
- Script bar: In the script bar you find all your current selected scripts. Therefore, it is easy to switch between different scripts and you do not have to open an extra Arduino IDE for every script.
- Arduino script editor: The program is written in the script editor. The programming language is a mix between C and C++. The editor highlights code in different colors which make the code faster to read. There have to be two functions in every script as shown in figure 2.6 (Arduino Programming Course, 2017).

The screenshot shows the Arduino IDE interface. The title bar reads "sketch_dec27b | Arduino 1.8.1". The menu bar includes "File", "Edit", "Sketch", "Tools", and "Help". Below the menu bar is a toolbar with icons for file operations and a search icon. The main editor area shows a sketch named "sketch_dec27b" with the following code:

```

1 void setup() {
2   // put your setup code here, to run once:
3
4 }
5
6 void loop() {
7   // put your main code here, to run repeatedly:
8
9 }

```

The code is color-coded: keywords like "void", "setup()", and "loop()" are in blue, comments are in grey, and the rest is in black. The IDE has a dark theme with a teal header and footer. The footer text reads "Arduino Yun on /dev/ttyACM0".

Figure 2.6: A Screenshot showing the 2 parts of Arduino sketch

- void setup (): The setup function will run only once when the board is connected with a power supply.
- void loop (): The loop function run as an open ended loop for the microcontroller. If the end of the loop function is reached, the script will continue with the first line of the loop function.
- Output console: In the output console you find errors if the syntax checks failed or you see the progress uploading a script to the microcontroller board.
- Selected board and settings: In the bottom right side you see the selected board from the settings and the selected COM port, where the board is connected to the PC to upload a script.

2.15.2 Arduino Libraries

Libraries are C or C++ files (.c, cpp) that offer extra functionality to sketches. Installing Arduino libraries can be done in three different ways.;

2.15.2.1 Using the Library Manager

The Library Manager can be used to connect a new library to the *Arduino* IDE (available from IDE version 1.6.2). Open the IDE and pick "Sketch" from the menu bar, then Include Library > Manage Libraries from the drop-down menu. The Library Manager appears, showing a list of libraries that are either installed or ready to be installed. To find it, scroll through the list, click it, and then choose the library edition you want to install. Finally, press install and wait for the new library to be installed by the IDE. Depending on your link speed, downloading can take some time. When it's finished, a tag named Installed should appear next to the Bridge library (Limor, 2018).

2.15.2.2 Importing a .zip Library

A ZIP file or folder is widely used to distribute libraries. The library's name is written in the folder's name. A.cpp file, a .h file, and sometimes a keywords.txt file, examples folder, and other library-specific files can be contained within the folder. You can now install third-party libraries in the IDE, beginning with version 1.0.5. Go to Sketch >

Include Library > Add.ZIP Library in the Arduino IDE to get started. Select "Add.ZIP Library" from the drop-down menu at the top. To get back to the Sketch > Include Library menu, select it from the drop-down menu. At the bottom of the drop-down menu, you can now find the library. It's all set to go in your drawing. In your Arduino sketches directory, the zip file would have been expanded into a libraries folder (Limor, 2018).

2.15.2.3 Manual installation

Manually adding a library requires downloading it as a ZIP file, expanding it, and placing it in the appropriate directory. File > Preferences > Sketchbook location lets you locate or alter the location of your sketchbook folder. Navigate to the location where you saved the library's ZIP file. Pick the main folder, which should have the library name, after extracting the ZIP file and all its folder structure into a temporary folder. It should go in your sketchbook's "libraries" folder. Go to Sketch > Include Library from the *Arduino* Software (IDE). Check the list and see if the library you just added is there (Limor, 2018).

2.15.3 Arduino Sketch Structure

The Arduino programming language has a simple structure and is divided into at least two sections. Blocks of statements are enclosed by these two necessary functions.

```
void setup ()
{
statements;
}
void loop ()
{
statements;
}
```

Where setup () is the preparation, loop () is the execution. Both functions are required for the program to work. The setup function should follow the declaration of any variables at the very beginning of the program. It is the first function to run in the program, is run only once, and is used to set pinMode or initialize serial communication. The loop function follows next and includes the code to be executed continuously – reading inputs,

triggering outputs, etc. This function is the core of all *Arduino* programs and does the bulk of the work (*Arduino Programming Course*, 2017).

2.15.4 Arduino Motors

DC motors, servo motors, and stepper motors are the three types of motors used with *Arduino*. *Arduino* boards can power a variety of servo motors using servo motors. This library is capable of controlling a large number of servos. It makes good use of timers: with only one timer, the library can control 12 servos. The general servo sketch is as demonstrated by by BARRAGAN <http://barraganstudio.com> and modified 8 Nov 2013 by Scott Fitzgerald available at <http://www.arduino.cc/en/Tutorial/Sweep> (Fitzgerald, 2013).

2.15.5 Type-K Thermocouple MAX775

The MAX6675 compensates for cold junctions and digitizes a K-Type thermocouple signal. The data is output in a read-only format with a 12-bit resolution and SPITM compatibility. This converter has a temperature resolution of 0.25°C, a temperature ranges of 0°C to +700°C, and thermocouple precision of 8 LSBs for 0-1024°C temperature bracket. The thermocouple is low necessitating the use of an amplifier to collect and amplify the signals. The thermocouple amplifier is specifically built to operate with thermocouples in order to perform the amplification task (Fahad, 2020). The Type-K Thermocouple is shown in figure 2.7.



Figure 2.7: A K-type MAX775 thermocouple

The general sketch for running the thermocouple to measure the temperature is described by Ahmad (2018) and Fahad (2020).

2.15.6 pH sensor in Arduino

The DFRobot Gravity is an analog pH meter V2 specially designed to measure the pH of the solution and read the acidity or alkalinity. The pH Sensor Kit has Signal Conversion Board (Transmitter) V2 and also pH Probe connected to each other. Various parts of the probe are shown in figure 2.8 (Alam, 2020).

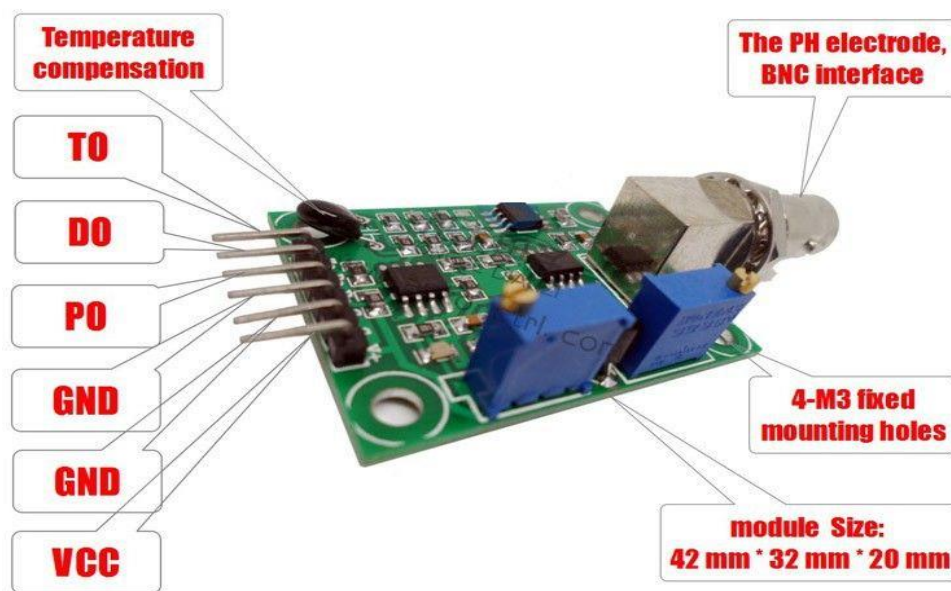


Figure 2.8: Various parts of the pH probe

2.15.7 SIM900 GSM GPRS Shield

The SIM900 is a full Quad-band GSM/GPRS device bundled as an SMT module that can be integrated into customer solutions. The SIM900 has an industry-standard interface and provides GSM/GPRS 850/900/1800/1900MHz audio, SMS, data, and fax output. SIM900 (figure 2.9) measures 24mm x 24mm x 3mm and therefore, can be incorporated in any portable devices (Last minute Engineers, (2020)).

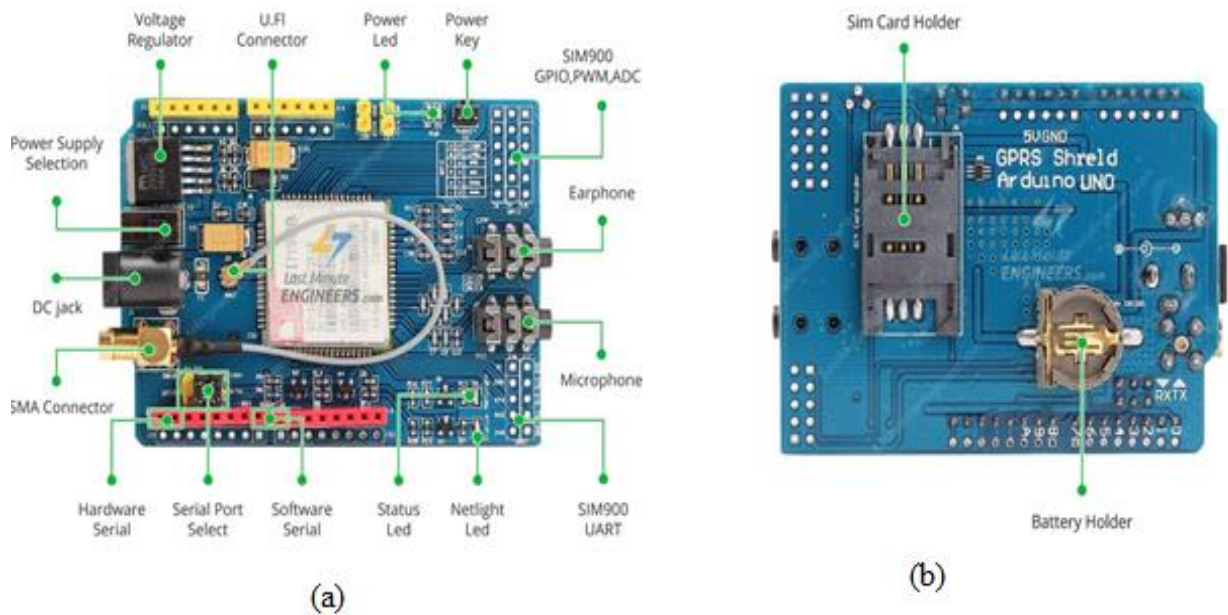


Figure 2.9: A SIM900 GSM/GPRS Shield (a) front side and (b) back side

The SIM900 consumes high power depending on the task with a maximum current of 2A. The *Arduino Code – Testing AT Commands* can be obtained from the Last Minute Engineers, (2020).

2.15.8 Gas detection in the environment

Gas detectors can be classified according to the operation mechanism (semiconductors, oxidation, catalytic, photo-ionization, infrared, etc.). Gas detectors come packaged into two main form factors: portable devices and fixed gas detectors (Rishabh *et al.*, 2018). The MQ2 sensor detects gas spillage at home and industry. It has very sensitive and fast in the qualification of H₂, CH₄, CO, Alcohol, Smoke, or Propane. A potentiometer may be used to adjust its detection levels. Among the best features of MQ2 are; a broad detection range, consistency and a quick and accurate response time.

Kumar *et al.* (2012) proposed a wireless sensor network which could show gas spillage location accurately. The plan was based on ZIGBEE and ARM7 and can sense gas leakage and forward the information of that location to the observer immediately. Anusha & Shaik (2012) in gas leakage study improved the work of Kumar *et al.*, (2012) by designing a system that could give leakage location in actual time.

Shital *et al.*, (2018), introduced a model device of an economical gas spillage sensor after investigating and documenting the merits and demerits of various sensors. They focused on LPG for residential, commercial and industrial usage. The device senses as gas leaks and gives a warning. The system's aim is to sense LPG gases e.g. flammable gases. Butane is permitted in the UK at a level of 600 ppm. The designed device ensures that the gas levels are constantly tracked. The system begins to issue early warning alarms at 100ms intervals if the gas level rises above the average threshold level of 400 ppm butane (LPG), indicating low-level gas leakage. The model initiates an audio alarms after every 50ms in case the levels exceed 575 ppm and a warning for the occupants to flee to safety (Shital *et al.*, 2018). Falohun *et al.*, (2016) suggested the application of a fan in automatic LPG detection and hazard control. Amsaveni *et al.*, (2015), suggested a system that could monitor and detect gas spillage and relay real-time data via real-time feed over the internet using Xively IoT platform (Amsaveni *et al.*, 2015). Further literature on the design and fabrication of gas leakage alarm systems can be found on Manichandana *et al.*, (2018).

2.15.8.1 MQ2 Gas Sensor

The MQ2 sensor (figure 2.10) has a Digital Pin which allows it to work without a microcontroller, which is useful when you only want to detect one gas.

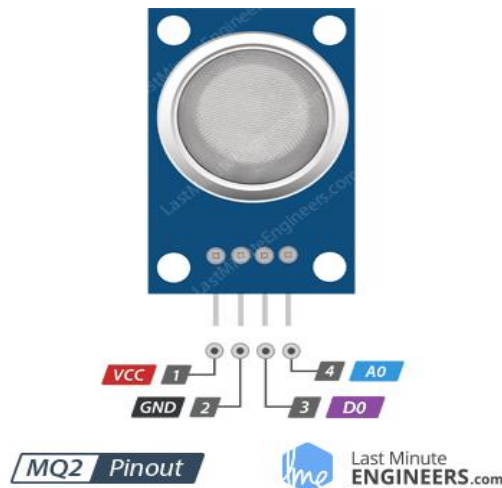


Figure 2.10: MQ2 gas sensor pins

2.15.8.2 Calibration of MQ2 module

The sensor is positioned near the smoke or gas to be sensed and adjusting the potentiometer till the Red LED begins to glow. The sensitivity is increased by turning the screw clockwise (figure 2.11), or decrease sensitivity by turning the screw anticlockwise.

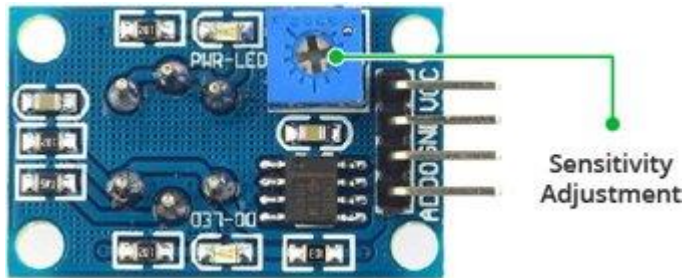


Figure 2.11: MQ2 gas sensor calibration

2.15.8.3 MQ-2 Sensor Gas Detection

A digital pin or an analog pin is used by the MQ sensor to detect gases. Simply supply 5V to the module, and you should see the power LED glow. The LED remains off when no gas leak is detected (0V). Pre-heating the sensor before use is highly recommended. In case of leakage, the digital pin will go high (5V), otherwise it will stay low (0V). Similar results are observable via the analog pin. A microcontroller is used to read the analog values (0-5V) which will be directly proportional to the gas concentration measured by the sensor. Riyaz (2019) and Mukherjee (2016) described the MQ2 gas and smoke detection Arduino code and therefore, one can randomly change the values to see how the sensor responds to various gas concentrations and change the software accordingly.

2.15.8.4 Biogas Monitoring using *Arduino*

Suruchi *et al.*, (2016) suggested that a biogas monitoring system for measuring volume using microcontroller & GSM to identify upcoming instabilities in anaerobic digesters before a crash happens. In a study using paper and mill effluents, treated in a upflow anaerobic sludge blanket reactor (UASB), an electronic system using Arduino platform

connected to a gas sensor was developed to measure and display the curve of daily methane production on processing (Ahmed *et al.*, 2017). The sensor sent the gas values in ppm to the Arduino board which transform the values to a plot on the computer display. In 2019, Sabran and Saharuddin design and manufacture of methane concentration gauges using Arduino and gas sensors as the main components. The measurement results are displayed on the LCD screen and picoscope measuring instrument. They reported highest concentration of methane gas in vegetable waste compared to other household wastes studied (Sabran and Saharuddin, 2019). Application of open source hardware devices are being introduced in different bio-energy projects due to their advantages of low cost, easy development and Internet sharing. Arduino-based microcontroller was employed in measurement system to perform biogas sensing (González and Calderon, 2018). They designed a device which monitors biogas concentration and the values are read in LCD or computer systems. However, they González and Calderon, 2018 suggested further works on integrating monitoring and supervisory system in order to enable real time visualization of the biogas composition and networking operation to provide cloud- enabled measurements storage.

Ahmed *et al.*, (2017) designed an integrated management system which offered an automatic monitoring thereby providing important supervision and planning functions that ensured continuous and efficient operation of the plant. The device displayed at any moment on the screen of a computer a curve showing the production of biogas (CH₄) as a time function. The program automatically warned the instructor of the methane production evolution by setting an alarm in case of an increase or deficit in produced quantity (Ahmed *et al.*, 2017). Methane content in biogas from an anaerobic digester was measured on-line by modifying an off-line measurement device that used a hydrocarbon sensor (MQ-4) and a pressure/temperature/humidity sensor (BME-280) integrated with an *Arduino* Uno. This modified on-line sensor was programmed to automatically measure methane composition by self-regulated introducing biogas sample and evacuating the device (Shunchang, 2020). In another study, an inexpensive, portable device to measure methane content in biogas samples was constructed. The central component of the device was an MQ-4 methane sensor (Shunchang *et al.*, 2019) This sensor, along with humidity,

temperature and pressure sensors, was enclosed in an airtight glass jar and interfaced with a programmable Arduino Uno clone for data logging and operation. The sensor was able to detect methane within the jar to as low as 400 ppm, but responded linearly to concentrations ranging from about 4000 to 110,000 ppm.

2.15.9 Flame Sensor

A flame detector shown in figure 2.12 (Arduino.cc, 2020) is a sensor that senses and responds to the presence of a flame or fire. Depending on the installation, sounding an alarm, deactivating a fuel line (such as a propane or natural gas line), and triggering a fire suppression system are all potential responses to a detected blaze.

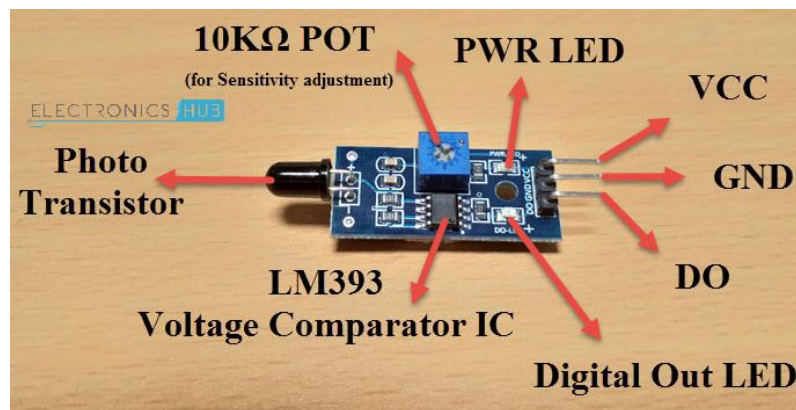


Figure 2.12: A flame sensor

Flame detection methods include ultraviolet detectors, near-IR array detectors, infrared (IR) detectors, infrared thermal cameras, and UV/IR detectors, among others. When a fire burns, it releases a small amount of infrared light, which is measured by the sensor module's Photodiode (IR receiver). An Op-Amp is used to note the voltage changes around the IR Receiver, so that if a fire is observed, the output pin (DO) will be 0V (LOW), and if there isn't, the output pin will be 5V (HIGH). Example of the flame detection can be obtained from similar code by Suryateja (2018), Fahad (2020) and Kumar (2018).

2.16 Microbial fuel cells

Electricigens refers to a class of microbes capable of oxidizing degradable matter using an electrode as the sole electron acceptor. The working principle of MFC is purely based on activities of these micro-organisms (Vilajeliu-Pons *et al.*, 2016). An MFC is made up of anodic and cathodic chamber linked by an ion-permeable membrane (Logan, 2006; Semenek and Franks, 2014). An electron is generated in the anodic chamber by oxidation of degradable material by electricigens. It travels via a conducting wire and meets the proton, combines with an acceptor to form a reduced product. Pure and mixed cultures have been utilized in MFCs. For example, *Escherichia coli*, *Shewanella*, *Enterococcus faecalis* (*E. faecalis*) etc. Li-ping and Song, 2016 noted that linking the electricigens to the electrode surface as the major setback in the application of MFCs in electricity generation.

2.17 Bio-slurry Application

During anaerobic digestion nutrients are transformed from organic states to dissolved states, making them more useful for plant uptake (Lansing *et al.*, 2010). The rate of bio-slurry application is 5 tons/ha in dry farming (SNV, 2011) to increase yield. Using more is sometimes suggested though not beyond 25 t/ha (Musisi, 2013). The bio-slurry can be applied to crops as a foliar fertilizer, in a liquid form (diluted), or in a dry, composted form. The liquid form can be applied directly to the crop by spraying or an irrigation canal. Besides, it can be used as a top dressing in which case it is diluted based on the digester type (SNV, 2011). Although the nitrogen levels are low, many farmers prefer the dried form because it is easier to transport. However, since the dried bio-slurry loses some of its nitrogen (particularly ammonium), the bio-nutrient slurry's value is reduced (Dahiya and Vasudevan, 1985; Singh *et al.*, 2007). Therefore, the dried form is the least efficient method of bio-slurry application. (SNV, 2011).

CHAPTER 3:

3.1 MATERIALS AND METHODS

The reagents, instrument, and procedure utilized to meet the study's goals are discussed.

3.2 Materials and Reagents

All the chemicals utilized were used as received without further purification. They were of general grade or analytical grade as specified in the procedures. They are categorized as follows: the biochemical analysis of cowdung, rumen fluid bacterial studies entailed use of blood agar and MacConkey nutrient agar. In proximate analysis a weighing balance (Kitchen balance – 10kg), Oven, thermometer, analytical grade HCl, H₂SO₄ were used. The following items were used in biogas production, 500 mL, 10 L, 20 L, 60L, 120L and 240 L bottles and plastic drums, polythene bags (2000mL), glass syringe (100mL), pH meter, thermometer, water bath, thermostatic heater, portable biogas analyzer (PG810), Analytical grade Sodium hydroxide and sulphuric acids were used to adjust the pH, N₂ and CO₂ were used to expel air in the digester and create the anaerobic condition. The instrument used were Agilent 6890N GC (equipped with an auto sample (Agilent 7683 Series Injector) and a micro-electron capture detector (μECD)), EDXRF. Digester design involved use of Flex pipe, plastic glue (100 mL), plastic tanks (500 mL – 3500 mL), elbow joints, knife, hacksaw, pliers, tubes, gate valve. The Ferrocement and the 14m³ were constructed using the following materials: cement, Dr. fixit waterproof, metal bars, binding wires, hoop iron, metallic plates, sand, ballast etc while in biogas upgrade experiments a fabricated digester, Zeolite rocks, steel wire, worn-out tyres, maize cobs and commercial desulphurizer (Lanneng -16 kPa) were used. The automation of the digester involved use of Arduino Uno Board, Takanawa 555 metal gear motors 12V-24V DC Reduction gear motor High torque Low noise, Towerflow MG995 and MG996 servo motors, a gravity analog pH sensor/meter pro kit for *Arduino* and K-Type thermocouple MAX6675. In microbial fuel cells a plastic container, wicks, agarose, sodium chloride, glucose, sugar, graphite rods, pHmeter, copper wire, thermometer, PVC pipes, market wastes were employed.

The following software was used in this study; Minitab 17, Origin 8, Microsoft excel 2013 and 2016, Matlab, R studio, R programming language, *Arduino* IDE.

3.3 Sampling Area

The rumen fluid used in this study was obtained from Dagoretti slaughterhouses ($1^{\circ}17'02.6''\text{S } 36^{\circ}41'02.2''\text{E}$) in Kiambu County, Kenya. The market wastes including vegetable and fruits wastes were obtained from Kangemi Market ($1^{\circ}15'52.9''\text{S } 36^{\circ}44'55.6''\text{E}$) and Wakulima Market ($1^{\circ}17'13.3''\text{S } 36^{\circ}49'56.2''\text{E}$) in Nairobi County, Kenya. A map of the sampling sites is shown in figure 3.1.

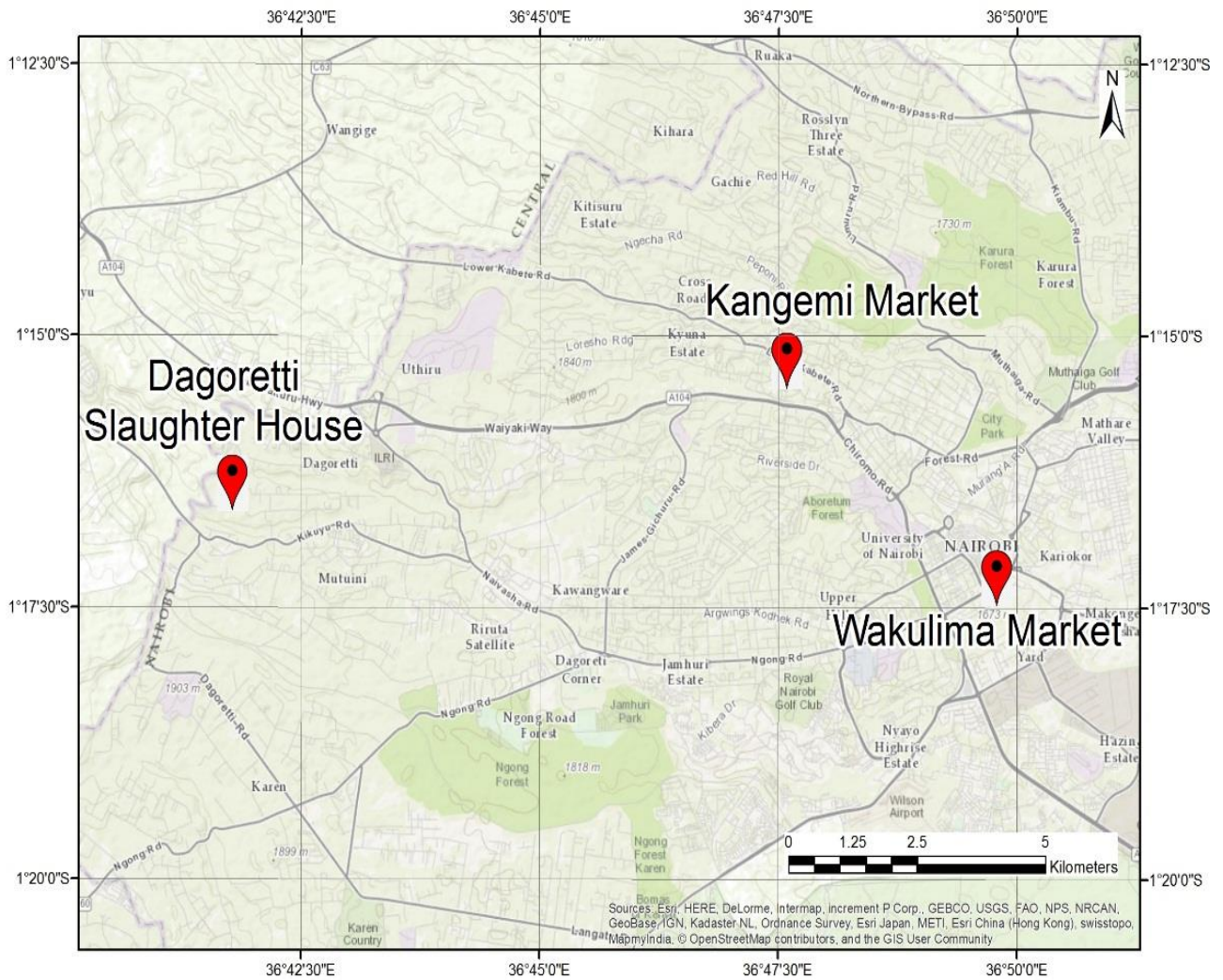


Figure 3.1: A map of the sampling points

3.4 Procedure

The procedures used in this study are outlined in this section. Unless otherwise stated, analytical grade reagents were used. The experiments were carried out in triplicate, and mean \pm standard deviation values reported.

3.4.1 Sample Collection

The market wastes were sampled in plastic buckets from Kangemi and Wakulima markets in Nairobi County and transported to the laboratory for analysis. Rumen fluid was collected in 5, 25 and 36-liter cooler box containers depending on the stage of the experiment from Dagoretti slaughterhouse and taken to the laboratory. Permission to collect the rumen fluid and market waste samples had been obtained from NACOSTI (Appendix 1) and the respective County government.

3.4.2 Pre-Treatment

The inorganic matter was removed from the market waste and discarded. The organic portion was sorted into fruits, vegetables and other organic matter, e.g. potato peels. The samples were then subjected to size reduction by chopping into smaller pieces using a knife followed by blending utilizing a kitchen blender to ease the process of digestion by bacteria.

3.4.3 Bacteria Total Count, Culture, Isolation and Identification

Rumen fluid and fresh cow dung were collected from Dagoretti (Kiambu County) slaughterhouse in 5-liter cooler box containers and sampling bags respectively, sealed and transported to the Microbiology laboratory at the College of Agriculture and Veterinary Sciences, the University of Nairobi for bacterial studies. The Standard Plate Count (SPC) method (LeChevallier *et al.*, 1980) was employed to give the total bacteria counts in the rumen fluid and cow dung samples. One milliliter/gram of the cow dung and rumen fluid slurry was aseptically transferred into 9 mL sterile distilled water to give a one in ten dilutions (1:in 10 dilution). The diluent was then serially diluted using 9 mL of sterile distilled water up to 10^{-6} dilutions. Using a sterile pipette, 1 mL each of 10^{-1} , 10^{-2} , 10^{-3} , 10^{-4} , 10^{-5} and 10^{-6} dilutions were plated on TSB agar.

³ and 10⁻⁵ dilutions were carefully and aseptically inoculated in triplicates by the pour plate techniques (i.e. 1 mL mixed onto molten agar) onto *Salmonella shigella* Nutrient, MacConkey, Eosine Methylene Blue agars for bacterial isolation, and on potato dextrose, Sabaraud dextrose and malt extract agars for fungi isolation. All the plates were incubated at 37° c for 24 hours for bacteria. The colony forming units were then calculated by multiplying the number of colonies by dilution factor and dividing by the amount of sample used.

3.4.4 Waste Analysis

Fresh solid vegetable and fruits market wastes; Avocado (*Persea americana*), Cabbage (*Brassica oleracea capitata*), Coriander (*Coriandrum sativum.*), Spinach (*Spinacia oleracea*), Kales (*Brassica oleracea acephala*), Pumpkin Leaves (*Cucurbita maxima*), *Kahurura* (*Cucumis ficifolia*), Pig Weed (*Amaranthus spp.*), African Nightshade (*Solanum nigrum*), Papaya (*Carica papaya*), *Togotia* (*Erucastrum arabicum*), comfrey (*Symphytum officinale*), Banana (*Musa spp*), Sweet Potato (*Ipomoea batatas*), Cucumber(*Cucumis sativus*), Watermelon (*Citrullus lanatus*), Tomato (*Lycopersicon lycopersicum*), Potato (*Solanum tuberosum*), Mango (*Mangifera indica*) and Courgette (*Cucurbita pepo*) henceforth referred as fruits and vegetable waste mixture(FVWM) were sliced into small pieces and then blended for toxic substances, macro and micronutrient, heavy metals analysis and proximate analysis studies.

3.4.4.1 Toxic Substances

The pesticide levels in the market wastes were determined by making a uniform waste mix of wastes from the fruits and vegetables and extracting using the QUECHERS method (Ukpebor and Ukpebor, 2016). The method involved extraction of the pesticides residues from FVMW with acetonitrile, phase separation with primary secondary amine and magnesium sulfate before the final injection solution was reconstituted in ethyl acetate and analysis done in gas chromatography coupled to a triple quadrupole mass spectrometer. (Donkor *et al.*, 2015). The pesticide levels in the waste mixture sample were determined by extracting using the soxhlet method and scanning the samples using GC-MS.

3.4.4.2 Macro and micronutrient and heavy metals analysis

About 500g of fruits and vegetable waste mixture (FVWM) were blended separately using a kitchen blender after chopping. The samples were mixed in a bigger container (110 liters) to make a homogenous waste mixer. The waste was divided into two whereby one was analyzed for elemental composition when fresh while the other one was allowed to undergo aerobic decomposition for three weeks. In both setups, the mixture was dried in an oven before being ground into a fine powder and made into a pallet. Analysis in triplicates was done using an X-Ray fluorescence spectrophotometer at the Institute of Nuclear Science, University of Nairobi as described by Khan *et al.*, (2011), Obiajunwa *et al.*, (2002) and Schramm, (2016).

3.4.4.3 Proximate analysis

The proximate composition was done on homogenized sample. The analysis included; energy, fat, nitrogen-free extract, ash, moisture content, protein, fiber, carbohydrates by the techniques of AOAC, (2003) as described in this section.

3.4.4.4 Moisture Content Analysis

Moisture level was obtained using the oven drying method (Carneiro *et al.*, 2018; Nielsen, 2010). About 1.0 g of market waste was weighed in a dried crucible. The sample was dried at 100-105⁰C for 6-12h to a constant weight. The sample was cooled for 30min in a desiccator before being weighed. The percentage of moisture was obtained using equation 3.1.

$$M = \frac{W_1 - W_2}{W_s} * 100 \dots \dots \dots (3.1)$$

W₁ is the Weight of crucible and sample before heating, W₂ is the crucible + sample weight after heating, W_s is the weight of sample + crucible before heating

Note: Further analysis was done using moisture free samples.

3.4.4.5 Determination of Ash

The ash levels were determined by heating the sample in a muffle furnace at 600⁰C for 1h, then cooling before weighing. One gram of each sample was ignited at 550⁰C for 2-4 h. Equations 3.2 (wet weight) and equation 3.3 (dry weight) were used to determine the ash levels.

$$Ash = \frac{W_3 - W_1}{W_s} * 100 \dots \dots \dots (3.2)$$

$$Ash(dry) = \frac{Ash(wet)}{100 - Moisture} * 100 \dots \dots \dots (3.3)$$

W₃ is the weight of crucible and ash, W₁ empty crucible weight and W_s crucible and sample weights before burning.

3.4.4.6 Determination of crude protein

Protein in the samples was determined using the Kjeldahl method (Chang & Zhang, 2017; Joanna & Barbano,1999). About 0.5-1.0 g of dried waste samples were digested by heating with H₂SO₄ plus digestion mixture comprising of potassium sulphate and selenium (catalyst). NaOH (0.1M) was added to make the digested mixture alkaline. This resulted in ammonium sulphate. Ammonia was collected in 2% boric acid solution before titrating against standard HCl. The total protein was determined using equations 3.4 and 3.5.

$$Crudeprotein = 6.25 * \%N \dots \dots \dots (3.4)$$

$$\%N = \frac{(S - B) * N * 0.0014 * D}{W_s * V} \dots \dots \dots (3.5)$$

Where S = Sample titration reading, B = Blank titration reading, N = Normality of HCl, D = Dilution of sample after digestion, V = Volume taken for distillation and 0.0014 = Milli equivalent weight of Nitrogen.

3.4.4.7 Determination of crude fat

The ether extract technique was used to determine total crude fat in the samples using the Soxhlet apparatus. About 1.5 -2.5g of dried samples was wrapped in filter paper, before placing in a fat-free thimble, and then introduced in the extraction tube. Weighed, cleaned and dried the receiving beaker and filled with petroleum ether and assembled the extraction apparatus. The extraction process was started. After 4-6 siphoning the ether was evaporated and disconnected the beaker before final siphoning. The extract was then transferred in a cleaned glass dish to a water bath after which ether was evaporated. The dish was then dried at 105⁰C for 2hrs and before cooling in a desiccator (Moreau & Winkler, 2011). Equation 3.6 was then employed for total crude fat. W_s is the weight of the sample and the crucible.

$$Crudefat = \frac{Weightofether\ extract}{W_s} * 100 \dots \dots \dots (3.6)$$

3.4.4.8 Determination of crude fiber

0.153g of the sample was weighed and transferred to the porous crucible. This was then placed into the Dosi-fiber unit. To each column, H₂SO₄ (150mL) solution and foam-suppresser was added dropwise. The heating element was powered while the cooling circuit was opened. On boiling, 30% power reduction was done for 30minutes. The acid in the sample was wholly removed by draining and rinsing with distilled water. This procedure was repeated using 1M KOH in place of 1M H₂SO₄. The sample was the dried at 150⁰C for 1h, cooled and weighed (W_1). The sample was further dried in a muffle furnace at 55⁰C for 3-4 hrs, cooled and re-weighed(W_2). Equation 3.7 was utilized in calculations of crude fibre.

$$crudefiber = \frac{W_1 - W_2}{W_s} * 100 \dots \dots \dots (3.7)$$

Where W_s initial weight of the sample, W_1 is crucible and sample weight after digestion and drying and W_2 is sample weight after drying.

3.4.4.9 Nitrogen free Extract

This represents the number of soluble carbohydrates and is calculated by differences after calculating all the other properties using equation 3.8

$$\%NFE = DM - (CL + C.P + Ash + \%C.F) \dots \dots \dots (3.8)$$

Where NFE is a nitrogen-free sample, D.M is the dry matter, C.L is crude lipids, C.P is crude protein and C.F is crude fibre (Nielsen, 2010).

3.4.4.10 Energy calculation

The energy content in the fruits and vegetable waste samples were calculated by summation of C.P and carbohydrates multiplied by four and C.L multiplied by 9 as per equation 3.9. The results were then reported as calories per 100gm of the sample (Nielsen, 2010)

$$Energy = C.P * 4 + C.L * 4 + C.L * 9 \dots \dots \dots (3.9)$$

3.5 Biogas Production

In this section, biogas recoveries from individual fruits and vegetables market waste is outlined. The samples were washed and blended before loading to digesters. Gravimetric and volumetric methods were employed in cumulative biogas measurements.

3.5.1 Digester Pressure Tests

Before biogas production experiments, pressure test was done for seven days to ensure all the anaerobic digestion containers were airtight and no gas losses were experienced during production. A *kPa* pressure gauge was used (figure 3.2).



Figure 3.2: Pressure test setup for 1 liter bottle.

Initially, the digester was loaded with the substrate and a pressure gauge was attached to the gas outlet. Then, pressure tests were done by placing reacting sodium bicarbonate with acetic acid in a basin and placing it on top of the substrate in the digester. The setup is shown in figure 3.3. The reaction of sodium bicarbonate with acetic acid generate carbon dioxide, which builds up pressure in the digester. The resultant pressure was recorded twice per day for a week. This was done to ensure that the digester is gas tight and no gas escapes during biogas generation.

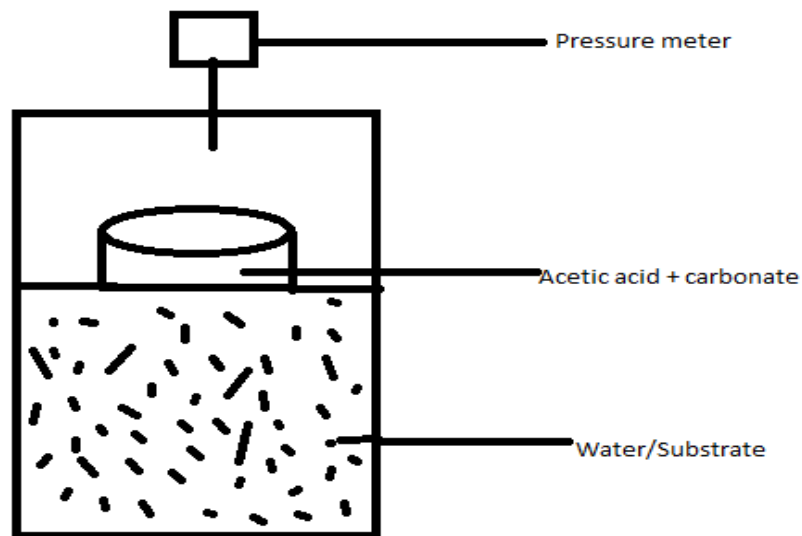


Figure 3.3: Pressure tests setup for 120l digester.

3.5.2 Biogas Measurement

Biogas produced was measured using two methods; gravimetric and volumetric. Gravimetrically, the substrate was loaded into the glass bottle and weighed after airtight sealing. The bottle was then placed in a water bath maintained at 37°C (Sasha et al., 2015). After every 24 hours, the setup was hand swirled, degassed and weighed as shown in figure 3.4.

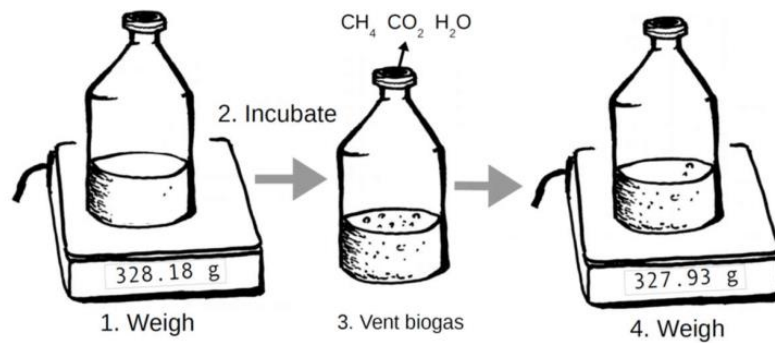


Figure 3.4: Schematics of gravimetric biogas methods (Sasha et al., 2015)

The volumetric biogas measurements involved loading the substrate to the conical flask/glass bottle and attaching a glass syringe as shown in figure 3.5. The pressure builds up resulting from biogas generated pushes the syringe. Cumulative biogas generated was recorded daily.

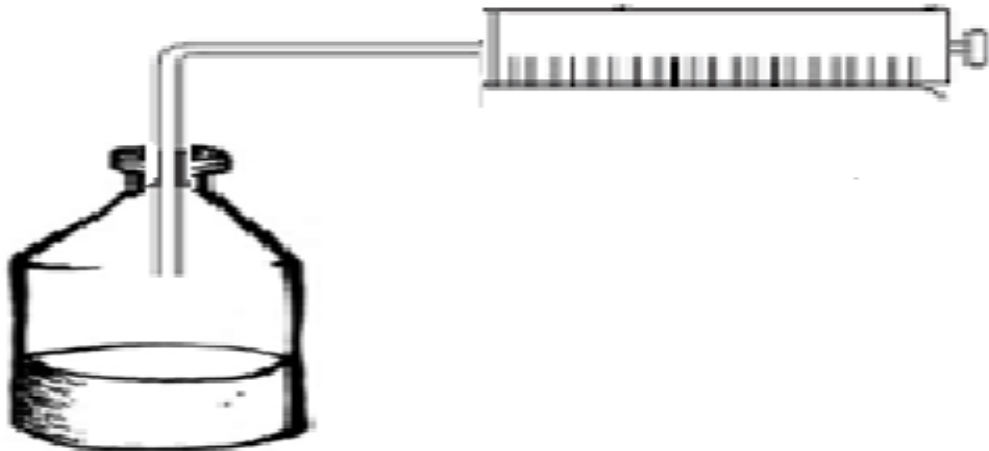


Figure 3.5: Volumetric biogas methods (Mbugua et al., 2020)

3.5.3 Biogas production at psychrophilic conditions

Market waste with different ratios of fats, proteins, and carbohydrates (based on the proximate matter analysis) was mixed with cow dung and rumen fluid as inoculum and employed for biogas production as per the procedures outlined in this section.

3.5.3.1 Biogas production from fruit wastes

About 250mL of blended Banana, avocado, watermelon, cucumber, georgette, tomato, potato, sweet potato, papaya and mango fruit wastes were loaded into 500mL plastic digester shown in figure 3.6 and biogas produced measured daily using a graduated glass(volumetric) syringe for seven days. The anaerobic digestion process was not inoculated and therefore, this was the control experiment. The same was repeated with Coriander (*Coriandrum sativum L.*), Spinach (*Spinacia oleracea*), kales (*Brassica oleracea acephala*), Pumpkin Leaves (*Cucurbita maxima*) Kahurura (*Cucumis ficifolia*), Pigweed (*Amaranthus spp.*), African Nightshade (*Solanum nigrum*) and comfrey (*Symphytun officinale*).



Figure 3.6 : Biogas production set up at psychrophilic conditions.

3.5.3.2 Biogas production from fruit wastes inoculated with cow dung

Banana, avocado, watermelon, cucumber, courgette, tomato, potato, sweet potato, papaya and mango fruits waste were collected from Kangemi/Wakulima market. They were separately reduced in size by chopping with a kitchen knife before blending. A blended mixture was made using 250mL of all the fruits and mixed thoroughly. The blended market wastes and cow dung were loaded into 500mL plastic digester shown in figure 3.7 in the ratio of 1:1 and biogas produced measured daily using a graduated glass syringe for seven days.

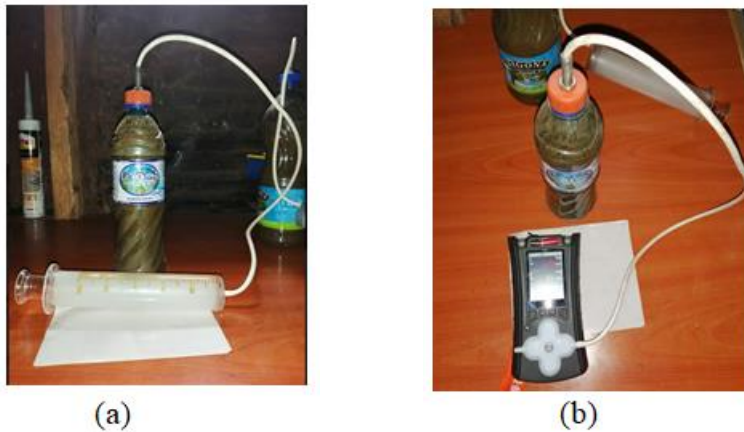


Figure 3.7: Biogas production measuring with a (a) glass syringe and (b) biogas analyzer.

3.5.3.3 Biogas production from fruit wastes inoculated with Rumen Fluid

Procedure 3.4.3.2 was repeated with rumen fluid for all the fruit and vegetables. The cumulative biogas produced at psychrophilic was measured and recorded daily for 7 days.

3.5.3.4 Biogas production from fruit wastes inoculated with Rumen Fluid

About 200mL of specific fruits and vegetable wastes were loaded into the reactor shown in figure 3.6. The inoculum was added to the wastes in a ratio of 1:1 and biogas production initiated at mesophilic conditions by placing the setup in a waterbath and maintaining it at 37°C. The operating pH was 6.8-7.2 at room temperature.

3.5.3.5 Biogas generation without inoculum

About 200mL of specific fruits and vegetable waste samples were blended and loaded into the bottle shown in figure 3.8. No inoculum was added to the wastes and biogas production initiated at mesophilic conditions. The operating pH was 6.8-7.2 while the temperature was maintained at 37°C using a water bath.



Figure 3.8: A set-up of biogas production at the mesophilic condition

3.5.3.6 Biogas generation with inoculum

The generation of biogas was done as described in procedure 3.4.3.5 with rumen fluid as the inoculum. Biogas production was done in a dark room to avoid sunlight or by covering the setup with dark material. The experimental design is shown in figure 3.9 where the waste was inoculated with rumen fluid in 1 liter and 5 liters reactors.



(a)



(b)

Figure 3.9: Biogas production at room temperature (a) 1 l reactor (b) 5 l reactor

3.5.3.7 Gas Collection, analysis and Recording

Daily gas production was collected with a lubricated calibrated syringe (100mL) or urine bag (2000mL). The biogas produced was analyzed using a Portable PG810 3 in 1 Multi-gas Detector from Henan, Inte Electrical Equipment Co. Ltd, China. It was fitted with three gas detection sensors in the following ranges; CH₄ (0-100%) CO₂ (0-100%) and H₂S (0-5000ppm). Figure 3.10 shows the biogas analyzer used in this study. A gas inlet and outlet were fixed to cover the gas sensors. Biogas stored in the urine bag and/or graduated syringe was then passed through the sensors and the composition displayed on the LCD screen.



Figure 3.10: GP810 multi-gas detector from Henan, China

Biogas quality/composition was measured after the seven days' retention time using a portable biogas analyzer, as shown in figure 3.11. Levels of CH₄, CO₂ and H₂S were measured and recorded.



Figure 3.11: Biogas analyzer measuring biogas quality from potato waste

The water vapor in the biogas was allowed to condense in the urine bag or the syringe before passing the biogas through the sensors.

3.5.4 Biogas production optimization

The biogas generation from wastes was optimized by varying the operating parameters as described in this section.

3.5.4.1 Waste pretreatments

Fruits and vegetable wastes were sampled and size reduction done by slicing and blending. The wastes were analyzed for proximate matter and the physicochemical properties as described in Kamau *et al.*, (2020). Twenty market waste comprising of fruits and vegetables were subjected to thermal, chemical and thermochemical pretreatment before biogas production at psychrophilic/mesophilic conditions. Further studies were carried out at thermo-chemical pretreated wastes based on the pretreatment preliminary results obtained.

3.5.4.1.1 Alkaline Pretreatment

Each waste was cut into small pieces before blending using a kitchen blender. The waste (100g) was then placed in a glass bottle, and 10mL 1M NaOH added. The mixture was thoroughly shaken before purging and sealing. The bottles were then placed in a water bath and maintained at 55⁰C for 24 hours, after which it was removed and allowed to stabilize for 6 hours at room temperature. The inoculum (1:1) was added, and then biogas generation was studied at 25⁰C for ten days. The same was done with the waste mixture(F.V.M.W.) for thermal and chemical pretreatment.

3.5.4.1.2 Acid Hydrolysis

200g of market waste was mixed with 20mL 0.1M HCl (pH 1) and pre-hydrolysis allowed for 24-48 hours at 37- 40⁰C with stirring. After the pretreatment step the setup was allowed to stabilize for 24 hours at room temperature, before loading to the digester and adjusting the pH to 6.8 – 7.2 using 0.1M NaOH. The inoculum was added (1:1), and

oxygen was driven off from the mixture using CO₂ to create an anaerobic environment before sealing. Cumulative biogas produced at mesophilic conditions was monitored for ten days. Figure 3.12 indicates the pretreatment setup.



Figure 3.12: A setup of fruits and vegetable market wastes pretreatment process
The same procedure was repeated using twenty fruits and vegetable markets wastes using NaOH in place of HCl to compare acid hydrolysis to alkaline pretreatment.

3.5.4.1.3 Large-Scale Waste Pretreatment

The above procedures were repeated using 350 g, 500 g, 2 Kg and 7 Kg mixed market wastes with inoculum at a 1:1 ration in 1.0, 1.5, 5 and 10 litres' digesters. The setup was removed from the water bath and allowed to stabilize for 6 hours before adjusting the pH to 6.8-7.2. The inoculum was then added and mixed thoroughly. Cumulative biogas generation was studied for 17 days' retention time. The setup is shown in figure 3.13.



Figure 3.13: Large scale biogas production from pretreated market wastes

3.5.4.2 Inoculum to substrate ratios

Biogas production was carried out at a mesophilic condition to assess the most appropriate inoculum to substrate ratio for biogas generation. Fruits and vegetable mix were inoculated using rumen fluid and cow dung at ratios of 1:1, 2:1 and 1:2 volume/volume and cumulative biogas production recorded for seven days.

3.5.4.3 Temperature

Laboratory scale studies were done at psychrophilic, mesophilic, and thermophilic conditions. The temperature brackets for batch reactors were 22-26°C, 35-37°C and 50-55°C using a water bath, as shown in figure 3.14. A thermostatic heater was used to warm the water. A thermometer was fitted in the water bath for temperature monitoring.



(a)



(b)

Figure 3.14: Setup for (a) psychrophilic and (b) mesophilic and thermophilic batch setup

3.5.4.4 Optimization of C: N ratio

Fruits and vegetable market wastes with different C: N ratios were loaded into anaerobic digesters and the biogas produced at mesophilic conditions measured. The market wastes ultimate properties i.e. the carbon and the nitrogen content were determined as per the procedures in waste analysis section.

3.5.4.5 Influence of carbohydrates, protein and fat content on biogas production

Market wastes with a different combination of carbohydrates, proteins and fat levels were loaded into anaerobic digesters and the biogas produced at mesophilic conditions measured. The waste to inoculum ratio of 1:1 was used without pH adjustment.

3.5.4.6 Influence of pH

In this set, the pH of each waste, rumen fluid, cow dung and waste mix were taken before loading to the digester and after seven days' retention time. The influence of pH was done by loading a waste to an inoculum ratio of 1:1 in the digester and pH adjusted using lemon juice and NaOH. The working pH was 5.13, 6.13 and 10.5. The cumulative daily gas production was measured daily using graduated polythene bags at thermophilic and mesophilic conditions.

3.5.4.7 Influence of Agitation

The influence of substrate stirring during the AD was investigated by loading cow dung to water ratio of 1:1 in 500 mL, 1 L, 5 L, and 10 L digesters. One set of the digesters was agitated after every 12hours while one set was un-stirred. Cumulative biogas generated was recorded daily for 30 days.

3.6 Modelling Studies

Batch digesters containing different ratios of carbohydrates, protein and fat were set up and gas production were done at different pH, temperature and other different operating parameters. Biogas production kinetics for describing and evaluating gas production was

done by fitting the experimental data to various documented models to predict gas production per given combinations of wastes.

Biogas recovery rates from market wastes in AD were modeled using exponential, linear and Gaussian plots at mesophilic conditions. The theoretical biochemical biogas potential of 20 market wastes was investigated using online biogas application by Sasha et al., (2018). The application which is built in R programming language is found at <https://cran.r-project.org/package=biogas>. The program can calculate BMP accurately from different biogas measurement methods (Hafner et al., 2018). The *Shiny* application was used to determine various parameters in biogas simulation and the screenshots of the application are shown in figure 3.15.

Figure 3.15: Screenshots of online biogas application

3.7 Biogas Upgrade

The upgrade experiments were performed using raw biogas from cow dung feedstock and market wastes. The raw biogas used in this study was generated from market wastes

inoculated with cow dung/rumen fluid in the ratio of 1:1 as recommended by Tira et al. (2015). The substrates (cow dung from dairy cows and water) was loaded into a 0.5 – 1.5 liters' digesters and biogas generated at psychrophilic conditions for a 10 days' retention time as described by Kamau et al. (2020). Raw biogas was also generated from market wastes at mesophilic conditions by inoculating market wastes mixture (F.V.M.W) with rumen fluid described by Kamau et al. (2020). The produced biogas was then stored in urine bags or tubes before being directed to biogas scrubbing unit. The upgrade cartridges were worn-out rubber tyres, natural zeolite rocks, commercial desulphurizer, maize cobs and steel wire. Figure 3.16 shows the upgrading cartridges.



Figure 3.16: The biogas upgrading cartridges; rubber tires, natural zeolite rocks, commercial desulphurizer, maize cobs and steel wire.

In figures 3.17 (a), the digesters were set at room temperature with the cartridges placed at the gas outlet channel for cleansing. In contrast, in figure 3.17 (b), the temperature was maintained at 36-37⁰C by warming water in a water bath.

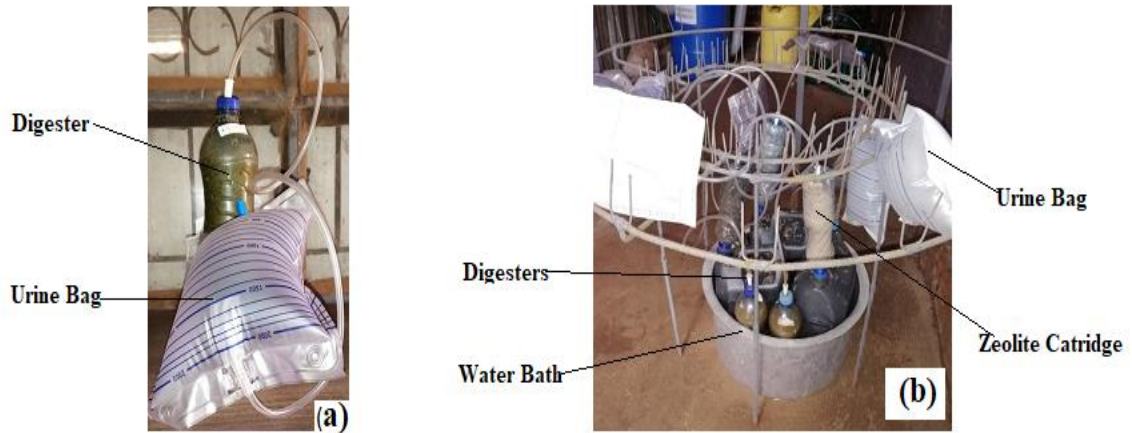


Figure 3.17: Biogas upgrade setups at (a) psychrophilic and (b) mesophilic conditions.

The scrubbing cartridges used in the lab scale and the pilot scale studies are shown in figures 3.17. The cartridges in the pilot scale upgrade were composed of well ground particles of rubber tires, natural zeolite rocks, commercial desulphurizer, maize cobs and steel wire.

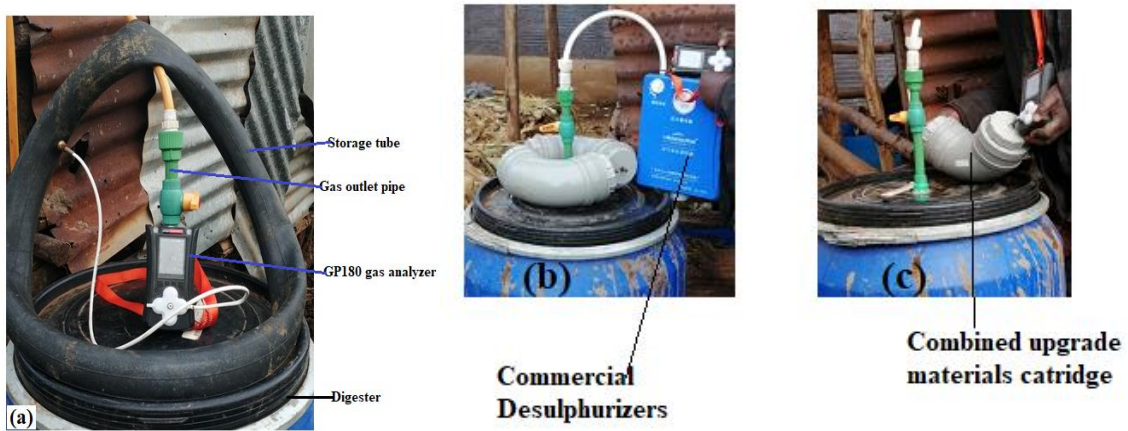


Figure 3.18 (a) Biogas composition analysis setup (b) Commercial desulphurizer (c) combined upgrade material.

3.7.1 Natural zeolite rock analysis

The natural zeolite rock samples (figure 3.09) were sampled from Eburru volcanic crater (0.63S, 36.23E), 8 Km North-West of Lake Naivasha within the Kenyan Rift Valley. The samples were taken from the base of a quarry, about 10 feet deep. The high upgrading

potential of the natural zeolite rocks from the preliminary studies necessitated its morphological analysis as described.



Figure 3.19: Natural zeolite rock

3.7.1.1 X-Ray Diffraction (XRD)

The zeolite rocks were ground and passed through 0.85 mm sieve before calcinating for 2 hours at 550 °C to discard the degradable matter (Waswa *et al.* 2020). 1.0 g of sample was prepared as a thin layer on a glass slide, subjected to x-ray beam rays using Cu-K α radiations ($k = 1.54184\text{\AA}$, 40 kV, 40 mA) with stepwise increase of $0.02^\circ\text{sec}^{-1}$ over $1^\circ\text{-}8^\circ$ and 2°min^{-1} over $8^\circ\text{-}90^\circ$ for small angle and wide angles respectively at room temperature (Toyara, 1986; Burton, 2009). The spectrum was recorded as intensity against 2Θ .

3.7.1.2 Scanning Electron Microscopy (SEM)

About 0.01g of powdered sample was dusted to form a thin coating on a double stick carbon tape, then a sufficient amount of powder was dissolved in water and the solution sonicated. A few drops of this solution were placed on a highly polished SEM mount of a silicon wafer, then allowed to dry before scanning them with a beam of incident electrons operated at 15-20 kV to form SEM images on the detector (Kliewer, 2009).

3.7.1.3 General Zeolite rock tests

The ground natural zeolite sample was subjected to elemental analysis according to Tran. *et al.*, (1993); Mehlich, 1953 to determine P, K, Na, Ca, Mg and Mn. Calometric procedures were employed to assess TOC (Gislason *et al.*, 2005) while Kjeldahl method was employed to assess the total nitrogen (Persson *et al.*, 2008). Trace elements, pH and the cation exchange capacity were determined as described by Turner *et al.*, (1966) and modified by Mbugua *et al.*, (2012).

The natural zeolite rocks were further powdered and packed in an airtight cartridge made from sealable u-shaped 4" elbow. After packing the rocks, both ends of the elbow were sealed and inlet and outlet channels made. Raw biogas was passed from the urine bag through the rocks and composition analysed. The composition before and after upgrade was done using a portable PG180 biogas analyser. The upgrading setup was as shown in figure 3.20, which showed biogas stored in a polythene bag, upgrading cartridge and a biogas analyzer.



Figure 3.20: The biogas upgrading set-up

3.8 Fabrication of a Digester

The fabrication of small and more efficient portable digester was done using readily accessible material, as shown in figure 3.21. Customization of the design of the available

digester was done to incorporate agitation and temperature regulation mechanism. This fabrication is described in steps. The detailed schematics with the specific measurement is described in appendix C.

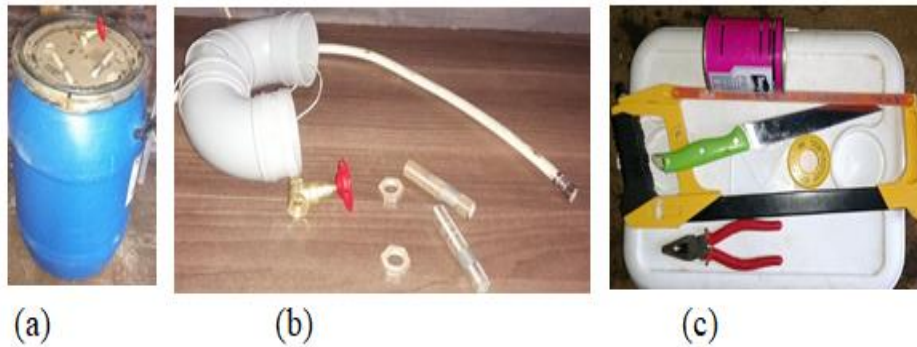


Figure 3.21: The (a) plastic drum (b) plumbing items (c) cutting material used for digester design

The following steps were followed in designing and fabrication of a portable biogas digester with a stirrer and a heating mechanism. The following steps were followed with the pictures shown in appendices (figure 5.5).

1. Fabrication of a stirrer. A wheel bearing was incorporated to ease the agitation mechanism using wind.
2. A hot water pipe was coiled around the stirrer
3. Two holes were made at the bottom and top of the plastic drum for the outlet and inlet respectively
4. Sockets were fitted for the inlet and outlet
5. The tank was made airtight to prevent leakages
6. Three holes were made on the top lid of the plastic container for the gas outlet, stirrer and temperature/pH/sampling point.
7. The assembled stirrer from step 2 was fitted inside the digester
8. The stirrer and the gas gate valve were fixed
9. The equipment was tested for water and gas leaks

3.9 Digester Automation Design

The detailed schematics with the specific measurement is described in appendix D. The biogas production was automated by employing automatic loading mechanisms, agitation mechanisms, temperature regulation and pH sensors and safety gas leakage and smoke sensing gadgets. The following devices and sensors were used in this section; *Arduino Uno R3*, servo motors, MQ2, MQ9, LED, LCD and jumper wires. The reactor automation was divided into two sections; hardware design and code development. In the hardware section, the component devices were connected using a design prototype done in DipTrace 3.3 platform, while in the second part, an *Arduino* sketch was done in *Arduino IDE*.

3.9.1 Loading rate

A mixing chamber was made using a 30-litre plastic basin with a gate valve at the bottom. The discharge rate was calculated using the formula 3.10

$$Q = A.V \dots \dots \dots (3.10)$$

Where Q is the digestate flow rate (m³/s or l/s), A is the area of the outlet pipe (m²) and V is the digestate velocity (m/s). The loading chamber is shown in figure 3.22. The loading rate is done automatically using *the Arduino* program, which automatically opens the inlet after every 24 hours. A well mixed substrate is prepared from the feedstock and water and thoroughly smoothed for free flow. The substrate is then loaded in the mixing chamber awaiting loading.



Figure 3.22: Substrate loading gate valve set up.

3.9.2 Temperature Monitoring using Arduino

The temperature in the digester is measured using a K type MAX 6675 thermocouple using an *Arduino* microcontroller. A 1602 LCD is attached, as shown in figure 3.23.

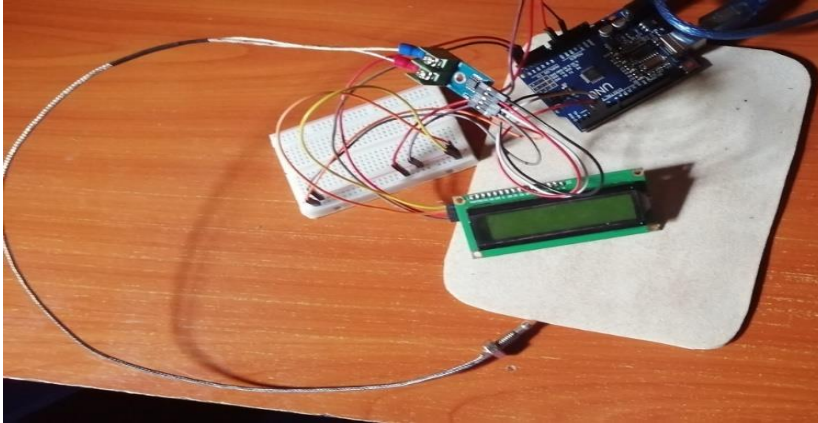


Figure 3.23: A schematic of thermocouple with an LCD.

A hot water chamber was made using a 5-liter plastic basic with a gate valve at the bottom. The discharge rate was calculated using the formula 3.10. A carrier pipe was inserted in the digester from the inlet and discharge of the cold water at the outlet. The setup is shown in figure 3.24.



Figure 3.24: Arduino controlled servo for warm water circulation

The water flow in the pipe is controlled using a microcontroller, which automatically opens and closes to allow water flow when the temperature is below 33⁰C and 55⁰C for mesophilic and thermophilic digestions, respectively.

3.9.3 Agitation mechanism

The agitation mechanism incorporates a fan, a bearing and a holder shaft, as shown in figure 3.25. The agitator is made up of a fan, bearings and a servo motor controlled by an *Arduino* board.

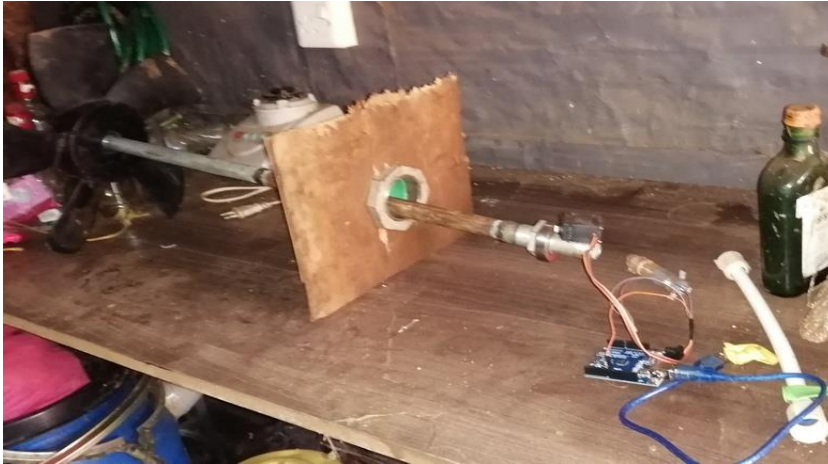


Figure 3.25: An Arduino servo-controlled agitator.

The agitation is automatically initiated using a microcontroller set to run after every 24 hours to ensure thorough mixing and uniform temperature in the digester.

3.9.4 pH Regulation Using pH Probe and Arduino

The pH probe board can supply a voltage output to the analog board that represents a pH value. Ideally, calibration is done to have a pH 0 at 0V and a pH of 14 illustrated by 5V. The probe has two potentiometers in the circuit; the offset regulation and the pH limit. The probe was connected to Arduino, as shown in figure 3.26 and the voltage of the P₀ pin adjusted using the offset regulation potentiometer to 2.5V, corresponding to a pH value of 7.00.

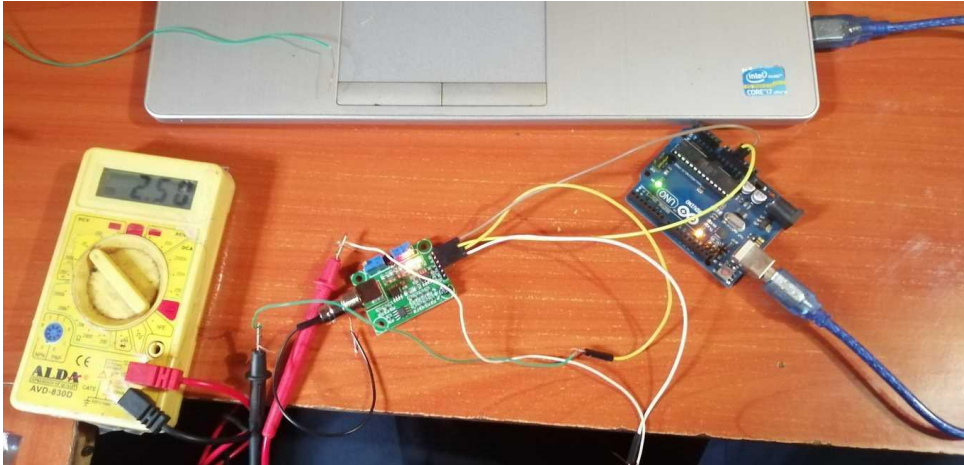


Figure 3.26: pH probe calibration using a multi-meter

Calibration of the pH module was also done using an offset sketch. The sketch reads the voltage from pin Po and displays it on the serial monitor. This entailed short-circuiting the inside of the BNC connector with the outside, as shown in figure 3.27, to simulate a neutral pH (pH7). The voltage was adjusted using the offset potentiometer to 2.50V.

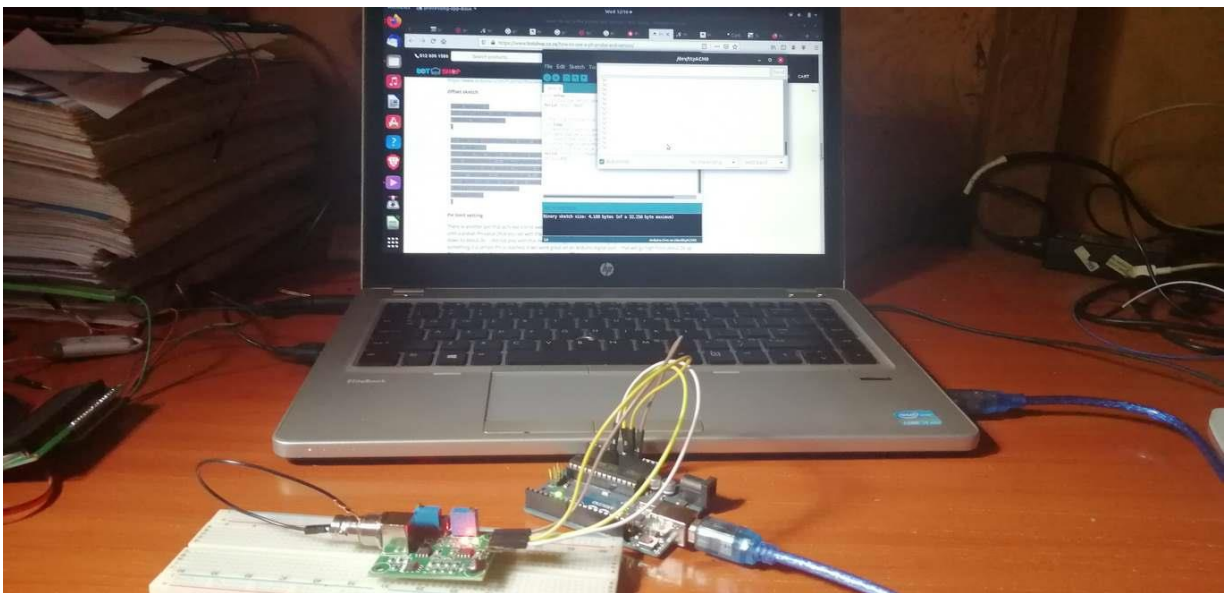


Figure 3.27: pH probe calibration using an offset code

The offset sketch employed in calibration of the pH module was obtained from <https://www.botshop.co.za/how-to-use-a-ph-probe-and-sensor/> and was written by Caballero, (2017).

The digesters pH was monitored using a portable pH meter and *Arduino* based pH probe fitted with temperature monitoring sensors, as shown in figure 3.28. Data logging was done using PLX DAQ V2.11 into excel after every one minute. Hourly readings were averaged and reported.

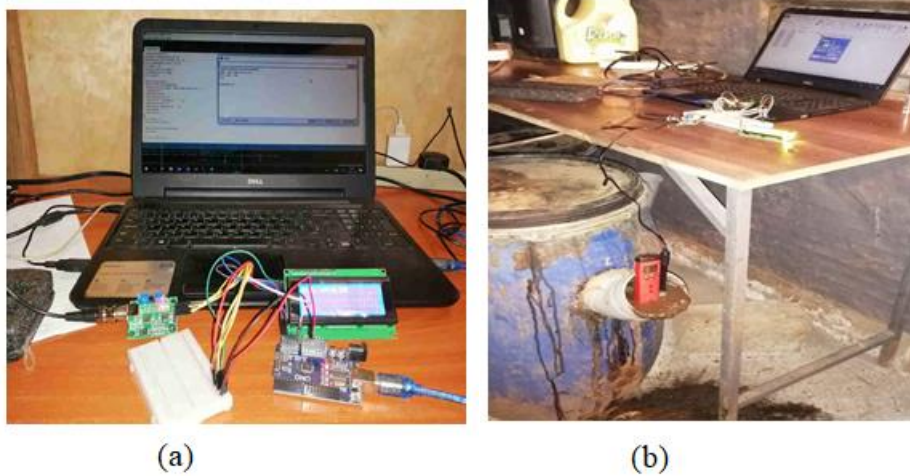


Figure 3.28: Digester pH monitoring with (a) *Arduino* and (b) portable pH meter

3.9.5 Re-engineered Digester Biogas Production

Four batch 120 liters' digesters were compared for biogas production for a 30 days' retention time. The digesters are shown in figure 3.29. Cow dung mixed with water in a ratio of 1:1 was used for biogas generation. They were labeled A, B, C, and D. Digester A was un-agitated with no pH or temperature regulation, digester B and C were agitated with temperature and pH regulation, respectively. In contrast, in digester D, both pH and temperature were regulated. The operation pH and temperature were 6.81- 7.10 and 36 – 37⁰C. An insulating material was used to cover the digester to prevent heat loss. The pH was controlled by adding 0.1M sodium hydroxide solution while the temperature was maintained by passing warm water through a pipe coiled inside the digester frequently.



Figure 3.29: The biogas digesters

The biogas produced was recorded for 30-day retention time for the four digesters running on a batch mode. Before that, the daily temperature in the digester was recorded on an excel sheet using PLX-DAQ V2 after every 3 minutes.

3.9.6 Automated Digester Biogas Production

Automation of biogas production was achieved using re-engineered digester design of the fabricated portable biogas digester. It incorporated micro-controllers in loading, temperature, pH regulation and agitation mechanisms. The micro-controllers included *Arduino Uno R3*, servo motors, MAX 6675 K type thermocouple, 16 x 2 LCD, DHT11 temperature humidity sensor, GSM sim900 modules and a pH sensor module.

The servo agitates the substrate for 3 minutes, after which temperature and pH values are taken, an alert in the form of an SMS was sent to a pre-registered number for regulatory action if the readings were not in the pre-set threshold. The project block and schematic diagrams are shown in figure 3.30 and 3.31.

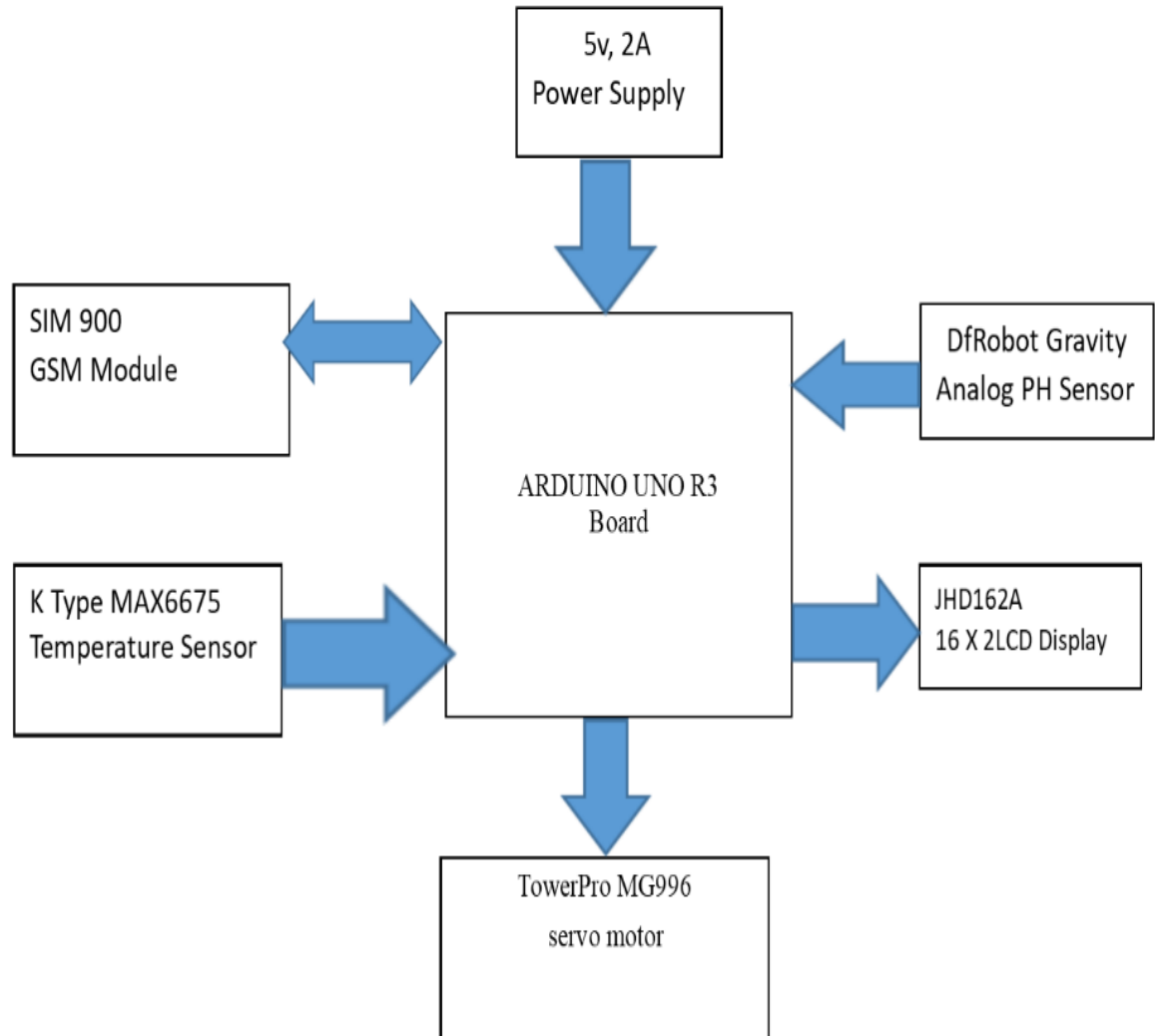


Figure 3.30: Block diagram of the automated digester

The automation model is powered by a computer via a USB port with a power back up automatically set in case of power outage. The components connections to the *Arduino* board pins were drawn using DipTrace 3.0 software and is shown in figure 3.31

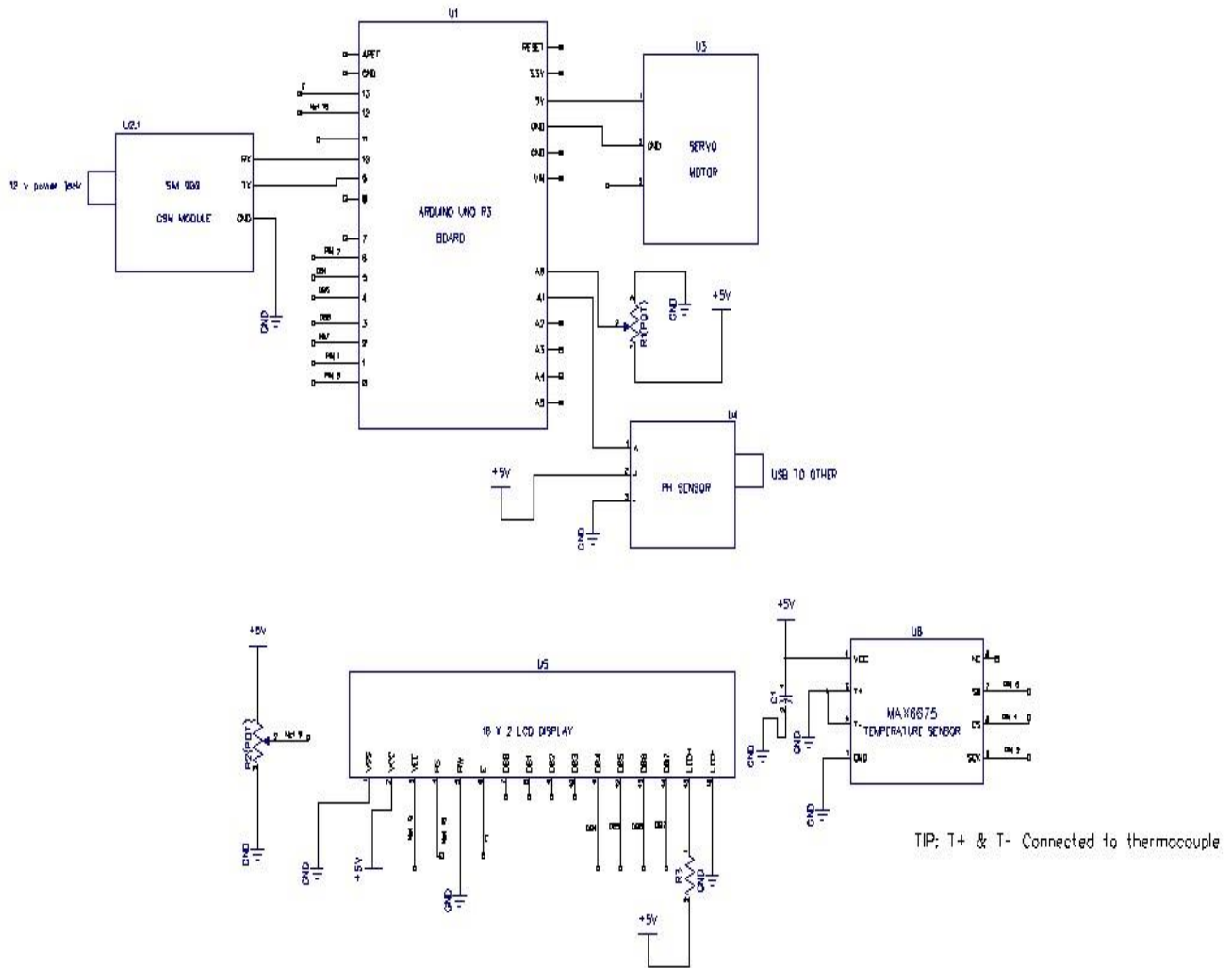


Figure 3.31: A schematic diagram of automation biogas production design

The prototype incorporates an *Arduino* micro-controller linked with a servo motor, analog pH sensor, K-type MAX6675 thermocouple and an LCD. The servo motors are used to regulate warm water flow and the loading rate as coded in the *Arduino* sketch. The K-type MAX6675 thermocouple is employed to monitor the digester temperature while the analog pH sensor monitors the digester pH. In case the preset threshold is exceeded, a phone call or an SMS is sent to a pre-registered number. The actual digester is shown in figure 3.32. The digester is fitted with an agitation motor and a warm water pipe is coiled in the digester. A gas outlet is made at the top cover of the digester cover. The portability of the digester is enhanced by placing the digester on a movable rack.



Figure 3.32: Automated biogas digester

3.9.7 Safety Measures in Biogas Production

The safety measures taken were to detect methane leakages which may result in flame and smoke. The alert system is to alert the user via the GSM module by call or SMS accompanied by an alarm buzzer and a LED blink.

3.9.7.1 Biogas Leakages Detection and Safety

In this section, an Internet of Things (IoT) based gas leak detection technique using the *Arduino UNO* module in conjunction with the SIM900 module and the high-sensitivity smoke and methane MQ-2 sensor was designed.

3.9.7.2 Methane, Fire and Smoke Detection

The following material was used in this study; *Arduino UNO R3* board, GSM SIM900 module with a 2A power supply, Flame sensor and an MQ-2. The block flow diagram

(figure 3.33) shows how the sensors, LCD and SIM900 are connected to the *Arduino* board.

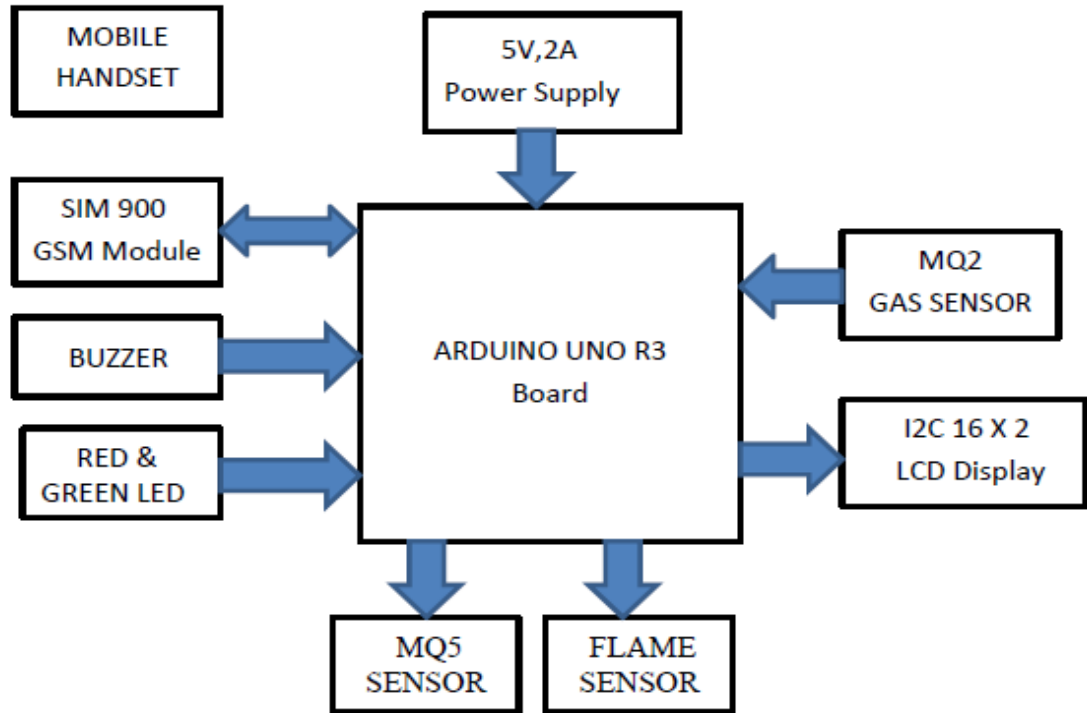


Figure 3.33: A block diagram of Arduino Based methane, Smoke & Fire Detection

The DipTrace 3.3 design tool was used to design the connection prototype while the software development was done in *Arduino* IDE platform. A programming code was used to run the devices with the prototype connections shown in figure 3.34.

The design was such that, whenever the MQ-2 sensor sense methane in the biogas utilization setup, an alarm is raised via the buzzer with red LED light on to indicate danger, a call is made to the pre-registered number with a warning message on the LCD and serial monitor. In the event there is fire or smoke which exceeds the set threshold, an alarm is raised via the buzzer with red LED light on to indicate danger, a call is made to the registered number with a warning message on the LCD and serial monitor.

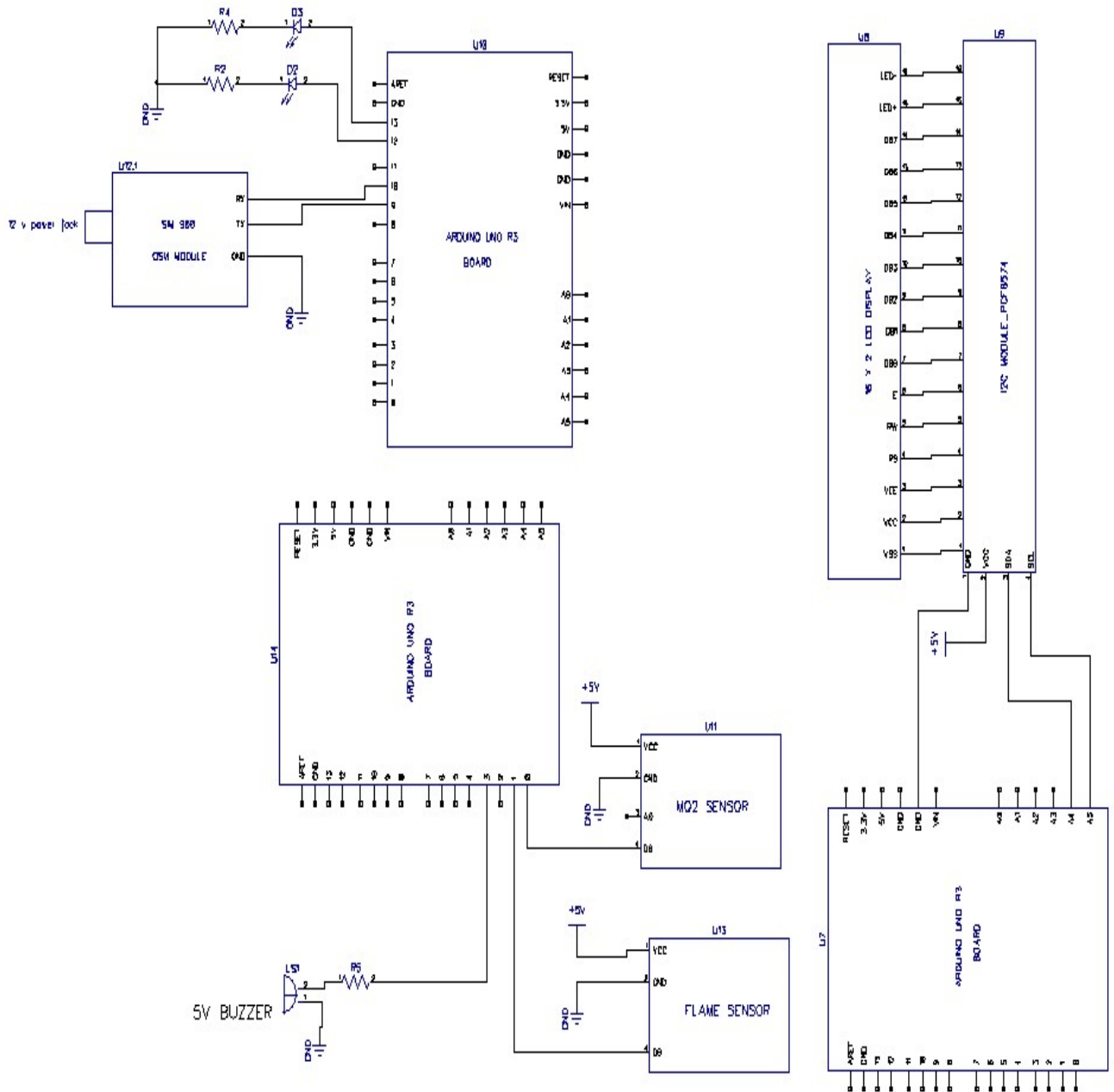


Figure 3.34. Prototype schematic diagram

3.10 Pilot Scale Set-Up

The pilot-scale experiments were done using 5liters, 10liters, 60liters, 120liters and 240 liters. The substrates were cow dung and market wastes. The inoculum for the market wastes was rumen fluid from Dagoretti slaughterhouse. The setup is shown in figure 3.35.

On cold days, the pilot scale digesters were covered with an insulating material like a dark blanket to prevent heat loss.

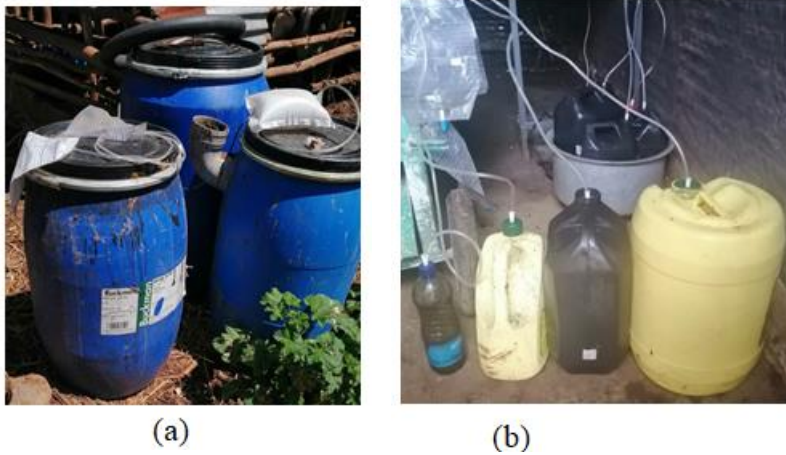


Figure 3.35: The pilot-scale biogas production setup (a) 120 – 240 liters (b) 5 – 20 liters
The pilot-scale upgrade setup was done using a desulphurizer cartridge, zeolite rocks cartridges and a mixture of zeolite rocks, maize cobs, steel wire, rubbers and desulphurizer pellets cartridge. The setups are shown in figure 3.36.



Figure 3.36: Pilot-scale biogas upgrade setup (a) using a desulphurizer (b) using zeolite

3.10.1 Solids Retention Time

Calculations of solids retention time were done using equation 3.11 (Al Seadi *et al.*, 2008)

$$S_{RT} = \frac{D_v * C}{F_{out} * C_{out}} \dots \dots \dots (3.11)$$

S_{RT} is the solid retention time, D_v is digester volume, C is microbes in the digester, F_{out} is the flow rate out of the reactor and C_{out} is the number of microbes flowing out of the digester.

3.10.2 Hydraulic Retention Time (HRT)

HRT is defined as the average time the reactor content remains in the AD compartment. It is given by equation 3.12

$$H_{RT} = \frac{D_v}{F} \dots \dots \dots (3.12)$$

H_{RT} is the hydraulic retention time, D_v is the volume of the reactor and F is the influent flow rate.

3.10.3 Organic Loading Rate

This depicts the quantity of substrate per digester capacity and is will be determined using equation 3.13

$$OLR = (V * C_{vs})/V_{reactor} \dots \dots \dots (3.13)$$

Where: OLR is the organic loading rate, V is the volumetric flow rate, C_{vs} is volatile solids concentration and $V_{reactor}$ is reactor volume (Burton *et al.*, 2003).

3.11 Fabrication of a Ferro-cement digester

A Ferro-cement digester with a 1450 liters' capacity was designed and fabricated using metal rods, cement, sand and ballasts as per the steps outlined in this section. The fabrication in pictures is shown in appendix (figures 5.8). Detailed description and schematics of the designed are attached in appendix E while the cost involved is shown in appendix J.

1. The metal framework was designed and molded
2. A hole was dug and the base was laid using concrete
3. The framework was fixed using concrete
4. Plywood was molded inside the framework to hold the concrete during plastering and fix the inlet and outlet.
5. The framework was bound with mesh wire
6. Plaster the digester with waterproof cement and allow 12 hours to cure.
7. Plaster the tank and smoothen using cement and allow curing process for 3 days
8. Fill the hole using the soil.
9. Fit in the warm water circulation pipe and the stirrer and seal the tank with a concrete cover.

3.12 Construction of a 14000 liters' digester

Construction of a 14000 liters' biogas plant for seven households cooking and lighting was done as per the steps. Detailed descriptions of the measurement and the design are attached in appendix F while the cost involved is shown in appendix J. The fabrication steps are shown in appendices (figures 5.10).

1. Site preparation was done by preparing a hole of 11ft diameter and 6.5ft deep with an outlet of 3 by 3 ft.
2. Construction blocks were made using cement, sand by compacting on a four-block plate
3. The foundation concrete was laid and spread smoothly at the base of the digester hole.
4. The foundation blocks were laid with significant consideration of the circular shape of the digester.
5. The walling blocks were laid up to a gas area and while fitting the inlet pipe
6. Close the digester by filling with blocks and maintain the measurements
7. Fill in the hole with the soil up to the gas area and compact as you prepare the inlet pot.
8. Fit the gas outlet using a threaded gas pipe and firmly fix it using concrete.

9. Paint the gas area with a brush and cement paste to fill in any gas leaks holes.
10. Construct the holding area of the substrate inlet and the outlet using waterproof cement.
11. Lay the first and the second plaster and smoothen on the gas area and inside the digester to ensure no gas leakages. Also, plaster the inlet and the outlet.
12. Cover the digester tank with soil and level the biogas area.
13. Fabricate the outlet cover.
14. Fix the pipes and finish up any other plumbing works

The operation process of both the ferro-cement and the 14 m³ digesters from loading to bio-slurry discharge is shown in appendices section (figures 5.11).

3.13 Microbial Fuel Cells

A H-shaped double chamber MFC was made using cheap material. Plastic containers with a diameter of 16.3 cm to 15.3 cm and a length of 7.4 cm to 9.4 cm, driller, adhesive glue, scissors, masking tape, wicks, PVC pipes and pipes joiners were used in MFC works. The anode was fed various fat, starch, and fat-containing substrate compositions, while the cathode was fed distilled water. A digital voltmeter was used to measure the amount of voltage produced.

3.13.1 Microbial Fuel Cells Construction

As anode and cathode chambers, two 1.2 liter containers were packed. The wire was inserted through two small holes drilled into the caps of the containers. A 5.7cm long and 0.7cm diameter graphite rod electrode was connected to one end of the copper wire. 2.5 litres of 1M NaCl, 3 percent agarose solution, and lamp wicks were used to make a salt bridge. The wicks were boiled in a NaCl and 3 % agarose solution for 10 minutes before being placed in the freezer at -4 °C to solidify. The solidified salt bridge was passed through PVC pipes and secured to the chambers with Araldite adhesive, ensuring that they were leak-proof.

3.13.2 Circuit Assembly

The double chamber MFC were put together as depicted in figure 3.37. The voltage and current were taken regularly via a multi-meter connected to copper wires joined to the carbon rods (Mbugua *et al.*, 2017).

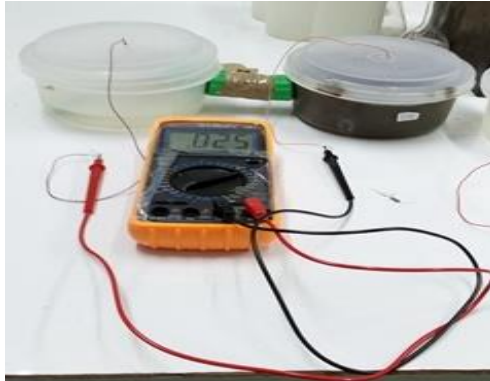


Figure 3.37: Set-up of H-shaped microbial fuel cells with a multi-meter

3.13.3 Resistance Variations

The anodic chamber was filled with 700 mL of cow-dung water mixture to characterize voltage, current, strength, and current and power densities through various resistors. The cathodic chamber, on the other hand, received 1 L of distilled water as a source of energy. As shown in figure 3.38, the MFC.



Figure 3.38: Set-up of H-shaped microbial fuel cells

The terminals from the cathodic and anodic chambers were connected with 1 Ω , 1 k Ω , 2 k Ω and 15 k Ω resistors. Regular voltage and current from the cells were measured across the connected resistors for 16 days.

3.13.3.1 Investigation of the potential of Fruit Wastes and Cow Dung

Around 500g each of watermelon, avocado, banana, tomato, and mango were diced, minced with a meat mincer, and homogenized then put into the anodic chamber. About 500mL distilled water was loaded in the cathodic chamber. A fruit mixture was also produced. To introduce the microbes, 250 mL cow dung in 205 mL water was added to each cell. The control experiment was 1000 mL cow dung in water. The current and voltage coming from the cells were measured every day for a period of 24 days.

3.13.3.2 Investigation of the potential of Fruit Wastes and Rumen Fluid

About 500g of watermelon, mango, avocado, tomato, and banana were cut into pieces, minced, homogenized and loaded to the anodic chamber to assess the potential of rumen waste in voltage generation from fruits wastes via MFC technology. About 250 mL rumen fluid from the Dagoretti slaughterhouse was added and mixed thoroughly. Voltage and current reading were done as described by Kamau *et al.*, (2017).

Before adding 250 mL rumen fluid, a mixture of the fruits waste was applied to the anodic chamber. In other experiments, 250mL, 350mL, and 500mL rumen fluid is mixed with mango and avocado. A salt bridge was used to link the set-ups to the cathodic chamber. A digital voltmeter was used to record current and voltage on a regular basis.

3.13.4 Microbial Fuel Cells Parameter Optimization

MFC operation conditions were analyzed in order to improve voltage generation. The electrode surface area, external resistance, and microbe concentrations operation conditions in tomatoes and avocado wastes were varied as described in this section.

3.13.4.1 Investigation of the effect of Electrode Surface Area

Before adding 500g of avocado to the anodic chamber, it was minced and blended. 500 mL rumen fluid was mixed thoroughly with the avocado in the same compartment.

Figure 3.39 illustrates how the electrodes were packed together. A salt bridge was used to

link the anodic-cathodic chambers. Three different carbon rods electrodes compartment A-0.01331 m², B-0.00666 m² and C-0.00399 m² were investigated for their influence on voltage generation from avocado in microbial fuel cells.

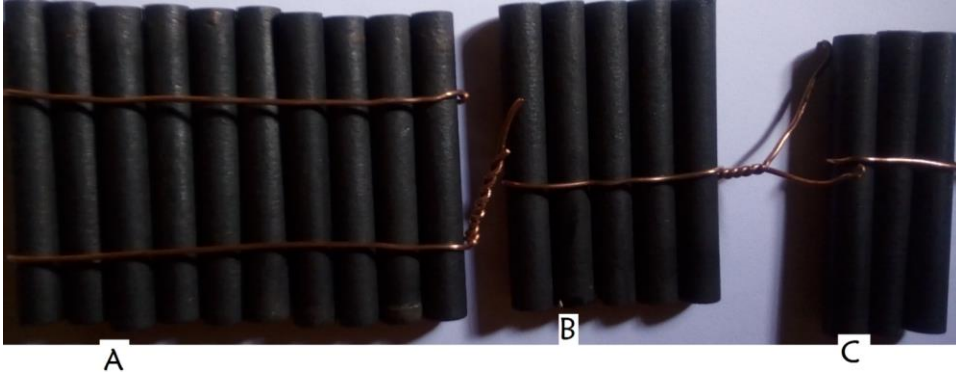


Figure 3.39: Carbon rods electrodes compartments A-0.01331 m² , B-0.00666 m² and C-0.00399 m²

3.13.4.2 Investigation of the influence of External Resistance

A H-shaped MFC were designed to investigate the effect of external resistance. About 500g avocado and 250mL rumen fluid were fed to the anodic chamber. Voltage and current across 1kΩ, 2kΩ, and 45 kΩ resistors were recorded daily as per Kamau et al., (2017).

3.13.4.3 Investigation of the influence of Microbe’s concentration

The anodic compartment was loaded with 500g of homogenized samples of avocado and tomato in a study to investigate impact of microbes levels on voltage generation. About 250, 300 and 500 milliliters of rumen fluid were applied. Voltage and current studies were done as described by Kamau *et al.*, (2017).

3.13.4.4 Data collection and observation

The generated voltage and current were registered every 24 hours for the specified number of days using a digital multi-meter. Equations 3.14 to 3.16 were used in calculations of power, current and power density.

$$P = VI \dots \dots \dots (3.14)$$

$$\text{CurrentDensity} = \frac{I}{A_{\text{area}}} \dots \dots \dots (3.15)$$

$$\text{PowerDensity} = \frac{\text{Power}}{A_{\text{area}}} \dots \dots \dots (3.16)$$

3.13.5 The Pilot Scale of Microbial Fuel cells

The microbial fuel cell pilot scale was set up using a 3.5l chambers, 6500cm³ surface is electrodes, 2.5g avocado and 1l rumen fluid. 15KΩ, 20kΩ, and 33KΩ resistors were attached to study the effect of external resistance to current and voltage. The voltage and current were recorded using a voltmeter. Light-emitting diodes fixed to circuit boards were attached to the terminals.

3.13.6 Degradation of chlorothalonil in microbial fuel cells

Studies of the amount of chlorothalonil degraded were done by adding 1g, 5g and 10g glucose to 10mL of 100ppm chlorothalonil stock solution to the anodic chamber containing blended decomposed tomatoes 10 days after voltage stabilization. A set without glucose was used as a control.

To study the effect of different concentrations of chlorothalonil, 10ppm, 20ppm with 2.5g glucose with tomato waste was added to the anodic chamber. Control was set using blended tomatoes without the pesticide.

Chlorothalonil degradation levels were obtained using the Shimadzu UV-Vis spectrophotometer. Voltage and current were recorded daily using a DT9205A digital multimeter for 30 days. The degradation plots were done using Minitab 17.

3.14 Digestate application in the container garden

A transplant of kale, spinach, tomato seedlings was done while maize, beans and peas were planted into a container garden, as shown in figure 3.40. Four gardens were set up comprising of a blank (where no manure/digestate was applied), ordinary dried manure set, cow dung set, and a digestate setup.

The soil used to grow the crops was investigated for fertility, as described in the analysis of the zeolite rocks section. The crop growth was monitored by measuring the increase of length after every 3 weeks and the physical appearance of the plant.



Figure 3.40: A picture of a container garden (a) bio-slurry, (b) cow dung, (c) dry manure (d) is the blank set (e) avocado

CHAPTER 4:

4.1 RESULTS AND DISCUSSIONS

For all the analytical studies, experimental were done in triplicates and meant used for all the plots in this research.

4.2 Food wastes

The general observation of the market waste pattern in the two markets was that individual fruit and vegetable wastage level depended on seasons and specific fruits or vegetable properties. For instance, leafy vegetable spoilage is higher than non-leafy vegetables. Sweet potatoes market life is higher compared to potatoes unless cuts were made during harvesting or transportation. The highly available vegetable waste in these two markets were kales and cabbages. *Cucumis ficifolia* and coriander were also observed to be among the most wasted leafy vegetable when in season. Spinach, pigweeds and African nightshade wastage were less frequent throughout this study. Tomato is the most consumed fruit in the world (FAOSTAT, 2019). The tomato wastage level was highest among the fruits followed by avocado when in season. Papaya and cucumber wastage was the least observed.

In most cases, FVMW result from spoilage of fresh fruits and vegetables during harvest, transportation and handling. These products are offered to the market for consumption, eventually ending up as wastes. The nutrient composition of these individual wastes was investigated to quantify the proximate composition. The Macro and micro-nutrient and heavy metals analysis, proximate and ultimate levels are presented in this section.

4.2.1 Macro and micro-nutrient and heavy metals analysis

Substrates with excess trace elements and other nutrients have been reported have low biogas yields (Matheri *et al.*, 2016). The table (Appendix B) shows the properties of the digested and fresh wastes after scanning for composition with an X-Ray fluorescence. The spectrum obtained is shown in figures 4.1 and 4.2. The levels of potassium, calcium,

zinc and zirconium were high in digested fruits and vegetable wastes in comparison to the fresh waste. This is explained by the fact that in digested wastes, the moisture content is lower and therefore the concentration of these elements is higher. This is evident in figures 4.1 and 4.2.

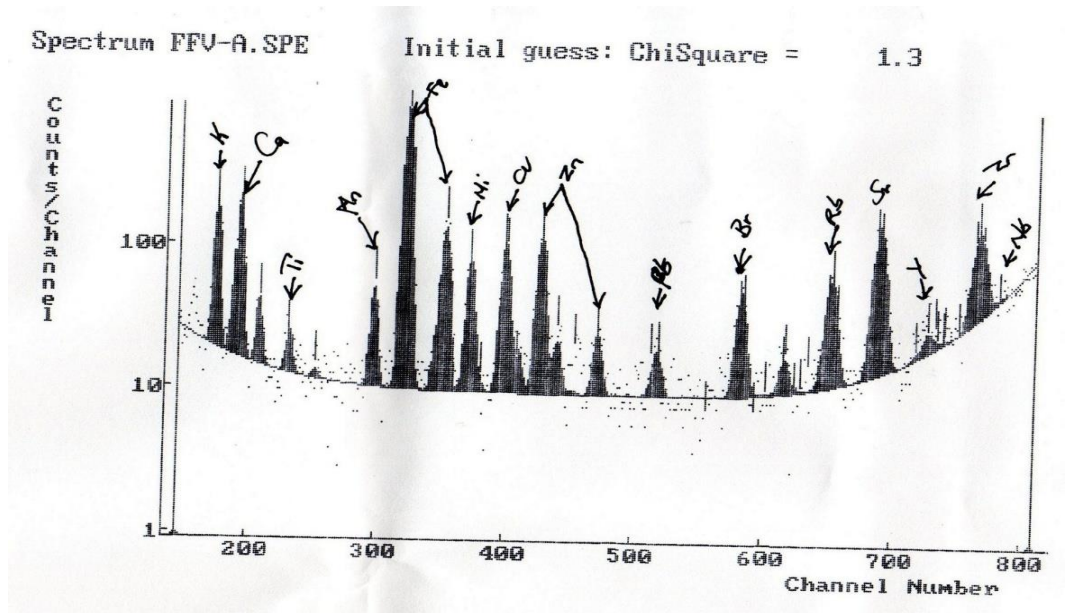


Figure 4.1: The XRF- spectrum for fresh wastes

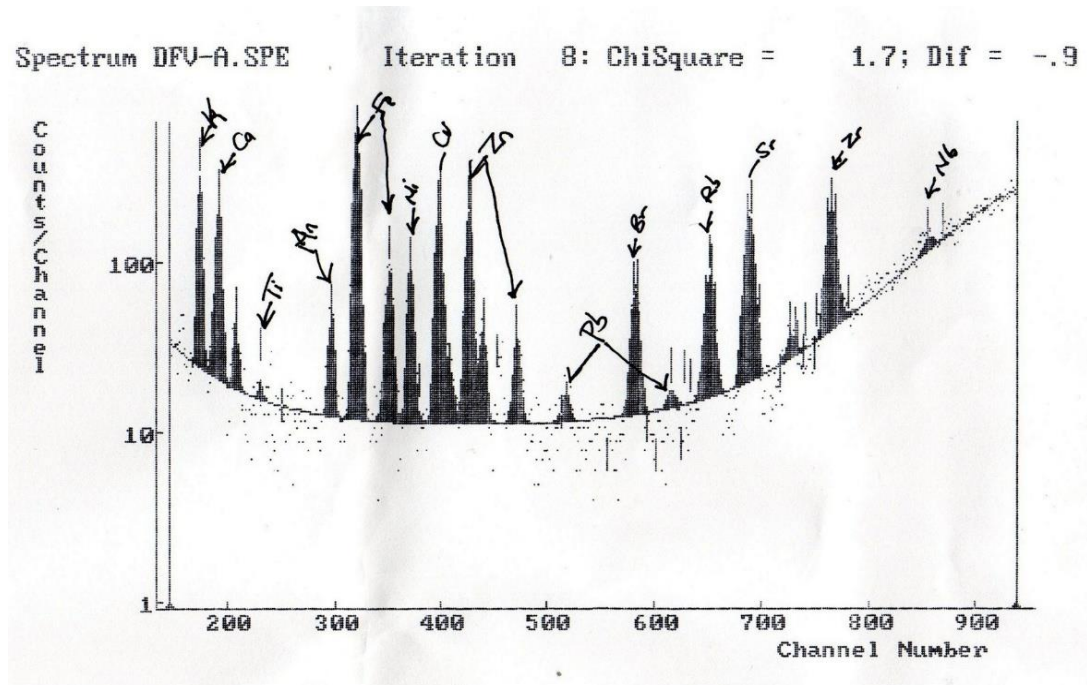


Figure 4.2: XRF- spectrum for digested wastes

The levels of lead, niobium, iron, manganese and titanium are higher in fresh wastes than in digested wastes. This means that these elements are utilized by microbes for growth and in the degradation process (Matheri *et al.*, 2016).

Figures 4.3 shows a graphical representation and comparison of fresh and digested wastes. The highest micronutrient was iron in both fresh and digested wastes. The observed trace elements levels in fresh wastes were 1.53% calcium, 280ppm manganese, 3742ppm iron and 15.10ppm lead. These levels are higher than the recommended limits from other studies. The recommended limits for the trace elements as suggested by Ariunbaatar *et al.*, (2016) are >0.54-40 ppm Ca, 0.003-0.06 ppm Co, 1-10 ppm Fe, 0.005-0.05 ppm Mo, 0.005-0.5 ppm, Ni (Weiland, 2006); 0.005-50 ppm Cr, Mg, Mn, Sn (Bischofsberger, 2005) as reported in Schattauer, *et al.*, (2011).

The Cd level were below the toxicity threshold of 0.18 mg/l at 0.09-0.18 mg/l bracket in both samples (Bożym *et al.*, 2015). Digestion of mixed substrates balances Cd in the reactor. The Mn levels were 4-19 mg/l and therefore, below the toxic limits of 50 mg/l (Bożym *et al.*, 2015). The results are similar to those observed for some wastes by Matheri *et al.*, (2016).

The general function of these elements in microorganisms range from involvement in the degradation of enzymatic compounds to simpler units to stimulating cell growth (Schattauer *et al.*, 2011). Other functions are highlighted in Matheri *et al.*, (2016).

The presence of trace matter in the feedstock influence methanogenesis, thereby dictating how much biogas is generated. Depending on the levels, they can be stimulating, inhibiting, or even toxic to the AD process (Şengör *et al.*, 2009; Oleszkiewicz and Sharma, 1990; Mudhoo and Kumar, 2013). The essential elements in micronutrients involved in AD efficiency are Co, Ni, Mo and Se. These elements are in the feedstock, and their deficiency leads to the poor performance of the AD (Lebuhn *et al.*, 2008; Schattauer *et al.*, 2011).

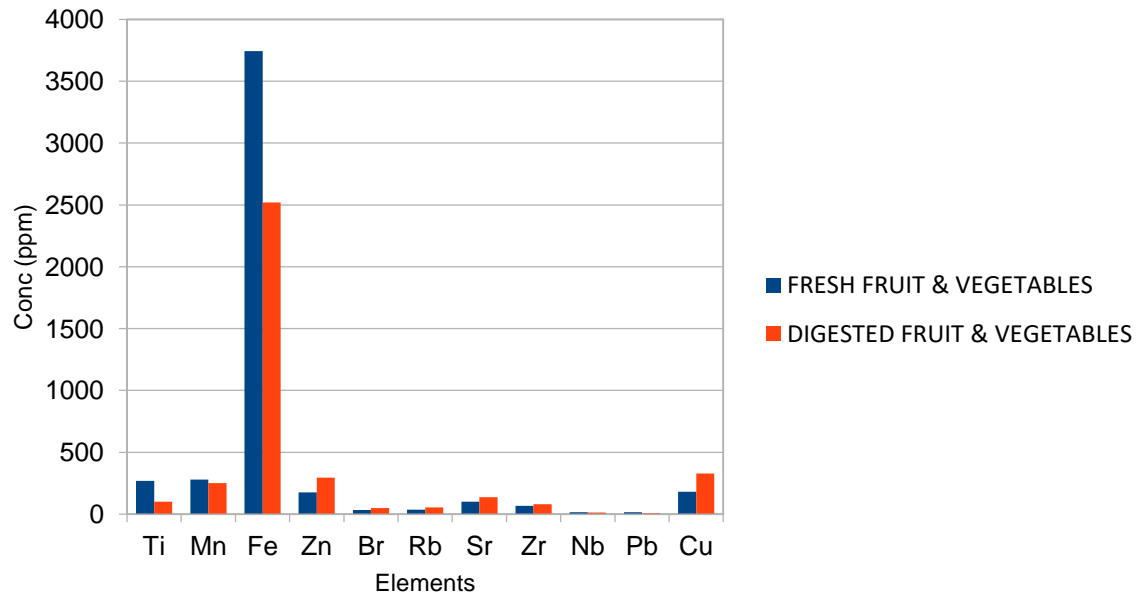


Figure 4.3: The elemental composition of fresh and digested wastes.

The investigated micronutrients were Zn, Mo, Mn, Cu, Ni and Co, while macro nutrients were K, Ca and Fe. These elements influence the substrate pH. Digestion at high trace elements level is effective at high pH (Kugelman and McCarty, 1965; Chen, *et al.*, 2008). The concentrations of lead and zinc were 15.10 ppm and 176 ppm, respectively. This represents the lead absorbed by the plants during growth and development and eventually ending up in the market. Toxic elements such as Cd, P, Cr and Pb dictates the amount of CH₄ and AD efficiency. Trace elements bind to thiols and other groups on protein molecules, displacing vital elements in enzyme prosthetic groups or interfering with enzymatic structure, making them poisonous. Sreekrishnan *et al.*, (2004), noted that K, Ca, Mg, Zn, Co and Cu speeds up biogas generation.

The percentages of potassium and calcium in the fresh and digested wastes are shown in figure 4.4. The percentages of calcium and potassium are higher in digested wastes compared to fresh scraps. This was observed due to lower levels of moisture in digested wastes. The potassium content evaluated ranged from 3.59 to 5.91 % in fresh wastes.

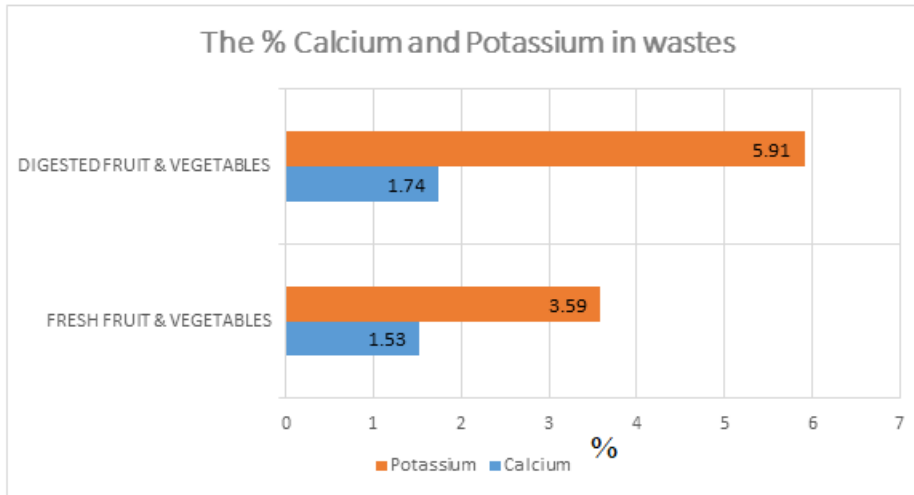


Figure 4.4: The % composition of fresh and digested wastes

Potassium and calcium are essential nutrients that catalyze the metabolism of microbes in biogas formation (Bożym *et al.*, 2015). Calcium moderate the substrate pH. Ca and K levels were below the toxic limit of 2800 mg/L and 3000 mg/L, respectively as specified by Bożym *et al.*, (2015); Takashima *et al.*, (1990). The observed macronutrients were potassium and calcium at 3.59 % and 1.5 3% respectively. Heavy metals in the samples like lead and zinc were at 15.10 ppm and 176.00 ppm respectively as shown in figure 4.3. Cr above 5 mg/L is toxic. The Cr levels were recorded at 3.69 ppm which was within the required range in this study (Khanzada *et al.*, 2008; Hussain *et al.*, 2009).

4.2.2 Pesticide levels

The pesticide levels in the mixed sample were determined using GC-MS, and the chromatogram obtained is shown in figure 4.5.

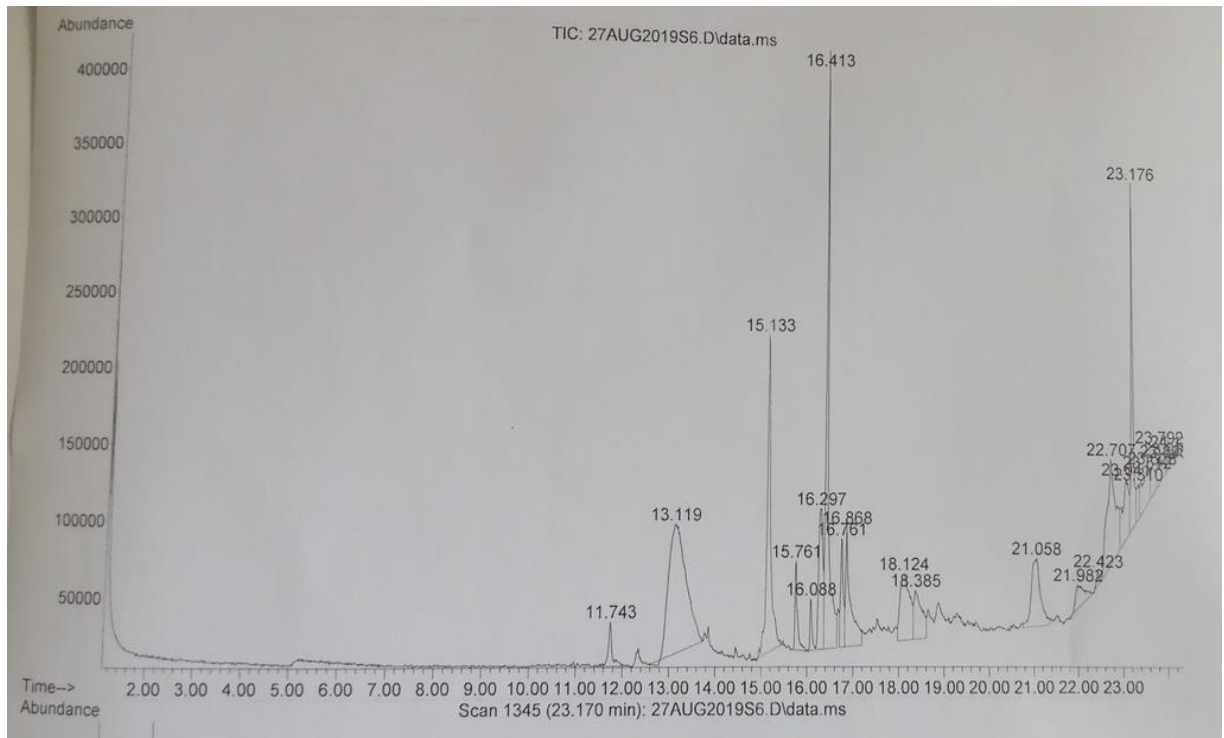


Figure 4.5: GC-MS chromatogram

The chromatogram in figure 4.5 showed that no pesticide residues were detected in the waste mixtures. The resultant peaks are for secondary metabolites in the plant waste matter. The presence of pesticides in the substrate utilized in anaerobic digestion affects microbe's activities. Thomas *et al.*, (2008); Brandli *et al.*, (2007) and Buyuksonmez *et al.*, (2000) had found some pesticides in compost and digestate, e.g., chlorothalonil after anaerobic digestion of substrates doped with pesticides. Khalil *et al.*, (2008) studied the influence of Mancozeb, Ametryne, and Niclosamide AD on the glucose AD by a mixed culture and reported inhibition of methanogenesis. In contrast, methanogenesis by *Methanosarcina barkeri* was not affected by Ametryne and Mancozeb. A study by Elefsiniotis and Li (2008) on biodegradation potential of 2,4-D and isoproturon and their effect on the performance of the anaerobic digestion process of sludge at mesophilic conditions. They reported complete removal of 2,4-D pesticide from the reactor while isoproturon biodegradation was practically negligible. They came to the conclusion that all reactors had a good digestion output, as evidenced by complete VFA utilization, significant gas production (containing 45 to 65 percent methane by volume), significant volatile suspended solids (VSS) reduction (42 to 50 percent), and pH and alkalinity

recovery (Elefsiniotis and Li, 2008). Dodemorph fungicide was stable in anaerobic digestion of biological waste (Vorkamp et al., 2003). Kupper, (2008), observed that 28 pesticides were detected from a sample size of 271 pesticides loaded in anaerobic digester. Furthermore, during composting, more than two-thirds of all pesticides found in the input materials dissipated at rates greater than 50%, whereas most triazoles levels decreased marginally or remained unchanged. Pesticides preferentially end up in presswater after solid–liquid separation, according to research on semi-dry thermophilic AD (Kupper, 2008).

4.2.3 Proximate analysis

The proximate study results on dry and fresh basis are shown in tables 4.1 and 4.2, respectively. The nitrogen-free extract (NFE) in proximate analysis represents sugars and starch and is obtained by difference rather than by measurement. NFE represents soluble carbohydrates, while crude fiber gives the insoluble carbohydrates (Dhont and Els, 2003). From table 4.1, the NFE reported in this study was in the range of 19.57 -62.90%. The levels were lowest in avocado wastes at 2.36%. The general trend for all the wastes was that higher proximate properties on a dry weight basis compared to fresh samples. This is explained by the dilution properties of the high moisture levels in fresh samples. The energy levels for the wastes were in the range of 189.95Kcal/100g in pigweed to 321.5 Kcal/100g in mango wastes. The ash content in dry wastes samples ranged from 2.81 % in sweet potato waste to 25.67 % in spinach waste samples.

Table 4.1: Proximate analysis on dry weight fruit and vegetable wastes

Sample	% Moisture	% Protein	% Fat	% Ash	% Fiber	% Carb.	% NFE	Energy (Kcal/100g)
Kales	10.53±1.09	21.68±0.99	3.22±0.08	18.45±3.88	15.00±1.11	31.12±1.22	31.12±1.90	240.18±15.00
Cabbage	5.13±0.11	16.12±3.90	0.96±0.03	9.70±1.99	10.38±1.77	57.71±5.55	57.71±3.90	303.96±13.00
Pumkin Leaves	8.77±0.23	25.99±2.33	2.12±0.05	23.86±0.75	10.72±0.76	28.54±2.68	28.54±1.89	238.01±16.99
<i>Cucumis ficifolia</i>	13.38±1.20	26.11±3.33	2.46±0.01	17.52±0.99	11.07±0.83	29.46±3.38	29.46±4.44	244.42±12.89
Pigweed	11.36±1.11	22.98±2.00	1.83±0.09	25.26±3.20	18.18±1.22	20.39±2.28	20.39±1.10	189.95±7.34
<i>Erucastrum arabicum</i>	10.63±2.90	26.57±2.56	1.85±0.15	18.76±1.33	15.81±2.38	26.38±5.76	26.38±2.22	228.45±10.99
Coriander	7.88±1.17	33.01±1.89	1.19±0.01	24.30±1.22	14.05±0.91	19.56±1.99	19.57±1.19	220.99±12.78
African nightshade	11.85±0.35	22.69±2.00	2.23±0.02	16.67±1.17	23.11±2.26	23.45±3.50	23.45±2.34	204.63±15.66
Spinach	6.73±0.67	22.80±1.89	2.52±0.11	25.67±33.77	13.74±1.99	28.54±2.00	28.54±4.03	228.04±8.09
Comfrey	14.96±1.22	21.71±2.09	1.98±0.17	23.13±2.56	13.85±1.56	24.37±1.22	24.37±1.22	202.14±7.78
Tomato	4.84±1.76	11.89±2.90	2.57±0.23	9.53±1.11	15.75±2.00	55.42±4.23	55.42±4.23	292.37±13.23
Potato	16.21±2.30	8.73±0.67	3.34±0.06	5.02±1.01	4.19±0.91	62.51±3.88	62.51±6.71	315.02±21.89
Sweet Potato	37.94±2.99	4.42±0.18	4.07±0.01	2.81±0.05	4.01±0.75	46.76±3.66	46.75±2.23	241.35±11.10
Pawpaw	10.78±1.90	6.36±0.71	3.15±0.45	4.65±0.88	12.16±1.11	62.91±2.22	62.90±9.77	305.39±14.23
Banana	25.7±3.66	11.89±1.11	1.97±0.01	6.53±0.21	4.85±0.22	49.06±4.34	49.06±3.44	261.53±9.84
Avocado	17.17±3.00	7.69±0.43	52.64±5.68	4.92±0.07	15.22±0.95	2.36±0.06	2.36±0.01	513.94±24.89
Courgette	4.65±0.87	22.92±2.35	5.48±0.09	15.58±0.98	14.87±0.88	36.50±1.99	36.50±1.29	287.01±10.00
Cucumber	4.14±0.09	12.65±1.27	5.19±0.45	11.14±2.67	18.75±1.22	48.13±2.22	48.13±2.88	289.83±12.89
Mango	13.18±3.44	6.61±0.44	5.23±0.67	3.33±0.10	9.74±0.78	61.91±1.50	61.91±2.78	321.15±23.00
Water Melon	7.14±0.88	12.72±2.67	4.63±0.01	10.49±0.76	15.68±1.11	49.34±3.77	49.34±2.89	289.91±56.78

From table 4.1, the proximate composition of the carbohydrates levels was higher compared to proteins and fats. This is because of sugars from the fundamental blocks in most tissues. This further translates to higher energy/100g of each waste. The values in table 4.1 are for dried wastes calculated from values in table 4.2. As expected, the

moisture levels are higher for fresh wastes compared to dried wastes. The proximate content of individual wastes on fresh weight basis is depicted in table 4.2.

Table 4.2: Proximate properties on wet weight fruit and vegetable wastes

Sample	% Moisture	% Protein	% Fat	% Ash	% Fiber	% Carb.	% NFE	Energy (Kcal/100g)
Kales	89.85±3.63	2.27±0.12	0.34±0.17	1.94±0.05	1.57±0.12	4.03±1.00	4.03±1.11	28.27±3.97
Cabbage	94.87±2.56	0.83±0.07	0.05±0.01	0.49±0.02	0.54±0.06	3.22±0.92	3.22±0.89	16.64±4.01
Pumkin Leaves	90.78±1.55	2.27±0.36	0.18±0.08	2.06±0.12	0.94±0.13	3.77±0.87	3.77±0.99	25.78±2.88
<i>Cucumis ficifolia</i>	86.62±2.98	3.49±0.72	0.33±0.11	2.34±0.05	1.48±0.52	5.74±1.02	5.74±1.04	39.89±2.37
Pigweed	88.64±2.00	2.61±0.55	0.21±0.7	2.86±0.01	2.06±0.78	3.62±0.85	3.62±0.88	26.81±7.00
<i>Erucastrum arabicum</i>	89.37±2.11	2.82±0.89	0.19±0.02	1.99±0.07	1.68±0.23	3.95±0.47	3.95±0.03	28.79±1.99
Coriander	92.12±4.47	2.6±0.23	0.09±0.03	1.91±0.05	1.12±0.09	2.16±0.36	2.16±0.08	19.85±1.97
A.Nightshade	88.15±1.99	2.68±0.36	0.26±0.10	1.97±0.03	2.73±0.11	4.12±0.56	4.21±1.10	29.91±1.13
Spinach	93.27±2.33	1.53±0.09	0.17±0.10	1.73±0.03	0.92±0.12	2.38±0.54	2.38±0.19	17.17±2.00
Comfrey	85.04±3.56	3.24±0.78	0.29±0.12	3.46±0.14	2.07±0.23	5.9±1.11	5.90±1.88	39.17±2.22
Tomato	95.16±4.00	0.57±0.01	0.12±0.01	0.46±0.01	0.76±0.01	2.93±0.09	15.08±1.11	2.93±0.05
Potato	83.78±4.23	1.41±0.87	0.54±0.21	0.81±0.02	1.74±0.14	11.72±1.00	57.38±6.88	11.72±0.99
Sweet Potato	62.05±2.99	1.67±0.09	1.54±0.14	1.06±0.05	1.51±0.23	32.17±2.31	149.22±20.01	32.17±2.44
Pawpaw	89.22±2.12	0.68±0.03	0.34±0.07	0.5±0.04	1.31±0.45	7.95±0.98	37.58±5.83	7.95±1.77
Banana	74.3±2.10	3.05±0.12	0.5±0.07	1.67±0.05	1.24±0.14	19.24±1.00	93.66±19.34	19.24±2.00
Avocado	82.83±3.00	1.32±0.14	9.03±1.36	0.84±0.02	2.61±0.98	3.37±0.55	100.03±12.90	3.37±1.11
Courgette	95.34±2.00	1.06±0.54	0.25±0.08	0.72±0.03	0.69±0.10	1.99±0.12	14.46±1.69	1.94±0.11
Cucumber	95.86±2.04	0.52±0.08	0.21±0.03	0.46±0.04	0.78±0.11	2.17±0.34	12.65±2.17	2.17±0.33
Mango	86.82±3.89	0.87±0.07	0.68±0.08	0.44±0.02	1.28±0.21	9.91±1.00	49.24±2.88	9.91±1.00
Water Melon	92.85±4.55	0.90±0.09	0.33±0.04	0.74±0.04	0.76±0.09	4.42±0.88	24.18±2.45	4.42±0.78

The moisture levels were in the range of 74.31 – 95.86% for all the wastes. Low percentages of proteins and fats were observed at 0.52 -3.49% and 0.09 – 1.54%,

respectively. Table 4.2 shows the percentage of moisture content in fruits and vegetable waste on an as-received basis. The total solids were computed by subtracting moisture levels from 100. In tomato waste, the moisture content was 95.16%. Mohammed *et al.* (2017) reported 90.75% moisture levels in tomato fruits. The percentage of moisture levels obtained was in range with previous studies by Oko-Ibom *et al.*, (2007), Adubofuor *et al.*, (2010) and Hossain *et al.*, (2010) who found moisture levels of 88.19 - 90.67%. The ash content shows the minerals/non-degradable matter in a sample when water and degradable matter are removed. Higher levels of ash levels were observed in leafy vegetables than in fruit wastes samples. For example, 2.06 – 2.46% ash levels were observed in *Cucumis ficifolia*, pumpkin leaves, pigweed, and highest in comfrey at 3.46%. The ash matter was lowest in fruit wastes, for example, 0.46% in tomatoes and cucumber. Watermelon Mango, avocado and pawpaw ash levels were 0.44, 0.84, 0.74 and 0.50%, respectively. From table 4.2, the highest NFE was reported in sweet potato, avocado and banana wastes at 32.17, 100.03, 93.66%, respectively, with the lowest being recorded in leafy vegetables like kales, spinach and coriander at 4.03, 2.38 and 2.16%, respectively.

The energy levels were computed as described by Pereira *et al.*, 2008. The energy per 100g of the sample was between 3.06 – 40.00kcal/100g and 189.95 – 513.94kcal/100g on a wet and dry basis, respectively. Previous studies on the energy levels of *Cucurbita moschata* and *Luffa acutangula* were estimated to be high compared to 248.8-307.1 kcal/100g reported in some Nigerian leafy vegetables (Isong *et al.*, 1999). Asibey-Berko & Tayie (1999) also found high energy content in some Ghanaian green leafy vegetables such as *Corchorus tridens* (283.1 kcal/100g) and sweet potato leaves (288.3 kcal/100g). The crude fat, proteins, fibre and carbohydrates are shown in table 4.2. High crude fat composition was registered in avocado at 9.03%, while protein was lowest in tomato at 0.57%. Low crude protein content in fruits had earlier been observed by Pugalenthi *et al.*, (2004). Roger *et al.*, (2005) reported that the protein level of green leafy vegetables range from 20.48-41.66% while in this study, 1.53 – 3.49% was observed. Roger *et al.*, (2005) worked on fresh samples while in this study, discarded samples were used hence the difference. The crude fiber in this study was in the range of 0.54 – 2.61%. The fiber

levels in pumpkin leaves are similar to the one obtained by Javid *et al.*, (2010), at 0.94%. The carbohydrates, proteins and fat levels in avocado were: 3.37, 1.32 and 9.03 % respectively while in mango, 9.91, 0.87 and 0.68 % were observed. The energy obtained for fresh waste was lowest in tomato, courgette and cucumber fruits wastes. The obtained results for crude fat, proteins, fiber and carbohydrates are shown in table 4.2.

4.2.4 Ultimate composition analysis

The ultimate analysis involved the determination of carbon, nitrogen, sulfur, hydrogen and oxygen in oven-dried market waste samples using CHNSO elemental analyser. The building blocks of these market wastes are made of carbon, hydrogen, oxygen, nitrogen and sulphur. They form the carbohydrates, protein and lipids units of the organic matter. The carbon levels were highest amongst the ultimate properties ranging from 47.13 – 83.20%. Cucumber and avocado carbon levels were 83.20 and 73.29 %, respectively. The observed levels of hydrogen were lowest in pawpaw at 6.55% and highest in avocado and cucumber at 11.05 and 11.59%, respectively. On average, most samples were observed to have hydrogen levels at 6.55 – 6.99%. The nitrogen content in the market waste samples was highest in coriander at 9.87%. Lower nitrogen levels were observed for fruit waste samples at the range of 3.05% -1.41%. In general, samples with high lipids levels possess long C-H chains. This translates to high methane potential though inhibit methanogenesis activities resulting to floatation of sludge (Neves *et al.*, 2009; Das & Mondal, 2016). For example, the lipids/fat levels in avocado in this study were observed at 9.03%. This carbon and hydrogen contents were 73.29 and 11.06 %. Similar findings were observed by Neves *et al.*, (2009) and Das & Mondal, (2016). The results obtained are shown in table 4.3.

Table 4.3: The ultimate analysis properties of fruits and vegetable waste

SAMPLE	%C	%H	%O	%N
Kales	50.34±2.89	6.77±0.77	36.71±5.76	6.18±1.12
Cabbage	47.45±7.23	6.48±1.88	42.97±9.91	3.11±0.08
Pumkin Leaves	50.48±10.11	6.85±1.56	35.31±7.55	7.36±1.22
<i>Cucumis ficifolia</i>	50.60±8.94	6.85±1.00	35.35±3.24	7.19±1.76
Pigweed	51.24±5.88	6.91±1.00	33.67±5.11	8.18±1.17
<i>Erucastrum arabicum</i>	50.71±10.11	6.85±0.12	34.74±2.99	7.78±0.09
Coriander	51.64±2.99	6.91±1.90	31.58±2.67	9.87±0.99
African nightshade	51.09±12.89	6.91±1.22	34.46±2.21	7.54±1.99
Spinach	50.69±11.92	6.81±1.09	35.71±3.77	6.80±0.12
Comfrey	50.32±6.13	6.84±1.18	35.59±2.61	7.24±1.71
Tomato	47.18±6.80	6.61±0.66	43.47±4.43	2.73±0.87
Potato	47.13±6.73	6.57±1.98	44.37±2.11	1.93±0.08
Sweet Potato	47.66±10.03	6.71±1.11	44.29±5.10	1.34±0.15
Pawpaw	46.85±6.13	6.55±0.72	45.20±8.93	1.41±0.02
Banana	47.44±6.32	6.58±0.76	42.99±2.66	2.99±0.15
Avocado	73.29±8.91	11.06±2.55	13.76±2.13	1.88±0.02
Courgette	51.06±7.81	6.99±1.11	36.28±3.46	5.67±1.06
Cucumber	83.20±14.11	11.59±1.88	0.01±0.00	5.21±0.74
Mango	47.73±6.44	6.70±2.63	44.16±6.67	1.41±0.01
Water Melon	48.68±8.67	6.78±0.77	41.49±7.44	3.05±0.06

Oxygen from the samples was obtained by summing up the carbon, hydrogen and nitrogen levels and subtracting from 100. It was assumed that these are the only elements making up the FVMW samples. The observed oxygen levels were lowest in cucumber at 0.01%, with all the other samples having oxygen levels at the range of 31.57 - 45.20%.

Asquer *et al.*, (2013) reported C, H and O in dry weight potatoes at 15 %, 6.5 % and 43

%, in fruits at 22 %, 6.5 % and 44 % and vegetables at 20 %, 6.5 %, 40 % respectively. The physical-chemical tests for specific fruits and vegetable wastes are shown in table 4.4. The TS were obtained by subtracting moisture content from 100. The fresh tomato waste was observed to have moisture levels of 95.16 compared to 4.84% on a dry weight basis. Deressa *et al.*, (2015) reported moisture content levels of 83.15%. Previous studies by Mohammed *et al.*, (2017) showed moisture content of 90.75%. Adubofuor *et al.*, (2010) reported ash content of 2.89 – 7.33% in tomato samples.

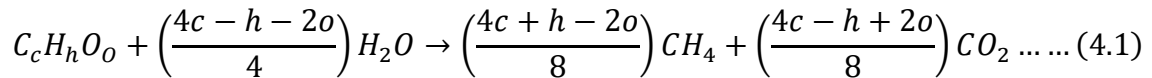
Table 4.4: Physical properties of various market wastes

Sample	% Moisture		Total Solids		% Ash		%Mineral Matter		%Volatile Matter		% Fixed Solids	
	WET	DRY	WET	DRY	WET	DRY	WET	DRY	WET	DRY	WET	DRY
Kales	89.85	10.53	10.15	89.47	1.94	18.45	2.134	20.295	8.21	71.02	6.27	52.57
Cabbage	94.87	5.13	5.13	94.87	0.49	9.7	0.539	10.67	4.64	85.17	4.15	75.47
Pumkin Leaves	90.78	8.77	9.22	91.23	2.06	23.86	2.266	26.246	7.16	67.37	5.1	43.51
<i>Cucumis ficifolia</i>	86.62	13.38	13.38	86.62	2.34	17.52	2.574	19.272	11.04	69.1	8.7	51.58
Pigweed	88.64	11.36	11.36	88.64	2.86	25.26	3.146	27.786	8.5	63.38	5.64	38.12
<i>Erucastrum arabicum</i>	89.37	10.63	10.63	89.37	1.99	18.76	2.189	20.636	8.64	70.61	6.65	51.85
Coriander	92.12	7.88	7.88	92.12	1.91	24.3	2.101	26.73	5.97	67.82	4.06	43.52
A. Nightshade	88.15	11.85	11.85	88.15	1.97	16.67	2.167	18.337	9.88	71.48	7.91	54.81
Spinach	93.27	6.73	6.73	93.27	1.73	25.67	1.903	28.237	5.00	67.6	3.27	41.93
Comfrey	85.04	14.96	14.96	85.04	3.46	23.13	3.806	25.443	11.5	61.91	8.04	38.78
Tomato	95.16	4.84	4.84	95.16	0.46	9.53	0.506	10.483	4.38	85.63	3.92	76.1
Potato	83.78	16.21	16.22	83.79	0.81	5.02	0.891	5.522	15.41	78.77	14.6	73.75
Sweet Potato	62.05	37.94	37.95	62.06	1.06	2.81	1.166	3.091	36.89	59.25	35.83	56.44
Pawpaw	89.22	10.78	10.78	89.22	0.50	4.65	0.55	5.115	10.28	84.57	9.78	79.92
Banana	74.3	25.70	25.70	74.30	1.67	6.53	1.837	7.183	24.03	67.77	22.36	61.24
Avocado	82.83	17.17	17.17	82.83	0.84	4.92	0.924	5.412	16.33	77.91	15.49	72.99
Courgette	95.34	4.65	4.66	95.35	0.72	15.58	0.792	17.138	3.94	79.77	3.22	64.19
Cucumber	95.86	4.14	4.14	95.86	0.46	11.14	0.506	12.254	3.68	84.72	3.22	73.58
Mango	86.82	13.18	13.18	86.82	0.44	3.33	0.484	3.663	12.74	83.49	12.3	80.16
Water Melon	92.85	7.14	7.15	92.86	0.74	10.49	0.814	11.539	6.41	82.37	5.67	71.88

The total solids volatile matter in these wastes were samples were reported at a range of 3.68 – 36.89 and 59.25- 85.63% on wet and dry weight, respectively. The TS of 29.5% and 11.8% were reported in banana and tomato, respectively, which are similar to what was obtained in this study at 25.70 and 4.84%, respectively. The obtained TS levels are

significant enough for AD of market wastes. Balsam (1996) reported that 7-9 % is the optimal TS levels for substrates employed in the biogas generation (Zennaki *et al.*, 1996). The instability of the AD was reported for substrates with TS below 7% (manure) with overloading reported for substrates with TS greater than 10% (Baserja, 1984). Similar results were reported for TS and VS for avocado 14.9, 13.55%, mango 9.01, 8.51%, papaya 6.08, 5.22% and watermelon 3.57, 2.43% (Gerardi, 2003).

The volatile matter represents the degradable portion of the samples during anaerobic digestion (Asquer *et al.*, 2013). The general observation was that the MM, VS and TS were higher in fruits than in vegetable wastes. This had earlier been reported by Asquer *et al.* in 2013. The TS of the fruits were on average, 7.5 - 23%, while in the vegetables, they are 3-11%. Moisture is a significant parameter that affects affecting AD of solid wastes Sadaka and Engler (2003). This is because water enables the growth and movement of microbes by dissolving and transporting nutrients in addition to lowering the mass of particulate substrate. In mathematical terms, water allows hydrolysis of the elemental composition of substrates, as shown in equation 4.1 (Speece, 1996).



Gelegenis *et al.*, (2007) noted that the water used in biogas generation during AD of organic substrate contain ultimate elements as shown by reaction equation 4.1. Alemu and Tesfaye (2019) reported similar results for organic carbon, total solids and moisture levels for mango, cabbage, papaya, potato, tomato and avocado. They said TS solids at 24.47% in avocado fruits and maximum moisture content of 95.02% in tomato fruits.

4.3 Inoculum studies

Theoretically, the inoculum is among the most critical parameter that dictates biogas generation and methane content in biogas (Moreno-Andrade and Buitrón, 2004). The inoculum was analyzed in terms of concentration, storage time and source. The two inocula used in waste digestion in this study were fresh cow dung and rumen fluid. They were analyzed for microbes (total viable count (TVC)) as per Miles and Misra (1938)

method as described in Okore (2004), as well as physicochemical properties according to AOAC, (2000), and the results were discussed.

4.3.1 Inoculum analysis

The results obtained for the bacteria counts from the rumen fluid and fresh cow dung are shown in table 4.5. The bacterial counts in manure were $1.50 \pm 0.02 * 10^{10}$ cfu/g, while in rumen fluid, it was $3.15 \pm 0.01 * 10^{10}$ cfu/mL. The results show twice as many microbes in rumen fluid compared to cow dung.

Table 4.5: Total microbes count from dung and rumen fluid samples.

Sample	Count	unit
Rumen fluid	$3.15 \pm 0.01 * 10^{10}$	cfu/mL
Cow dung	$1.50 \pm 0.02 * 10^{10}$	cfu/g

Deepa *et al.*, (2018) observed highest bacterial colony counts in cow rumen fluid (434.33) followed by goat (262.67) and chicken (170.67) in a colony counts study of bacterial species from rumen fluids of different animals. Ozbayram *et al.*, (2018) and Liu *et al.*, (2016) observed twice as many microbes in rumen waste compared to manure. The standard of any manure employed in anaerobic degradation is determined by the total viable count (Ezekoye and Ezekoye, 2009). Total cfu/g of bacteria of $(1.78 - 2.84 \pm 0.01 \times 10^5)$ cfu/g) was reported in three samples of cow dung collected from different farm by Kiyasudeen *et al.*, (2015). The serial dilution methods developed by (Frazier and Westhoff, 1995; Talaro, 2009) were used to assess the bacterial population. The total viable count (TVC) is a critical metric for determining the quality of dung for use as manure or as a biofuel source. Gagandeep's, (2017) study enumerated TVC in three cow dung samples ranging from $1.9 * 10^6$ to $2.8 * 10^6$ cfu/g. Ambar *et al.*, (2017) reported TVC of $9.55 * 10^8$ and $1.32 * 10^8$ cfu/g, respectively in cow manure and cow rumen waste. Van Vliet *et al.*, 2007 observed 3,700 µg of C/g of dry matter in dung depending on the protein composition of cow's diet. Moreno-Andrade and Buitrón (2004), showed that the inoculum concentration of dictates the speed of substrate biodegradation. The

time elapsed from sampling has no significant influence on microbial degradation waste (Shelton and Tiedje, 1984). However, rumen waste should be used within four days of sampling. Inoculum sources influence the substrate degradability due to different levels of microbial population and diversity (Moreno-Andrade and Buitrón, 2004; Tabatabaei *et al.*, 2010).

Further, table 4.6 present some biochemical analysis results for the slaughterhouse waste and the cow dung used as inoculum in this study. The samples pH was in the bracket of 7.23 – 7.30 for the two samples, which is the optimal pH for biogas generation. The observed TS was 26.30% and 21.32% in rumen waste and dung, respectively. Budiyo *et al.* (2011) obtained comparable data., at 20.23±1.94% in cow dung.

Table 4.6: Cow dung and slaughterhouse waste biochemical properties

Parameters	Rumen waste	Cow dung
pH	7.23±0.11	7.30±0.52
Total solids (%)	26.30±1.20	21.32±1.00
Volatile solids (%)	81.69±1.52	73.50±2.20
Nitrogen (%)	1.92±0.02	3.21±0.09
Carbon (%)	56.87±2.22	54.60±1.26
C:N	29.62±0.51	17.06±0.50

The TS, MC, VS, FS, nitrogen content, organic carbon % and C/N ratio of goat manure and cow rumen fluid were 97.1, 2.9, 63.8, 36.2, 2.5, 40.1 and 16.0% for goat manure and 36.0, 64.6, 73.2, 26.8, 1.6, 54.3 and 33.0% for rumen fluid, respectively (Gammaa *et al.*, 2015) which is comparable with the current study.

Budiyo *et al.*, (2011) further reported VS at 18.11±1.70%, which relates well with the results of this study of 73.50 ± 2.20% in cow dung calculated from TS. The reported carbon and nitrogen levels from dung and rumen wastes were 56.87 ± 2.22 and 54.60 ± 1.26 and 1.92 ± 0.02 and 3.2 ± 0.09%, respectively. Pratima and Bhakta (2015) reported similar results for C: N ratio of 22.75 and 19.81 in slaughterhouse matter and dung, respectively. Osman *et al.*, 2015 showed that TS, MC, VS, FS, nitrogen content (N),

organic carbon (C) and C/N ratio OF 36.0, 64.6, 73.2, 26.8, 1.6, 54.3 and 33.0% respectively in rumen fluid. The cow dung pH value and moisture level obtained in this study of 7.30 and 73.70% were in range with those obtained by Chinwendu *et al.*, (2013) reported of 7.10 and 68.55%. Similar results were obtained from three cowdung samples from different farm by Kiyasudeen *et al.*, 2015 of 80.73 – 90.21%. A total carbon (41.89±0.11%), total nitrogen (2.65±0.01%), crude protein (16.90±0.06%) and organic matter (75.40±0.2%) were reported by Kiyasudeen *et al.*, 2015 which are similar with the levels obtained in this study. The pH values (7.23) and volatile matter (81.69%) obtained in this study are in line with those observed by Chaudhry (2008) who observed a pH range of 6.8 – 7.3 and volatile matter of 82.4 % from slaughtered cow rumen content.

Similarly, Kiyasudeen *et al.*, (2015) noted a pH bracket of 6.6 – 7.5 from three cow dung samples from different farms. The percentage total carbon (54.60) and nitrogen (3.21) obtained in the current study also related to those obtained by Kiyasudeen *et al.*, (2015) of 41.89 and 2.65, respectively. Carbon and nitrogen are the main nutrients required by micro-organisms (Doerr and Lehmkuhl, 2008). The optimum C/N ratio for biogas production is 20 to 35:1 (Kamau *et al.*, 2020). Annor *et al.*, (2018) calculated C/N ratio from his study at 35: 1.48. which compares with the one obtained in this study at 17.06:1 in dung. Chenamani, (2018) reported that the volatile solids ranging from 70% to 90% were present in Kumasi abattoir waste with a pH range of 6 – 8. Higher volatile solids content is important as they reflect the amount of the total gases that can be produced from the substrate. Further, the moisture content for cattle rumen content waste varied between 78% and 88%. The total solids values for rumen content ranged from 10% to 20% while most of the sample total solids were below 15% (Chenamani, 2018). Investigations by Na Li *et al.*, (2018) and Deepanraj *et al.*, (2015) showed that rumen waste content which has 10% total solids is best suitable for anaerobic digestion.

Chenamani (2018) reported lower Nitrogen levels of 1.8% to 2.8% in rumen matter which correlate with the ones obtained in this study at 1.92%. Therefore, the rumen content might be considered more suitable for biogas production, as it contains low nitrogen, to form low ammonium nitrate. High ammonium nitrate inhibits biogas production from growth and function. The carbon content level varying from 40% to 50%

reported by Chenamani (2018) were lower than 56.87% reported in this study. Gammaa et al. (2015) showed that Cattle manure had 73.2% moisture content, 36.0% total solids, 26.8% Ash content, 73.2% volatile solids, 54.3% carbon and 1.6% nitrogen content.

Chudoba *et al.*, (1991) noted that ISR is a vital factor in batch tests. In an inter-laboratory study, ISR was highlighted as an essential factor in AD process. Bio-methane potential (BMP) calculations are based on ISR to control the AD process. $ISR \geq 2.1$ is the recommended concentration for the total breakdown of organic matter (Chudoba *et al.*, 1991). The trace elements in the inoculums used in these studies are shown in table 4.7. Most components were higher in the rumen fluid matter as compared to cow dung.

Table 4.7: Trace elements in the inoculums

ELEMENTS	COW DUNG (mg/l)	RUMEN MATTER (mg/l)
Calcium	3.09±0.02	3.92±1.32
Potassium	5.01±1.11	5.22±1.55
Aluminium	0.05±0.01	0.21±0.02
Copper	3.78±0.05	2.47±0.09
Cobalt	1.28±0.01	2.33±0.55
Zinc	1.44±0.04	1.62±0.22
Cadmium	0.09±0.01	0.11±0.01
Iron	2.54±0.11	2.89±0.90
Manganese	4.37±0.52	4.65±1.22
Nickel	0.09±0.02	0.27±0.07
Silver	0.34±0.11	0.44±0.05
Molybdenum	2.66±0.23	3.01±1.12
Phosphorus	1.47±0.07	1.52±0.04

The reported concentrations of calcium and potassium were 3.09 ± 0.02 and 3.92 ± 1.32 and 5.01 ± 1.11 and 5.22 ± 1.55 ppm in cow dung and rumen waste, respectively. The trace elements in the inocula are as reported in table 4.7. These trace elements are essential for microbial growth. The influence of trace content on biogas and CH₄ generation inhibition has been reported by Dokulilová *et al.*, (2018). Atkinson *et al.*, (1958) and Sager, (2007) reported trace elements like Hg, Be, Cd and Co in manure samples with Pb, Ag and Sb at trace levels. Faridullah *et al.*, (2014) reported a pH of 7.5 in fresh cow dung and P, K, Ca and Mg levels of 119, 81.6, 263.2, 70, 8.3 ppm respectively. The trace elements levels in rumen and dung are highly influenced by the animal diets and water intake (Spears, 2003).

4.4 Biogas production

This section present and discussed the biogas production from market wastes using cow dung or rumen fluid as inoculum. Unless otherwise stated, the inoculum to substrate ratio was 1:1 without initial pH adjustments. Further, the wastes were sorted into the organic and inorganic matter, after which the substrate was washed, sliced, and blended before introducing to the digesters. Biogas generated from individual wastes is reported.

4.4.1 Pressure Tests

This test is vital to ensure no biogas leakages from the digester for accurate reporting. The tests were carried out for the different types and capacities digesters employed in this study. This involved reacting vinegar with baking soda at an enclosed system. The results (figure 4.6) obtained showed that pressure remained constant throughout the test period for all the digesters used in this study. This revealed the absence of leakages in the digester and, therefore, accurate measurement of the produced biogas. Results may have been affected by temperature, pressure gauge accuracy.

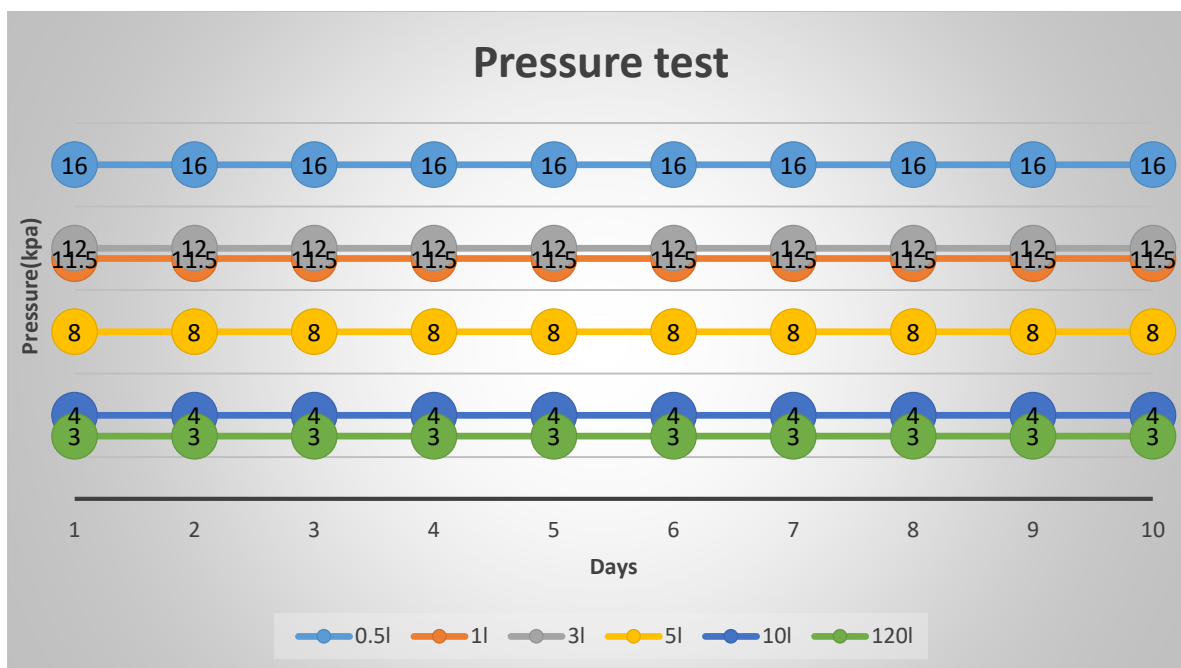


Figure 4.6: Pressure tests line plots

For the 0.5 L digesters, the pressure readings were 16 kpa while the pressure gauge reading remained 8 kpa for 5 L digester. The tests were carried out for 10 days as depicted in figure 4.6. The pressure tests were important for accurate measurement of biogas generated ensuring that no gas leaks.

4.4.2 Biogas Measurement

The quantity of biogas recovered from wastes can be quantified manometrically, volumetrically or gravimetrically (Valero *et al.*, 2016). At laboratory scale two methods are employed in BPM tests to measure biogas generated: volumetrically by providing constant pressure and measuring the volume of biogas by displacement volume devices, or manometrically by keeping the volume constant and measuring increases in pressure (Rozzi and Remigi, 2004; Parajuli, 2011; Pham *et al.*, 2013). Gravimetrically, the bottles are weighed after venting biogas that accumulated during each measurement interval, and a sub sample is analyzed for composition (Alduchov and Eskridge, 1996). In the current study, gravimetric and volumetric biogas measurement method were compared. The results obtained are shown in figure 4.7

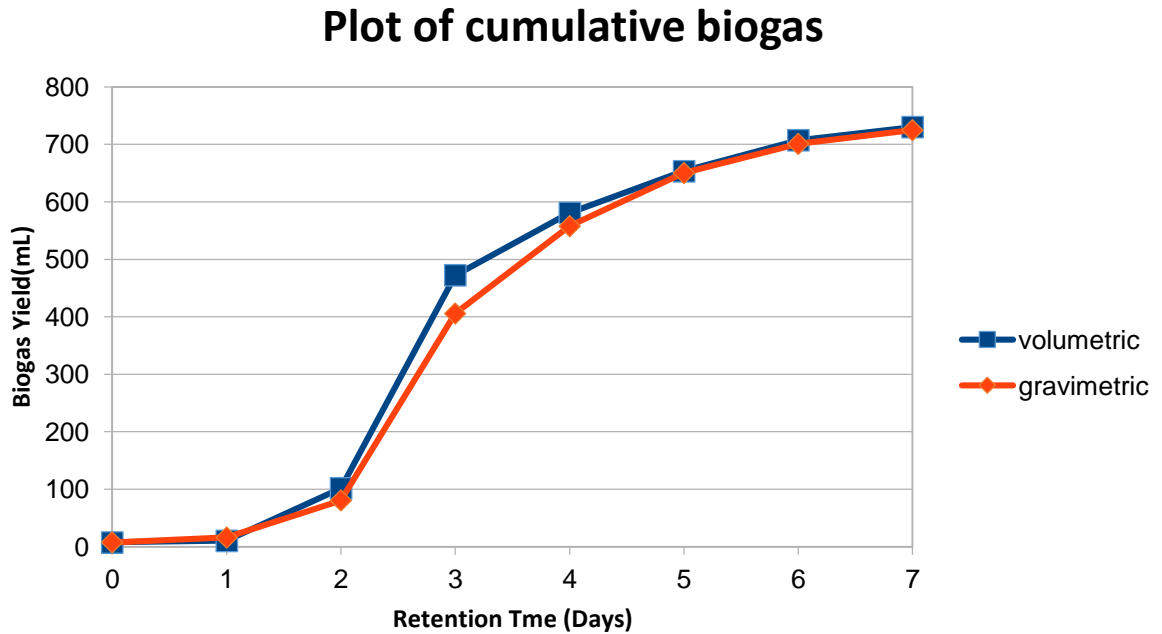


Figure 4.7: Plot of volumetric and gravimetric measured biogas

The change in mass of the bottle (reactor) was recorded and the conversion to volume achieved as demonstrated by Hafner *et al.*, (2019). From these plots, there was no major variation in biogas yield measured between the two methods. The average measured biogas measured was 408.05 mL and 392.94 mL for volumetric and gravimetric, respectively. The variation resulted from standardization and conversion of loss in mass using the online application. Volumetric method was adopted henceforth in this work unless otherwise stated.

Waste digestion to biogas (control study) was done at psychrophilic state for the fruits and vegetable wastes without inoculation. This was the control for the fruits and vegetable wastes at psychrophilic conditions. The volumetric biogas produced for the seven days' retention time is illustrated in figure 4.8. Low biogas yields were observed in banana and sweet potato wastes at 20mL and 24mL, respectively. The operation temperature was in the range of 20⁰C – 27⁰C depending on day's weather. The fruits waste mix cumulatively produced the highest gas amongst the fruits samples at 247mL on day 7. This is explained by the availability of higher levels of proximate properties in comparison to individual fruit samples as earlier noted by Kamau *et al.*, (2020).

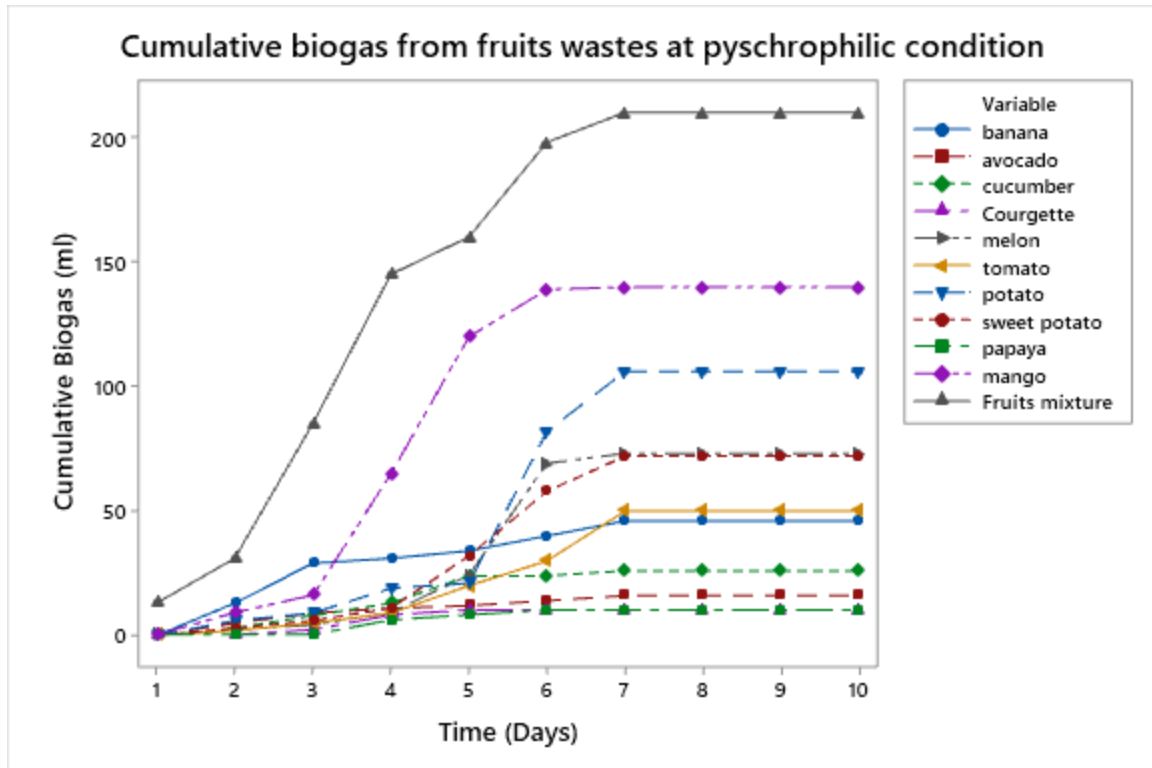


Figure 4.8: Biogas produced from fruit wastes at psychrophilic conditions

Pathogenic microfloras are some of the habitat of fruits surfaces, though non-pathogens, and opportunist pathogens are also observed (Alegbeleye *et al.*, 2018). The fruits skin covers it from yeast, molds and bacteria attacks. The micro-organisms come from soil insects and air and farmers (Al-Kharousi *et al.*, 2016). Among the most common microbes on fruits skin surfaces are; *Staphylococcus*, *Enterobacter*, *Shigella*, *Salmonella*, *E. coli*, *Bacillus cereus*, *Pseudomonas*, *Erwinia*, *Enterobacter*, and *Lactobacillus sp.* (Pao, 1997), *Rhizopus*, *Aspergillus*, *Penicillium*, *Eurotium*, *Wallemia*, *Saccharomyces*, *Zygosaccharomyces*, *Hanseniaspora*, *Candida*, *Debaryomyces*, and *Pichia sp.* (Kalia and Gupta, 2006). These microbes are responsible for decay and decomposition of the fruits waste anaerobically or aerobically (Alegbeleye *et al.*, 2018; Al-Kharousi *et al.*, 2016). Further, the biogas generation from leafy vegetables was carried out, and the results obtained were used to plot figure 4.9. The figure shows green vegetable mixture samples cumulatively yielded highest biogas followed by kales wastes at 167 mL.

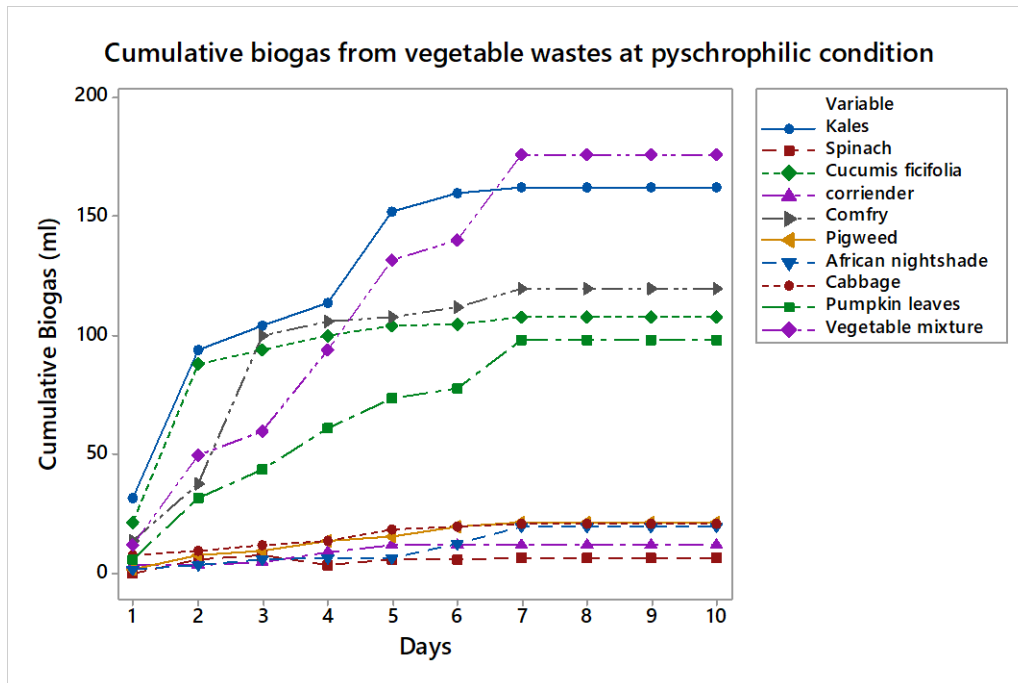


Figure 4.9: Biogas produced from vegetable wastes at psychrophilic conditions

Biogas production is positively influenced by the presence of microbes from the bovine stomach (Kamau *et al.*, 2020). These microbes produce biogas by breaking down the fruits and vegetable wastes. In figures 4.8, 4.9 and 4.10, the wastes were digested without any inoculum. Low biogas yields were observed in fruits and leafy vegetables. The gas produced had low levels of methane at levels ranging from 23.09 % to 47.34 %. The production rates plateaued around day 5, with abrupt pH changes being observed. Figure 4.10 showed a combined bar graph plots of cumulative biogas production for the control experiment at room temperature conditions.

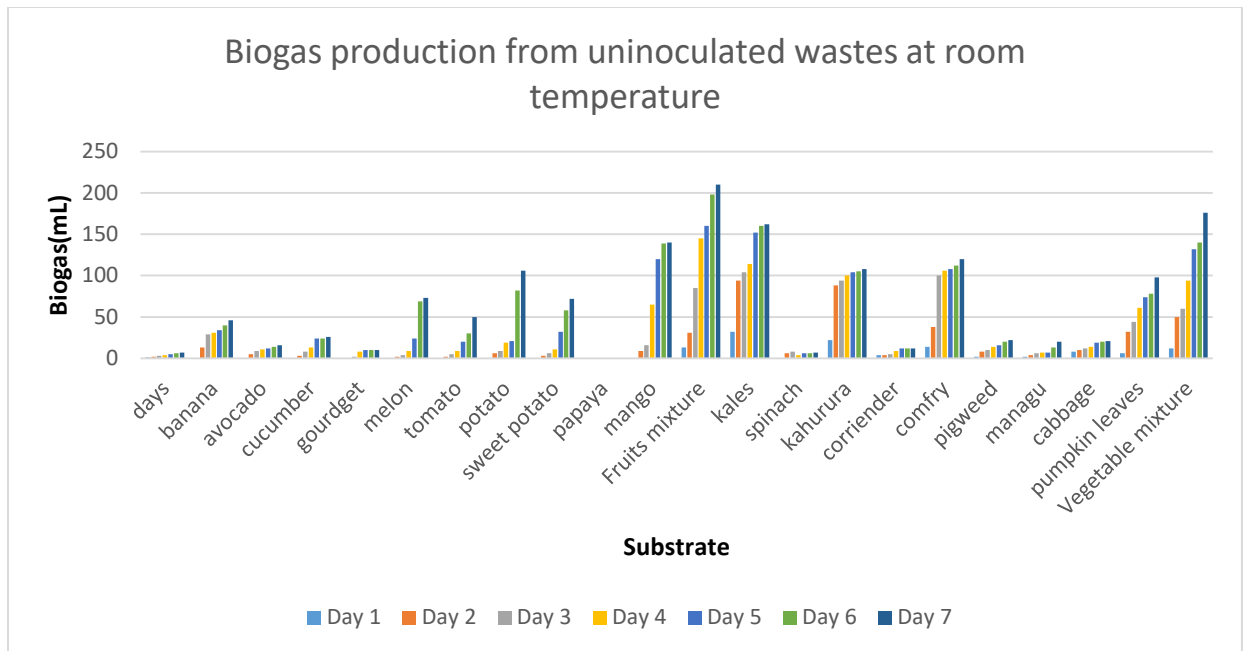


Figure 4.10: Biogas produced from wastes at psychrophilic conditions

Biogas production was observed to be high for the fruits mixture compared to vegetable mixtures. This is explained by the low lignin levels and high volatile matter and low C: N ratio in fruit wastes. High carbon levels and low nitrogen content in leafy vegetables leads to higher C: N ratio, which inhibits biogas generation emanating from ammonia formation in the reactor. In the event C: N is beyond the limit, the low yield was witnessed because acidogens depletes nitrogen more rapidly than methanogens. If too low, bacteria consume up nitrogen for growth. Carbon deficiency leads to low acid formation, and therefore, pH rises due to NH_4^+ (Yen & Brune, 2007), which adversely affects biogas production. Higher biogas production from fruits compared to leafy vegetables had previously been observed by Kamau *et al.*, (2020) using fruits and market waste samples.

In figure 4.11, biogas production was observed for thirty days' retention time. The wastes were inoculated with rumen fluid from Dagoretti slaughterhouse. Psychrophilic conditions were assumed at 22 – 27°C. Biogas generated was highest in FVMW mixtures at 1400mL reported in day 6. The biogas generated was rich in methane at 46 – 63%. The

rate of production was high from day one to day 6 or 7 after which gas production stabilized.

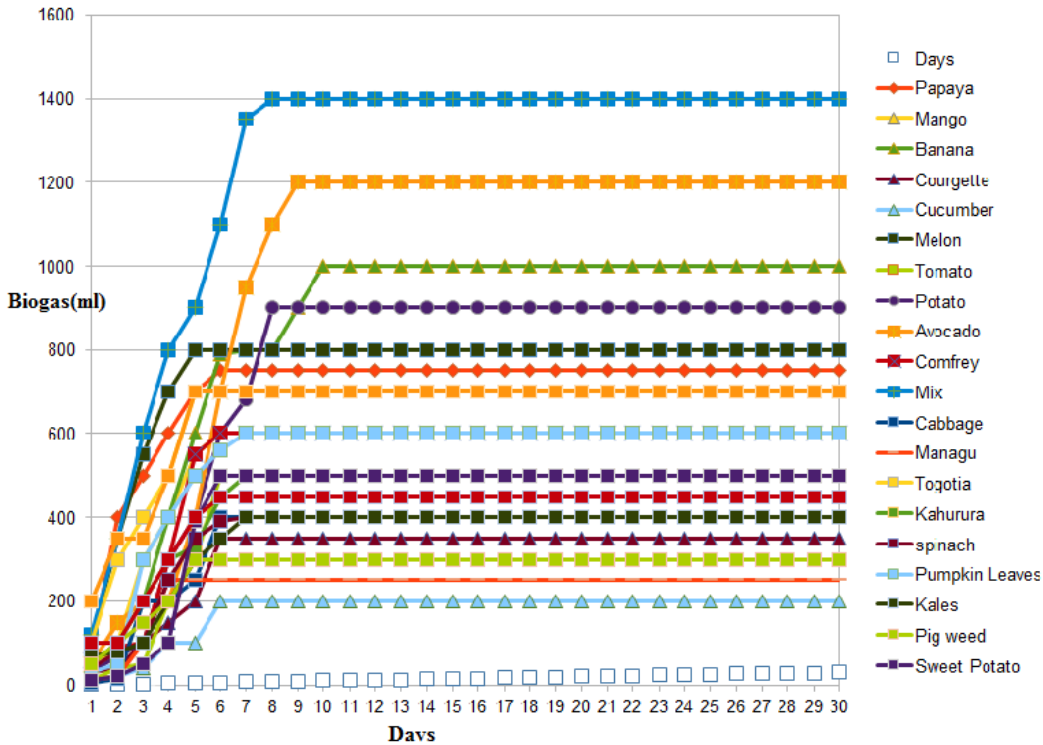


Figure 4.11: Biogas produced from market wastes mixtures at psychrophilic conditions

The general trend of the market wastes was high biogas production in wastes with high levels of fat like avocado at 1200 mL on day 9. Mbugua *et al.*, (2019) observed high biogas from avocado wastes co-digested with cow dung. The pH of the digester becomes acidic with time and therefore, biogas production is slowed. The high concentration of microbes in the rumen wastes means that there is completion for available substrate and therefore increased rate of biogas formation. The volatile matter was depleted by day 7, and therefore the microbes start dying, which eventually translates to a downward trend of biogas yield. Figure 4.11 illustrates the cumulative biogas generated. As shown in figure 4.11, biogas generated from cucumber and African nightshade(manage) was lowest at 200mL and 230 mL, respectively. Low fats and carbohydrate levels explain this trend. Burade and Bhagat, (2016) used fruits wastes as substrate. They observed that the biogas generation is affected by temperature and inoculum. In addition, gas generation was low in winter at 75 mL after

30th day. This was the general trend observed in this study; gas production was higher during sunny warm days compared to cold days. Co-digestion of FVMW with rumen fluid increased biogas produced a twenty to fifty-fold for most wastes. For instance, uninoculated banana waste produced 45 mL on day seven while the introduction of rumen fluid resulted in gas production of 1000 mL. This was also witnessed for other wastes.

4.4.3 Influence of different inoculum on biogas production

Waste conversion to renewable energy involves microbial degradation. The degradation rate is highly influenced by microbial counts, temperature, pH, among other operating conditions. From the bacterial count studies, it is evident that the rumen waste inoculum produced the highest biogas, as shown in figure 4.12. Ruminant animal's rumen harbors anaerobes which breakdown cellulosic matter (Aurora, 1983).

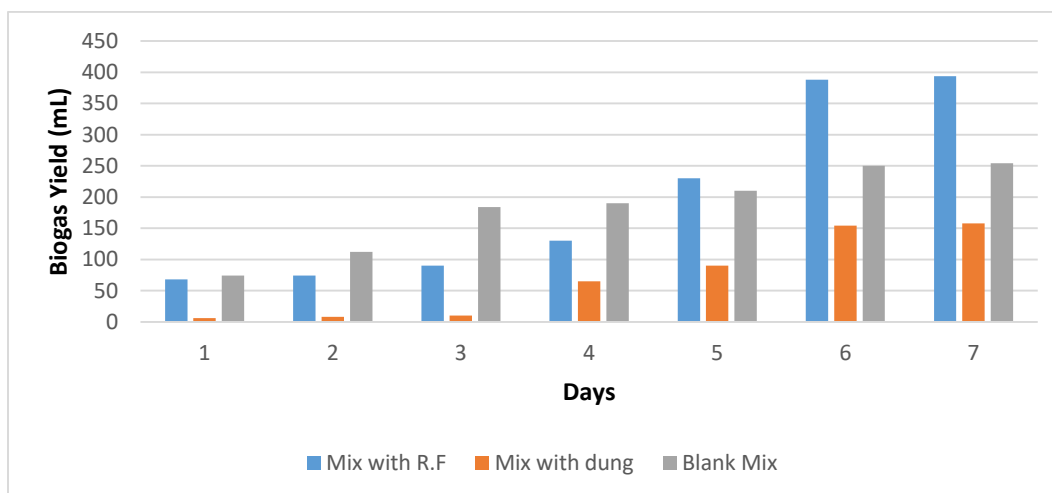


Figure 4.12: Biogas produced from market wastes inoculated with dung and rumen at psychrophilic conditions.

The high COD, BOD, and moisture content of abattoir effluent make it ideal for anaerobic digestion. The abattoir wastewater also includes high amounts of suspended organic solids, such as fat, oil, fur, feathers, manure, grit, and undigested feed, all of which contribute to the slow biodegradability of organic matter (Zafar, 2020).

Co-digestion of FVMW with rumen fluid recorded the highest biogas production at 390 mL on day seven compared to 170 mL for dung with FVMW and 260 mL for the blank

mix. The fact that the lower rate of anaerobic digestion is shown by waste inoculated with cow dung suggested that other factors inhibit biogas production using cow dung. The C:N ratios and the influence of pH plays a bigger role in this waste to biogas conversion. The high rate of production was witnessed for blank waste compared to the co-digested wastes. This is because the microbes require time to adapt to the substrate environment before they initiate digestion as reported by Demirel and Scherer, (2008). The methane levels of the cumulative biogas from the three substrates was 27%, 52% and 57% for blank FVMW, FVMW in cow dung and FVMW in rumen waste. The presence of methanogenic bacterial community in dung and rumen fluid account for this observation. Biogas yields is highly dependent on microbial activities. Cow dung is widely employed as a substrate in the biogas field. The CH₄ in biogas is influenced by operation parameters and the substrate type and ranges between 55% and 80% (Vintilă, *et al.*, 2012; Dobre *et al.*, 2009). In figure 4.13, curves of biogas production from market wastes inoculated with cow dung while figure 4.13 showed the same with rumen fluid inoculum. The lower productions in some fruits can be attributed to low temperatures and pH of the substrates.

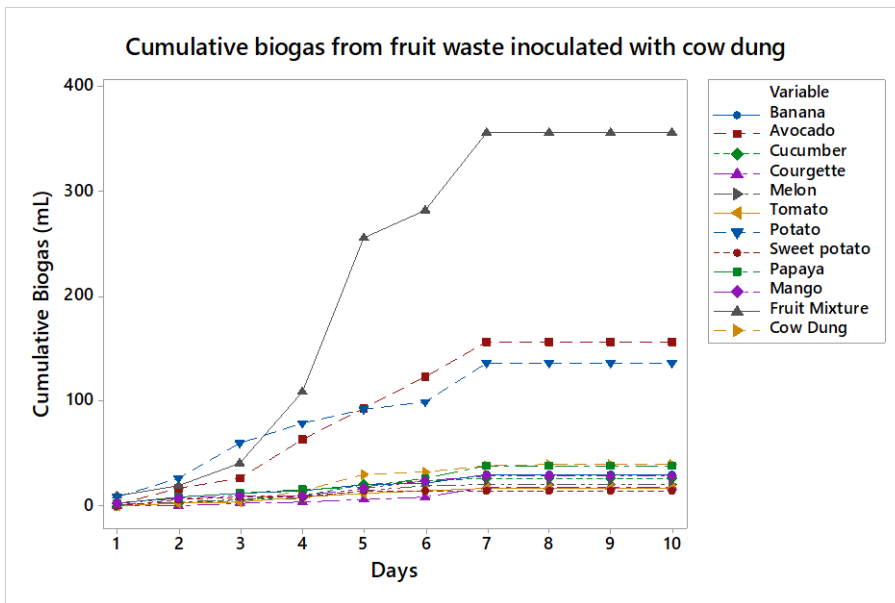


Figure 4.13: Biogas produced from fruit wastes inoculated with cow dung at psychrophilic conditions.

Lower levels of biogas production were reported for most wastes in fruits compared to the fruits mixture inoculated in cow dung. The cumulative biogas produced was 370 mL, 140 mL and 125 mL in fruit mixture, avocado and potato wastes respectively.

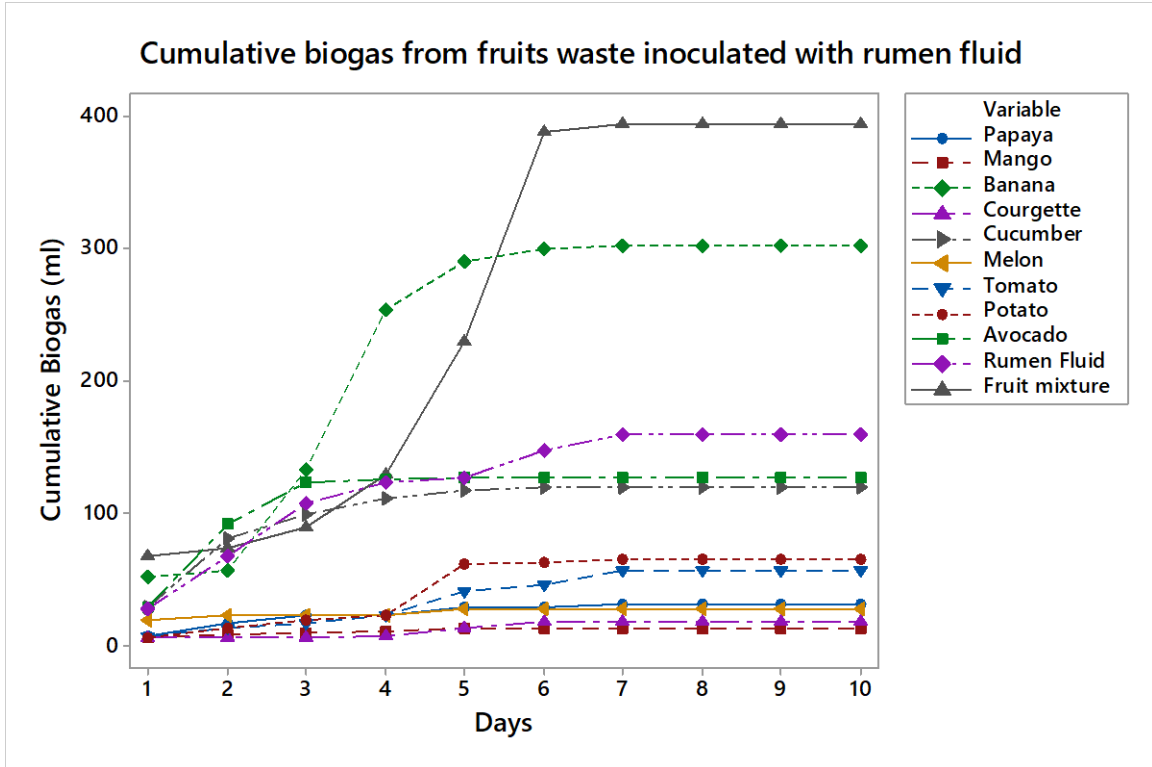


Figure 4.14: Biogas produced from market wastes inoculated with rumen fluid at psychrophilic conditions

In figure 4.14, avocado fruit waste was observed to produce the highest biogas followed by comfrey at 210 mL on day 7. Again, the effects of pH and temperature come into play for these wastes. The co-digestion of these wastes was started at a neutral pH of around 6.73- 7.23 but by day 5, the pH for most setups was lower at 4.34 – 5.50. This had also been studied by Adekunle and Okolie, (2015). The AD biochemical reaction can be divided into acid and methane formation steps. The acidogens and the methanogens vary in kinetics, physiology, sensitivity to environmental conditions and nutritional requirements (Pohland and Ghosh, 1971). The acidogens multiply at a higher rate (1–1.5 days) than the methanogens (5–15 days) (Gerardi, 2003).

Since higher cumulative biogas production was observed from wastes inoculated with rumen fluid, the rumen fluid waste was adopted as the main inoculum in this study.

Various investigations were done, including effects of different temperatures, C: N ratios and proximate properties on biogas production from market wastes. Figure 4.15 shows biogas production from un-inoculated wastes at mesophilic conditions. The lag phase is significantly reduced by co-digestion with rumen fluid which increased CH₄ formation and concentration (Ambar *et al.*, 2017).

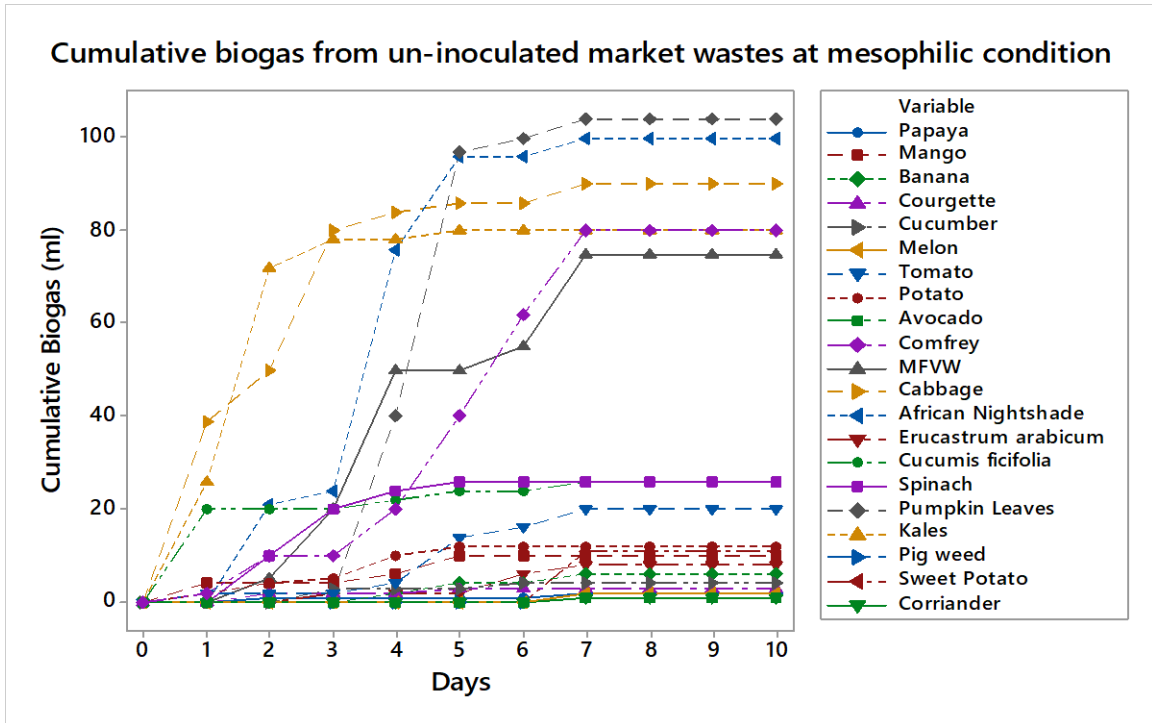


Figure 4.15: Biogas production from un-inoculated market waste at mesophilic conditions

The generated biogas at mesophilic condition was low ranging from 1- 120 mL in all the wastes. The methane levels were in the range of 34 – 47%. Biogas generation was initiated by co-digesting FVMW with rumen matter at three distinct temperatures. Methanogens are categorized into psychrophiles, mesophiles and thermophiles based on optimal temperatures of operations. The two inocula were compared for biogas generation for seven days. Figures 4.16, 4.17 and 4.18 show a comparison of daily biogas produced at three different temperatures using cow dung and rumen fluid inoculum with market wastes feedstock.

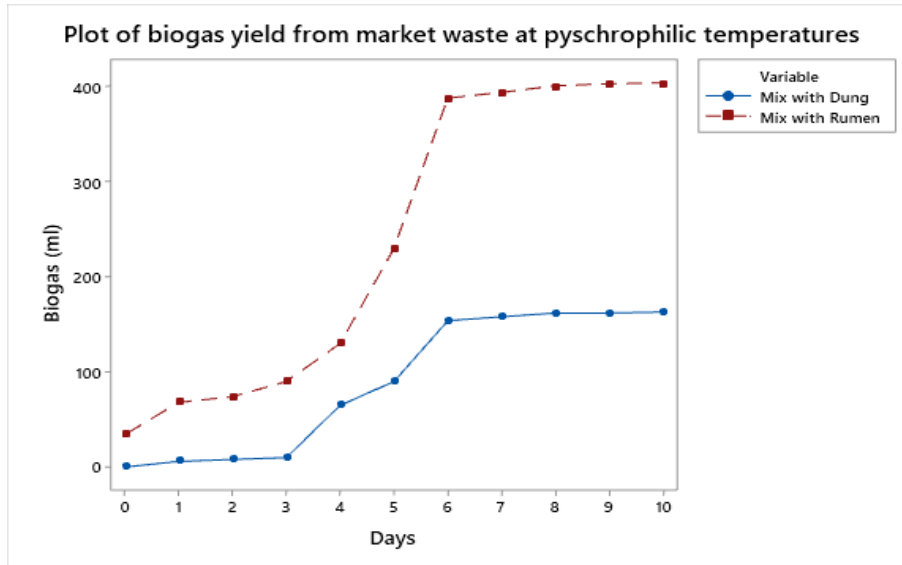


Figure 4.16: Surface plot of biogas production from market waste at psychrophilic temperatures.

During the seven days' retention time, rumen waste inoculated digester produced three times more biogas compared to cow dung. For instance, at day seven, rumen waste produced 457mL compared to 147mL for cow dung. This is explained by the high microbial community in rumen fluid. The findings revealed that adding rumen decreased the lag phase (hydrolysis and acidogenesis) prior to the production of methane. The peak in biogas production occurred after 20 days while inoculating with rumen matter, while the peak occurs later, after 30 days, in the control sample (Pertiwinigrum *et al.*, 2017).

In figure 4.17, biogas generation was initiated at 37 °C as described above. The amount of biogas generated was significantly higher in rumen waste as observed for the psychrophilic temperatures. The cumulative production was highest on day seven at 2900mL and 490mL for rumen and cow dung inoculum respectively. It was observed that biogas generated at mesophilic temperatures was three to seven times more compared to psychrophilic temperature. In addition, the rate of biogas generation was highly influenced by temperature.

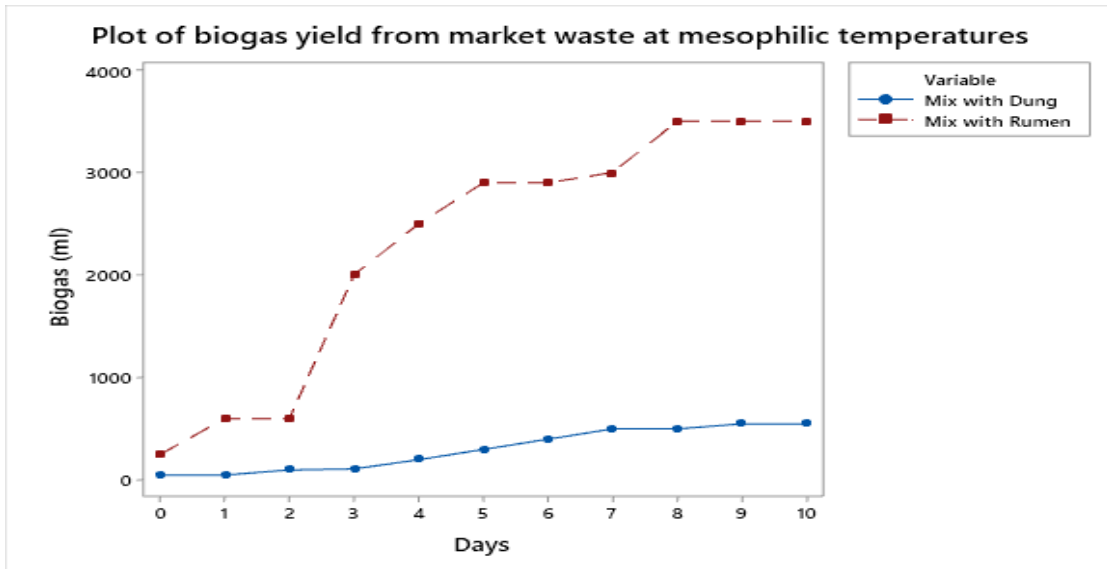


Figure 4.17: Surface plot of biogas production from market waste at mesophilic temperatures.

As shown in figure 4.18, the rate biogas generation at thermophilic temperature is higher compared to mesophilic and psychrophilic temperatures. The highest production was recorded in rumen inoculated reactors at 3200 mL compared to 530 mL in cow dung digester. In the thermophilic temperatures, the rate of the biochemical reactions is high, which implicitly result in high CH₄ yield.

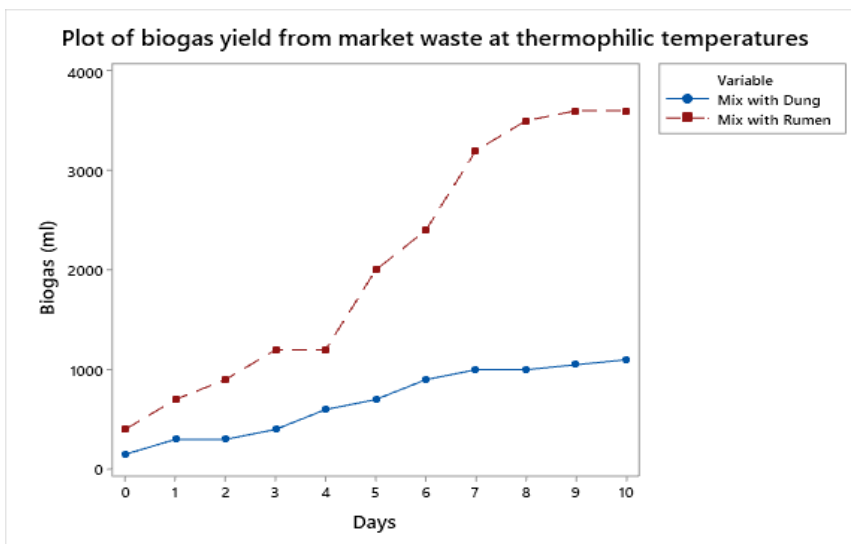


Figure 4.18: Surface plot of biogas production from market waste at thermophilic temperatures.

It was observed that thermophilic methanogens are very sensitive to temperature fluctuations ($\pm 1\text{ }^{\circ}\text{C}$), and have a longer lag phase. On the other hand, microbes at mesophilic temperatures can survive $\pm 3\text{ }^{\circ}\text{C}$ changes with low impact on biogas generation. Angelidaki, (2002) reported that thermophilic reactors have the higher substrate to biogas conversion rate than in mesophilic conditions.

Biogas generated from different market wastes inoculated with rumen waste and control at mesophilic temperatures is shown in figure 4.19 and 4.20, respectively. From the bar graph in figure 4.20, high biogas levels were recorded for African nightshade, cabbages, pumpkin leaves, kales, comfrey and mix samples at 100mL, 90mL, 104mL, 80mL, 80mL and 75mL respectively. This was the control for the mesophilic digesters as it was not inoculated. Lower percentages of methane content were observed at 39 - 48% in biogas. The pH drops were higher at mesophilic temperatures compared to psychrophilic temperatures. At higher temperatures, the acid build-up is high due to higher substrate degradation rate leading to pH drops and therefore, inhibition of anaerobic digestion.

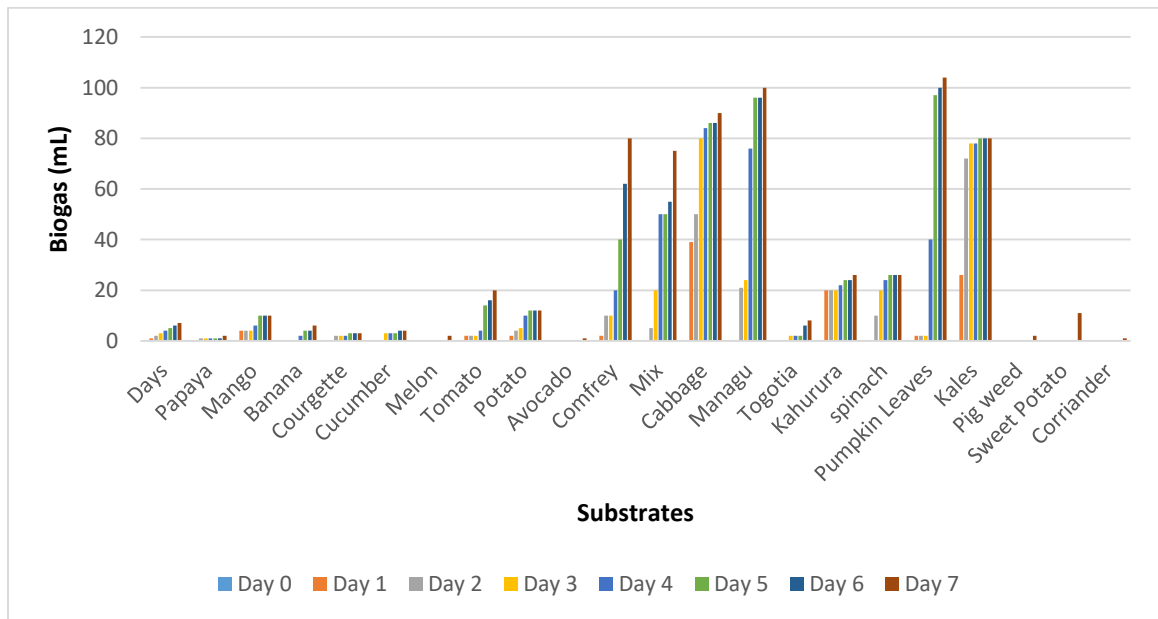


Figure 4.19: Mesophilic(37⁰C) biogas production from un-inoculated market wastes

High biogas generation was observed for wastes inoculated with rumen waste. From figure 4.19, high cumulative biogas was observed in FVMW sample at 3500mL followed

by sweet potato, potato and banana wastes at 2000 mL, 1700 mL and 1500 mL respectively. Pages *et al.*, (2011) reported that co-digestion increased biogas significantly.

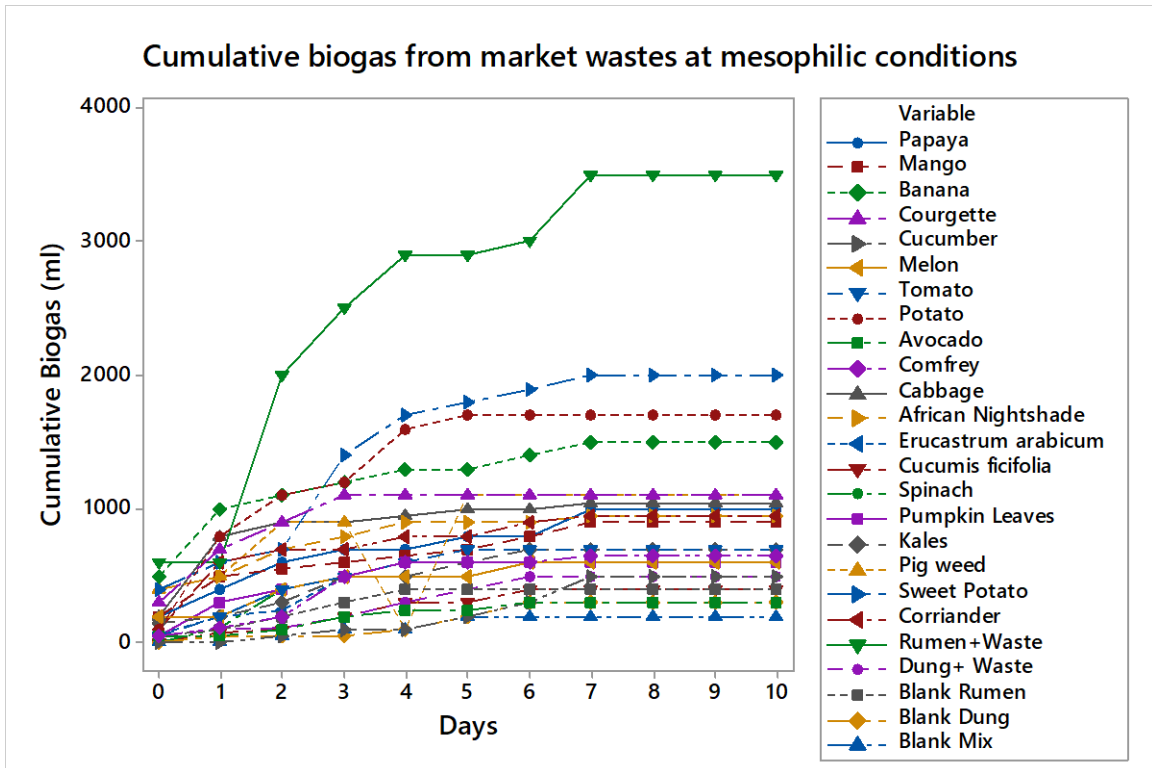


Figure 4.20: Mesophilic (37 °C) biogas production from inoculated market wastes

The results are explained by the fact that methanogens in rumen wastes degrade the volatile matter in the wastes generating biogas. In the FVMW sample, there is the availability of high levels of nutrients required for microbe activity and well as for breakdown to biogas. The balance between carbon and nitrogen in the waste mixture also explains the high production rate and levels. Further, in figure 4.20, control experiments were set by studying biogas production from un-inoculated waste mixtures, blank rumen waste and blank dung as well as inoculating the wastes mixtures with dung and rumen wastes. Un-inoculated wastes produced 300 mL, blank rumen and dung 700m while co-digestion of waste with dung and rumen produced 1000 mL and 3500 mL respectively.

Biogas generation from wastes at (55 °C) was initiated by co-digesting individual wastes with rumen wastes in a ratio of 1:1 and maintaining the digester temperatures at (55 °C)

using a water bath.

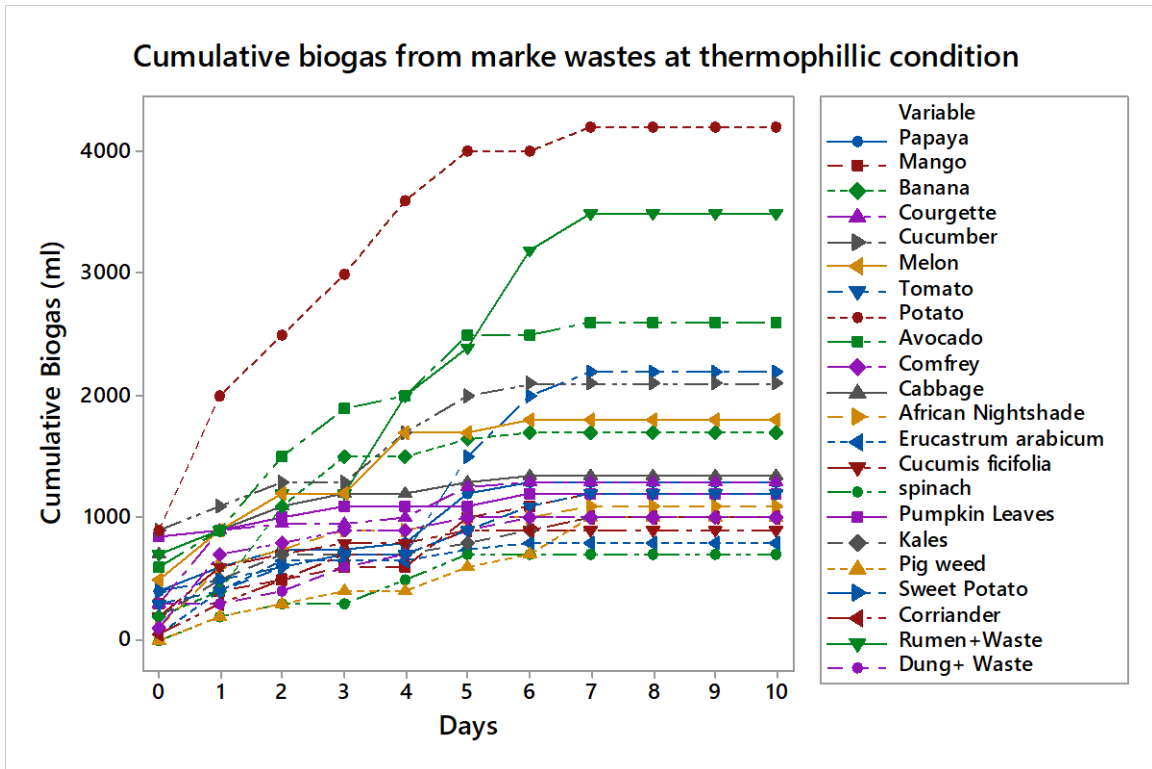


Figure 4.21: Thermophilic(55 °C) biogas production from inoculated market wastes

Potato wastes produced the highest cumulative biogas at 4200 mL on day seven compared to 700 mL from spinach waste. Avocado at 2500 mL and 2200 mL from sweet potato wastes were also among the highest biogas producing wastes. High-fat levels in avocado and high carbohydrates levels in potato and sweet potato wastes explains the high production levels. The imbalance between carbon and nitrogen in leafy vegetables like spinach account for the low production levels. Thermophilic temperatures favour a high rate of degradation of organic matter which implicitly increases biogas methane yield (Angelidaki, 2002). For example, in mesophilic temperatures, potato produced 1700 mL while FVMW produced 3500 mL while at thermophilic temperatures, potato produces 4200 mL while FVMW produces 3500 mL. Higher rates were observed in thermophilic compared to mesophilic temperatures.

4.4.4 Optimization Studies

Biogas production is highly influenced by substrate type, substrate alkaline and acidic pretreatments, C: N ratio, digester design, temperature, LR, pH and HRT. (Dioha *et al.*, 2013; Bożym *et al.*, 2015; Matheri *et al.*, 2015).

4.4.4.1 Waste pretreatment

Tables 4.1 and 4.2 show the proximate properties (dry and fresh weights) of various fruit waste from Nairobi County. Table 4.4 shows the physical properties of the market wastes on a dry and fresh weights basis. These properties influence the pretreatment process. For example, Peces *et al.*, (2015) observed that substrate pretreatment is highly influenced by moisture levels. At low temperature pre-hydrolysis (60 °C) biogas generation from brewers grain is enhanced by 6 % and by 14 % for ultrasound pretreatment (1000 kJkgTS⁻¹). However, a study by Chen *et al.*, (2019) reported no significant difference in methane production for the three moisture contents studied during pretreatment (54%, 70 %, and 77 %) of the rose stalk.

Different waste pretreatment results in different biogas generation levels for similar wastes. In thermal pretreatment setups, the highest cumulative biogas obtained was 2384 mL, 4126 mL and 5207 mL for 500 mL, 1 liter and 1.5 liters' digesters, respectively, compared to 2297 mL 3139 mL and 4127 mL in chemical pretreatment for similar digesters. The highest cumulative biogas was reported in the thermochemical methods at 3579 mL, 4888 mL and 6160 mL for 500 mL, 1liter and 1.5 liters' digesters, respectively, as shown in figure 4.22. The gravimetric biogas measurement method was applied in this pretreatment section.

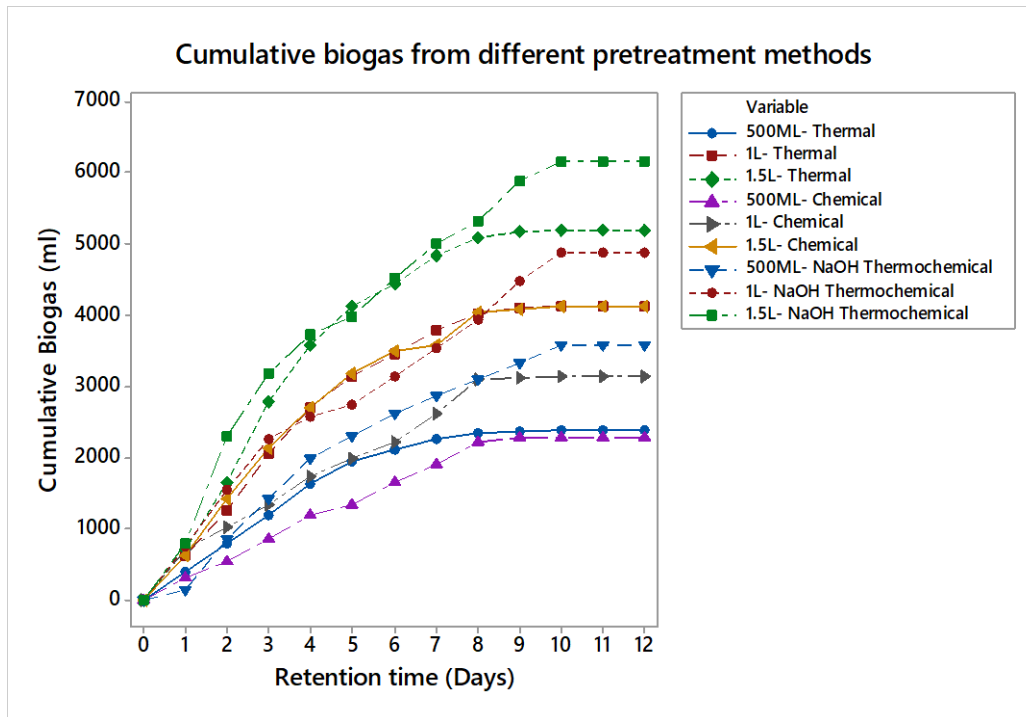


Figure 4.22: Cumulative biogas produced from F.V.M.W. with varying pretreatment methods

In thermal treatment, the substrate building blocks are disintegrated by heat, thereby increasing the substrate surface area. In figure 4.23, acidic hydrolysis and alkaline pretreatment thermochemical methods were compared. Higher cumulative biogas production was evident in NaOH digesters compared to HCl hydrolysis at 2909mL, 422mL and 5137mL in 500mL, 1liter, and 1.5liter HCl pretreated digesters, respectively compared to 3579mL, 4888mL and 6160mL NaOH waste pretreated, respectively. The acetate groups are separated from hemicellulose in alkali pretreatment, rendering the hemicellulose more available to hydrolytic enzymes. It strengthens digestibility. The addition of alkali also induces lignocellulose swelling which is a secondary influence (Kong *et al.*, 1992). Swelling occurs, resulting in an increase in internal surface area, a decrease in degree of polymerization, a decrease in crystallinity, and the separation of structural linkages between lignin and carbohydrates, resulting in an increase in cellulose hydrolysis (Kleinert, 1966). Alkali pretreatment appears to be a more efficient choice for pretreatment purposes (Damisa *et al.*, 2008). Mancini *et al.*, (2018) employed different chemicals in the pretreatment of wheat straws, the organic solvent N-methylmorpholine

N-oxide (N.M.M.O.) for 3 hours at 120 °C, the organosol method, using organic solvent (ethanol) at 180 °C for one hour and employing NaOH at 30 °C for 24 h. The study observed that a cumulative biomethane recoveries of 274 mL CH₄/gVS from untreated feedstock.

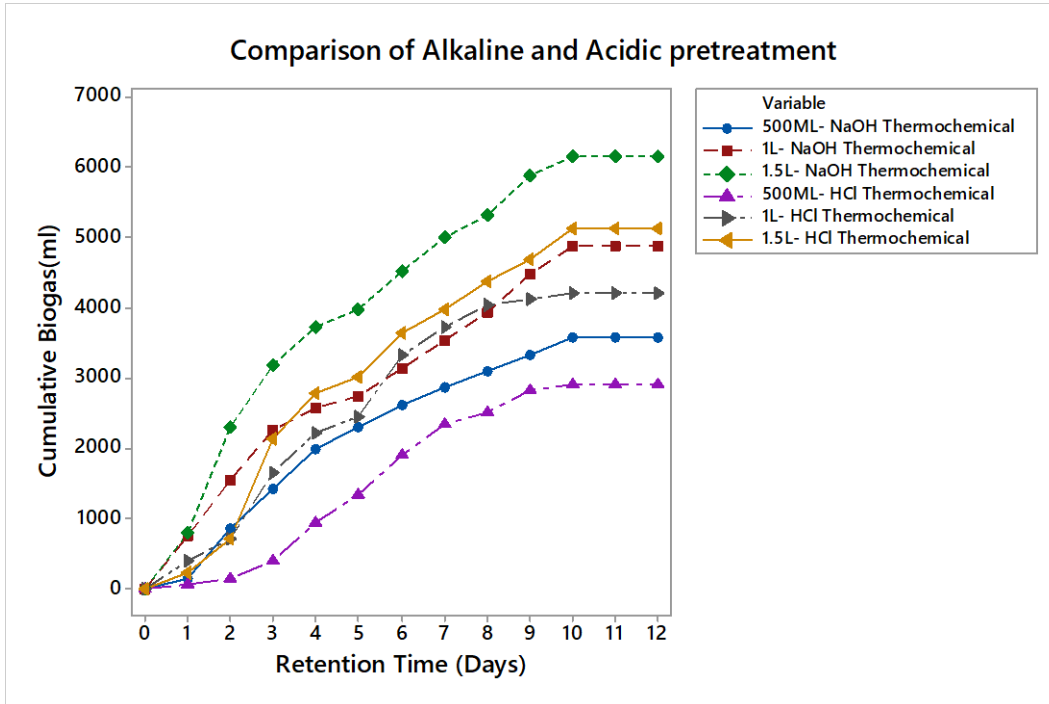


Figure 4.23 : Cumulative biogas generated from alkaline and acidic pretreated F.V.M.W.

On the other hand, acid pretreatment, mostly diluted acid pretreatments, increased cellulose accessibility mainly by solubilizing hemicellulose. In figure 4.24, the cumulative biogas generated from the market wastes pretreated with NaOH is shown. Low cumulative biogas is recorded in spinach waste at 1069mL, while the highest was recorded in avocado fruit wastes at 4705mL. This is explained by the high-fat content in avocado (9.03 ± 1.36) compared to spinach (0.17 ± 0.10). In general, wastes with high fat, carbohydrates and protein content recorded higher biogas production (Kamau et al., 2020).

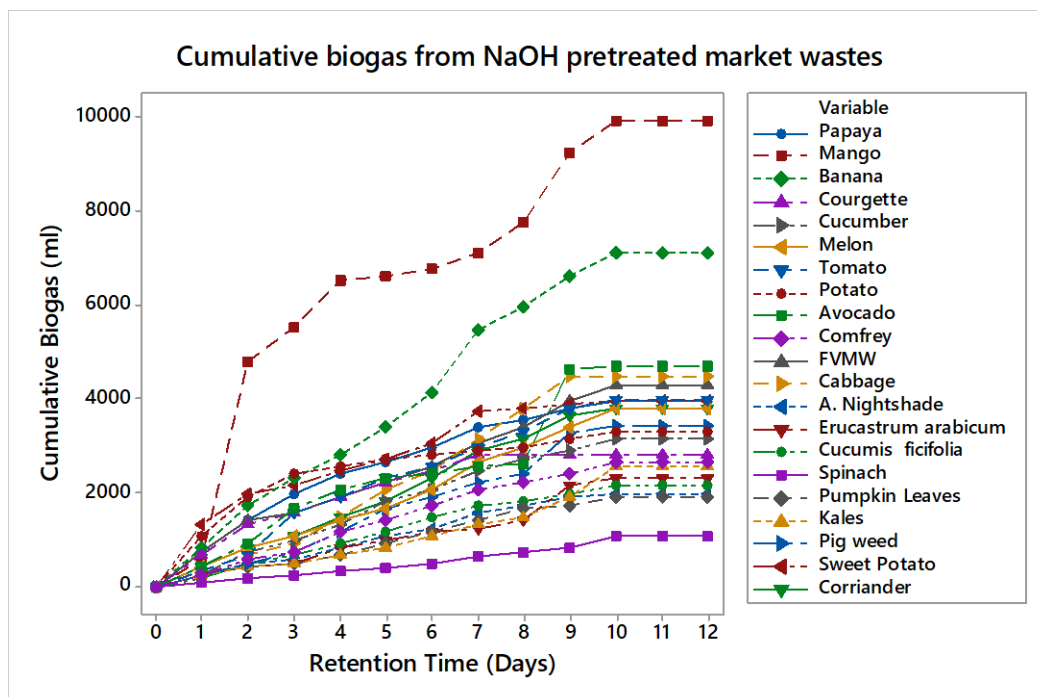


Figure 4.24 : Biogas generated from NaOH pretreated market wastes

The influence of the alkali pretreatment in mesophilic biogas generation is influenced by the level of decay of the organic waste. For all the wastes, a 10 - 20% increase in biogas production was observed except for avocado, banana and mango, which recorded more than 40-50% biogas increment. Owing to their structure and composition, the lignocellulosic materials are hydrolysis resistant. Lignin is also partially solubilized by pretreatment with alkali, enabling cellulose and hemicellulose to be more available. Lime, KOH and NaOH are the most common alkali employed in pre-treatment (Monlau *et al.*, 2013; Bochmann and Montgomery, 2013). Alkali pretreatment contributes to salt build-up and increased pH during continuous fermentation. The high concentration of salt and the effects on the balance of ammonium-ammonia prevent methanisation (Chen *et al.*, 2008). The feedstock's pretreatment efficiency depends on its proximate matter, temperature, incubation time (Raveendran *et al.*, 2015). Acid hydrolysis resulted in almost similar biogas generation levels as alkaline pretreatment. Higher production levels were witnessed in courgette and *Erucastrum arabicum* at 5490 mL and 5210 mL, respectively, as shown in figure 4.25.

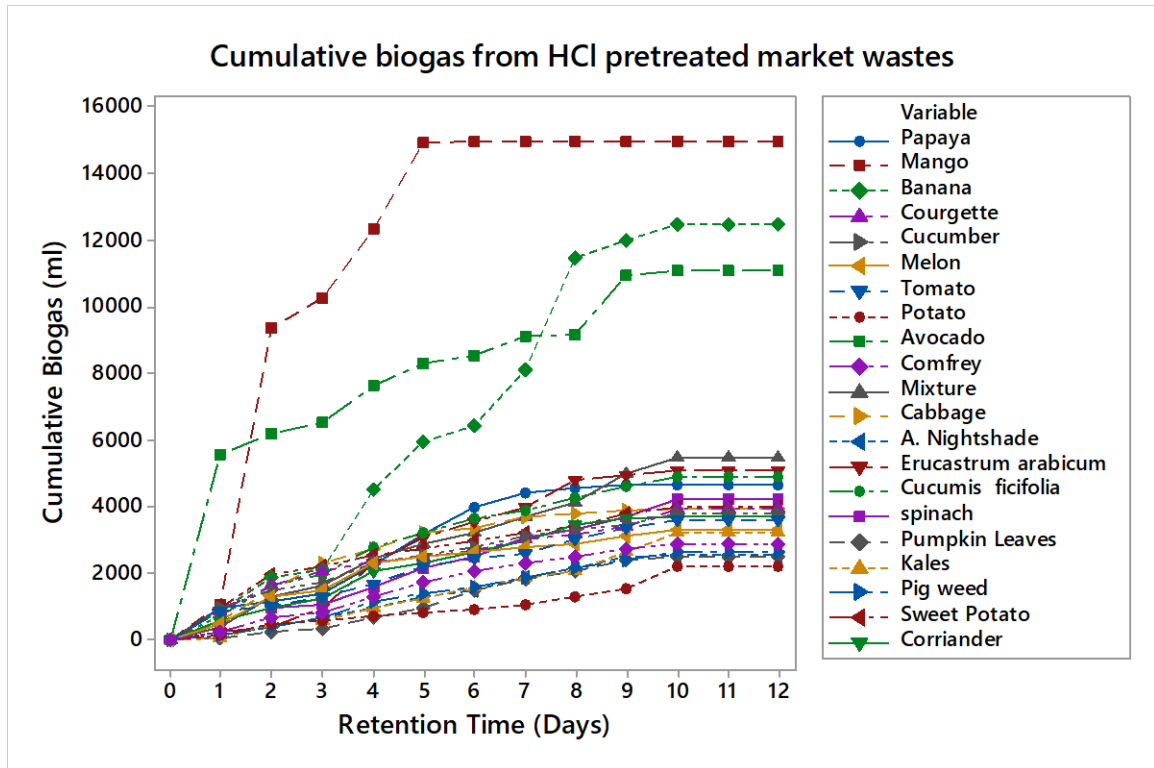


Figure 4.25: Biogas generated from HCl pretreated market wastes

Sludge disintegration and cell lysis are caused by acid pretreatment, which produces intracellular organics that become more bioavailable and thus improves the rate and efficiency of the digestion method (Eskicioglu *et al.*, 2007). The H-bond, Van der Waals forces and covalent bonds in lignocellulosic matter are disrupted during pretreatment resulting in breakdown of hemicellulose and the reduction of cellulose (Li *et al.*, 2010). In a study by Devlin *et al.* (2011) wastewater was digested using HCl at pH 2, 35 °C and 12-day HRT resulting to 14.3 % increment in CH₄ production in comparison to untreated WAS. Dilute H₂SO₄ pretreatment was used by Taherdanak *et al.* (2018) to enhance bio-methane yield from the wheat plant at mesophilic AD. An optimal CH₄ yield which was 15.5 percent higher compared to untreated wheat plant was obtained at 121 °C after pretreatment for 120 minutes.

The influence of alkaline and acidic pretreatment of market wastes on cumulative biogas generation is comparable. Proximate properties, pH and temperature, are the significant

factors that influence biogas production. This is because the waste collected is at the decomposing stage, and therefore, lignin is already disintegrating. However, based on waste and the decay level, pretreatment influence biogas production levels. For example, the cumulative biogas from untreated avocado, mango and banana wastes at mesophilic anaerobic digestion is 300 mL, 900 mL and 1500 mL, respectively. Figure 4.26 shows that pretreating these wastes with HCl results in 11088 mL, 14798 mL and 12476 mL in avocado, mango and banana wastes while pretreating with NaOH gives 4705mL, 9922 mL and 7113 mL, respectively.

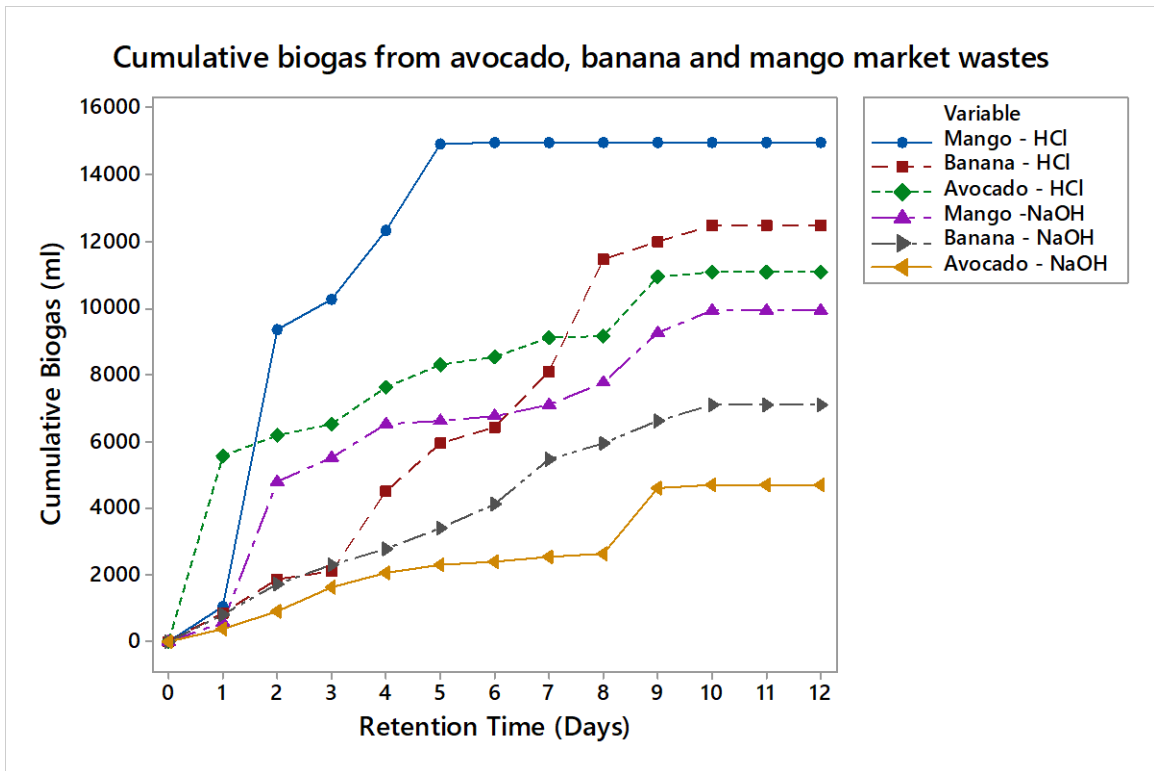


Figure 4.26: Biogas generated from NaOH and HCl pretreated avocado, mango and banana wastes

The influence of acidic thermochemical pretreatment resulted in over 30-fold increment in biogas generation in avocado, 16-fold increment in mango and 8-fold increment in banana. The same was observed with alkaline thermochemical pretreatment with 15-fold, 11-fold and a 5-fold increment in avocado, mango and banana, respectively.

In the pilot-scale studies, the influence of the amount of substrate, pretreatment chemical and retention time on cumulative biogas generation is shown in figure 4.27. The highest levels of biogas were generated from wastes treated with HCl at 34400 mL measured volumetrically using urinebags from a 10 liters' digester.

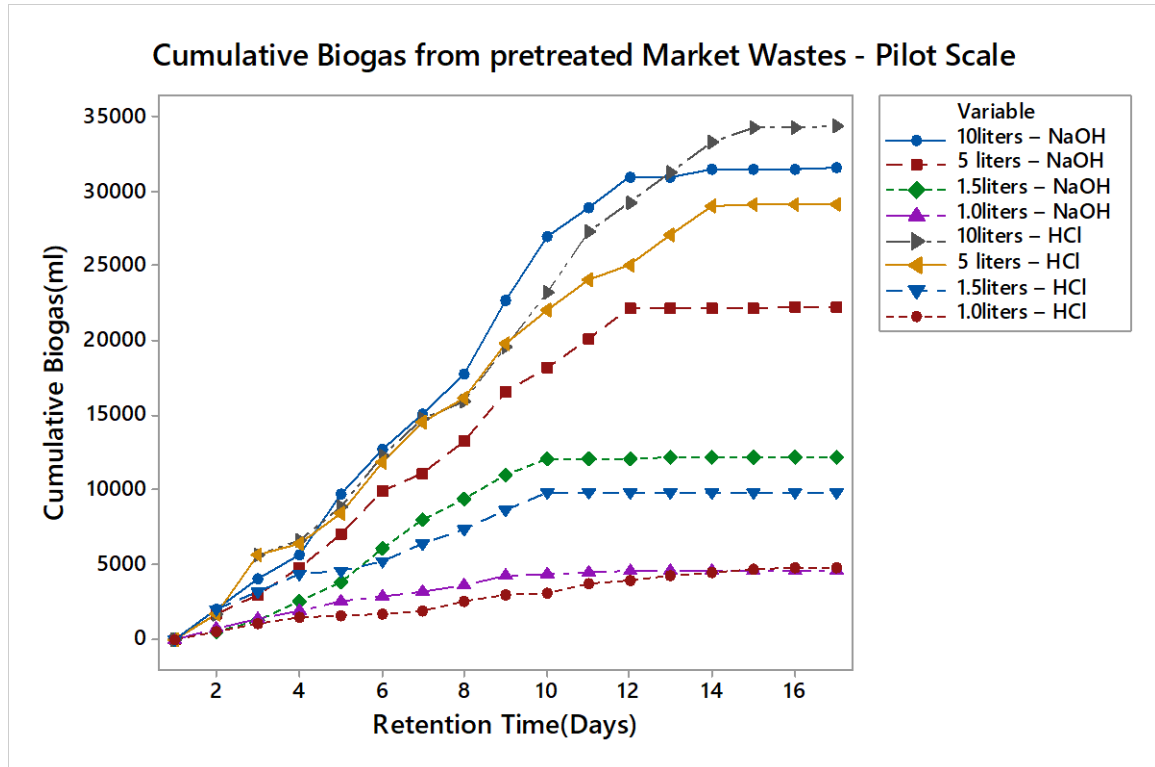


Figure 4.27: Cumulative biogas produced from pretreated F.V.M.W. at pilot scale

4.4.4.2 Inoculum to substrate ratios

In literature, cow dung, slaughterhouse waste and wastewater treatment have widely been employed in biogas production studies. The most widely used is cow dung due to its availability, especially in the agricultural area. In this section, rumen fluid inoculum was compared to cow dung in market waste biogas generation at 1:1, 1:2 and 2:1 ratios of waste to inoculum. The resulting cumulative biogas plots are shown in figures 4.28 and 4.29, while a comparison of the two inocula used in waste digestion is shown in figure 4.30. The ratio of 1:1 yielded more biogas in comparison to 2:1 and 1:2 waste to rumen waste ratios. The substrate to inoculum balance is essential in AD due to pH, C: N and

microbial community concentration. In 2:1 proportion, the available substrate is high leading to high C: N. The wastes pH is also likely to fluctuate over time and inhibit biogas generation. In 1:2, the high microbial community accounts for a higher production rate during the first days, but as the volatile matter is depleted, the production goes down. This is depicted in figure 4.28.

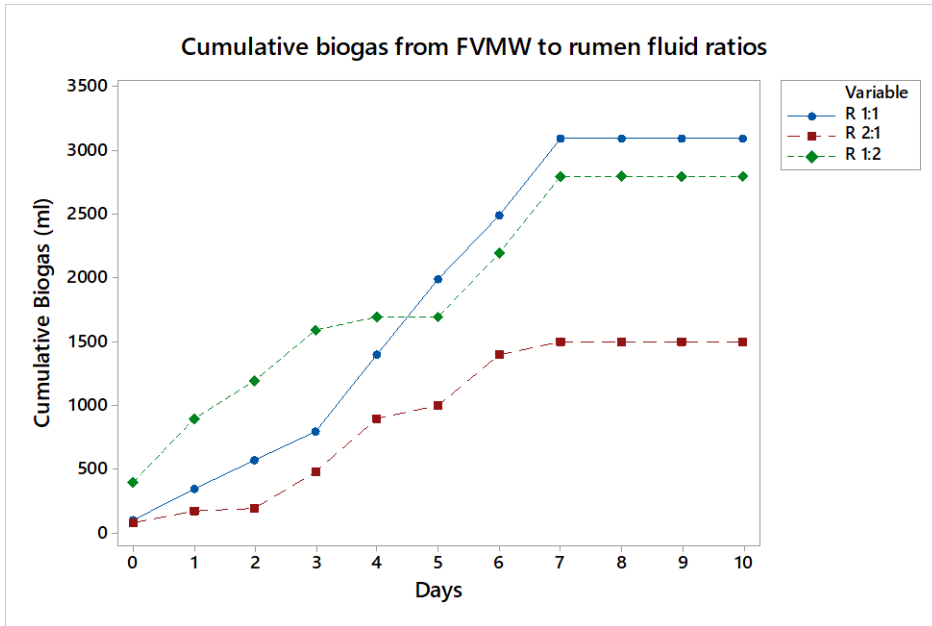


Figure 4.28: Plot of biogas produced for wastes to fluid rumen ratios

In figure 4.29, the 1:2 ratios were observed to have a higher production rate compared to 1:1 and 2:1. Cow dung has high nitrogen and this leads to ammonia inhibition during AD process. 1:2 ratio trend is because dung serves as a habitat of methanogens and substrate. This means that the available nutrients for microbial action. In 2:1 ratio, the cumulative production was 750 mL compared to 1300 mL and 1450 mL in 1:1 and 1:2 ratios.

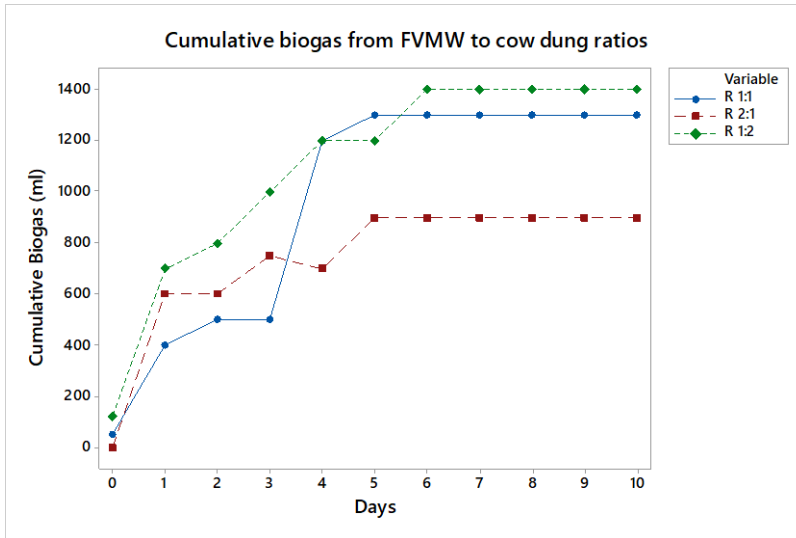


Figure 4.29: Plot of biogas produced for wastes to cow dung ratios

The wastes co-digestion with rumen and dung at different ratios was observed to be influenced by the inoculum utilized. In general, the 1:1 ratio of rumen produced 3100 mL of biogas compared to 1300 mL of 1:1 ratio of dung. This showed the influence of the microbial community in the biogas generation. High methane levels were observed by inoculation of market wastes with cowdung and rumen fluid as earlier observed by Kamau *et al.*, (2020).

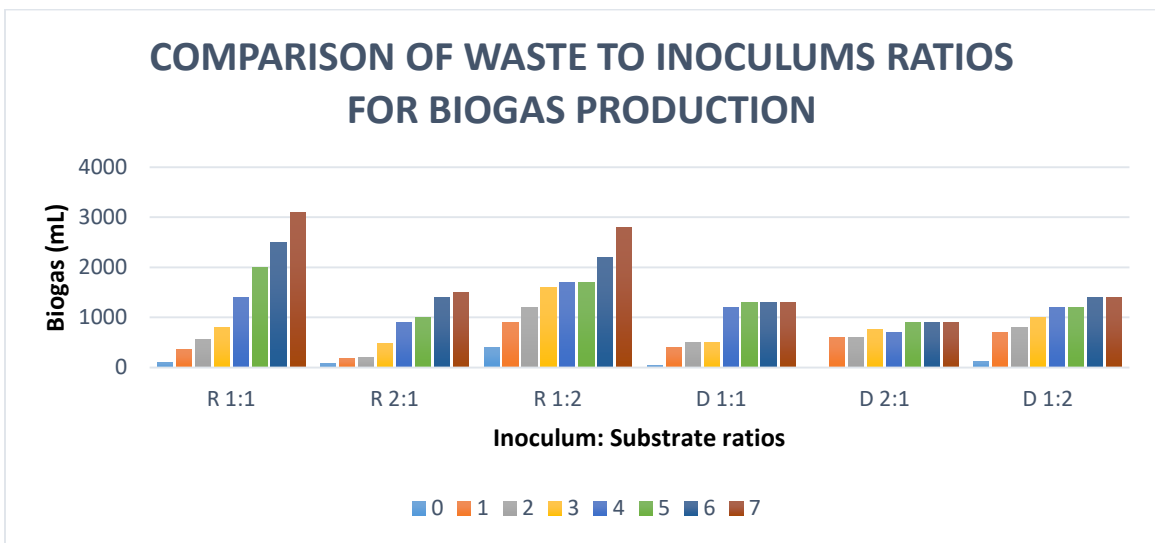


Figure 4.30: Plot of biogas produced for wastes to different inoculum ratios

The 2:1 ratio of dung cumulatively produced 900 mL of biogas compared to 1500 mL similar ratio for rumen waste. In 1:2 ratios, the generation was 2800 mL and 1400 mL for rumen and dung respectively. This confirmed the influence of microbial community population in biogas generation.

4.4.4.3 Temperature

Psychrophilic (<25 °C), mesophilic (30 – 40 °C) and thermophilic (50–65 °C) conditions are the three temperature ranges of AD (Sean *et al.*, 2006; US Department of Energy, 2013). Figure 4.31 shows biogas production at a psychrophilic condition where different wastes mixtures were used. The set up was left in a cold room at 14 °C – 19 °C where no biogas generation was observed for the first five days except for the 5litres waste in rumen fluid. After transferring the setup to 24 °C – 27 °C in day 4, biogas production was observed.

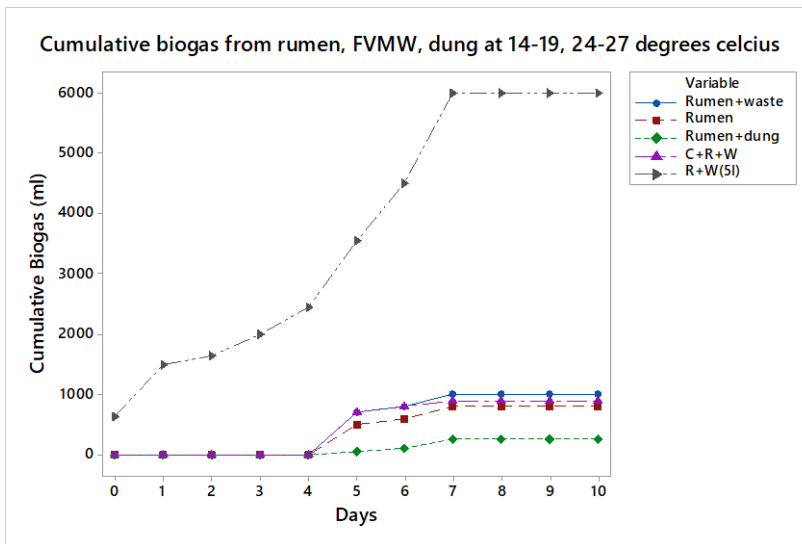


Figure 4.31: Biogas production at temperature ranges of 14 °C – 19 °C and 24 °C – 27 °C

Between 14 °C – 19 °C no biogas was observed for 1liter digester. Transferring the 1-liter digesters to an environment with 24 °C – 27 °C initiated biogas production with cow dung rumen and FVMW(C+R+W) digester recording a 790 mL biogas production. The digester containing FVMW and rumen waste (5 L) did not register adversely change from

temperature fluctuations from 14 °C – 27 °C. Cu *et al.*, (2012) noted low biogas generation was recorded during winter. The rate of biogas generation was lower at 14°C – 19 °C with 2700 mL cumulative biogas which later increased exponentially at 24 °C – 27 °C to 5800 mL from day 5 to day 8. A 1 liter digesters containing FVMW inoculated with rumen wastes were set up at three different temperatures. The digesters were operated at a 7 days’ retention time. Low productions were witnessed for psychrophilic temperatures with less than 700 mL biogas generation for the 7 days. This is explained by low microbial activities leading to slow hydrolysis of the substrate. The mesophilic digester recorded production of 3400 mL for the 7 days. This is five times more compared to psychrophilic temperatures. High biogas generation was recorded at thermophilic temperature with more than 4500 mL biogas production for the 7 days HRT as displayed in figure 4.32.

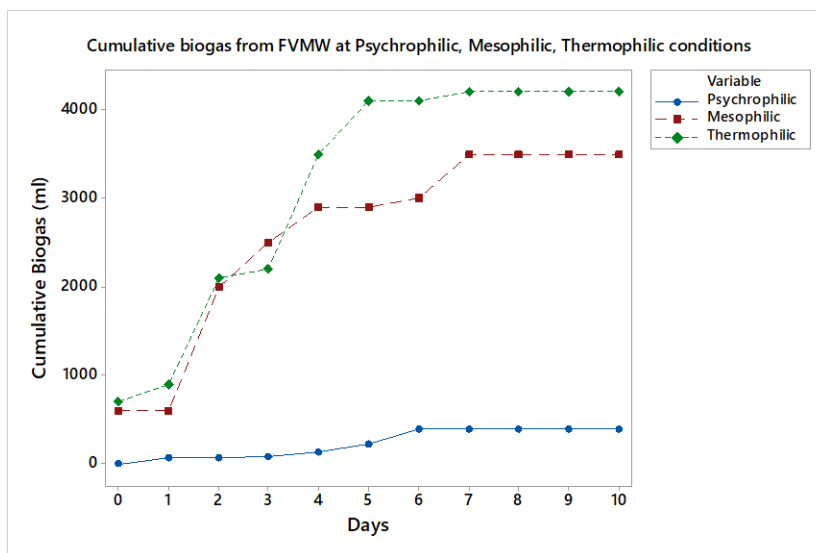


Figure 4.32: Plot of biogas generation at different temperatures

At mesophilic conditions, the digestion rate was slow and the biogas yield is low. However, biogas generation at mesophilic condition is preferred due to low heat cost compared to the thermophilic state (Cu *et al.*, 2012). The effectiveness and stability of the AD reactions are highly influenced by temperature and feedstock (Chae *et al.*, 2008). Arikan *et al.*, (2015), noted that temperatures impact microbial concentration, thermodynamic and kinetics of AD as well as products stoichiometry. The optimum

temperatures observed for this study is thermophilic production at 55-56 °C. This is similar to the observations by Deressa *et al.*, (2015), who reported that fruits and vegetable wastes digestion is affected by temperature. Griffin *et al.*, (1998) reported that methanogens growth and activity is highly affected by temperature. AD ammonia inhibition depends directly on the temperature. Lower temperatures result in reduced inhibition. Operating at temperatures below 50 °C, lowers thermophiles growth rate and this can lead to their discharge due to a growth rate lower than the hydraulic retention time at a time (Angelidaki *et al.*, 2002). The digester pH is also directly influenced by temperature. While the temperature is increasing, the carbon dioxide solubility decrease; this is why in the case of thermophilic digesters the pH value is higher than in the mesophilic ones where the carbon dioxide will dissolve easily and will produce carbonic acid in reaction with the water, increasing the acidity (Angelidaki *et al.*, 2002).

4.4.4.4 Optimization of C: N ratio

In this section, the impact of C: N on the AD performance at mesophilic and thermophilic conditions was studied. A C/N ratio range of 9 to about 50 was investigated. This range exceeded 20-30 bracket which always reported in research works. In the current study, the fruits and vegetable wastes showed high bio-methane yield in the researched C/N brackets as earlier shown by (Guarino *et al.*, (2016). The average C/N of individual waste is show in table 4.8

Table 4.8: The C: N ratio of market wastes

Waste	C: N	Waste	C: N
Kales	8.14±0.55	Tomato	17.23±0.43
Cabbage	15.26±0.22	Potato	24.36±0.52
Pumpkin Leaves	6.85±0.94	Sweet Potato	35.54±0.43
<i>Cucumis ficifolia</i>	7.03±0.09	Pawpaw	33.26±0.81
Pigweed	6.25±0.92	Banana	15.86±0.24
<i>Erucastrum arabicum</i>	6.51±0.64	Avocado	38.92±0.73
Coriander	5.23±0.03	Courgette	9.00±0.30
A.nightshade	6.77±0.36	Cucumber	15.94±0.81
Spinach	7.45±0.96	Mango	33.90±0.13
Comfrey	6.94±0.51	WaterMelon	15.94±0.81

In this case, we considered coriander, courgette, banana, potato and avocado, which had C: N ratios of 5.23, 9.00, 15.86, 24.36 and 38.92 respectively. The biogas production at mesophilic conditions is plotted in figure 4.33.

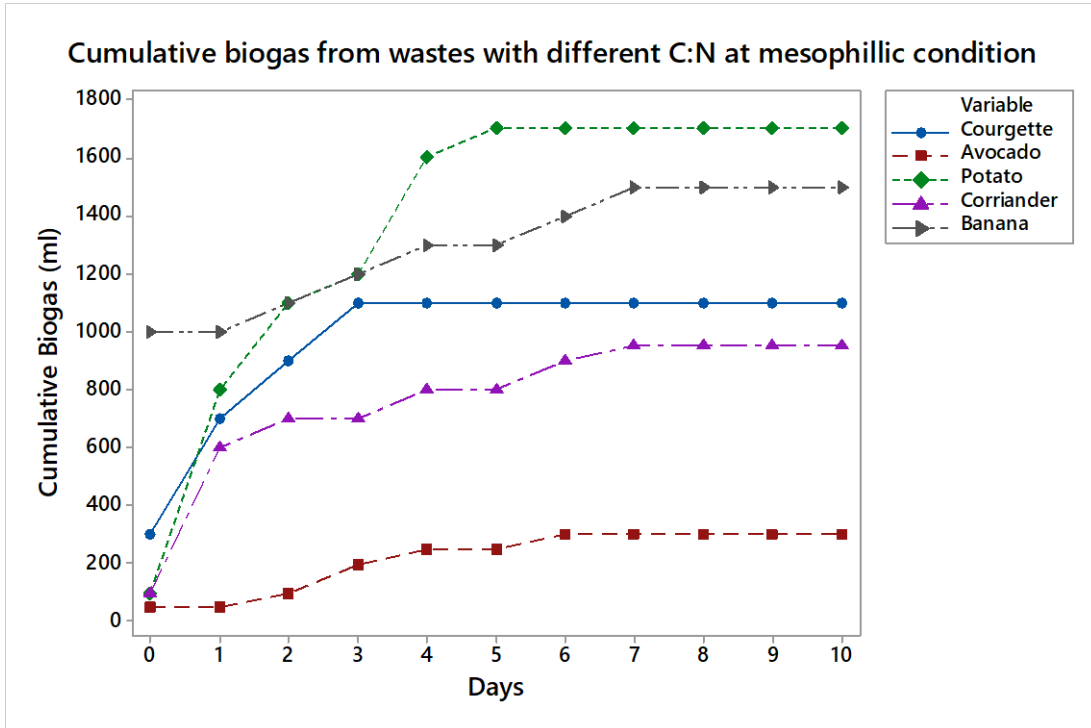


Figure 4.33: Biogas production from market wastes with different C: N ratios at mesophilic condition

Similar plots of biogas generated at different C: N ratio under thermophilic temperatures is shown in figure 4.34. At low C/N ratio, nitrogen is formed and accumulate as ammonia which raised the reactor pH. A pH value greater than 8.5, poisons methanogens leading to low biogas yield (Oghenero *et al.*, 2016).

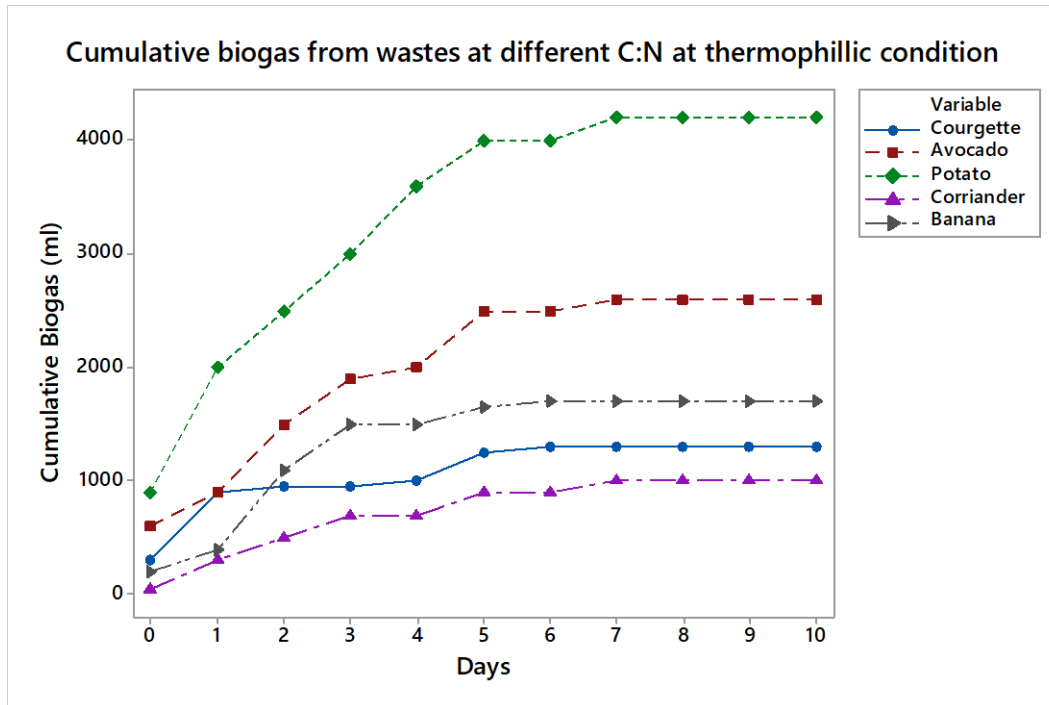


Figure 4.34: Biogas production at thermophilic condition with distinct C: N ratios

While various C: N ratios were used, it was observed that the best working range was between 20-30:1 as earlier noted by Guarino *et al.*, (2016) and Garba *et al.*, (1998). The avocado containing the highest C: N ratio of 38.92 had the lowest biogas production at mesophilic conditions ranging from 50-300mL while at thermophilic conditions, the volume was 600 - 2600mL. On the other hand, coriander with a 5.23 C: N had the lowest biogas generation, as shown in figures 4.33 and 4.34.

The results obtained in this research are in consistence with others obtained, e.g. For anaerobic digestion of palm wastes, Al Juhaimi *et al.*, (2014) utilized a C/N ratio of 30. For municipal waste, Rao and Singh (2004) determined a maximum C: N of 25; for buffalo dung biogas recoveries were done at C: N of 30 (Yasin and Wasim, 2011). Nonetheless, C: N brackets outside this ranges have been reported e.g. Tewelde *et al.*, (2012), discovered a C: N of 17 while digesting brewery waste. According to Dioha *et al.*, 2013, the best C/N ratio is 20–30:1. In contrast to 20 and 25, a C: N of 30 is said to have generated more CH₄ (Achmad *et al.*, 2011).

4.4.4.5 Influence of carbohydrates, protein and fat content on biogas production

Theoretical biogas yields largely depend on lipids, carbohydrates and proteins levels (Das & Mondal, 2016). The main proximate properties involve analysis of moisture, carbohydrates, protein and fat content (tables 4.1 & 4.2). The influence of these properties on biogas production is discussed.

The moisture content of the wastes was in the range of 74.30 – 95.86% on a fresh weight basis. Biogas production requires feedstock to be in a fluid state for ease in the microbial breakdown. The hydrolysis step is highly influenced by the moisture content. In this step, the complex substrate is broken down into small units that are highly eased by moisture (Ralph & Dong, 2010). In figure 4.35, scatter plots of cucumber and banana wastes with a moisture content of 95.86 and 74.30 % are shown.

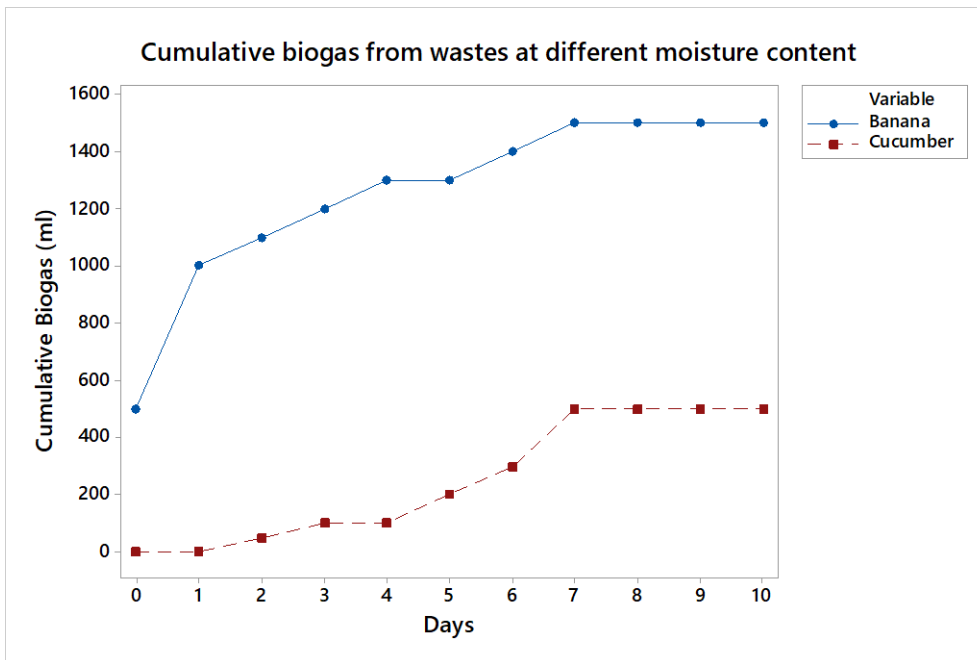
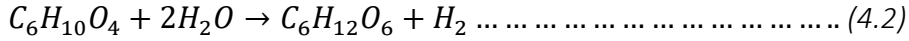


Figure 4.35: Influence of moisture content on biogas production.

In the hydrolysis step, water is used in the conversion of complex substrate carbohydrates, proteins and fat to simpler matter like sugars, amino acids and fatty acids respectively. The general reaction is shown by equation 4.2 proposed by Ostrem & Themelis (2004).



Low biogas is reported in cucumber despite the high moisture content against high cumulative biogas generation from banana wastes with lower moisture levels. Moisture level in substrate influence the hydrolysis process, which can only increase the rate of breakdown and not the methane potential of a substrate (Kamau et al., 2020).

The carbohydrates levels were reported to be the highest among the proximate properties investigated in this study. The highest amount was reported in sweet potato at 32.17 and lowest in courgette at 1.99%. The biogas generation levels are shown in figure 4.36.

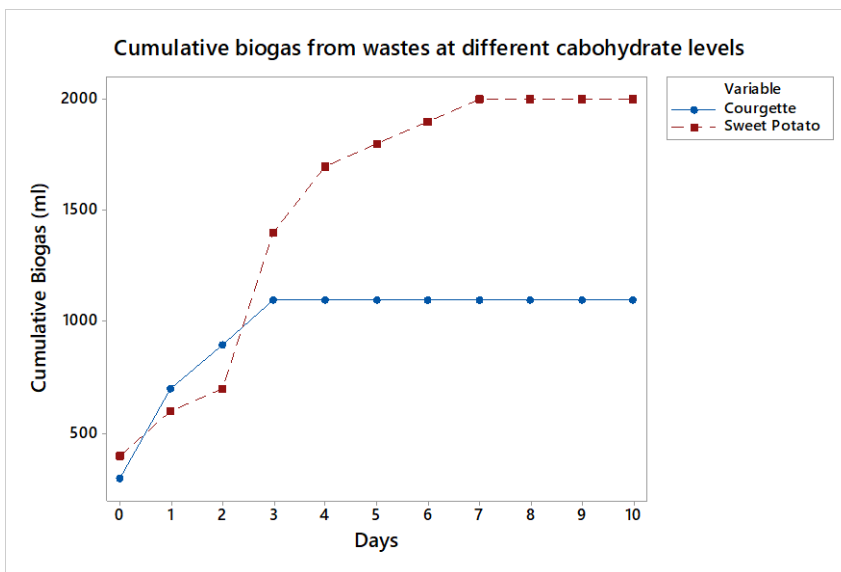
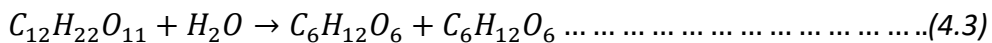


Figure 4.36: Influence of carbohydrates content on biogas production.

The carbohydrate or the complex sugars are broken down into monosaccharides e.g. lactose into galactose and glucose as shown in equation 4.3.



It is evident from figure 4.36 that biogas generation is highly dependent on the carbohydrates level in the sample. It was observed that at high carbohydrate levels, high biogas was generated (Alibardi and Cossu, 2016). The fat levels amongst the substrates were higher in avocado at 9.03% and lowest in kales and cabbages at 0.09 and 0.05 %

respectively. The obtained thermophilic production at different levels is shown in figure 4.37.

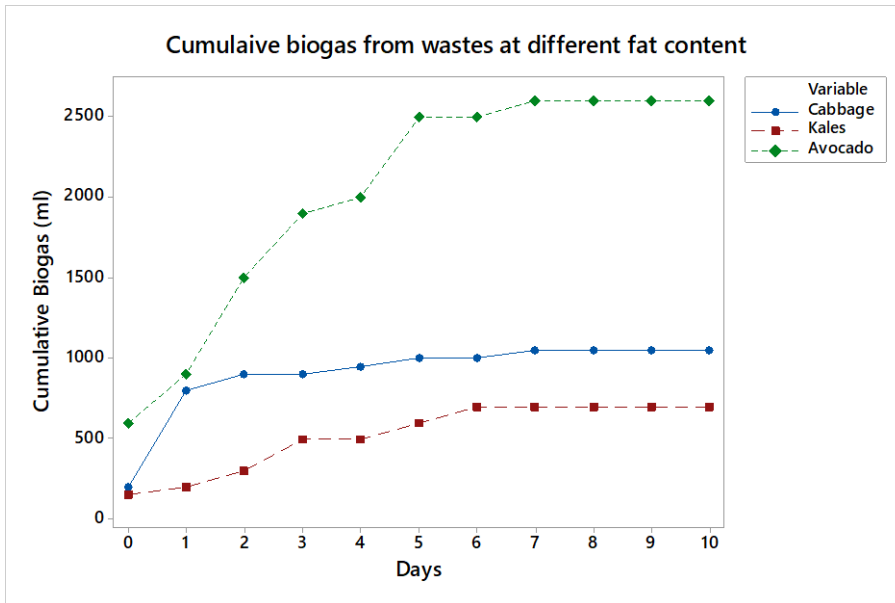
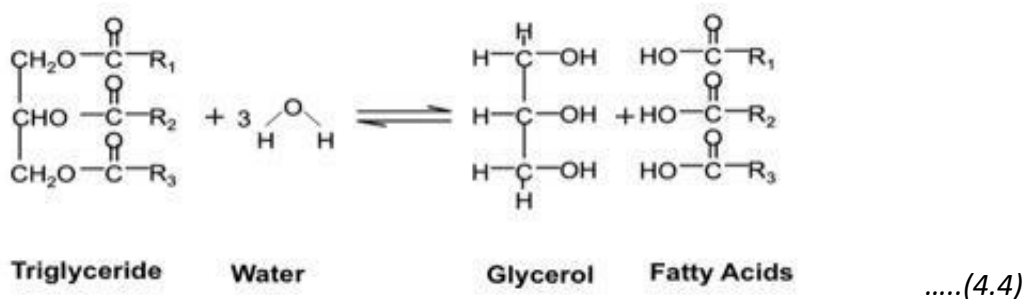


Figure 4.37: Influence of fat content on biogas production.

It was noted that the fat content influenced biogas generation in waste to biogas conversion. High-fat levels translated to high biogas production. The overall biogas produced by the avocado substrate was in 600-2600 mL range for the seven days' retention time. Fat is converted to fatty acids in the hydrolysis step as described in the reaction proposed by Philip (2014).



Among the proximate matter, lipids contribute largely to biogas formation though with longer HRT because of slow bio-degradability. Proteins and carbohydrates have fast digestion rate though the yield is low (Das & Mondal, 2016).

The protein levels were lowest in tomato wastes at 0.58 and highest in *Cucumis ficifolia* wastes at 3.49 %. The overall biogas production at these levels is shown in figure 4.38.

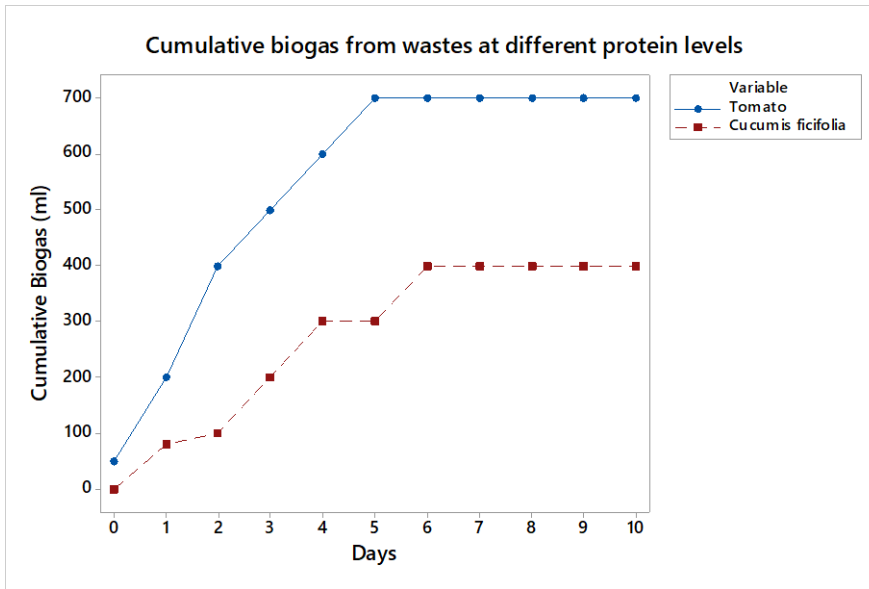
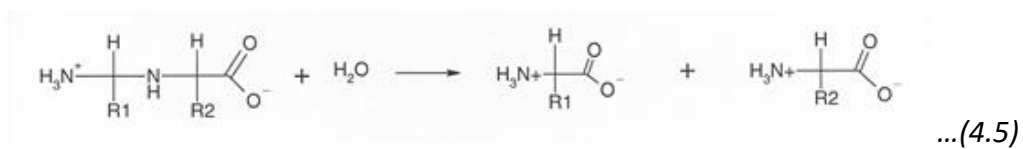


Figure 4.38: Influence of protein content on biogas production.

The observed trend is that the higher the protein levels, the lower the biogas production. The protein content influences the levels of ammonia and hydrogen sulfide in the digester. This translates to some inhibition of microbial activities, consequently influencing biogas productions. The resulting equation is shown in equation 4.5 (Dana and Corey, 2014); Arthur and John, 2006),



Biswas *et al.*, (2007) studied the effects of carbohydrates, protein and fat on biogas generation using vegetable waste, oil cake and whey. They observed that methane production was dependent on these proximate proprieties. This was also reported by Biswas *et al.*, (2007) and Tekin and Dalgıç, (2000). With a fixed slurry concentration, methane levels decreased with an increase in carbohydrates concentration because at high levels of carbohydrates, acidogenic bacteria growth is favoured producing volatile fatty acids like butyric and valeric which inhibit methanogens growth and therefore, low

methane generation. Besides, high protein content leads to low methane formation due to the formation of ammonia at the acetogenesis step (Biswas *et al.*, 2007).

On the other hand, fat content favours methane production due to the availability of long fatty acids being converted to methane (Yanyany *et al.*, 2016; Yang *et al.*, 2015).

Baserga reported biogas yield of 790, 1250 and 700 L/Kg of organic matter and methane levels of 50, 68 and 71 % for carbohydrates, fats and proteins respectively.

4.4.4.6 Influence of pH

The pH value provides an estimate of the fermentation process's state. For AD, a pH range of 6.5 - 7.5 is ideal (Lazor *et al.*, 2010; Pratima & Bhakta, 2015). Some of the feeding materials tend to decrease the pH of the digestate. The daily changes in pH of the individual wastes are shown in figure 4.39. The pH decreased with HRT for all the wastes besides the waste mixture and courgette wastes which increased from 6.23-6.43 and 5.98-6.06 respectively. The most significant decrease was observed in FVMW uninoculated mixture. The drop was from a pH of 5.23 to 3.47. In potato waste, the pH dropped from 6.49 – 4.78.

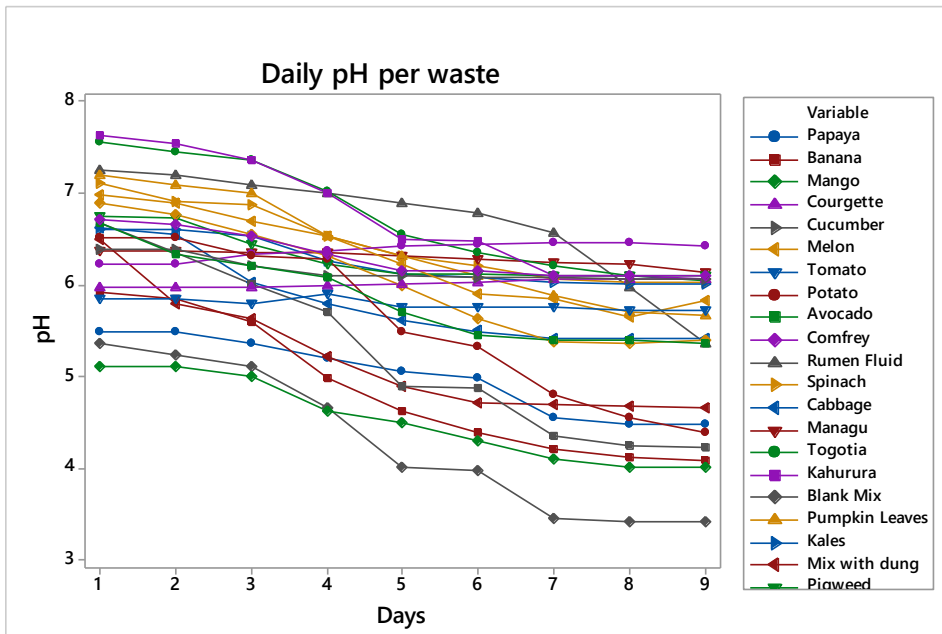


Figure 4.39: Daily pH changes per waste.

The final pH readings for each waste were recorded in table 4.9 with slight drops in initial pH being recorded for all the wastes. For leafy vegetables, kales pH dropped from 6.61 to 6.02 with 7.21 to 5.68 decline witnessed in pumpkin leaves.

Table 4.9: The pH of the substrate before and after loading to the digester.

Substrate	Before	After	Substrate	Before	After
Kales	6.61	6.02	Sweet Potato	6.68	4.25
Cabbage	6.62	5.42	Banana	5.92	4.08
Spinach	7.12	6.03	Pigweed	6.76	6.11
<i>Erucastrum arabicium</i>	7.57	6.05	African Nightshade	6.37	6.14
Comfrey	6.72	6.10	Blank Mix	5.37	3.42
Pumpkin leaves	7.21	5.68	Blank Dung	7.64	5.82
Coriander	6.89	5.37	Blank Rumen	7.25	5.36
<i>Cucumis ficifolia</i>	7.64	6.06	Waste+Rumen	6.23	6.47
Cucumber	6.40	6.07	Waste+Dung	6.50	4.68
Courgette	5.98	6.06	Water	7.36	
Mango	5.12	4.01	Papaya	5.49	5.49
Avocado	6.68	5.36	Tomato	5.86	5.73
Melon	6.98	5.83	Potato	6.51	4.39

In general, lower drops in pH were recorded in leafy vegetables compared to fruits wastes. This is because leafy vegetable wastes have high moisture content which acts as a solvent, thereby diluting the blended wastes. The pH decrease was higher in wastes with low moisture content like potato and sweet potato wastes. In FVMW inoculated with rumen wastes pH increased from 6.23 to 6.47 within 7 days. This was observed due to substrate inoculum digestion product balance. Blank rumen and blank mix dropped by 1.89 and 1.95 respectively. The increment on inoculating the waste with rumen was 0.24. In figure 4.40, biogas production was investigated concerning initial pH. This was done by inoculating the FVMW with rumen waste at a preset initial pH ranging from 5.83 to 12.67.

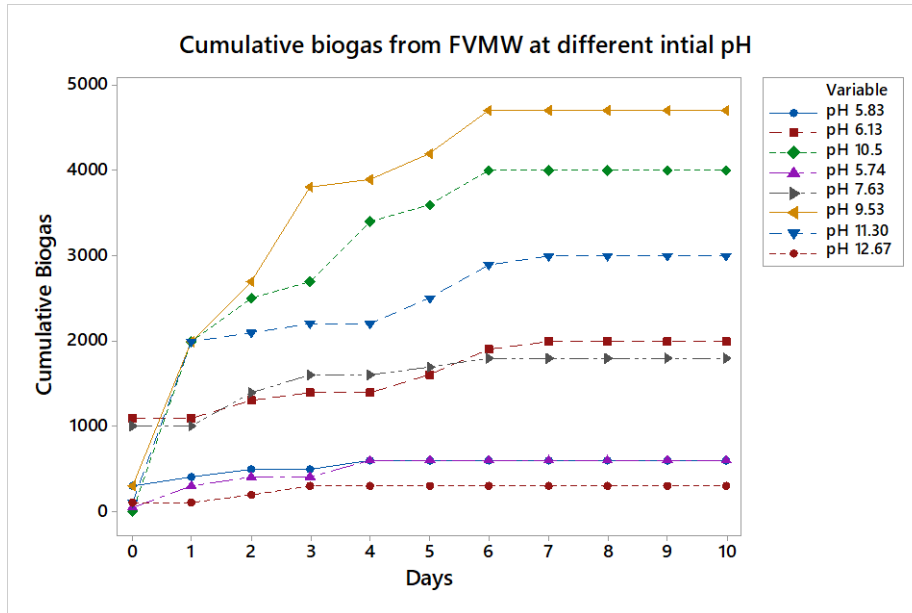


Figure 4.40: Plot of influence of pH on biogas production

Cun-fang Liu *et al.* (2008) reported that a lowering the pH can inhibit gas generation and results to accumulation of acids. Jayaraj *et al.*, (2014) investigated influence of pH on biogas yield from food waste in reactors maintained at pH 5, 6, 7, 8 and 9 at mesophilic temperatures. In anaerobic digestion, all life processes are carried out at well-defined values of pH. The pH of the optimal hydrolytic stage is between 5 - 6 (Castillo *et al.*, 2006; Vavilin *et al.*, 2008; Veeken *et al.*, 2000) and for methane production stage, the optimal pH value varies between 6.5 – 8 (Converti *et al.*, 1999). If the pH value decreases below 6, methane production is strongly inhibited. The temperature of the reaction medium influences the pH value. While the temperature is increasing, the carbon dioxide solubility decrease; this is why in the case of thermophilic digesters the pH value is higher than in the mesophilic ones where the carbon dioxide will dissolve easy and will produce carbonic acid in reaction with the water, increasing the acidity (Babel *et al.*, 2004). During the digestion process, the pH value may increase because of the ammonia presence resulted either by the protein degradation or by its presence in the charging flux; also it can decrease if VFA will accumulate in the reaction medium. The reaction medium must provide sufficient buffering capacity to neutralize VFA accumulation (Neves *et al.*, 2003). Dobre *et al.*, (2014) noted that methanogens metabolic rates are

affected by pH variation. Any changes outside their operations spectrum halts biogas generation.

4.4.4.7 Influence of Co-digestion

The effect of multi-substrate degradation of market waste with dung and rumen matter is shown in figure 4.41. Blank FVMW produced the least biogas at 500mL compared to dung and rumen 700mL recorded in day two of digestion. After day 2, the available substrate in dung and rumen was depleted and therefore no further increment in biogas produced. Co-digestion of market waste with dung recorded a cumulative biogas generation of 900mL compared to 3500mL in waste co-digested with rumen waste.

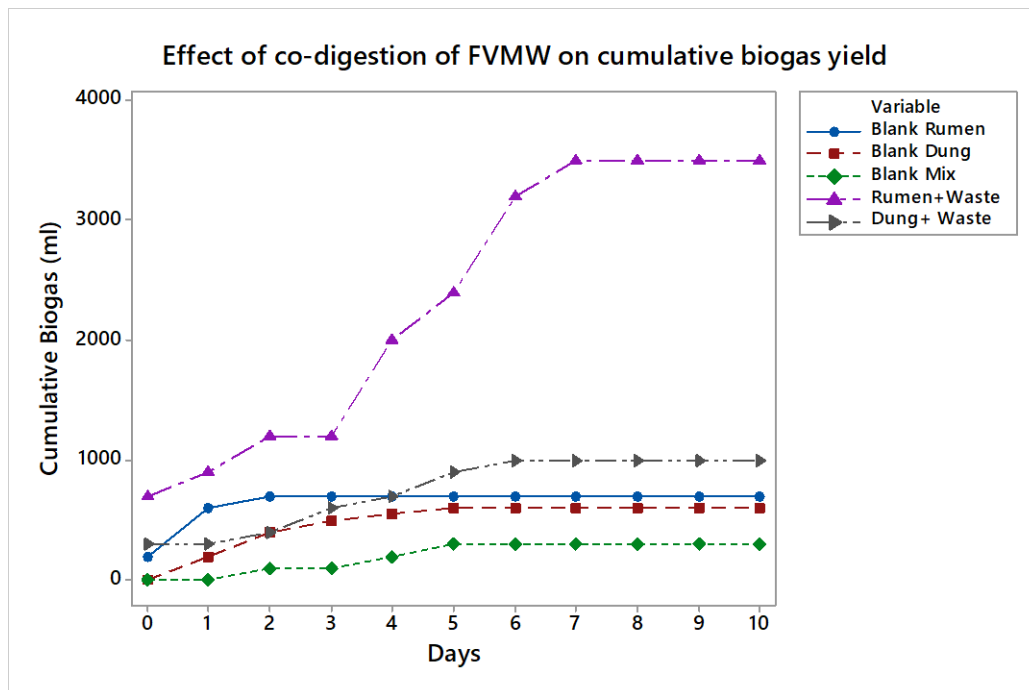


Figure 4.41: Biogas generation from co-digested substrates

The microbes in rumen and dung significantly influence the rate of substrate breakdown as shown by lower production in un-inoculated waste. Further co-digestion also increased biogas yield significantly as demonstrated by high production in dung and rumen co digested wastes.

Co-digesting result in increased biogas generation. For instance, a 65% CH₄ was reported (Lehtomäki *et al.*, 2007) by co-digestion of cattle dung with molasses (Sarker & Møller,

2013; Sarker & Møller, 2014), energy crops (Lehtomäki et al., 2007), food wastes (El-Mashad & Zhang, 2010), agro wastes (Cavinato et al., 2010), FVMW (Callaghan et al., 2002; Poulsen et al., 2016).

Majeed and Malik (2018) investigated the effects of co-digesting fruit and vegetables with cow dung at mesophilic temperature (35°C-40°C). They discovered that the FVCW (fruit vegetable –cow dung) ratio of 0.5 -1.5:1.0 created the most biogas and had the highest CH₄ levels, at 2134.15 mL/g VS.

4.4.4.8 Influence of Agitation

Thorough mixing of the substrate during digestion ensures uniformity in the digester, uniform temperature and even distribution of the microbes. This was reported to increase biogas yields 5-10 folds compared to the un-agitated digester. In this study, biogas production in the agitated digester (A) was more than five times compared to the un-stirred digester, as shown in figures 4.42. The study was carried out in different capacity digesters ranging from 500 mL – 10 litres. The agitated 10-liter digester produced 8700 mL biogas compared to 2800 mL in the un-agitated digester. A 5-liter digester generated 7000 mL biogas compared to 1400 mL in the un-agitated digester. Agitating the biogas ensured that the trapped gases are set free and this increased the cumulative gas recorded. Further, stirring ensured uniform distribution of nutrients for microbial enhancement. The results observed correlated with those shown for vegetable and fruits and other substrates.

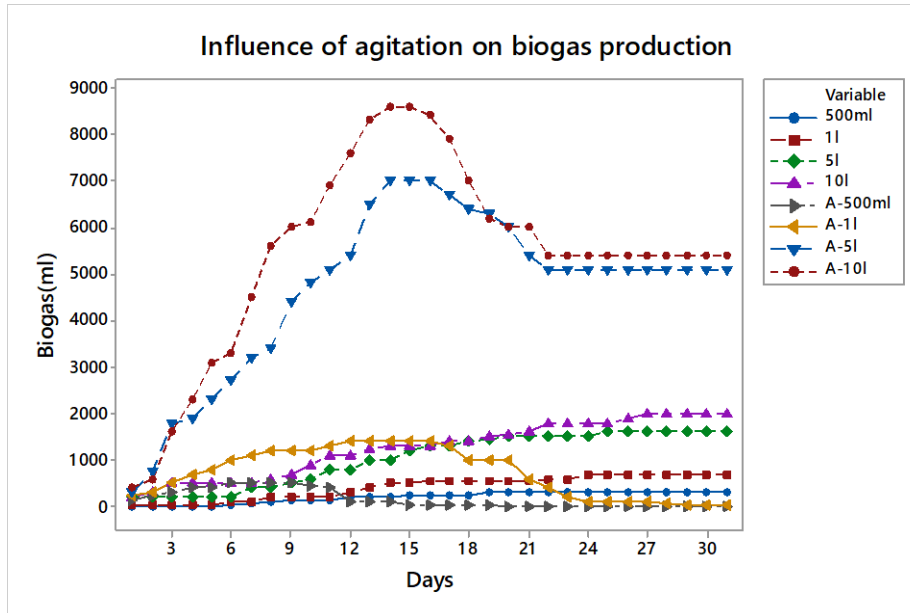


Figure 4.42: Plot of biogas production from agitated and un-agitated digesters.

Rusin, Chamradova & Grycova, (2017) reported that stirring doubles biogas yields for the same HRT. Trisakti *et al.*, (2017) assessed the effect of agitation on biogas production on methanogenesis stage. The results showed that the highest production of total VFA achieved was 5,766.61 mg/L at agitation rate of 200 rpm, with the concentration of acetic acid, propionic acid, and butyric acid were 1889.23, 1161.43 and 2725.95 mg/L, respectively. In another study on effects of agitation on acidogenesis, Trisakti *et al.*, (2017) reported that the highest growth of microorganisms was achieved at HRT 4.0 day with microorganism concentration of 20.62 mg VSS/L and COD reduction was 15.7%. The most increased production of total VFA reached was 5,766.61 mg/L at agitation rate 200 rpm, with the concentration of acetic acid, propionic acid, and butyric acid were 1889.23, 1161.43 and 2725.95 mg/L, respectively. At the same time, VS decomposition and COD removals were 16.61 and 38.79%, respectively.

4.5 Biogas upgrade

The trace amount of CO₂, H₂O and H₂S in raw biogas lower its calorific value, cause corrosion and makes it hard to compress biogas into the cylinder. To use biogas as LPG, purification is vital (Divyang *et al.*, 2016).

4.14.1 Characterization of Eburru Zeolite Rocks

The characterization of the Eburru zeolite rock sample was carried out to assess their properties and ascertain their effectiveness for formulation and utilization in biogas upgrading to bio-methane. Figure 4.43 shows the X-ray diffraction peaks comparable to the those observed by Treacy *et al.*, (2001), having 2θ values of characteristic artificial zeolite A at 7.2° , 10.3° , 12.6° , 16.2° , 21.8° , 24° , 26.2° , 27.2° , 30° , 30.9° , 31.1° , 32.6° , 33.4° and 34.3° as shown in figure 4.43.

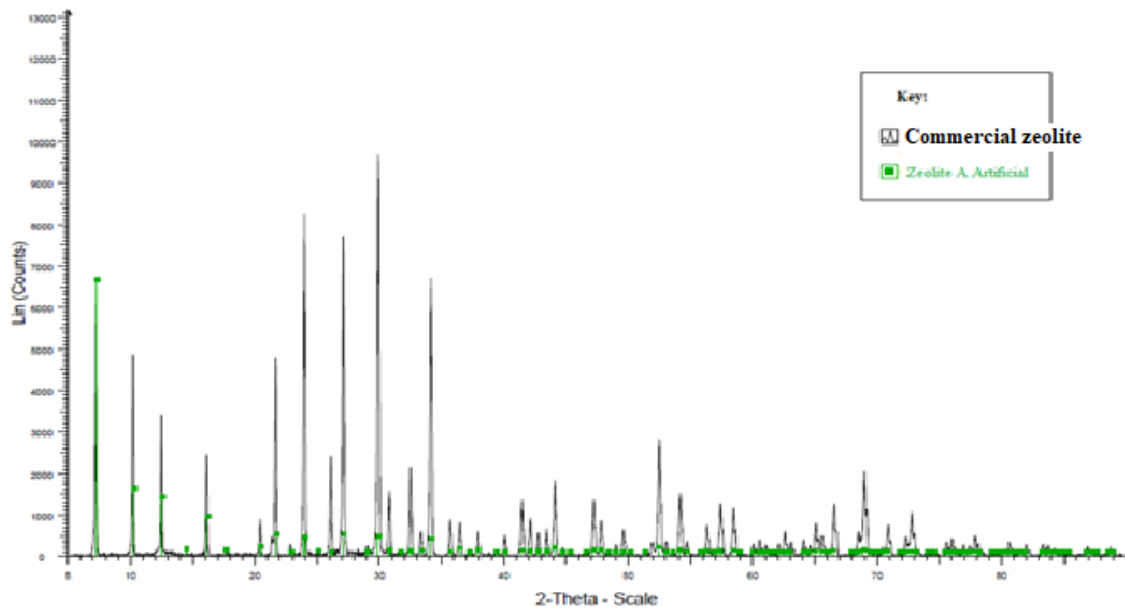


Figure 4.43: XRD spectra of commercial zeolite rocks sample

The XRD characterization of Eburru zeolite rocks showed distinct spectrum (figure 4.44), with diffraction properties data tabulated in Table 4.10.

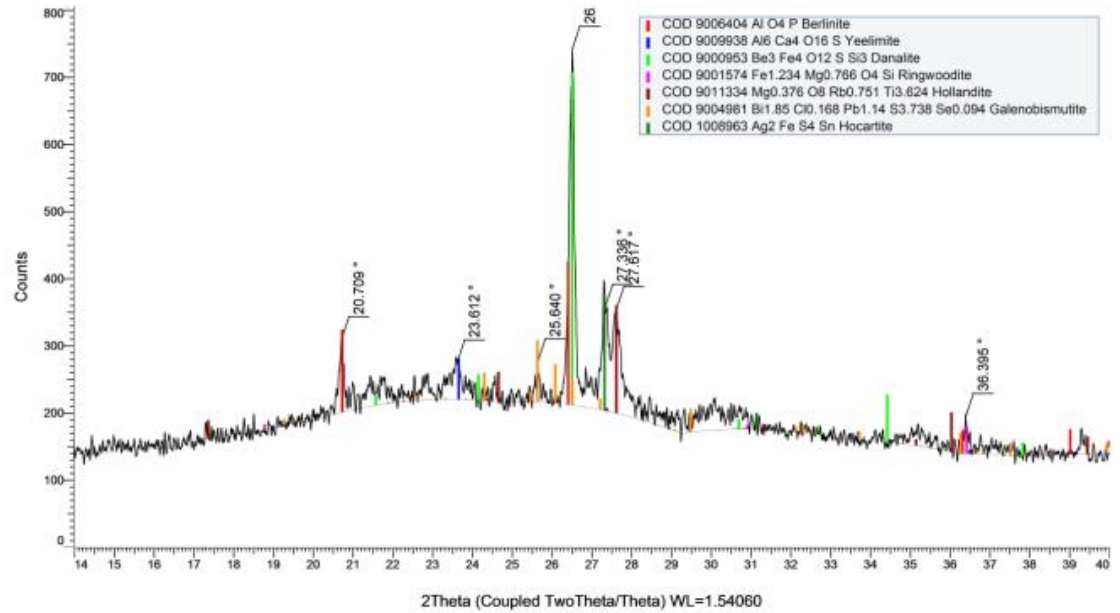


Figure 4.44: Eburru zeolite rocks XRD spectrum

Table 4.10: Diffraction parameter data for Eburru zeolite rocks sample

Index	Angle	d Value	Rel. Intensity
2	23.612 °	3.76492 Å	10.3 %
7	36.395 °	2.46657 Å	10.6 %
3	25.640 °	3.47156 Å	11.3 %
1	20.709 °	4.28560 Å	20.4 %
5	27.336 °	3.25990 Å	29.1 %
6	27.617 °	3.22740 Å	29.2 %
4	26.512 °	3.35935 Å	100.0 %

The dominant minerals of Hollandite, Donalite and Berlinite were noted at 21.6 %, 41.2 % and 14.3 %, respectively. For each of the minerals present, their chemical formulae were determined as recorded in Table 4.11.

Table 4.11: Formulation of Eburru zeolite rocks sample

Index	Compound Name	Formula	Pattern Number	I/Ic DB	S-Q
5	Hollandite	$Mg_{0.376}O_8Rb_{0.751}Ti_{3.624}$	COD 9011334	3.190	21.6 %
4	Ringwoodite	$Fe_{1.234}Mg_{0.766}O_4Si$	COD 9001574	3.610	5.0 %
6	Galenobismutite	$Bi_{1.85}C_{10.168}Pb_{1.14}S_{3.738}Se_{0.094}$	COD 9004981	7.580	5.2 %
3	Danalite	$Be_3Fe_4O_{12}SSi_3$	COD 9000953	5.170	41.2 %
2	Yeelimite	$Al_6Ca_4O_{16}S$	COD 9009938	3.630	7.2 %
1	Berlinite	AlO_4P	COD 9006404	6.390	14.3 %
7	Hocartite	Ag_2FeS_4Sn	COD 1008963	13.790	5.4 %

The EDX characterization of Eburru zeolite rocks sample showed aluminum and silicon oxides levels of 18.8 % and 37.4 %, respectively, while Fe, K, Mn, etc oxides were also observed (Table 4.12).

Table 4.12: The EDX content of Eburru zeolite rocks

Analyte	Result %	Standard Deviation	Line	Intensity (cps/ uA)
SiO ₂	37.410	0.433	SiK α	0.7178
Fe ₂ O ₃	21.389	0.069	FeK α	116.996
K ₂ O	20.671	0.149	K K α	1.8806
Al ₂ O ₃	18.764	1.649	AlK α	0.0294
ZrO ₂	0.609	0.004	ZrK α	29.8216
MnO	0.585	0.014	MnK α	2.8732
CaO	0.194	0.033	CaK α	0.2792
NbO	0.100	0.002	NbK α	5.9555
SO ₃	0.075	0.004	S K α	0.0746
Y ₂ O ₃	0.074	0.002	Y K α	3.6852
ZnO	0.074	0.003	ZnK α	1.6514
Rb ₂ O	0.057	0.002	RbK α	2.8905

FTIR characterization of Eburru zeolite rocks sample generated the spectrum below (Figure 4.45) and data in table 4.13.

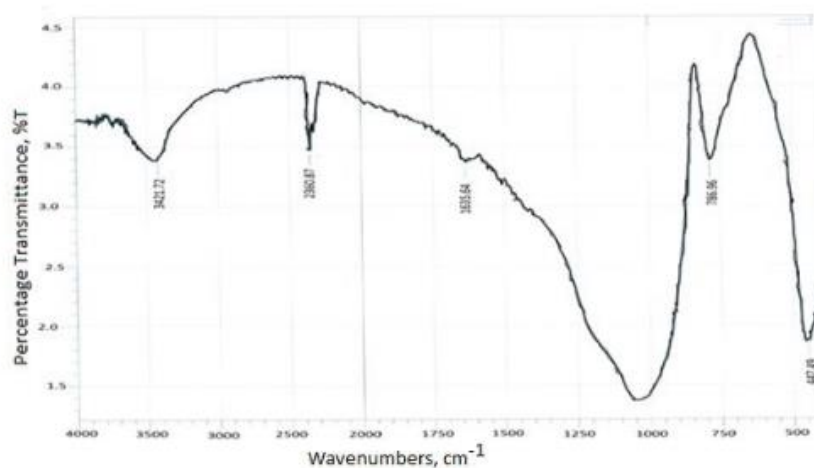


Figure 4.45: FT-IR spectra of Eburru zeolite rocks sample

Table 4.13: The Infrared band location of Eburru zeolite materials

Commercial zeolite rocks	Eburru zeolite rocks	Assignments
3471.87	3421.72	H-O-H Stretching of absorbed water
2357.01	2360.87	H-O-H overtone in plane bending
1654.92	1635.64	H-O-H Bending of water
-	786.96	Si-O quartz
663.51	-	Si-O-Si Bending
-	447.49	Si-O-Si Bending for internal tetrahedral

Mozgawa *et al.*, (2005) attributed bond bridge vibration to a range of wave numbers. Notably, Si-O(Si) and Si-O(Al) could have asymmetric elongating vibrations nearing 1006 cm^{-1} , Si-O-Si symmetric vibration nears 726 cm^{-1} . On the other hand, Si-O-Al symmetric stretching vibration bridge bonds near 670 cm^{-1} , vibrations around 550 cm^{-1} could be thought of symmetric stretching of bridge bonds and bending for Si-O-Si and O-

Si-O correspondingly, while lower wavenumbers of between 466 cm^{-1} and 250 cm^{-1} could correspond to distinctive bending vibrations occurring in four membered rings (Wlodzimier et al, 2011), of which similar peak was exhibited by Eburru zeolite rock sample at around 447.49 cm^{-1} suggesting that this particular sample had strong fundamental vibrations of alumino silicate framework composition in comparison to their natural rock samples.

The SEM of the natural zeolitic rock illustrated that particles had uneven sizes (figure 4.46) with irregularly shaped crystals.

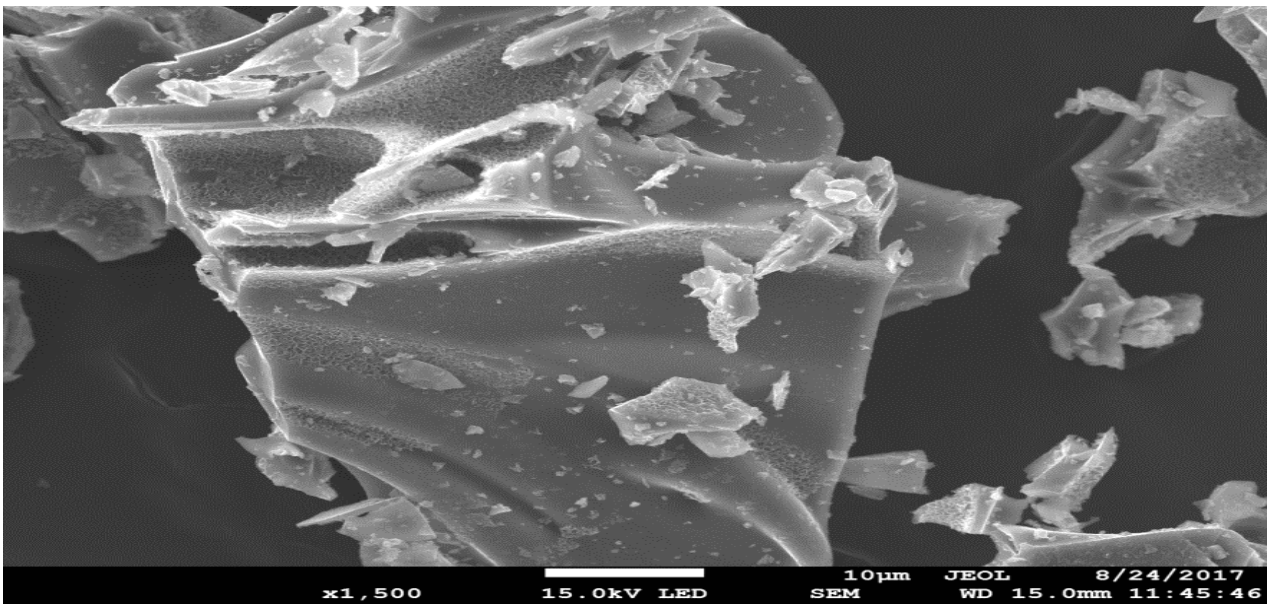


Figure 4.46: The SEM images of Eburru zeolitic rock.

The general soil/sediment analysis process done on the natural zeolitic rock samples before calcination gave the information recorded in table 4.14 below. The percentage magnesium is 0.59 ± 0.07 compared to 0.62 ± 0.04 , 4.70 ± 0.11 , 0.84 ± 0.03 levels of potassium, calcium and sodium respectively. Cations present in the zeolite could be in the form of K^+ , Na^+ , Ca^{2+} , or Mg^{2+} , and in all cases acid-base interaction between the zeolite and H_2S can occur and an example is shown in equation 4.6.

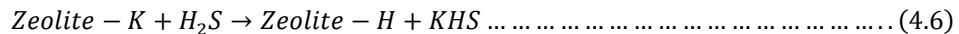
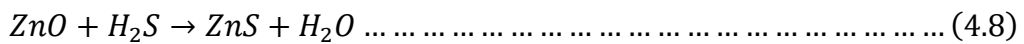
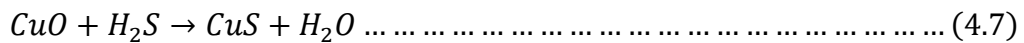


Table 4.14: Composition properties of zeolite rocks

Parameter	%	Parameter	%
Zeolite rock pH	8.38±0.52	Magnesium (me%)	0.59±0.07
Total Nitrogen (%)	0.10±0.02	Manganese (me%)	0.20±0.01
Total Org. Carbon (%)	0.94±0.04	Copper (ppm)	1.36±0.05
Phosphorus (ppm)	3.40±0.12	Iron (ppm)	13.34±1.29
Potassium (me%)	0.62±0.04	Zinc (ppm)	10.22±1.88
Calcium (me%)	4.70±0.11	Sodium (me%)	0.84±0.03
Elect. Cond. mS/cm	0.23±0.01		

The rock samples were moderately alkaline, with minimum organic content. Beside silicon and aluminum, which form the main components of zeolites were below detection limits, elements like Iron, Zinc and Calcium as indicated in table 4.14 were also present. Utilisation of Cu and Zn modified zeolites adsorbents was observed to be enhanced by (CuO or ZnO) as indicated by equations 4.7 and 4.8 (Micoli *et al.*, 2014):



4.14.2 Biogas from cow dung upgrade

The initial biogas composition levels were >20.00±2.69%, 56.04±7.56% and 226.96±6.87ppm for CO₂, CH₄ and H₂S, respectively. Higher CO₂ in biogas had been observed to lower the calorific value of biogas and has a small Wobble index (Tira *et al.*, 2015). The upgrade experiments were aimed at removing carbon dioxide and hydrogen sulphide resulting in higher methane levels. The H₂S levels compared well with those observed by Tira *et al.*, (2015) at 245.35 ppm.

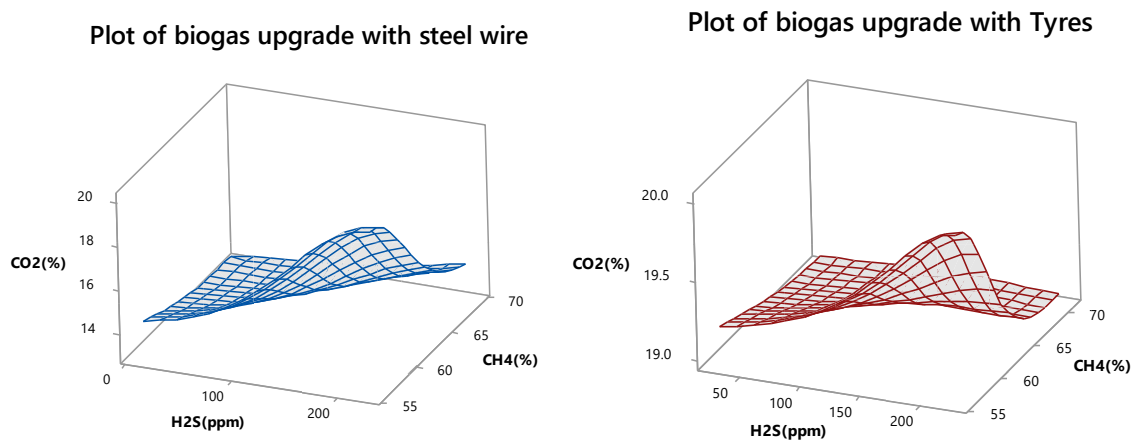


Figure 4.47: Biogas upgrade levels using steel wire and tyres

From figures 4.47, steel wire removed about 4.09% of CO₂ and 26.7ppm of H₂S compared to 1.99% of CO₂ and 166.70ppm of H₂S by tyres. The methane levels in upgraded biogas were in the range of 72 -75% for both agents. These results agree with those reported by Nallamothu, Teferra and Rao (2013) who utilized steel wool, water and silica gel to upgrade raw biogas containing to about 60-70% CH₄, 30-40% CO₂, traces of H₂S and water vapor. To test the efficiency of biogas purification, bio-methane and raw marsh gas were compared by warming 500 mL of water. Upgraded biogas heated the water in 4.54 ± 0.03 minutes while raw gas took 5.62 ± 0.02 minutes. The iron oxide in steel wire reacts with H₂S in biogas forming solid FeS₃ and water (Salihua and Alama, 2015).

Figures 4.48 shows the upgraded levels by maize cobs and desulphurizer. Previous studies by Tira *et al.*, (2018) reported that increasing corn cobs activated carbon resulted in higher CO₂ removal rates. The results showed low upgrading capacity in maize cobs compared to the other agents used at 2% CO₂ and 7% H₂S.

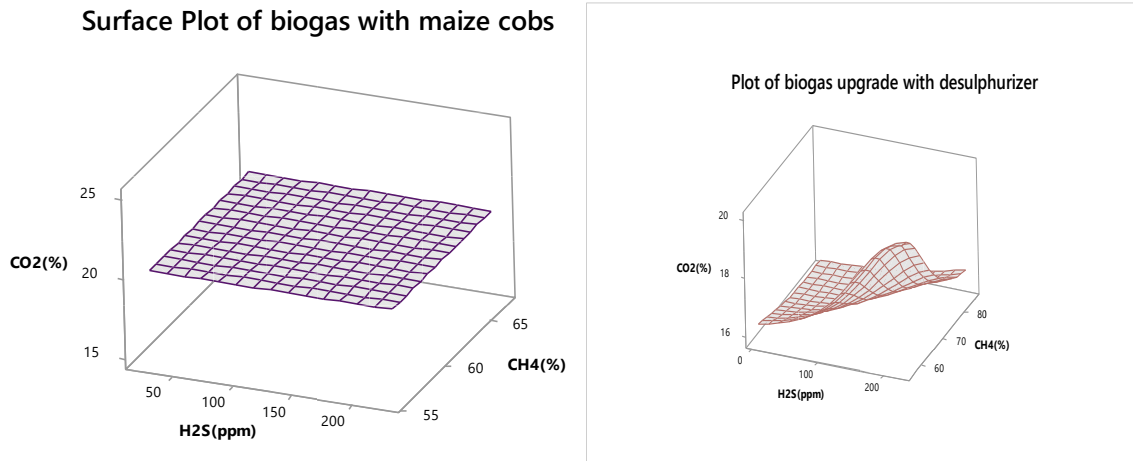


Figure 4.48: Biogas upgrade using maize cobs and desulphurizer

Desulphurizer recorded highest upgrade level for H₂S by reducing the H₂S to about 17ppm from the initial 226.7ppm. In figure 4.49, the results obtained using zeolite rocks are shown. Zeolite rocks removed about 13.09% CO₂ and 200ppm H₂S upgrading the methane levels to about 95%.

Plot of biogas upgrade with Zeolitic rocks

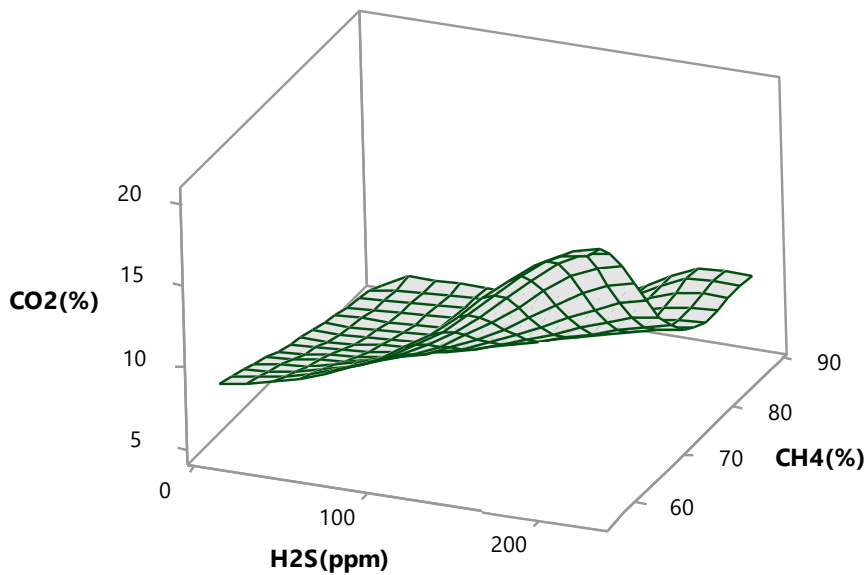


Figure 4.49: Biogas upgrade using zeolite rocks

The results obtained are comparable with those reported by Rzepka *et al.*, (2019), who used pellets of nano-sized zeolite with clay binder for biogas upgrading. A study of

biogas upgrading by scrubbing using iron oxide (steel wool) showed that the scrubbing system enriched CH₄ by about 95 % or higher subject to inlet flow and water pressure (Katara and Rahi, 2016). Further, H₂S in biogas reacts with Fe₂O₃ to form Fe₂S₃.

The CO₂ adsorption onto the zeolite surfaces was higher than other upgrading material at 75%, as shown in figure 4.50. The high efficiency of zeolite results from its bigger porous size translating to deeper penetration (Tira *et al.*, 2018).

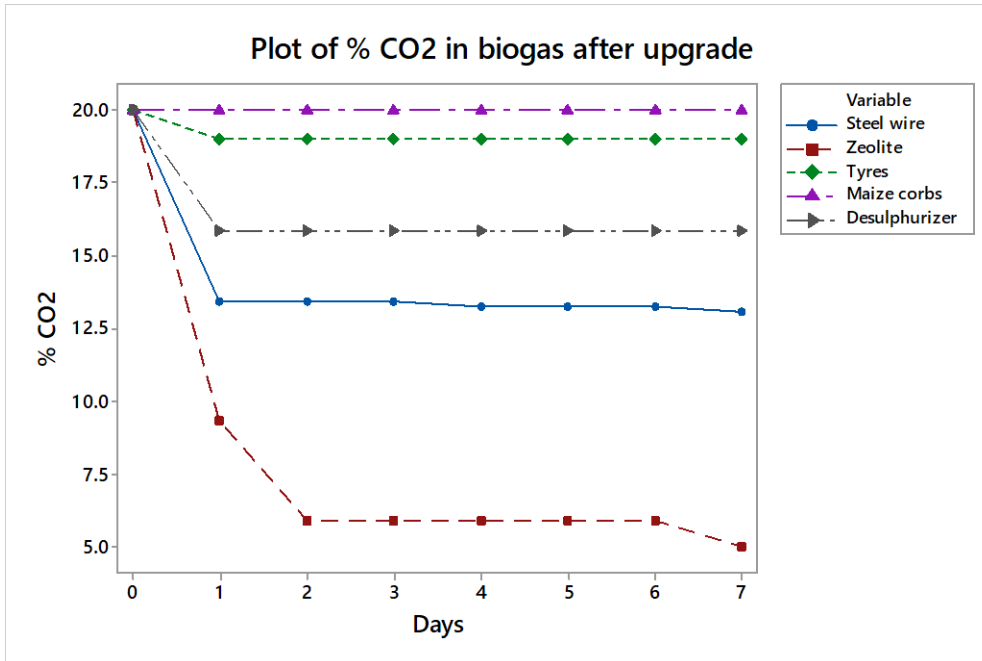


Figure 4.50: Plot of carbon dioxide levels after upgrade

It is clear from figure 4.50 that maize cobs and tires efficiency in biogas upgraded is low for CO₂ removal with removal levels of less than 3%. High CO₂ removal levels is recorded for zeolite rocks with more than 70%. Tira *et al.*, 2018; Valerio *et al.*, 2016; Vijayanand and Singaravelu, 2016; Rzepka *et al.*, 2019 other research reported CO₂ removal levels of 69 – 83% after the upgrade. The adsorption of CO₂ was predominantly occurred by Van der Waal’s force. The attractive force between CO₂, H₂S molecules and adsorbent was higher compared to that of CH₄ and adsorbent. This resulted in more impurities gases CO₂ being more tightly bound in adsorbent, while CH₄ molecules tended to pass through the adsorbent in the absence of a bond (Papagiannakis and Hountalas, 2004).

In terms of H₂S removal from raw biogas, lower levels were witnessed in tires at 35.24% reduction. Steel wires and desulphurizer reduction rates were higher at 93.83% and 97.67% respectively (figure 4.51).

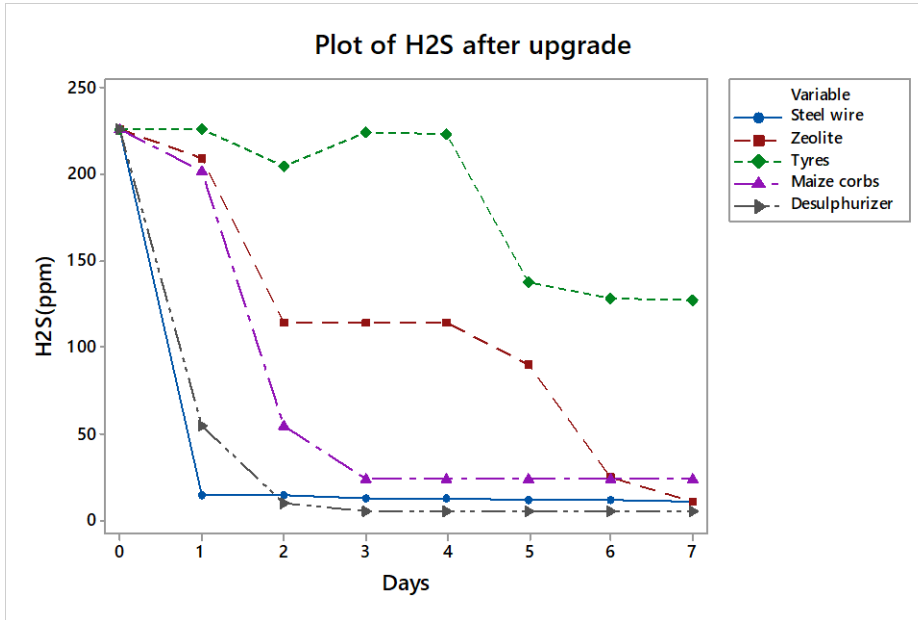
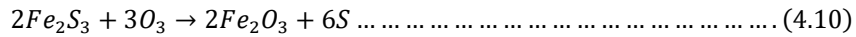
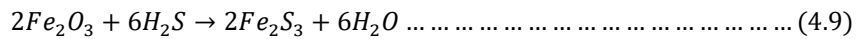


Figure 4.51: Plot of hydrogen sulfide levels after upgrade

Iron oxide reacts with hydrogen sulphide, thereby removing H₂S from the reactor. Raw biogas is pumped through steel wool, and therefore, iron oxide is converted into elemental sulphur (Suryansh and Dal, 2016) as shown in equations 4.9 and 4.10.



The methane levels obtained after passing raw biogas through upgrading cartridges is shown in figure 4.52. The highest methane levels were recorded in desulphurizer agent at 95%, followed by 89.9% in zeolite rocks. This confirmed why desulphurizer is widely employed in the cleaning of biogas.

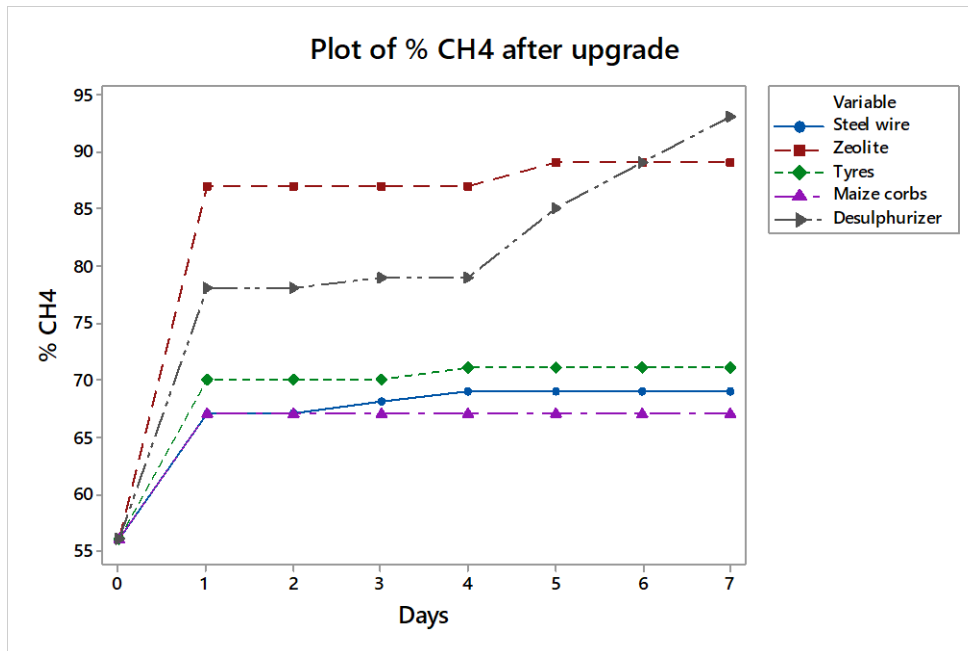


Figure 4.52: The % methane after raw biogas upgrade

The results confirm that the zeolitic rocks are superior to tires, maize cobs, steel wire and desulphurizer in improving biogas quality. The desulphurizer material suited best in the removal of hydrogen sulphide with up to 97.78 % removal. The upgrading efficiency of desulphurizer, combined with zeolite material in pilot-scale was in the range of 87.67 – 93.93 % methane and CO₂ removal rate of 53.20 – 77.76 %.

In another study on biogas upgrading, raw biogas was generated from market wastes inoculated with rumen waste. The initial composition of biogas from market waste was 20% carbon dioxide, 54% methane and 327.50 ppm hydrogen sulfide. The results obtained after the upgrade using different cartridges are shown in figure 4.53. The CO₂ removal rate was highest in zeolite rocks at 80% and lowest in tires at 2%. The other agents removed CO₂ (50-52 %) range. Methane levels in the upgraded biogas were 67 - 92% for all the cartridges employed in the upgrade experiments, as shown in figures 4.53. The overall removal of hydrogen sulphide was highest in steel wire with over 99.64% removal and lowest in tires with 83.51 %.

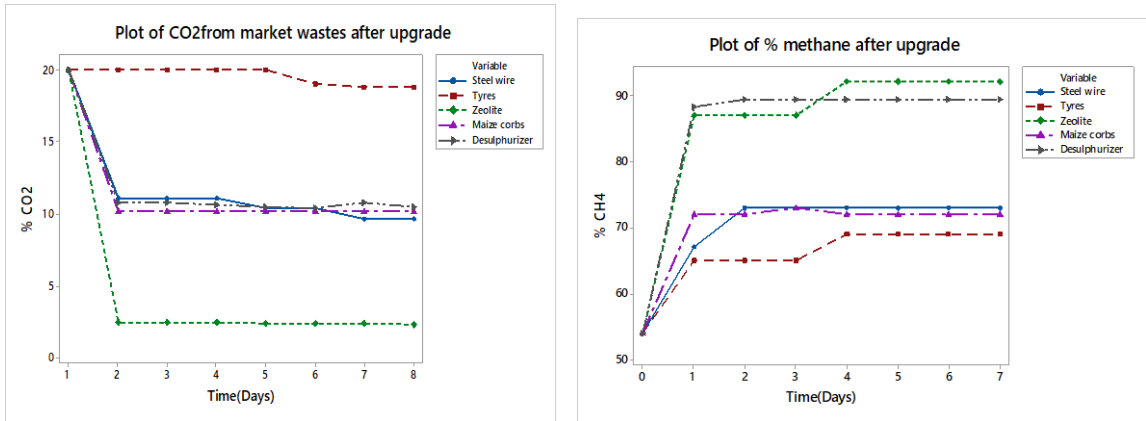


Figure 4.53: Plot of % methane and carbon dioxide after upgrade

The pilot-scale upgrade level is shown in figure 4.54. The highest upgrade levels were observed in desulphurizer and zeolite rocks as recorded in lab-scale experiments.

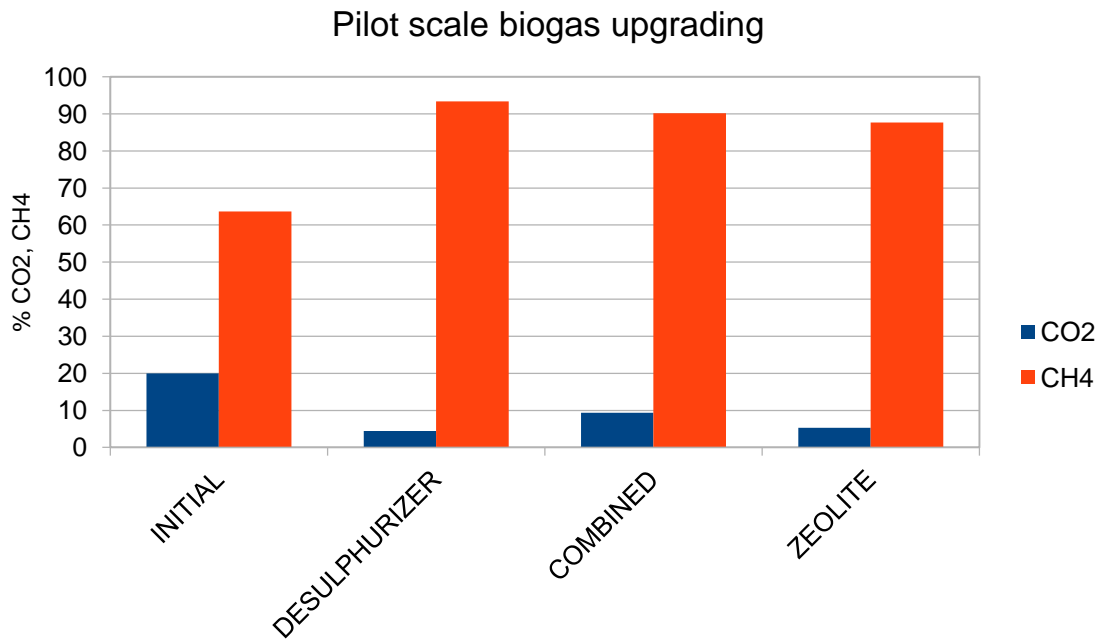


Figure 4.54: Pilot-scale CO₂ and CH₄ levels after clean up

From figure 4.54, CO₂ was reduced from the initial 20% in raw biogas to 4.48, 9.36 and 5.26% by desulphurizer, combined agents and zeolite rocks respectively. The initial levels of hydrogen sulphide were 162±15.36 ppm with reduction of up to 2.00±1.73 ppm, 6.66±0.51 ppm, 3.67±1.53 ppm for desulphurizer, combined agents and zeolite rocks respectively.

4.15 Simulation and modeling

Validated mathematical models built from mechanistic studies that lead to a more indepth understanding of the very complex transport phenomena, microbial biochemical kinetics, and stoichiometric relationships associated with anaerobic digestion can be used to improve the design and optimization of anaerobic digestion processes for biogas development (Bharati and Shinkar, 2014). Various kinetic models were used to match the obtained data in this section.

4.15.1 Anaerobic Digestion Kinetic Study

The performance of AD digester can be predicted by the AD Kinetic studies. The limiting parameters can also be highlighted by the kinetic studies. The performance of the AD process was investigated using first-order kinetic models (Llabres and Mata., 1987; Mata., *et al.*, 1993).

4.15.1.1 Linear kinetic model

The model suggest that biogas generated rises with HRT as per equation 4.11(Ghatak and Mahanta, 2014).

$$B_1 = a_1 + b_1 t \dots \dots \dots (4.11)$$

Where B_1 is the biogas production rate ($L\ kg^{-1}\ d^{-1}$) at time t (day), t is the time (day) over the digestion period, a_1 is intercept ($L\ kg^{-1}\ d^{-1}$) and b_1 is slope ($L\ kg^{-1}\ d^{-2}$). For rising limb, b_1 is positive, whereas b_1 is negative for falling limb. The obtained data were fitted onto the linear kinetic model and coefficient of determination R^2 got was in the range of 0.63 to 0.98. The plots are shown in Figure 4.55.

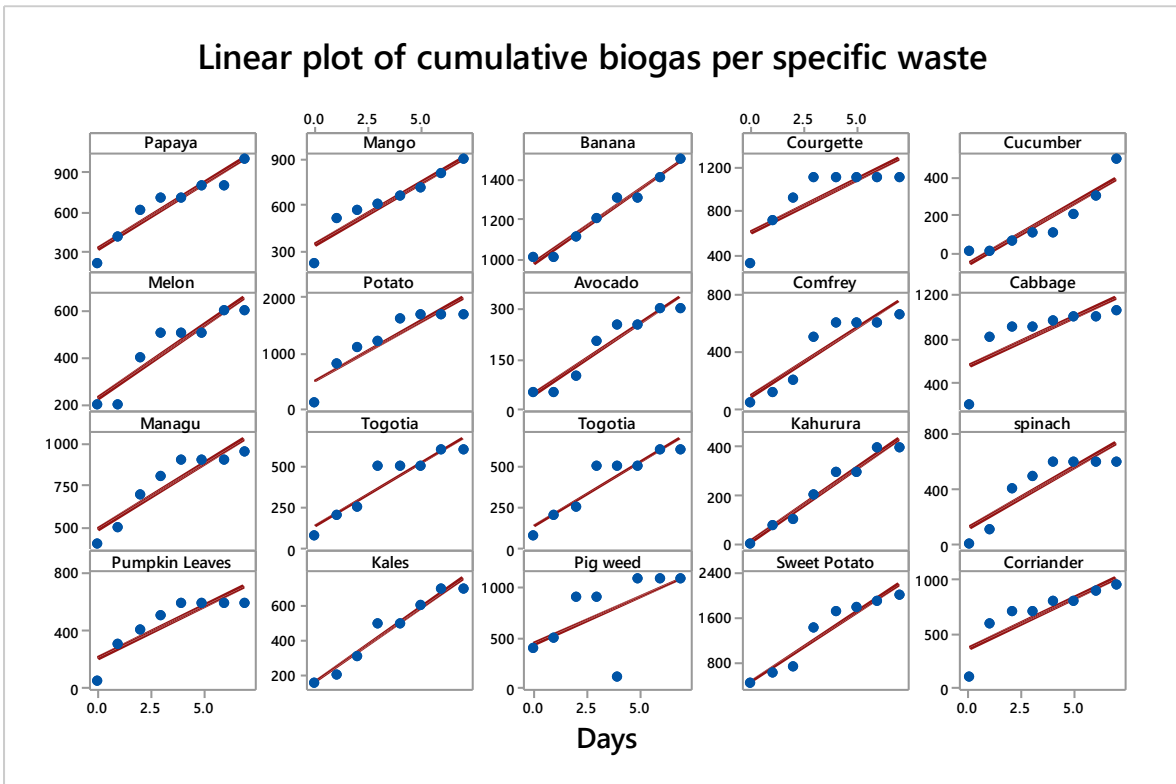
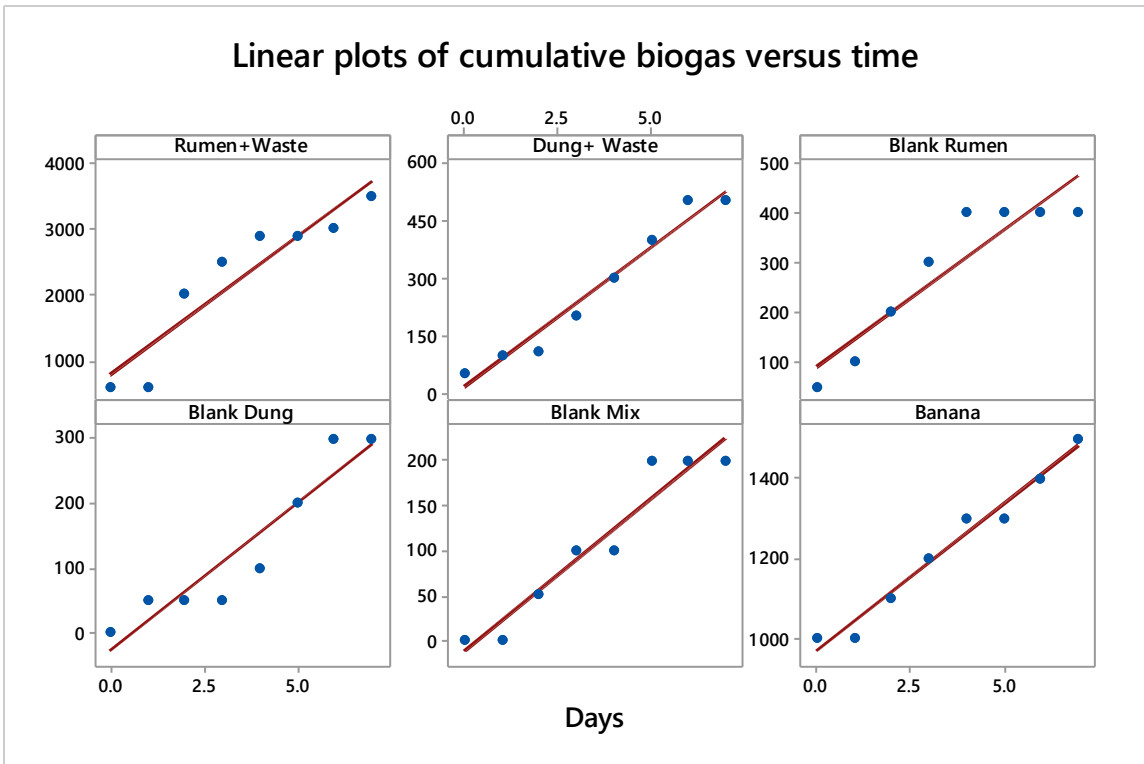


Figure 4.55: Plot of the linear model for market wastes biogas production

From figure 4.55, the slope represents feedstock’s digestion rate. The rate is highest in rumen inoculated digester compared to the cow dung inoculated digesters. This is due to the high microbe counts in rumen compared to the counts in manure translating to high competition for substrate depletion.

4.15.1.2 Exponential kinetic model

The exponential model proposes exponential increase in biogas formed with time (equation 4.12) (Kumar *et al.*, 2004; Aritra and Mondal, 2015).

$$B_1 = a_1 + b_e \exp(c_e t) \dots \dots \dots (4.12)$$

Where B_1 is the biogas production rate ($L\ kg^{-1}\ d^{-1}$) at time t (day), t is the time (day) over the digestion period, a_1 is intercept ($L\ kg^{-1}\ d^{-1}$) and b_1 is the slope ($L\ kg^{-1}\ d^{-2}$) and c is a constant (d^{-1}). For the upward limb, b_1 is positive and b_1 is negative for downward limb. The experimental data plot is shown in figure 4.56, with y representing the cumulative biogas produced in mL/day. The coefficient of determination was in the range of 0.78 to 0.99.

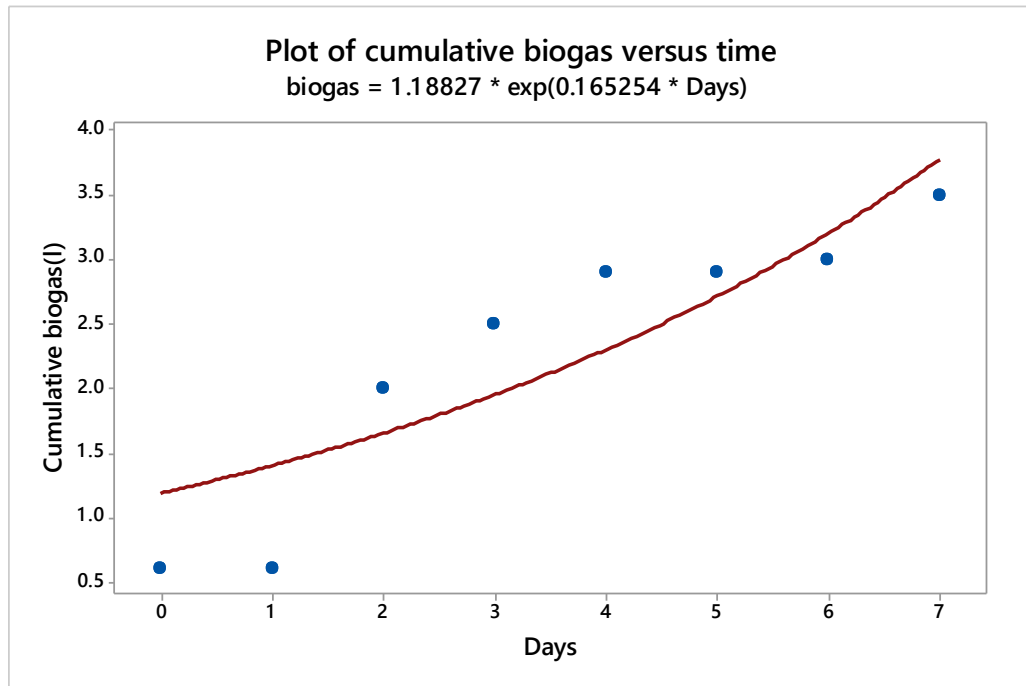


Figure 4.56: The exponential plot for FVMW mixture biogas production

Figure 4.57 depicts the exponential curves of the cumulative biogas generated from banana market waste inoculated with rumen waste. The correlation of the operation parameters relates highly with R^2 of 0.97.

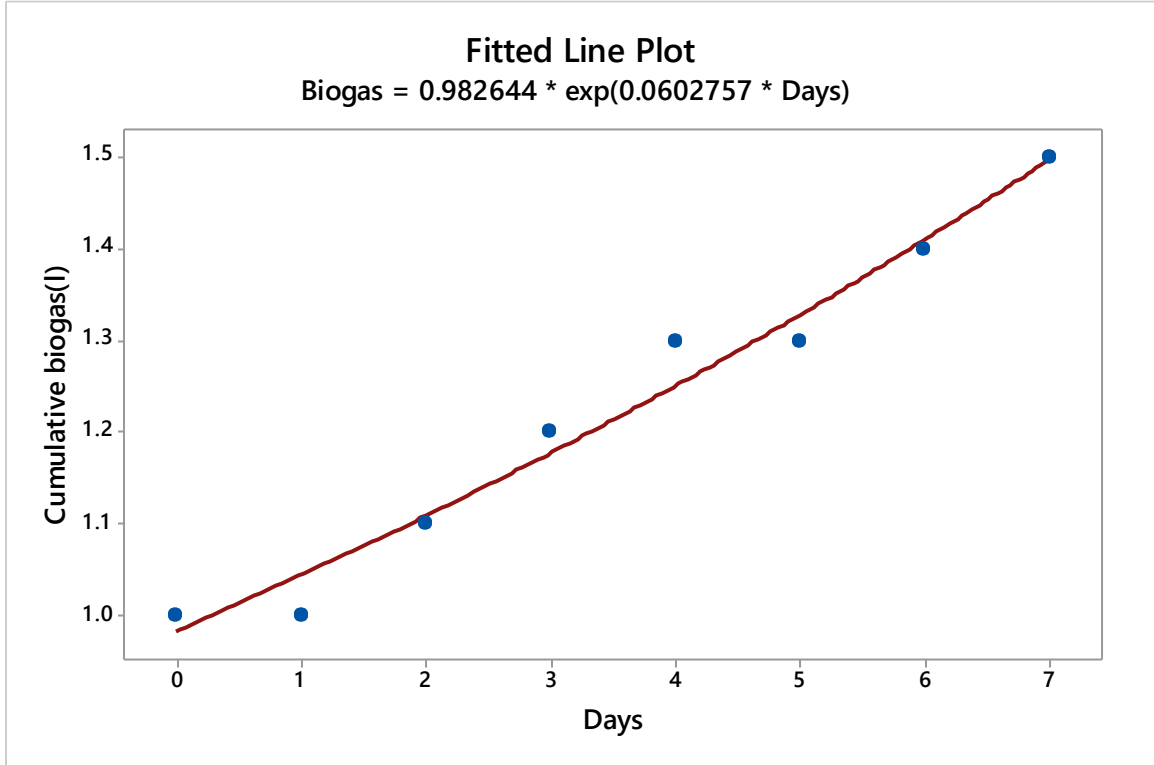


Figure 4.57: Exponential plot for banana wastes biogas production

4.15.1.3 Gaussian Kinetic Model

Assuming that biogas generation rates and microbial kinetic growth and its decay would follow the normal distribution throughout the breakdown period, the Gaussian equation, presented in equation 4.13 (Aritra and Mondal, 2015; Lo *et al.*, 2010) was employed to predict biogas recoveries rate including ascending and descending limb.

$$B_1 = a_1 \exp\left(-0.5 \left(\frac{t - t_0}{b}\right)^2\right) \dots \dots \dots (4.13)$$

Where t_0 is the time (day) where the peak (maximal) biogas generation rates occurred. The obtained normal distribution curves for the growth are shown in figure 4.58 for the blanks and the market wastes production.

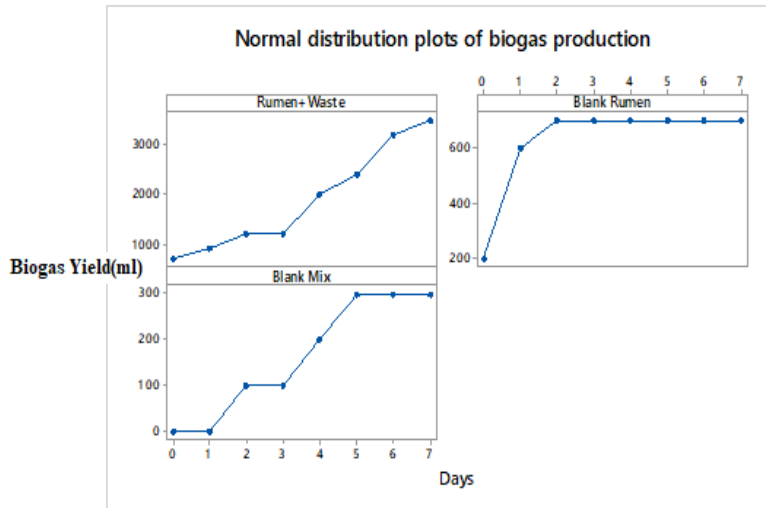


Figure 4.58: The normal distribution curves for biogas production.

According to the Gaussian plot in figure 4.58, the plots rise from day one of digestion and plateau when microbial activities stop showing depletion of substrates. The curves start to drop, indicating no further biogas production. This is the point at which loading should be done for a continuously operated digester. The coefficients of determination were 0.83, 0.96 and 0.95 for blank waste, waste + rumen and blank rumen, respectively. The trend is very pronounced in bank rumen, where the rate of substrate breakdown is very high and stops in day two, where the curve flattens. As for the blank waste mixture, the bacteria in the wastes take time to adjust to the environment in the digester for about 3 days and then production is halted at day 5 due to pH changes (Mbugua *et al.*, 2020). The growth and development of the microbes are clearly shown in blank waste and waste inoculated with rumen waste. Initially, the microbe's concentration is low and require time to adapt at lag phase. The concertation increases rapidly and high biogas generation is witnessed (growth phase). This phase terminates when cells compete for diminishing substrate and therefore, replication equals death (stationary phase). The stationary phase ends when death is higher than reproduction and biogas generation decreases rapidly (death phase) (Velázquez-Martí *et al.*, 2018).

4.15.1.4 Modified Gompertz Equation

The experimental data from the co-digestion of market waste with rumen matter was investigated for its alignment to the modified Gompertz equation 4.14.

$$P = \gamma_m \cdot \exp \left\{ -\exp \left[\frac{u \cdot e}{\gamma_m} (\lambda - t) + 1 \right] \right\} \dots \dots \dots (4.14)$$

The resultant curve is indicated in figure 4.59.

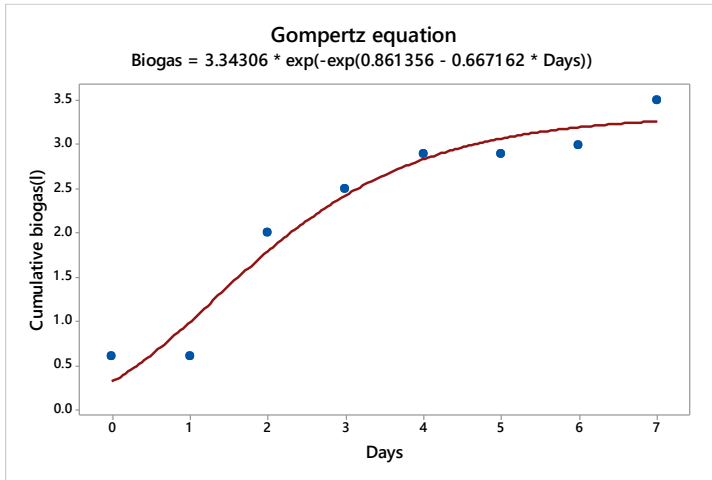


Figure 4.59: The Gompertz plot for FVMW plus rumen biogas production

In the simulation section, the coefficient of determination of FVMW inoculated with rumen was 0.96 and the plot is shown in figure 4.59. Biogas generation rate (μ_m) and lag phase period (λ) was found to be 3.34mL/gm/day and 0.86 days at 55°C while the biogas generation (P) was estimated at 49.09 mL/gm. This is consistent with the results reported for cow dung waste at the thermophilic temperature at 39.10mL/g biogas produced at a production rate of 1.40 mL/g/day and a lag phase 6.22 day (Ghatak and Mahanta, 2014).

4.15.1.5 Methane Energy Value

Methane energy value (MEV) model was employed, which estimates methane yield from the nutrient composition of energy crops in mono fermentation via regression models (Angelidaki *et al.*, 1993; Batstone *et al.*, 2000; Henze *et al.*, 1986; McCarty and Mosey, 1991; Pavlostathis and Gossett, 1986). The MEV was computed using equation 4.15

$$MEV(1_N CH_4 kg^{-1} VS) = x1 * XP + x2 * XL + x3 * XF + x4 * XX \dots \dots \dots (4.15)$$

Where VS is volatile solids, XP is crude proteins, XL is crude lipids, XF is crude fiber and XX is the nitrogen free extract. The MEV of a substrate showed the energy figure, which can be recorded from an organic matter. The results obtained are shown in table 4.15, and it was observed to be highly influenced by the proximate properties of the waste.

Table 4.15: The methane energy values

Sample	% Fiber	%Protein	% Fat	% NFE	MEV ($1_NCH_4kg^{-1}VS$)	Energy (Kcal/100g)
Kales	15.01	21.68	3.22	31.12	430.91	240.18±15.00
Cabbage	10.38	16.12	0.96	57.71	659.48	303.96±13.00
Pumkin Leaves	10.72	25.99	2.12	28.54	401.89	238.01±16.99
<i>Cucumis ficifolia</i>	11.07	26.11	2.46	29.46	413.52	244.42±12.89
Pigweed	18.18	22.98	1.83	20.39	332.87	189.95±7.34
<i>Erucastrum arabicum</i>	15.81	26.57	1.85	26.38	396.49	228.45±10.99
Coriander	14.05	33.01	1.19	19.57	340.45	220.99±12.78
African nightshade	23.11	22.69	2.23	23.45	378.59	204.63±15.66
Spinach	13.74	22.8	2.52	28.54	402.58	228.04±8.09
Comfrey	13.85	21.71	1.98	24.37	356.32	202.14±7.78
Tomato	15.75	11.89	2.57	55.42	644.83	292.37±13.23
Potato	4.19	8.73	3.34	62.51	673.88	315.02±21.89
Sweet Potato	4.01	4.42	4.07	46.75	505.00	241.35±11.10
Pawpaw	12.16	6.36	3.15	62.9	694.01	305.39±14,23
Banana	4.85	11.89	1.97	49.06	546.73	261.53±9.84
Avocado	15.22	7.69	52.64	2.36	250.25	513.94±24.89
Courgette	14.87	22.92	5.48	36.5	494.81	287.01±10.00
Cucumber	18.75	12.65	5.19	48.13	591.07	289.83±12.89
Mango	9.74	6.61	5.23	61.91	683.84	321.15±23.00
Water Melon	15.68	12.72	4.63	49.34	592.49	289.91±56.78

From table 4.15, the MEV was twice as much as the energy value of the waste. For instance, the MEV for tomato was 644.83 kcal/kg compared to 292.37292.37kcal/100g energy. The MEV of avocado was 250.25 kcal/kg compared to the energy value of 513 kCal/100g.

4.15.2 Bio-methane Potential studies

Equations 2.10 and 2.11 (in chapter 2) were employed in computation of methane yield capacity of the wastes (Buswell and Mueller, 1952) while (BMP_{OFC}) was calculated as per Lesteur *et al.*, (2010) description while theoretical, equations 2.21, 2.22, 2.23 and 2.25 (in chapter 2) were employed and the results given in table 4.16. Only the mean of the BMP calculations is reported.

Table 4.16: Table of Experimental and theoretical BMPs

SAMPLE	% CARB.	% PROTEIN	% FAT	BMP _{CHNO} (ml/g.VS)	BMP _{OFC} (ml/g.VS)	TBMP mlCH ₄ gVS ⁻¹
Kales	31.12	21.68	3.22	269.33	236.7135	449.6350
Cabbage	57.71	16.12	0.96	329.18	319.4614	491.6115
Pumpkin Leaves	28.54	25.99	2.12	268.84	247.3729	452.9704
Cucumis ficifolia	29.46	26.11	2.46	276.70	251.7895	492.8013
Pigweed	20.39	22.98	1.83	217.15	198.6179	494.8469
Erucastrum arabicum	26.38	26.57	1.85	260.02	241.283	502.3386
Coriander	19.56	33.01	1.19	256.97	244.9157	494.5887
A. nightshade	23.45	22.69	2.23	232.47	209.8825	503.2272
Spinach	28.54	22.8	2.52	257.08	231.5546	501.9992
Comfrey	24.37	21.71	1.98	228.89	208.8372	495.7319
Tomato	55.42	11.89	2.57	315.02	288.9935	490.9395
Potato	62.51	8.73	3.34	336.58	302.7512	454.7203
Sweet Potato	46.76	4.42	4.07	257.24	216.0185	454.5800
Pawpaw	62.9	6.36	3.15	324.52	292.6125	467.3760
Banana	49.06	11.89	1.97	282.54	262.5934	451.7274
Avocado	2.36	7.69	52.64	581.70	48.47017	456.3218
Courgette	36.50	22.92	5.48	320.72	265.2138	930.5539
Cucumber	48.13	12.65	5.19	315.11	262.5361	508.9576
Mango	61.91	6.61	5.23	342.74	289.7651	1065.510
Watermelon	49.34	12.72	4.63	314.80	267.8991	467.7762
Waste Mixture	38.2205	17.277	5.43	299.38	244.3641	478.3047

From table 4.16, BMP_{CHNO} and BMP_{OFC} are similar. The theoretical values ($TBMP_{mLCH_4gVS^{-1}}$) was highest. This is explained by the fact that some VM is used for microbe's development and metabolism as the other fraction converted to CH_4 (Ali *et al.*, 2018). Lower BMP was recorded for BMP_{thCOD} ranging from 47.9458 $mL/g.COD$ in comfrey to 4325.9308 $mL/g.COD$ in cucumber. The BMP was in the sequence of 51.14803 $mL/g.COD$, 244.3641 $mL/g.VS$, 299.38 $mL/g.VS$ and 478.3047 $mLCH_4gVS^{-1}$ for BMP_{thCOD} , BMP_{OFC} , BMP_{CHNO} and TBMP for FVMW inoculated with rumen. According to these results, the best-recommended BMP calculation method is BMP_{OFC} or BMP_{CHNO} when proximate and ultimate properties are known. These two methods represent the actual properties of the samples. Further, the low BMP_{exp} values are explained by the fact that lignin is non-digestible, whereas the theoretical BMPs are calculated with an assumption of 100% digestibility (Wall *et al.*, 2013). These methods do not consider the substrates used for cell growth and therefore, they might be erroneous (Raposo *et al.*, 2011). The theoretical BMP of 20 market wastes was also studied using online biogas application by Sasha *et al.*, (2018). The application which is built in R programming language is found at <https://cran.r-project.org/package=biogas>. This determination was based on the feedstocks macromolecular content. The resultant equation and methane potential are shown in the table (appendix C).

4.15.3 Anaerobic Biodegradability

Most digestibility methods assume that all reactor content is degradable and therefore, BMP studies are done to compensate for this assumption (Raposo *et al.*, 2011). The elemental bio-digestibility (BD_{ele}) was computed using equation 4.16 (Raposo *et al.*, 2011)

$$BD_{ele} = \frac{BMP_{exp}}{BMP_{CHNO}} \dots \dots \dots (4.16)$$

Where BD_{ele} is bio-digestibility

Based on the VS content, the feedstock digestibility (BD_{exp}) was calculated using equation 4.17 (Nielfa, 2015).

$$BD_{expVS} = \frac{VS_i - VS_f}{VS_i} * 100 \dots \dots \dots (4.17)$$

Where BD_{expVS} is bio-digestibility in terms of volatile msolids, VS_i is initial volatile solids and VS_f is final volatile solids.

Depending on the lignin matter (X_i), the digestability (BD_{LB}) was evaluated as per equation 4.18 (Chandler *et al.*, 1980).

$$BD_{LB} = (0.83 - (0.028 * X_i)) * 100 \dots \dots \dots (4.18)$$

The obtained results are shown in table 4.17.

Table 4.17: Table of of different feedstock’s biodegradability

Substrate	BD_{exp}	BD_{LB}	BD_{ele}
Kales	86.24±2.34	77.40±1.09	83.91±2.11
Cabbage	83.19±1.00	73.90±1.20	80.50±1.53
Pumkin Leaves	84.64±2.19	75.72±3.01	79.60±1.00
<i>Cucumis ficifolia</i>	77.36±3.99	71.81±3.00	81.98±1.54
Pigweed	85.88±0.99	68.36±1.26	81.51±1.64
<i>Erucastrum arabicum</i>	76.85±5.87	72.08±2.78	73.07±1.88
Coriander	85.43±0.89	69.28±2.89	77.83±1.93
A. nightshade	80.77±2.33	74.04±1.66	76.57±1.07
Spinach	80.00±1.50	74.88±2.06	77.80±0.87
Comfrey	86.96±7.00	71.80±1.96	78.64±1.90
Tomato	82.19±3.33	72.92±2.00	79.36±1.98
Potato	84.10±2.12	76.56±1.19	80.22±1.22
Sweet Potato	84.82±7.88	70.43±2.36	77.75±0.68
Pawpaw	84.73±5.63	76.56±1.88	77.04±0.89
Banana	86.27±5.73	74.04±2.05	75.74±1.45
Avocado	84.08±0.82	76.56±2.76	77.36±0.95
Courgette	77.16±1.26	68.16±1.33	74.83±1.55
Cucumber	78.26±3.56	69.28±1.25	76.16±1.67
Mango	81.95±0.99	77.12±2.89	79.07±1.88
WaterMelon	76.61±.32	71.82±1.22	74.65±1.00
FVMW Mix	93.48±1.11	77.76±1.26	83.51±1.78

The three substrate degradability methods gave almost the same results. For example, watermelon sample digestibility was 76.61 ± 3.32 , 71.82 ± 1.22 and 74.65 ± 1.00 representing BD_{exp} , BD_{LB} and BD_{ele} , respectively. From BD_{ele} calculations, substrates decomposition magnitude is shown which classifies biomass as degradable or non degradable. Ali *et al.*, 2018 noted that lignin decreased digestibility of a matter three times. The variation of BMP studies based on the digestibility has been reported but vary accordingly (Lesteur *et al.*, 2010; Chandra *et al.*, 2013).

4.16 Pilot Scale Experiments

The pilot-scale experiments were done using 5liters, 10liters, 60liters, 160 liters and 240 liters' capacity plastic containers and the results were discussed. In figure 4.60, cumulative biogas produced from waste inoculated with rumen using a 5liter digester is shown. The cumulative biogas generated increased with an increase in retention time. The influence of temperature is very pronounced as the production rate is three times higher in thermophilic setups compared to psychrophilic production.

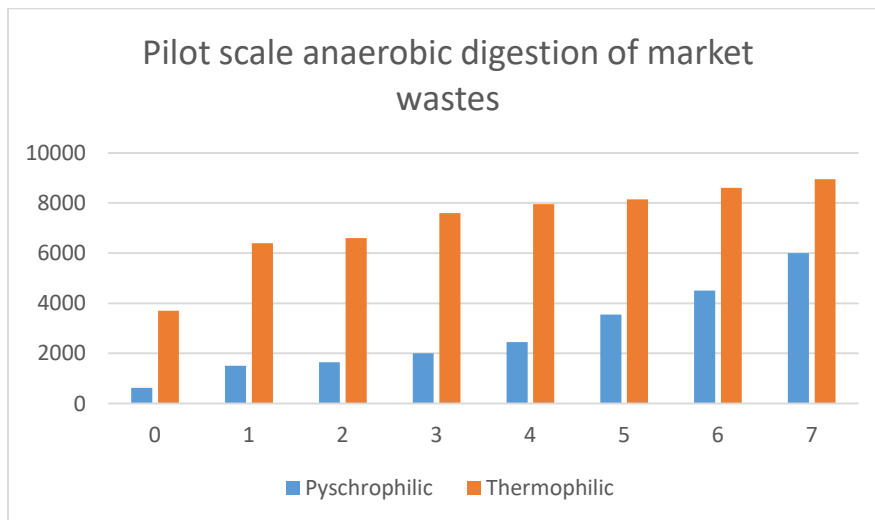


Figure 4.60: Bar graphs of pilot-scale biogas production at thermophilic and psychrophilic temperatures

For example, on day seven, the psychrophilic and thermophilic biogas generated was 6000mL and 8950mL, respectively. Biogas generation started immediately after setting up the digesters with 600mL and 3700mL recorded in psychrophilic and thermophilic

setups. The high microbe concentration in rumen fluid accounted for this observation, as reported by Mbugua *et al.*, (2020).

Mesophilic biogas generation is the most common due to the high production rate and lower temperatures and operations cost. Figure 4.61 shows the cumulative production of 5 litres digester at mesophilic conditions.

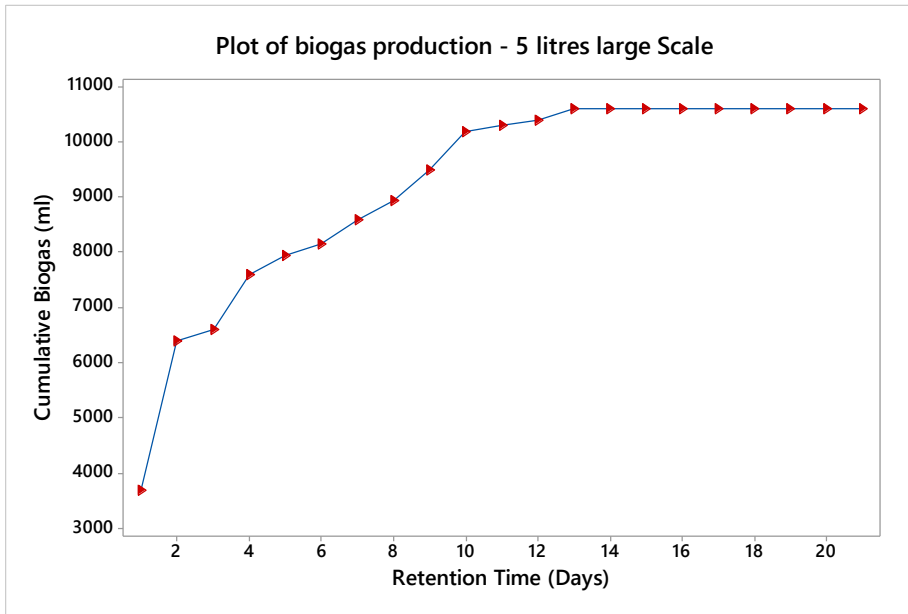


Figure 4.61: Time graph of cumulative biogas produced in a 5l large-scale digester. The gas generated from FVMW co-digested with cow dung showed a high increase in production for the first two days and after that a normal increment for the entire digestion period. Cumulatively, about 9000mL of biogas was generated. Production from another pilot scale at psychrophilic conditions is shown in figure 4.62 and 4.63. The production was higher on warmer days compared to cold days. In figure 4.62, pilot scale set up of cow dung shows that biogas generation was higher in larger volume digesters as expected at around 100l in 8 days for 240l digester and 75l for 120-liter digester. Large volumes mean high concentration of microbes translating to higher microbial activities and subsequently higher productions.

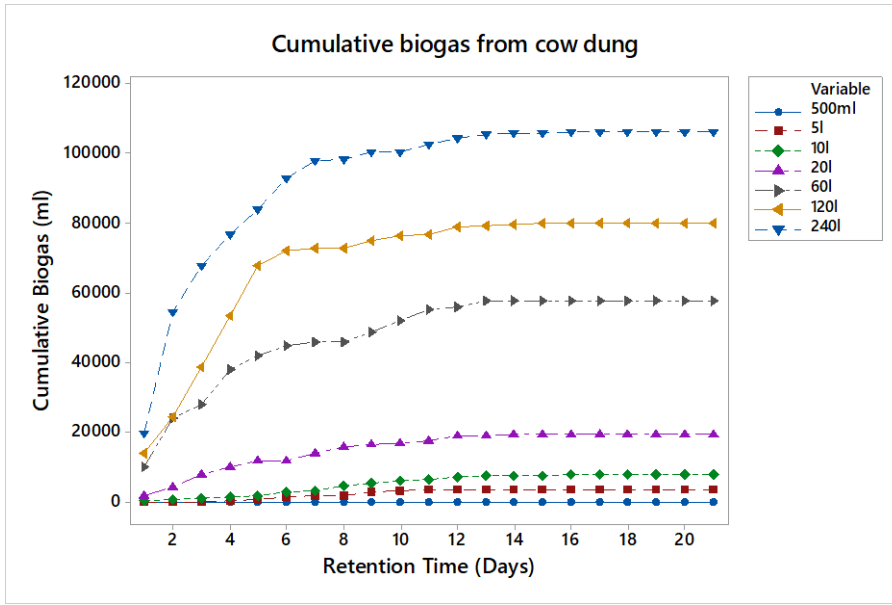


Figure 4.62: Plot of cow dung psychrophilic biogas generation

Cow dung is widely employed for biogas generation in Kenya (Mbugua *et al.*, 2020). This study suggested a minimum of 240liter digester capacity for biogas generation.

In figure 4.63, biogas was generated by co-digesting FVMW and dung and the results show that bigger volume digester produced a higher amount of biogas.

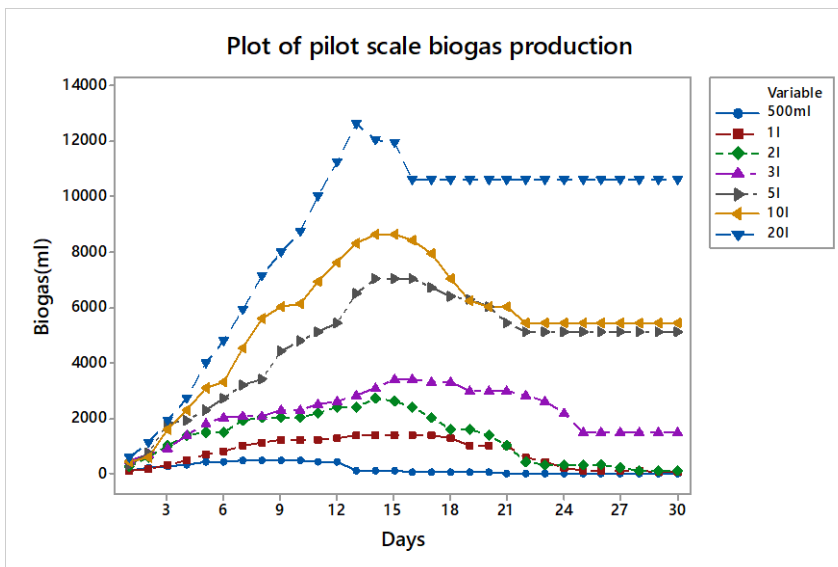


Figure 4.63: Plot of psychrophilic biogas production from FVMW mixture + cow dung

In the mesophilic setup, biogas was produced at 37 °C and the results obtained are shown in figure 4.64, which is three times more than what was generated from psychrophilic experiments. The cumulative biogas generated from 20 l digester was about 57000 mL compared to 90 mL in 500 mL digester within the same retention time.

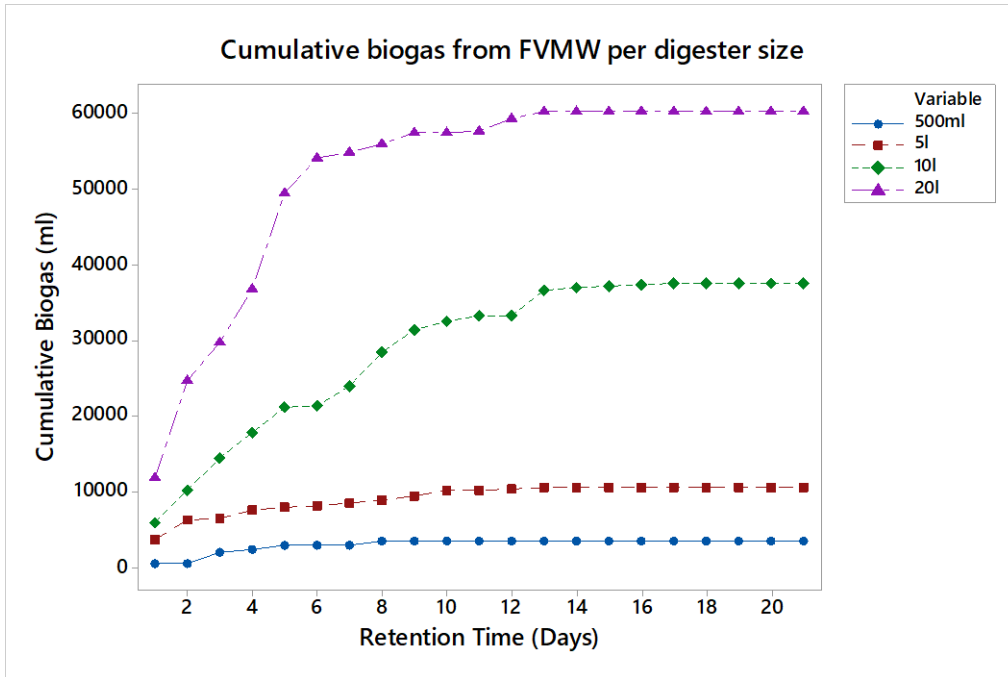


Figure 4.64: A plot of mesophilic biogas production from FVMW + rumen

Figure 4.64 clearly shows the influence of inoculum concentration and source as a significant factor that influences biogas generation. This was earlier studied by Ali *et al.*, (2018), who noted that source of inoculum and concentration influence biogas generation capacity in co-digestion experiments.

4.7 Biogas digester design

The working digester was fabricated from a 60l capacity plastic drum and is shown in figure 4.65. The outlets and the inlet were made using a 4inch pipes while a stirrer was made from rust-resistant metal pipe. Detailed description and schematic of the digester is shown in the appendix C.



Figure 4.65: A 60l portable digester with a stirrer and hot water circulation pipe

The stirrer has a handle for manual agitation, as shown in figure 4.65. The warm water circulation pipe pass water from the inlet to the outlet with the more significant portion of the pipe coiled in the tank. The digester was scaled up to 120 L and 240 liters with time, as shown in figure 4.66.



Figure 4.66: A 120 liter digester biogas production

The main advantage of the digester design shown in figure 4.67 is portability and easy cleaning of the pipes in case of clogging. Biogas generated from this digester is not enough to cook and hence scaling up was done to 240 liters. Besides, a 1.45 m³ Ferro-cement digesters and 14 m³ brick digesters were constructed are shown in figures 4.62.

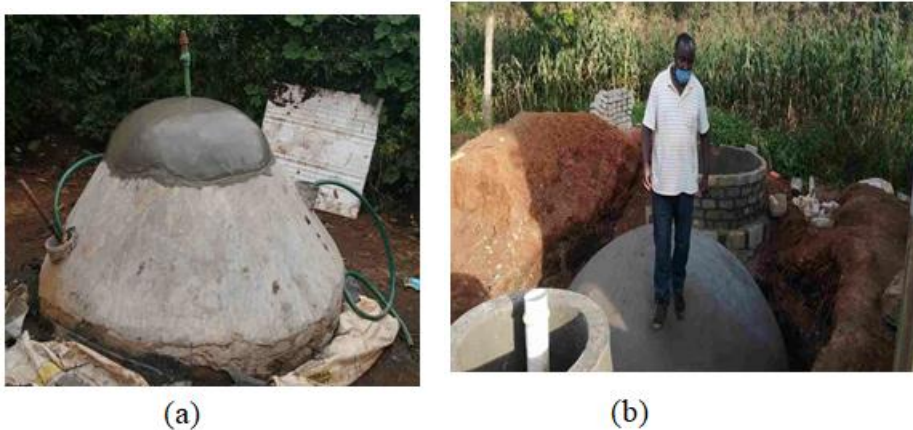


Figure 4.67: A (a) 1.45 m³ Ferro-cement digesters and (b) 14 m³ brick digesters

The temperature regulation in the 1.45 m³ Ferro-cement digesters was achieved by circulating warm water in the pipe while agitation was via a manual hand stirrer. The 1.45m³ Ferro-cement digesters consumed little resources compared to brick digester of the same capacity. Biogas generated from this digester was enough to cook for a family of 5 people for 5 hours with continuous burning. As per our earlier observation, temperature regulation and agitation increased biogas production exponentially. A 12 m³ and a 14 m³ capacity digester were set up in two different sites. Biogas was generated using cow dung for 12 m³ and FVMW co-digested with cow dung for 14 m³ digester.

4.7.1 Operation of Ferro-Cement and 14 m³ Digesters

In this section, the loading, digestion of substrate, retention, production of biogas and discharge of slurry is described for the fabricated ferro-cement and the 14m³ digesters (pictures in appendix, figures 5.11). The steps are as follow;

1. The market waste, cow dung and rumen waste are obtained from the markets, cow shed and slaughter house respectively. Size reduction of market wastes is done by

means of panga and homogenized with a blender (in case of bulky wastes, a petrol engine chopper is used) before thermochemical pretreatment is done to increase digestibility of the lignin matter. For cow dung and rumen waste, the solid matter is hand removed for easy flow to the digestion chamber.

2. The substrate is loaded into the inlet tank before mixing with water in a ratio of 1:1. The substrate was then agitated to obtain a free flowing feedstock. The inlet was opened for the substrate to get into the digestion chamber.
3. The substrate is fed until the substrate area is fully covered allowing only one gas escape route i.e. the gas outlet. This is shown in the figures below. Once the substrate area is covered, the digestion process is given time for gas formation.
4. Once the gas form in the chamber, it fills the gas area and the pressure build up in the chamber results in displacement of the digested matter from the chamber to the outlet tank. If the gas formed is not used and fills the gas area, the slurry fills in the compensation tank, resulting to out flow to the garden. If the gas is used, the pressure is lowered and therefore, the slurry remains in the compensation tank.
5. The gas outlet pipe was connected to a valve which was used as a pressure control. Initially, the valve was closed until gas build up in the gas area. The valve was then opened for gas distribution purposes.
6. A water trap is installed few meters from the gas outlet pipe to discharge water vapor condensed in the pipe. The trap is opened frequently to discharge water.
7. The gas was then distributed to the kitchens and cleansed using a de-sulphurizer or the zeolite rocks cartridge before connecting to a burner. The biogas composition is analyzed before and after cleaning to determine the burning efficiency of the gas. The results obtained showed that before treatment, the methane, carbon dioxide and hydrogen sulfide were 67%, 17% and 19ppm while after upgrade, the levels were 93%, 4% and 4ppm respectively. At high pressure, biogas burns without clean up step.
8. The slurry flows to the garden via a trench for crop production. It is nutrient rich and the high moisture content made it suitable for crop growth.

It was observed that in 14m³, the lag phase was 3 weeks due to high protein levels in cow dung waste. This resulted in ammonia inhibition and therefore, a gas formed was not combustible. After the third week, the microbes adapted to the digester temperature with an exponential increase in methanogenic microbes, which resulted in higher methane levels and consequently combustion was achieved. The gas produced was used for cooking for a family of 9 people with more than 12 hours of continuous burning without depleting the gas. On the other hand, the 14 m³ lag phase was less than a week. Biogas generated was distributed to 3 family's kitchens with an average of 5 people. The gas was enough to cook supper and warm bathing water for family members without depletion. The loading rate was 20 kg and 30 kg of waste per day for the 12 m³ and a 14 m³ digesters.

4.7.2 Temperature Regulation in the digester

Warm water maintained at 37 °C and 55 °C for mesophilic and thermophilic temperatures respectively was achieved by first studying the heat loss from water in a basin and further in piped water and in 20 L and 60 L loaded digester. The temperature drop with time shows that the decline is higher in the first minutes. For example, a temperature drops from 55°C to 27 °C was witnessed in 80 minutes. While 40 °C to 29 °C was recorded within 30 minutes for 20-liter digester and 44 °C to 26 °C was witnessed for 60-liter digester within 26 minutes.

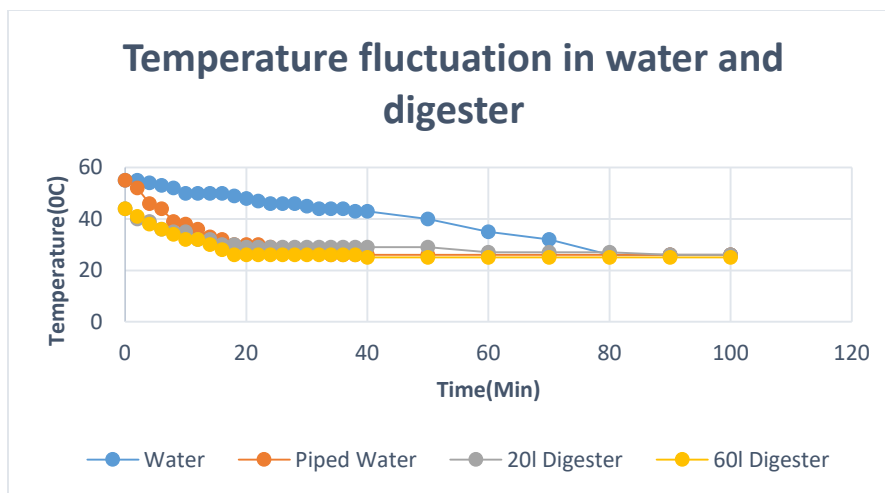


Figure 4.68: Plot of temperature changes in water

figure 4.68 showed that to maintain the digester temperature, frequent water pumping was required, which is subject to the digester size. The bigger the digester, the higher the rate of passing the water.

4.8 Biogas digester Automation

Biogas automation was divided into four main sections. The sections are loading rate, agitation, temperature and pH regulation. The loading rate was automated using a gate $\frac{3}{4}$ ' valve fitted with *Arduino* board. A servo motor was programmed to open a $\frac{3}{4}$ ' gate valve for 3 minutes and then close. The program was designed to run after every 24 hours.

After loading, the program was designed to agitate the substrate for thorough mixing of feedstock and inoculum. This was done using a DC motor commanded via *Arduino uno* R3 board and powered by a 9V battery. The final set up is shown in figure 4.69.

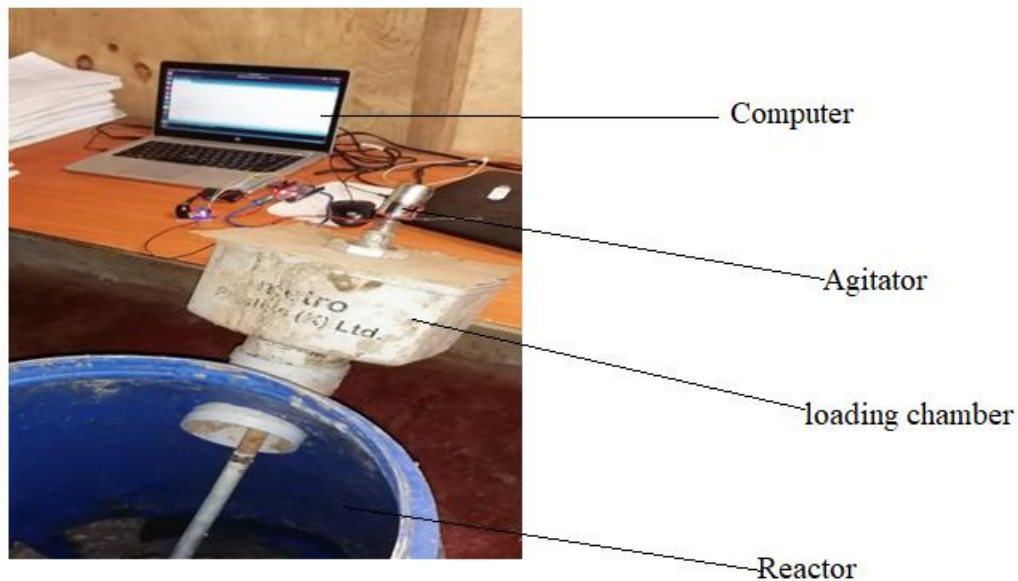


Figure 4.69: DC-motor anaerobic digester agitator

The agitator was commanded to run for three minutes and after that delay for 24 hours till the next loading using the *Arduino* sketch shown in appendix G. The well-stirred digester has been reported to increase biogas generation tenfold (Rusin *et al.*, 2017). It ensured uniform microbes distribution as well as even temperature and pH in the digestion chamber. In figure 4.69, *Arduino* microcontroller was employed in temperature monitoring and recording using a MAX6675 thermocouple sensor with an LCD. The

temperature readings were automatically recorded in the excel sheet using PLX-DAQ V₂ application using the Arduino sketch and the excel data used to plot figures 4.70 and 4.71.

Figure 4.70 showed that the temperature fluctuation at night was 2.5 °C. This mean that in a temperature-regulated digester, more regulation is required at night for optimum biogas generation.

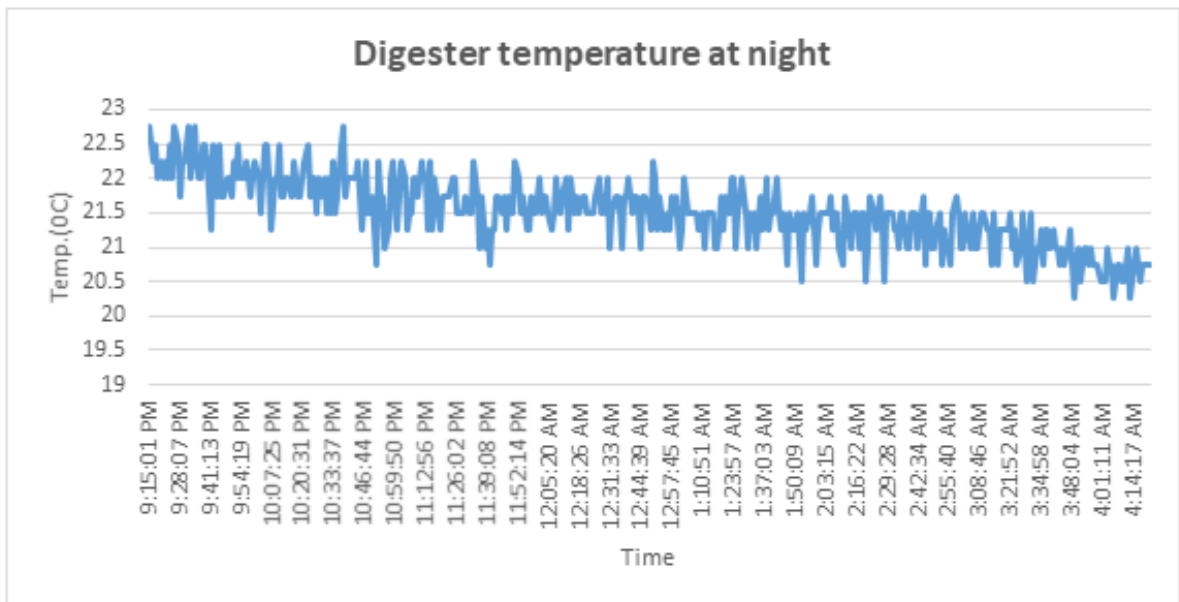


Figure 4.70: Digester temperature at night

In figure 4.71, the day time temperature regulation was observed to range from 0.5 °C to 3.5 °C. This showed the reason why digester temperature regulation was vital during anaerobic digestion.

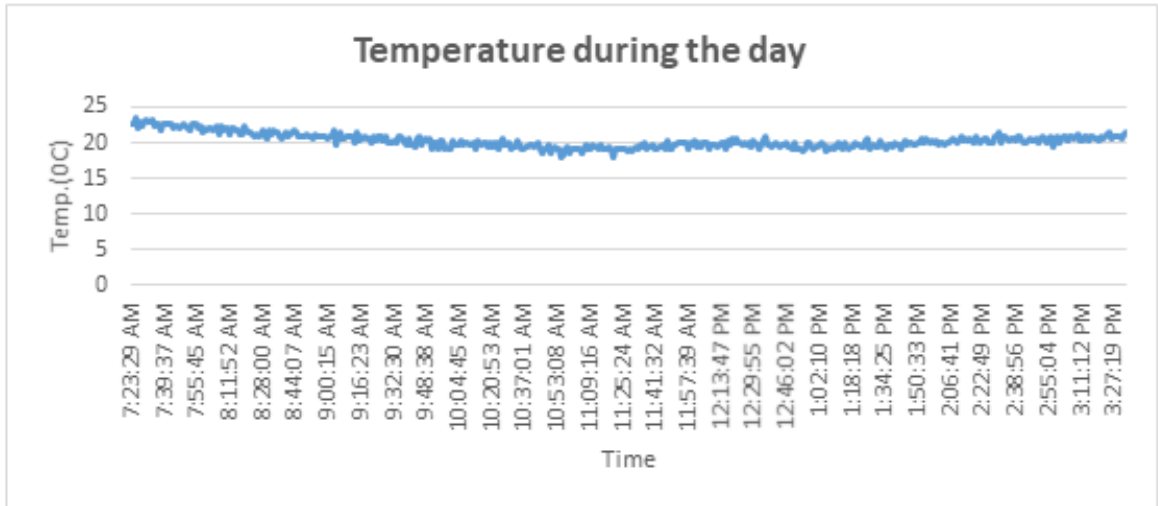


Figure 4.71: Digester temperature at night

The digester pH values were automatically logged into an excel sheet using a PLX DAQ V₂ application using the Arduino sketch. The observed pH values fluctuated with less than 0.40 for the twenty-four hours of the study. It was observed that the temperature of the digester highly influenced fluctuation. The pH increased with decrease in temperatures and is shown in figure 4.72.

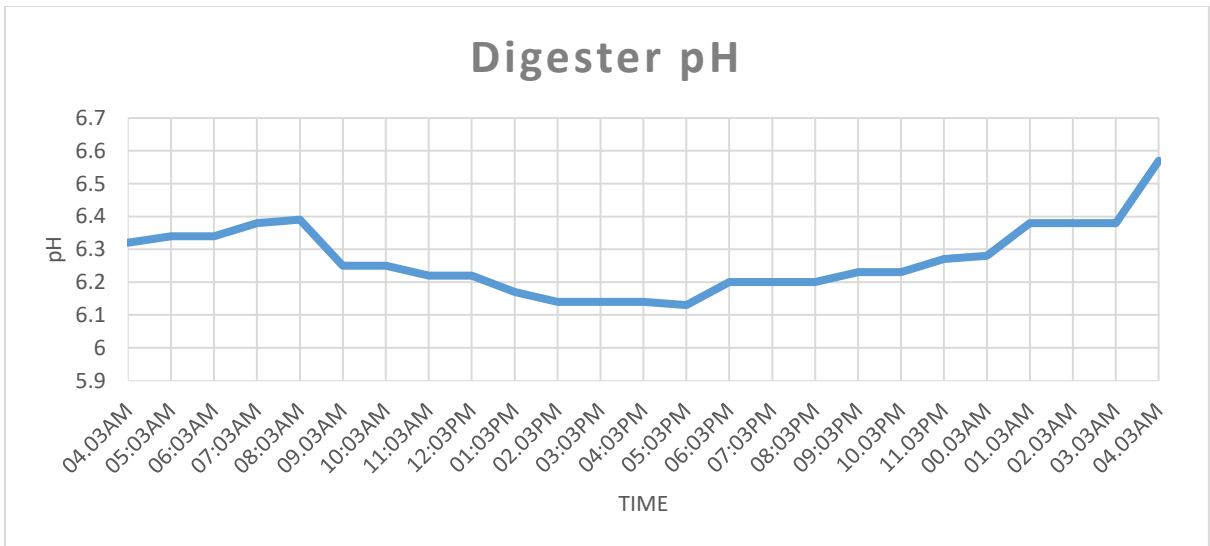


Figure 4.72: Plot of digester pH

The pH of the digester was highly dependent on the substrate type and digester temperature. This necessitated the need for both pH and temperature monitoring daily for optimal performance of the digester. This is achievable via IoT technology using simple programmable devices like *Arduino*.

The final automation section involved a combination of the four areas discussed in this section. The last automation connection is shown in figure 4.73. more details about the design and connections can be obtained from the patent No. KE/P/2020/3707.

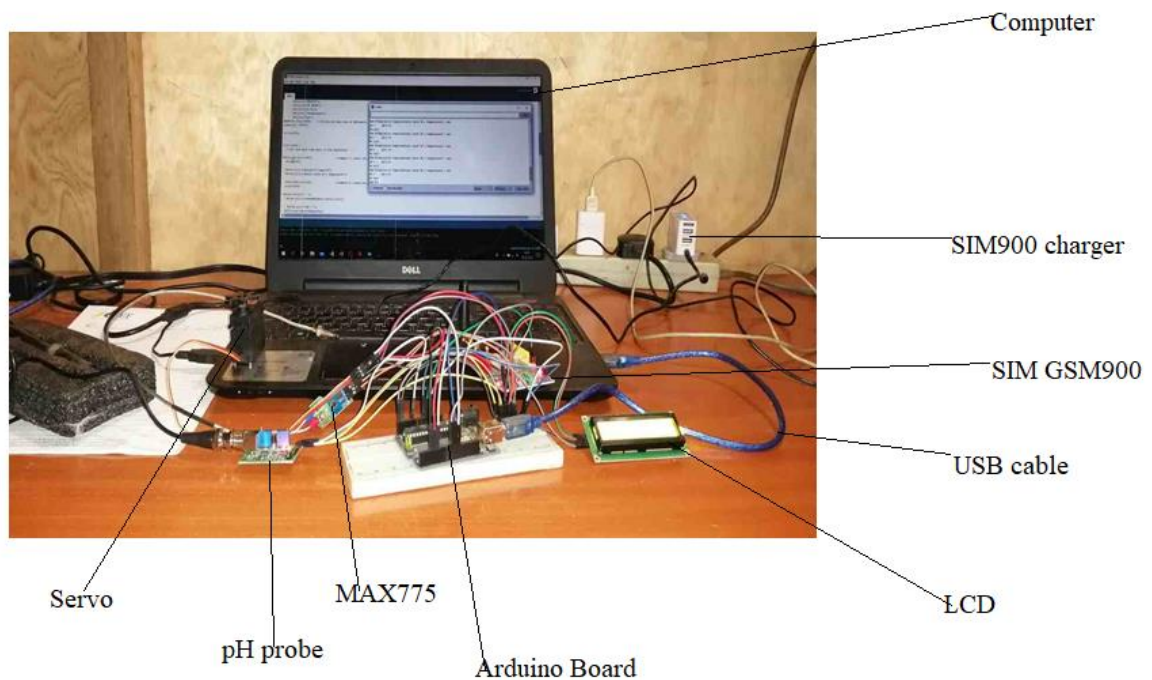


Figure 4.73: Final biogas digester automation connections

The working principle is such that the servo/DC motor agitates the substrate for 3 minutes after which temperature and pH values are taken, an alert by SMS sent to a pre-registered number for regulatory action if the readings are not in the pre-set threshold. The re-engineered digester biogas production was compared to the un-agitated digester, pH and temperature regulated stirred digesters. The accumulation of biogas obtained is shown in figure 4.74. The Arduino programming code can be obtained from the patent no. KE/P/2020/3707 titled ‘Biogas digester automation’.

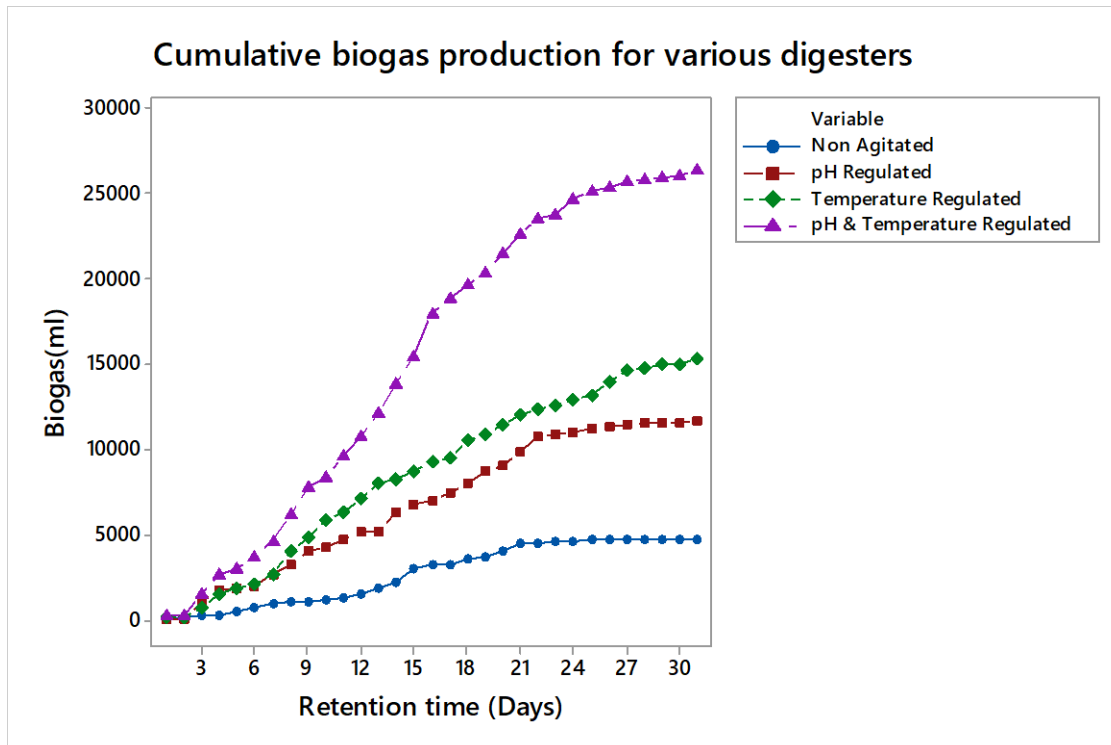


Figure 4.74: Cumulative biogas for different digesters

The results obtained in this study showed that the cumulative biogas generated from the automated reactor was 26400 mL, while the un-agitated digester is 4700 mL.

Temperature and pH regulation were noted to influence biogas yields with aggregate production being 11800 mL and 15300 mL for pH and temperature regulated digesters, respectively. Monitoring and adjustment of pH and temperature and agitation increased biogas production six-fold in comparison to the un-agitated digester. The microbial activities in the digester entail process, which frequently alters the pH. The initial pH of the feedstock was low during the preparation of the feed since wastes are acidic, and thus, buffer solution was used to adjust the pH (Kamau *et al.*, 2020). Liu *et al.*, (2008) reported that pH is a significant factor that influences digester performance. pH drop has been reported to inhibit methanogenesis and led to less biogas production (Chen *et al.*, 2014). Yang *et al.*, (2015), proposed that adjusting the digester pH led to an increase in biogas production (Eramati & Ossein, 2017). This was because acetogenic microbes converted organic matter to weak organic acids (Velmurugan and Alwar, 2011).

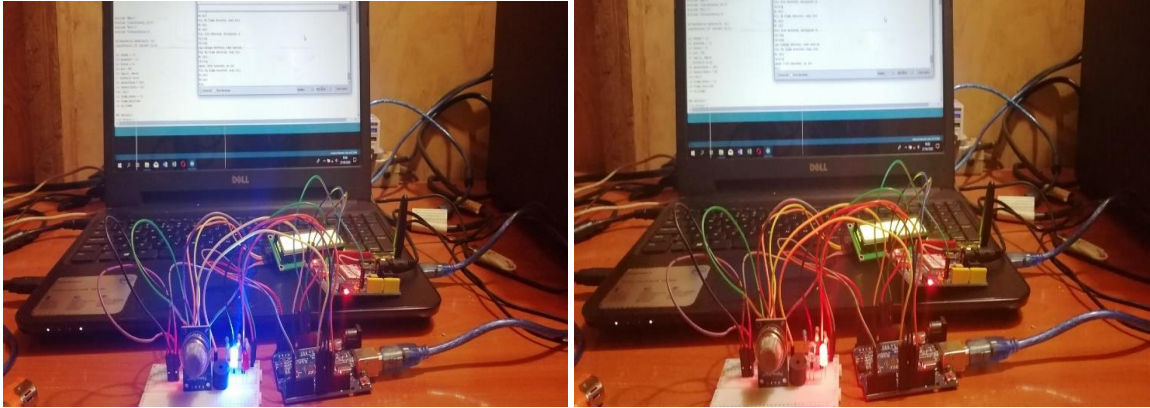


Figure 4.76: LED display when (a) all is running well (b) in the event of smoke, fire or methane leak

The gas and smoke sensors were operated by a command an Arduino code/sketch as shown in appendix I. Similar devices have been developed for LPG leakage systems with similar functionalities. For example, Asmita *et al.*, (2018) proposed a gas spillage detector framework that utilizes IoT innovation, which additionally has smart alarming methods like calling, sending SMS and email to the concerned user. In a research study by Carmela and Ana, 2017, a gadget was invented to distinguish and quantify CH₄ gas incombustible gas store zones. The gadget measured the air and water quality, as well as any parameter changes because of gas spillage in the environment. The detection unit quantified CH₄ and CO₂ gases in the surroundings. The gadget uploaded the sensor data to an MYSQL databank on Raspberry Pi 3. A research investigation by Falohun *et al.*, (2014) presented an LPG detection unit utilizing an MQ-9. No reported work on biogas leakage detection using Arduino is documented in the literature.

4.10 Microbial Fuel Cells

When microbial colonies from the anaerobic anodic chambers were cultured, isolated and identified, the following plates were obtained in MacConkey and blood agar. In figure 4.77, the rumen sample was stained in a dish and three distinct cultures isolated.



Figure 4.77: Anodic chamber sample stained plate

The isolates were then removed from the initial plate and cultured in blood and MacConkey agar, as shown in figures 4.78.

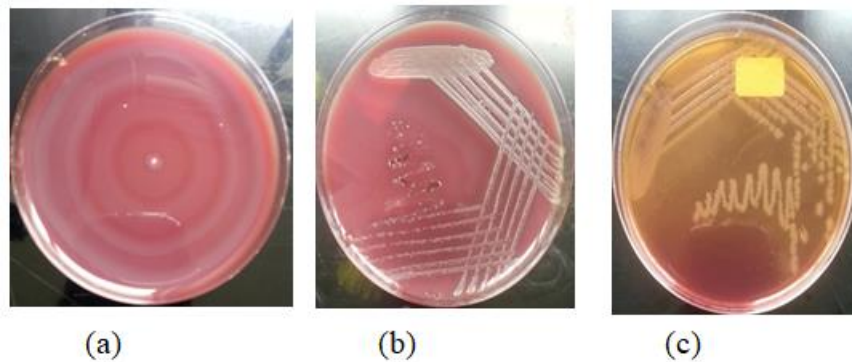


Figure 4.78: Plates of microbes in the anodic chamber of MFC (a) and (b) in blood agar and (c) in McKonkey agar

Microscopic and biochemical studies of the cultures confirmed that *Proteus* and *Clostridium spp.* were found in the anodic compartment of MFC. The images obtained from an electron microscope is shown in figure 4.79. These results compare with a previous study by Gagandeep *et al.*, (2017) who identified *Bacillus subtilis*, *Clostridium Spp*, *Peptostreptococcus Species*, *Bacillus Cereus* and *Bacteroides Species* in the anodic chamber of a running MFC which aided in electricity generation in the MFC. The isolated microbes found in this study are also comparable to others (Adegunloye, 2007; Gopinath, 2014; Shiv, 2012; Nene, 1999; Sawant, 2007 and Kartikey, 2016).

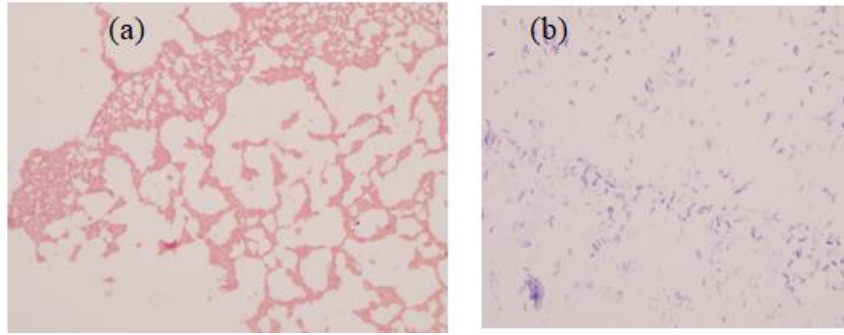


Figure 4.79: Electron microscope images of (a) *Proteus* and (b) *Clostridium spp.* bacteria

Proteus spp is a gram-negative *proteo*-bacteria found in decomposing animal matter, sewage and manure soil. It is also widely seen in the mammalian intestine. *Proteus Vulgaris* commonly grow in the MacConkey agar culture plate. *Clostridium* is a rod-shaped genus of gram-positive bacteria that are obligate anaerobes. This means that they are killed by exposure to atmospheric oxygen (20.9 5%) (Haryy, 1996); Brooks *et al.*, 2007). The voltage produced from decaying tomato wastes is shown by plots figure 4.80. In a study using five cultures, *Paracoccus homiensis* and *Pseudomonas aeruginosa* produced the maximum voltage of 320 mV and 300 mV, respectively. *Bacillus thuringiensis* had the least voltage of 150 mV. Likewise, *Paracoccus sp* and *Pseudomonas sp* gave the maximum current of 10 mA and 20 mA, respectively (Mathuriya and Sharma, 2009). MFC performance differs for every bacterium. For example, 10.89 mA and 10.45 mA current were generated by *Saccharomyces cerevisiae* and *Clostridium acetobutylicum* after 10 days of operation (Mathuriya and Sharma, 2009).

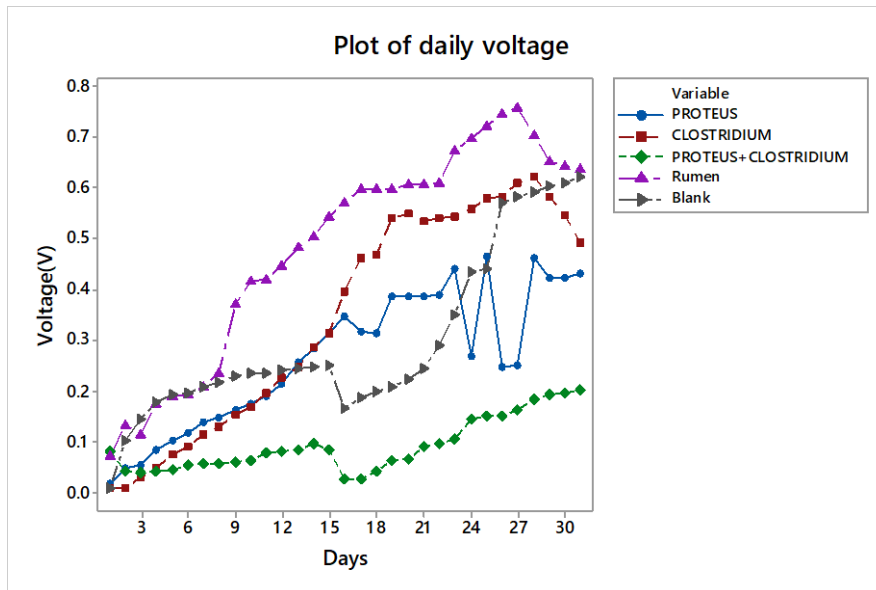


Figure 4.80: Plot of daily voltage using different culture

Low voltage was recorded in a mixed culture of *Clostridium* and *Proteus* compared to pure cultures. This is explained by the fact that the two cultures require individual time to adapt to the anodic chamber environment in addition to collective time to adapt as a mixed culture (Aritra and Mondal, 2015). This contradicts what was observed by Fatemi *et al.*, 2012, who claimed that diverse culture produced more voltage than pure ones.

Rismani-Yazdi *et al.*, (2007) used rumen microorganisms as inoculum to produce electricity from cellulose, in an H-type MFC; the voltage reached a steady-state level of 470 ± 2 mV after 14 days and an external load of 1000Ω . In another study, the voltage was generated using *Clostridium cellulolyticum* utilizing cellulose as a substrate (Ren *et al.*, 2007) while electron transfer *Geobacter sulfurreducens* was used.

The daily current generated is shown in figure 4.81. Rumen fluid inoculated set up registered the highest current explained by a higher microbe's population resulting in a higher substrate breakdown rate (Mbugua *et al.*, 2017) as per the total viable count data.

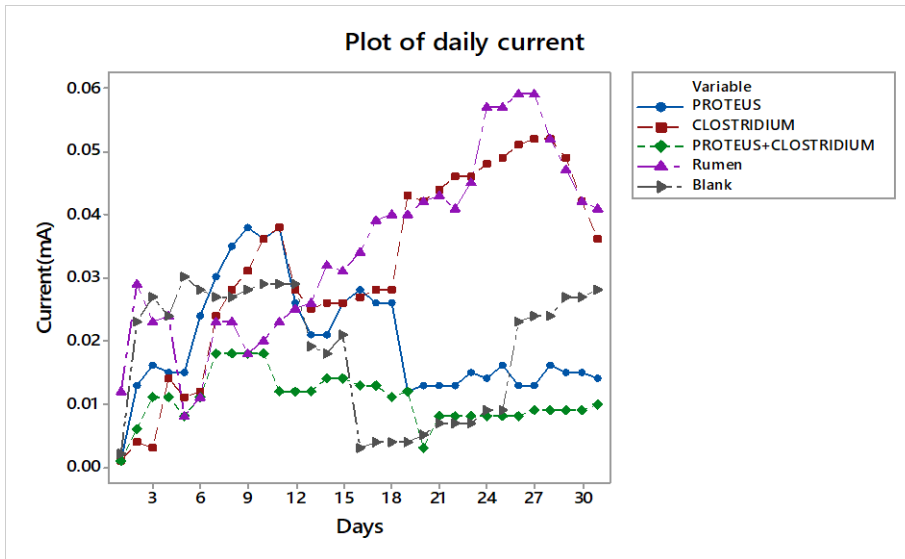


Figure 4.81: Plot of current daily production for different cultures.

The current generated using *Proteus* was highest on the 10th day at 0.038 mA with a voltage of 0.191 V. In another study using the same culture, a voltage of 0.5 V was recorded at 37 °C (Namjoon *et al.*, 2002). The figure (4.82) shows daily power calculated by multiplying voltage by current. Power was highest in the set inoculated with rumen fluid followed by the set with *Clostridium*. Co-digestion of tomato waste with rumen for electricity generation means a high concentration of microbes and therefore, high microbial activities leading to high voltage.

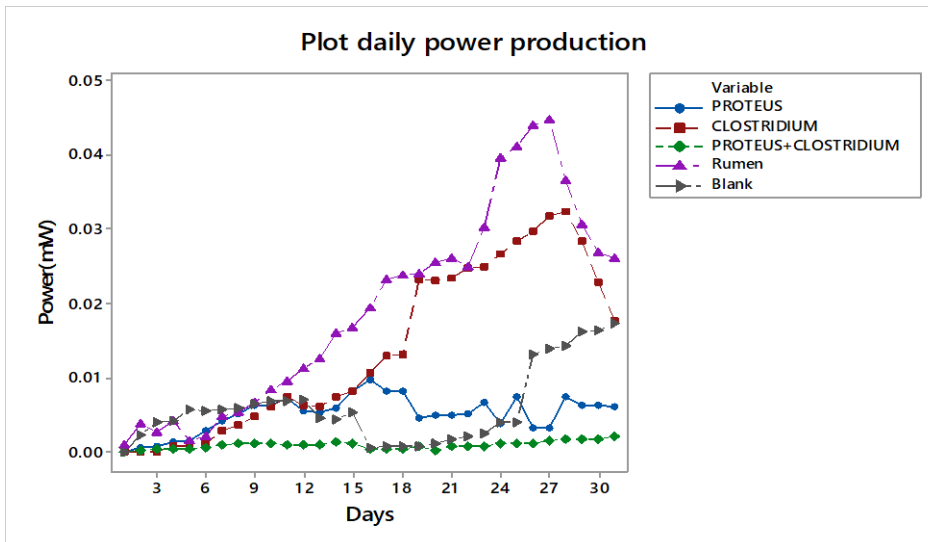


Figure 4.82: Plot of daily power production for different microbes.

The current density shown in figure 4.83 was obtained by dividing current with the anodic electrode surface area.

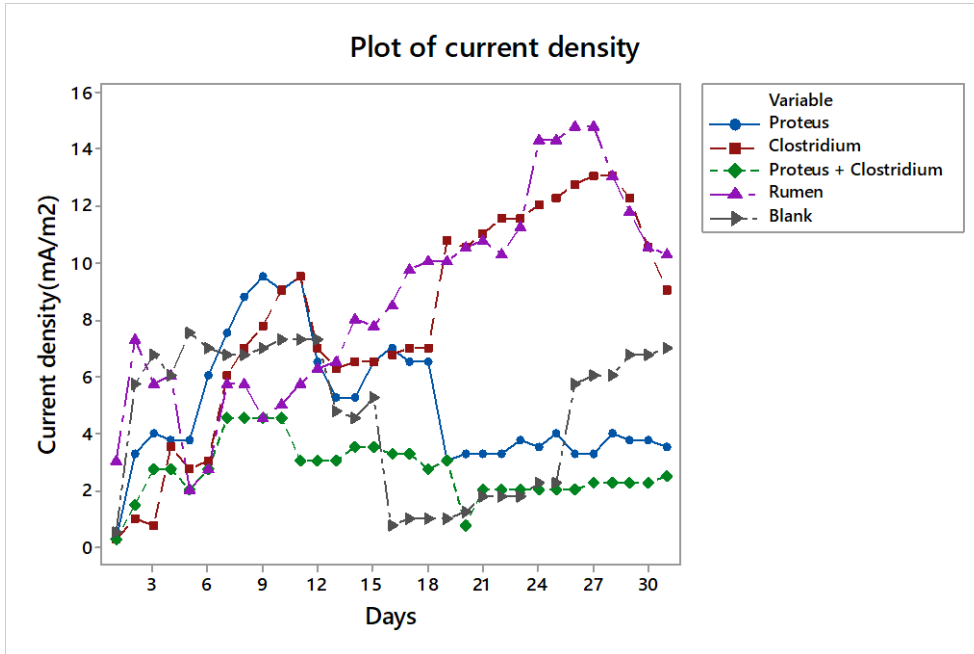


Figure 4.83: Plot of daily current density for different cultures.

The figure (4.83) showed that when produced current is divided by the electrode surface area, 14mA/m² current density is observed from rumen-tomato setup. Low current density was observed in blank tomato waste mixture and from the mixed culture of *Proteus and clostridium*. The results are consistent with those reported by Cao *et al.*, (2019) of a range of 31 mA/m² and the Coulombic efficiency reached 81% when using glucose as the substrate and *β-proteobacteria* (Chaudhuri and Lovley, 2003). Jiang *et al.*, (2006) isolated *Clostridium spp* from the soil whose membrane-bound cytochromes was responsible for direct electron transfer (Park *et al.*, 2001) and generated a current density of 12 mA/m². Figure 4.84 shows surface plots of daily power and current densities for the different cultures.

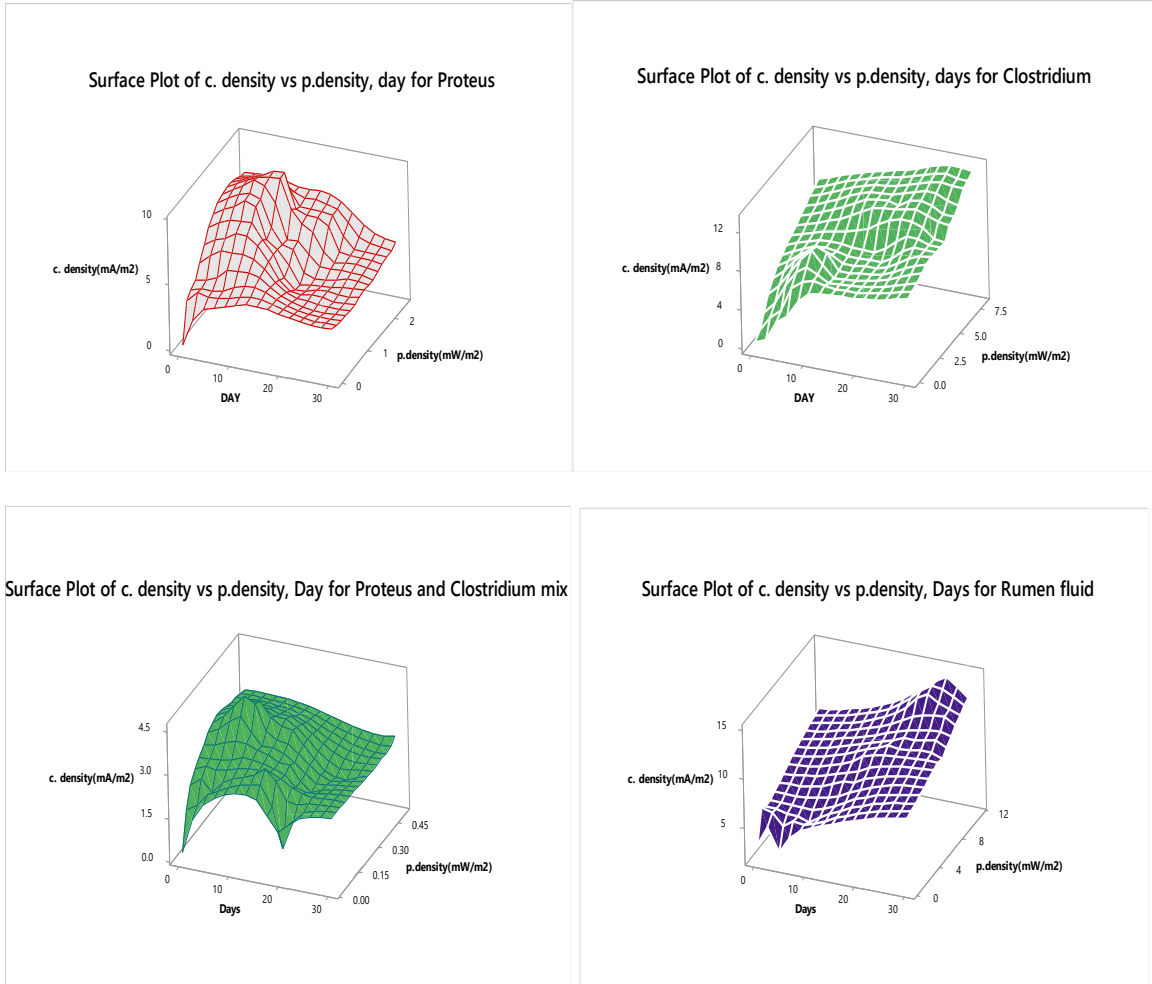


Figure 4.84: Surface plots of daily power and current densities

The power density obtained was highest in rumen MFC due to increased microbial concentration and diversity at 12 mW/m². The lower power density was recorded in mixed culture at 0.45 mW/m². Power density is the leading property to assess the performance of the MFC. Further, low power and power density witnessed showed that electricity generation originated from microbial catalysis rather than chemical reactions.

4.10.1 Pure culture voltage modelling

The modelling assumed that the voltage generation rate rises with time (equation 4.19).

$$V = a + bt \dots \dots \dots (4.19)$$

Where V is the voltage generated, a is the intercept, b is the slope and t represents the time of the study when voltage reading was taken. Besides, voltage production was simulated using the Gompertz equation 4.20.

$$V = ae^{-be^{-ct}} \dots \dots \dots (4.20)$$

The experimental voltage generated from decaying tomato wastes by *Proteus spp.*, *Clostridium spp.*, *Proteus spp.* + *Clostridium spp.* and rumen fluid microbes were fitted in linear, logistic and Gompertz growth models. The results for the linear and Gompertz fitting obtained are shown in figures 4.85.

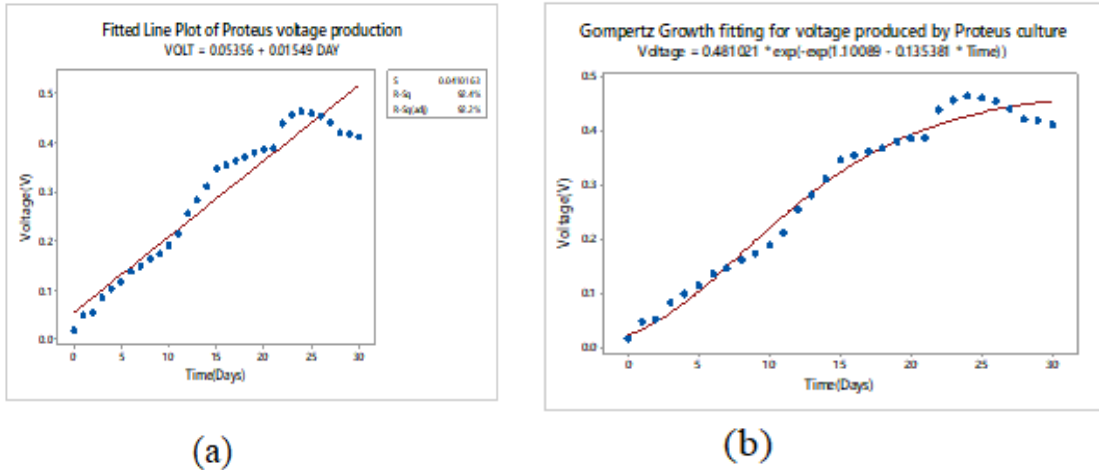


Figure 4.85: Fitted plots for voltage generation by *Proteus* a) linear b) Gompertz
 The results shown in figure 4.85 show that the growth of *Proteus* culture, which translates to voltage production is well explained by the Gompertz equation growth model with regression values of 0.996 compared to 0.927 obtained in linear data fitting. The same is well reflected by the simulating growth model of *Clostridium spp.* as shown in figure 4.86. In both cases, the voltage generated from the pure cultures cannot be explained linearly due to low R² of 0.91 and 0.922 for *Clostridium spp.* and *Proteus* respectively compared to 0.96 and 0.98 for the Gompertz equation fitting.

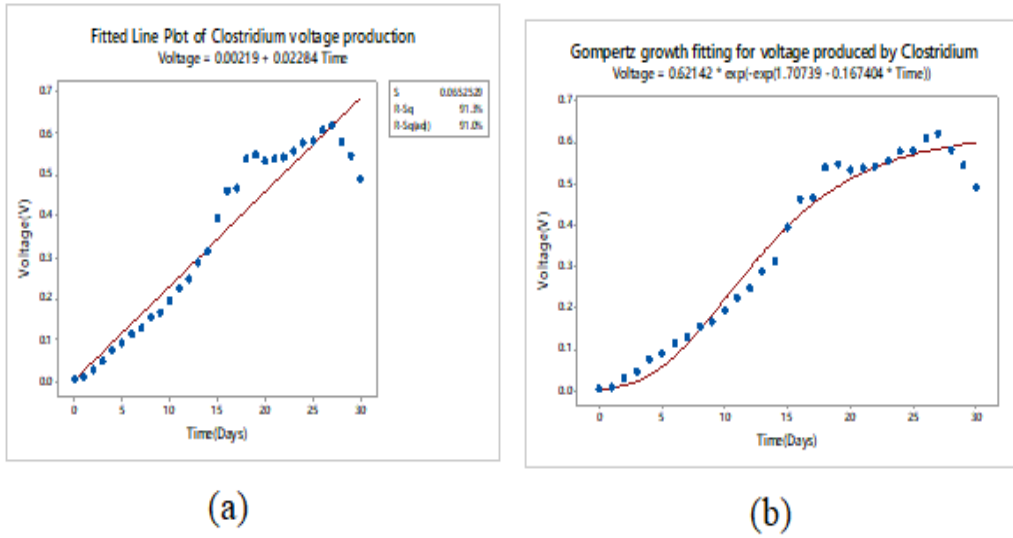


Figure 4.86: Fitted plots for voltage generation by *Clostridium spp* a) linear b) Gompertz

Figures 4.82 and 4.83 shows the best fits for the rumen fluid voltage and the *Clostridium spp.* + *Proteus* culture mix simulated models. The voltage produced from rotten tomato wastes by rumen fluid microbes is better explained by the Gompertz growth model while the mixed culture voltage fitted the linear model best. Only the best-fit curves are shown.

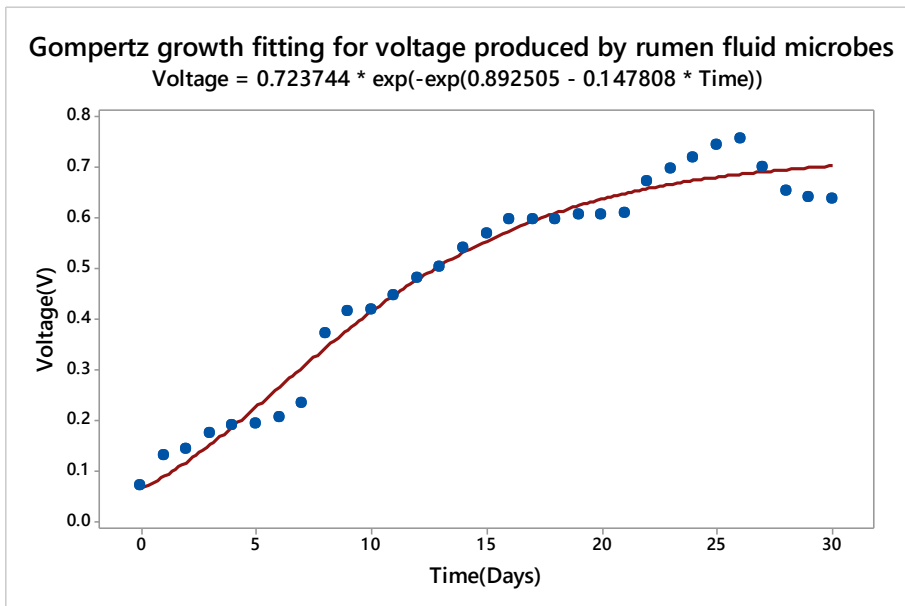


Figure 4.87: Gompertz fitted plots for voltage generation by rumen fluid microbes

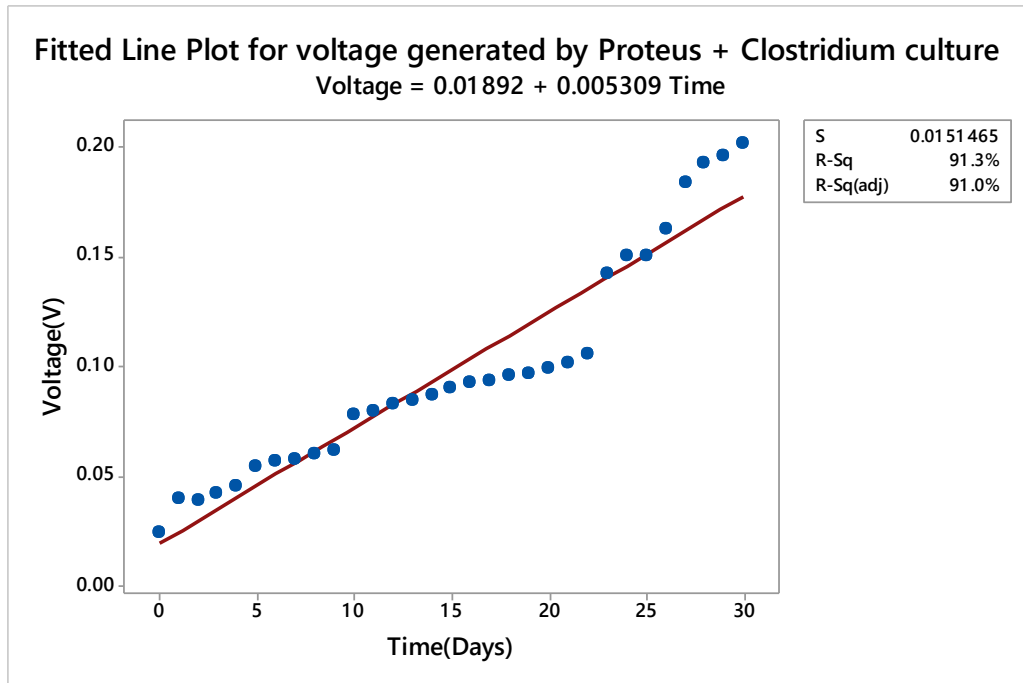


Figure 4.88: Linear fitted plots for voltage generation by *Clostridium spp*+ *proteus* cultures

The regression coefficient of the *Clostridium ssp.* + *Proteus* culture mix was 0.91 for linear plot compared to 0.67 for the Gompertz plot. This means that the Gompertz model should be employed in explaining electricity generation from MFC with a high concentration of microbes.

4.10.2 Influence of External Resistance

The plots in figure 4.89 represent voltage generated from MFC on varying external resistance. The open circuit generated the highest voltage, according to the model. In contrast to the other resistors, the 15 kΩ resistor recorded the highest voltage. Kamau *et al.*, (2017) had previously observed similar results. The obtained results are also consistent with Ohm's law.

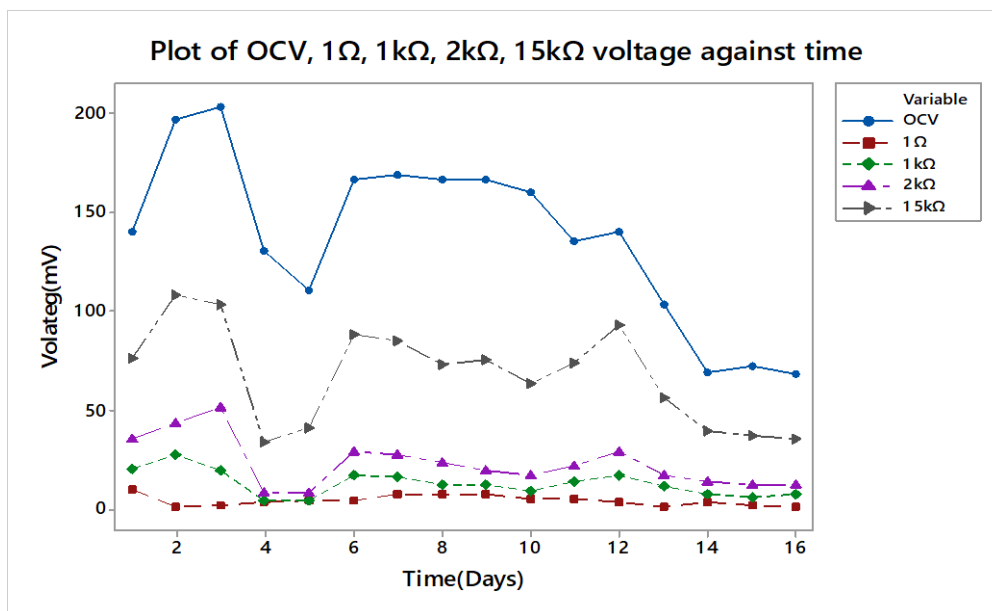


Figure 4.89: Plot of voltage across different resistors and open circuit.

For the first three days, the obtained voltage rose, then decline. The upward trend is due to the microbes in cow dung competing for available substrates as food. The microbes begin to die as fresh dung is depleted, resulting in a downward voltage trend.

Menicucci *et al.* (2016) reported a drop in voltage with decline of the external resistance. This was due to the current-limiting electrode's limits on electrode reaction kinetics, mass transfer, and charge-transfer processes. In other studies, an external load increment of 0 to 4,000 Ω , resulted to a cell voltage rise, reaching an optimum of 358 mV at 4,000 Ω (Ghangrekar and Shinde., 2007). Rismani-Yazdi *et al.* (2011) found similar cathode potentials at various external resistances. However, when various external resistances were used, the anode potential differed. Higher anode potentials were found in MFCs with lower external resistance. Song *et al.*, (2010) used a sediment microbial fuel cell and found similar results (SMFC). Cow dung bio-catalysis of fruit wastes to electricity in MFC, resulted to the daily voltage shown in Figure 4.90. On days 5 and 12, banana wastes had the lowest reported voltage, ranging from 0.021V to 0.23V. Methanogenic bacteria found in cow dung decomposed organic substrates (Mwaniki *et al.*, 2016). Days 6 to 16 yielded voltage ranging from 0.03 to 0.357 V in avocado wastes. The high voltage

observed is due to the energy released when breaking down avocado's high fat-content.

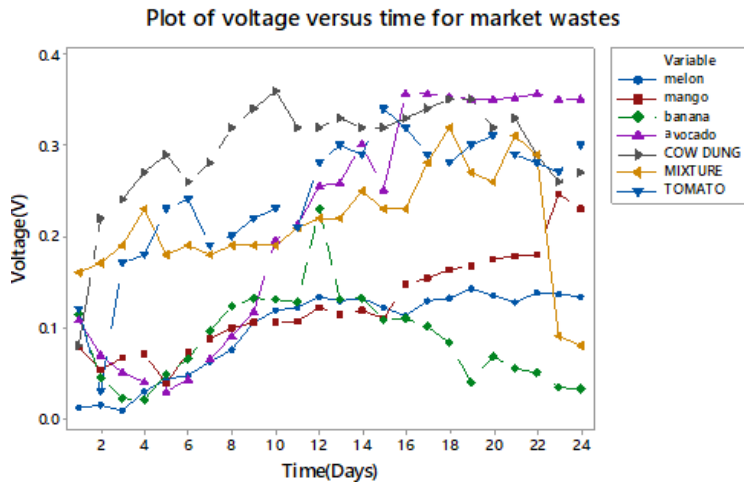


Figure 4.90: Plot of daily voltage for different fruit wastes using cow dung

In the first ten days, the voltage obtained from fresh cow dung was at its peak. This was due to the high microbe concentration and low lignin content in the dung. When the microbes' food in the manure runs out, the pattern reverses. The high voltage in cow dung waste is clarified by a balanced C: N ratio for microbe activities and a stable pH. Fruit waste pH is poor, as previously discussed in biogas production, and microbes need time (lag phase) to adjust to the anodic chamber environment before voltage generation. By multiplying current by voltage, power was obtained. As shown in figure 4.91, the banana had the lowest power and the avocado had the highest.



Figure 4.91: Plot of power against time generated by other fruits wastes.

Power production and coulombic performance are used to assess the efficiency of MFCs (Bruce et al., 2006). Watermelon powder had a power range of 0.000081 to 0.01206 mW, whereas the fruits mixture powder had a power range of 0.00008 to 0.01024 mW. From day 3 to day 16, a 0.00002 to 0.029988mW power increase was noted in avocado's, which gradually decreased. Power is typically characterized per reactor parameters, such as electrode surface area, to show the efficiency of MFC systems. The anode is where wastes are biologically converted into energy (Rabaey et al., 2004; Park and Zeikus., 2003, Liu et al., 2004; Park et al., 1999. Equations 4.21 and 4.22 were used to compute the current density and power density where A is the electrode surface area, and I is the current.

$$CurrentDensity = \frac{I}{A_{area}} \dots \dots \dots (4.21)$$

$$PowerDensity = \frac{Power}{A_{area}} \dots \dots \dots (4.22)$$

On day 7, as shown in figure 4.92, the observed current density was highest in avocado at 63.11044 mA/m² and lowest in banana at 1.50263 mA/m².

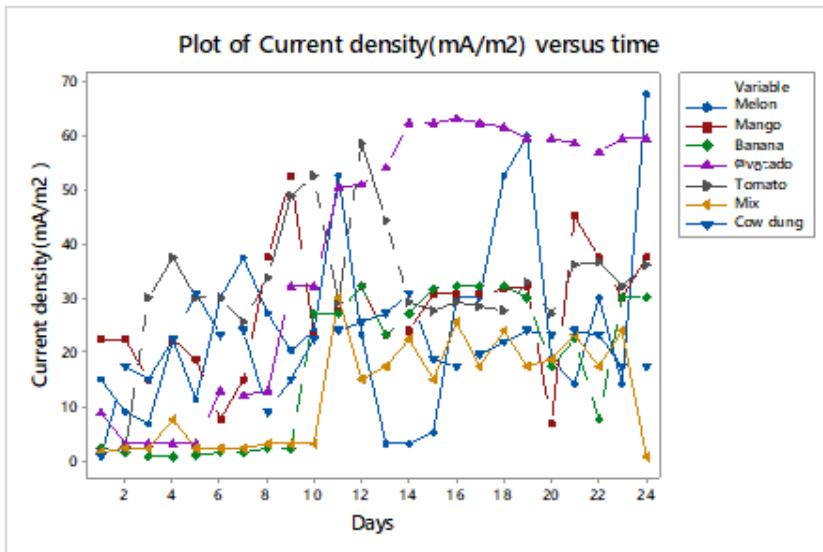


Figure 4.92: Plot of current density against time.

Figure 4.93 depicts the power density plot. The highest power density (PD) was recorded in avocado then tomato, as per the plots. In this analysis, the banana and the fruit mixture had the lowest power density.

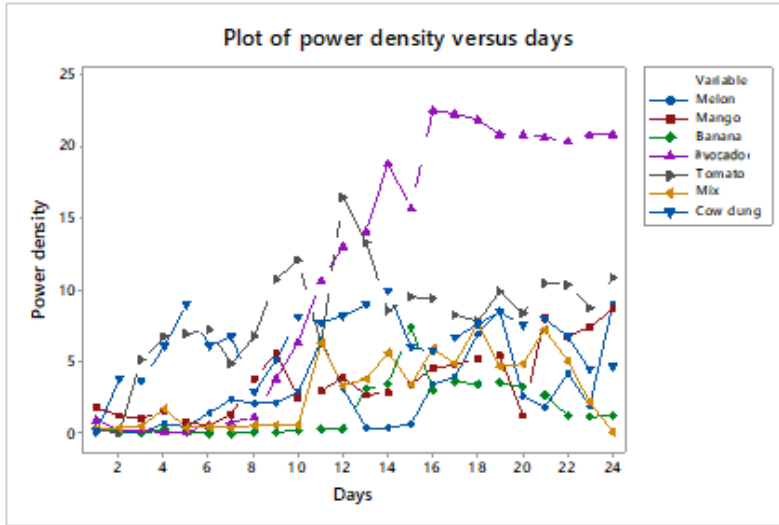


Figure 4.93: Plot of power density against time.

Figure 4.94 depicts a plot of PD versus CD. Power rises with the current until it reaches a limit of 22.53 mW for avocado, then drops due to ohmic losses and electrode over-potentials. This is true for all of the fruits examined in the current study.

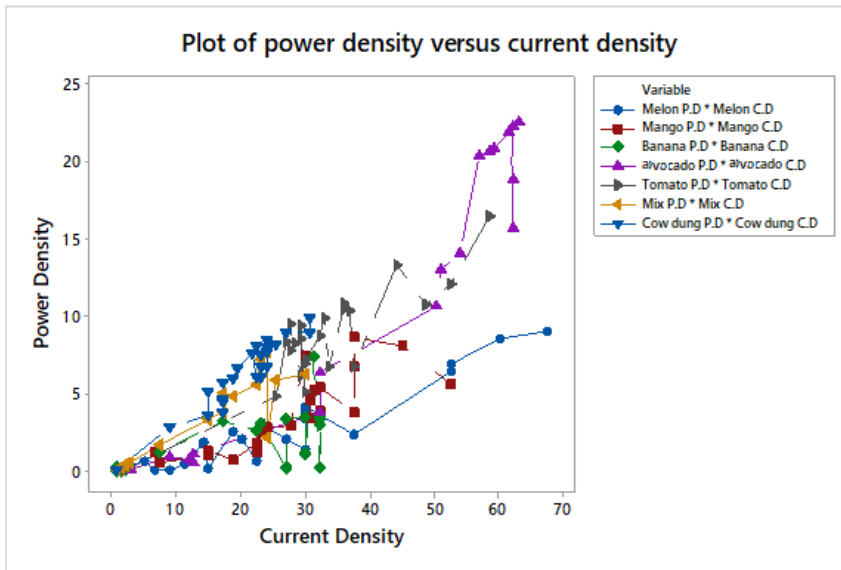


Figure 4.94: Plot of power density versus current density for fruits waste in cow dung

4.10.3 Rumen fluid

The voltage and power obtained from avocado and tomato wastes were as shown in figures 4.95 and 4.96. Tomato was recorded the highest voltage while inoculated with 500mL rumen fluid in tomato. High digestion rate due to high microbe count in the 500 mL rumen matter explains this observation. The avocado waste with 250 mL rumen fluid generated the lowest strength.

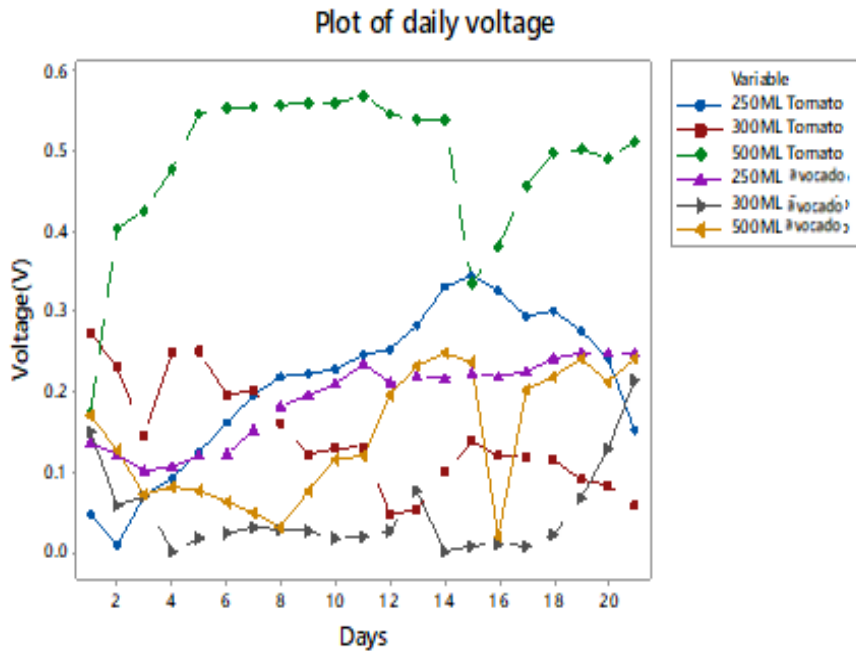


Figure 4.95: Plot of voltage versus days of tomato and avocado inoculated with rumen waste

These findings are consistent with a study that found that the rate of microbial metabolism at the anode increased as the electrical potential of the anode increases; thus, the rate of microbial metabolism in response to electron concentration or electrical potential determines the amount of electricity produced in the MFC (Ieropoulos *et al.*, 2006; Park *et al.*, 2000; Tender *et al.*, 2008).

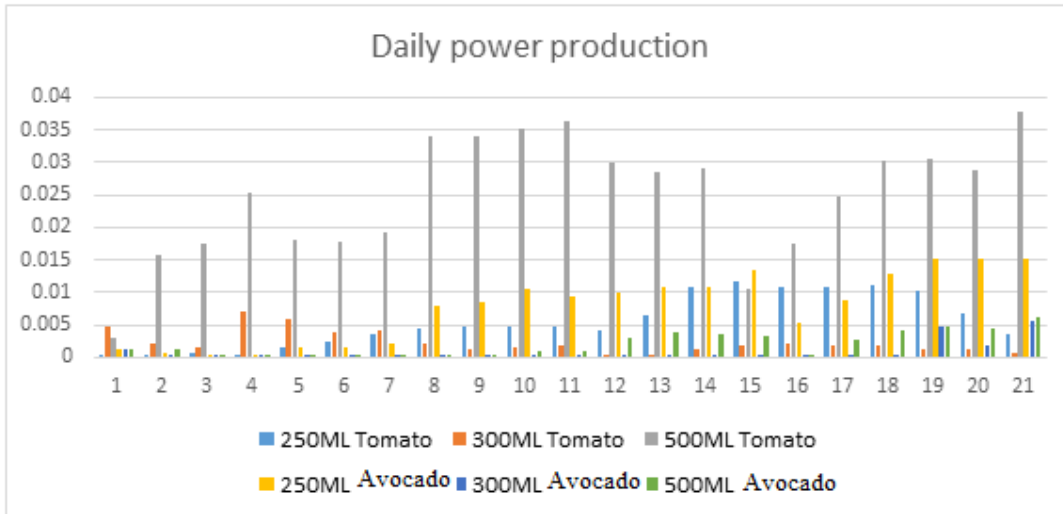


Figure 4.96: Bar graphs of power generated from tomato and avocado wastes

Figure 4.97 shows the daily voltage plotted for the fruits mixture as rumen fluid concentrations were varied. The highest voltage was found in 350 mL of rumen fluid. This could be due to the microbes having nearly enough food to last the duration of the study. Figure 4.97 shows that after the first 24 hours, the 500 mL rumen fluid had the highest voltage. Because microbes compete for food, this results in a high rate of electron production. The rate of voltage production in the 250 mL rumen fluid remained constant throughout the experiment. This is explained by the microbes having almost enough food and the available food is incomplete.

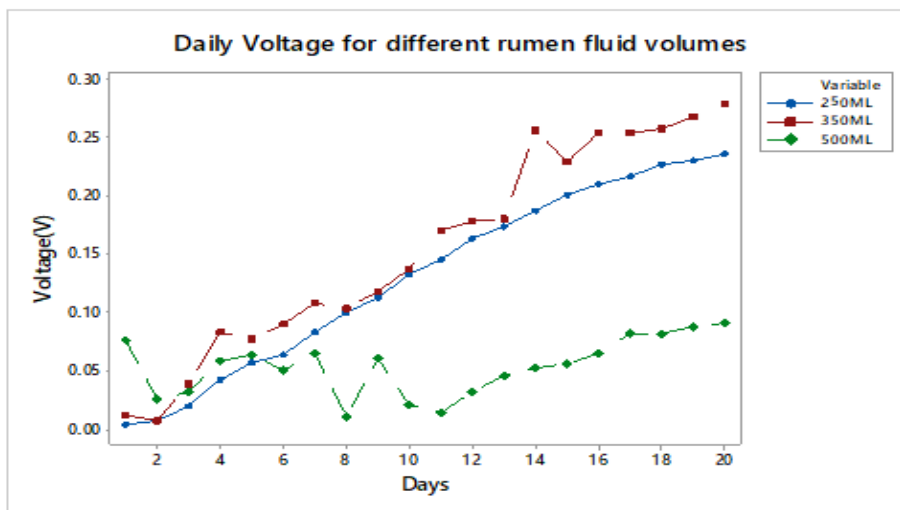


Figure 4.97: Plot of voltage produced by varying amount of rumen matter

The current yield from fruit waste mixture and 250mL rumen fluid array was highest. The continuous release of electrons by mango and avocado 1:1 mixture, as previously stated, explains this scenario which translated to the highest power (calculated using equation 4.23) output (figure 4.98).

$$P = VI \dots \dots \dots (4.23)$$

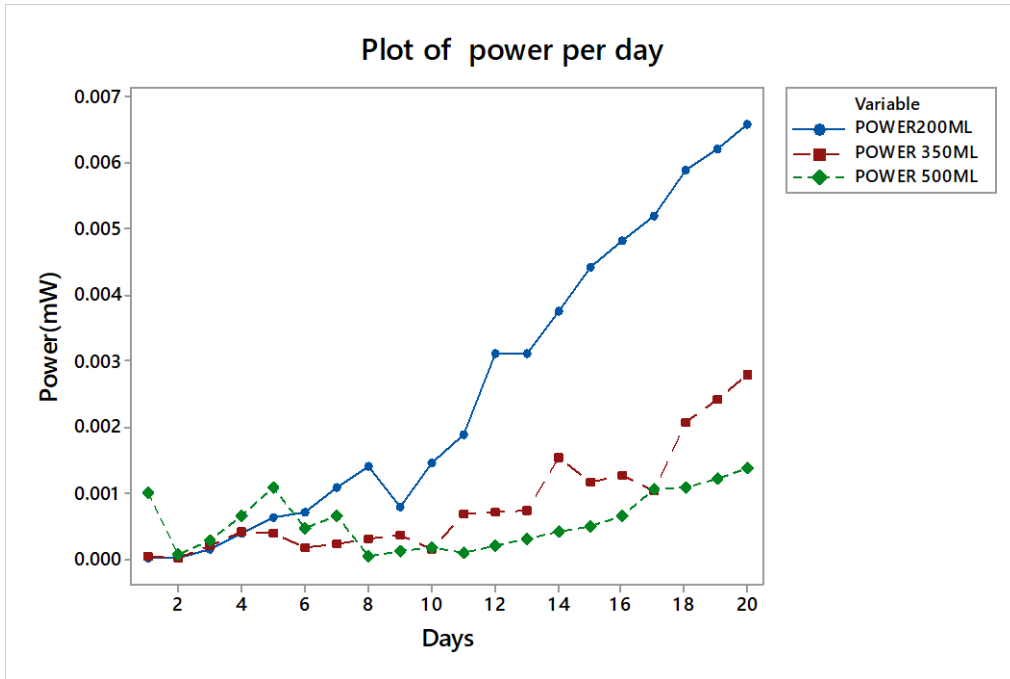


Figure 4.98: Power generated by 1:1 avocado, mango mixture to rumen fluid.

On day 15, an optimal voltage (0.449V) was observed in avocado sample by varying the anodic electrode surface area. Figure 4.99 showed the voltage (V), power (Mw), and current (A) from the three-electrode surface areas tested.

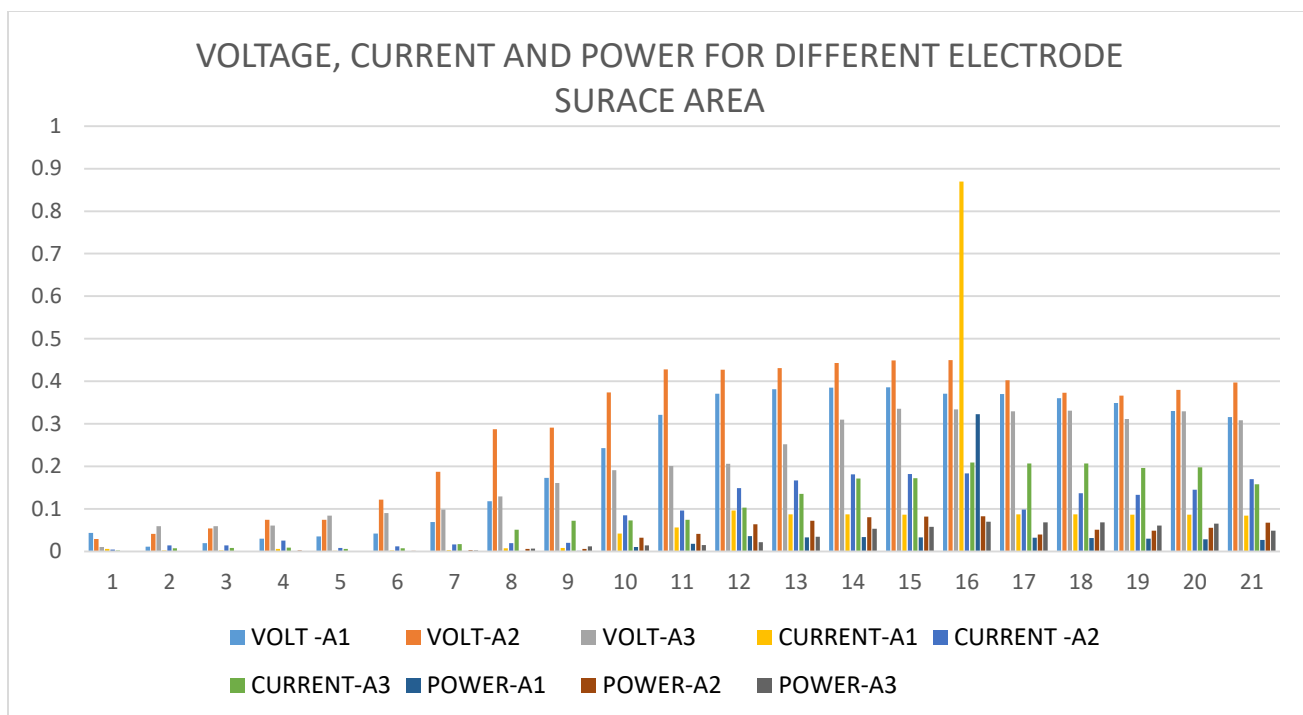


Figure 4.99: Bar graphs showing effect of A1-0.00399m², A2-0.00666m² and A3-0.01331m² electrode S/A.

On day 15, the highest current was obtained at 0.209mA from a 0.01331m² electrode surface area while day one current was the least. This is because all of the electrons yielded during the substrate decomposition secured an adsorption position on the electrode surface. The quantity of electrons emitted per unit surface of the electrode was indicated by the current density. Equation 4.21 was used to calculate the current density with figure 4.100 showing the resultant plots.

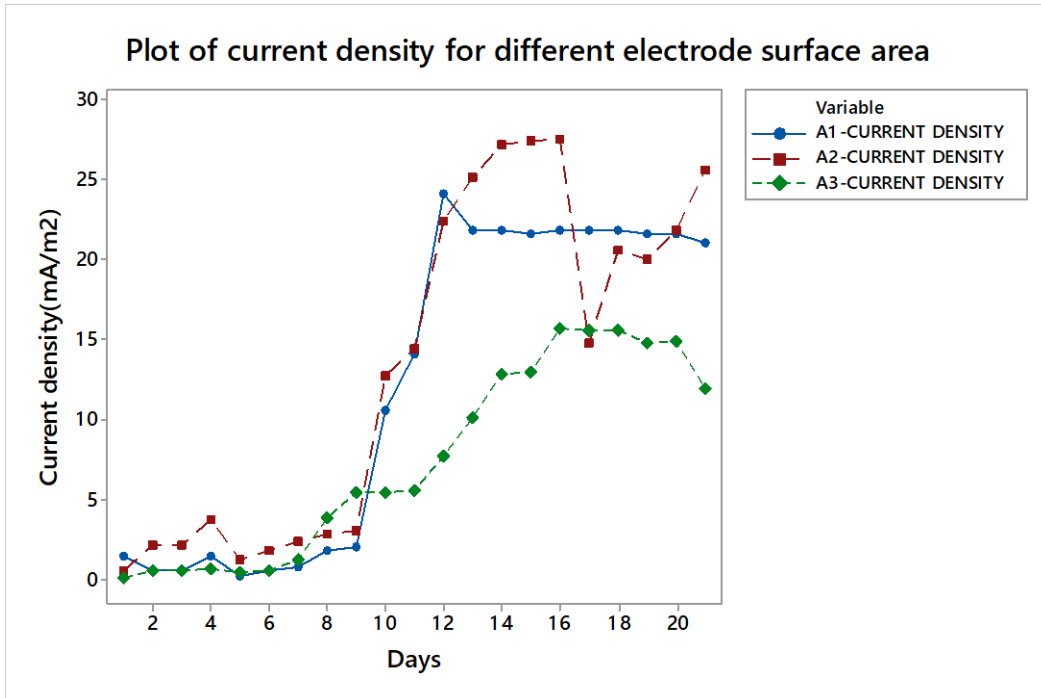


Figure 4.100: Current density plots for different electrode surface area

Figure 4.101 showed the power density(PD) computed (eq. 4.22) with electrodes of various surface areas. The 0.00666m² electrode surface produced the highest power density, as shown in the graph.

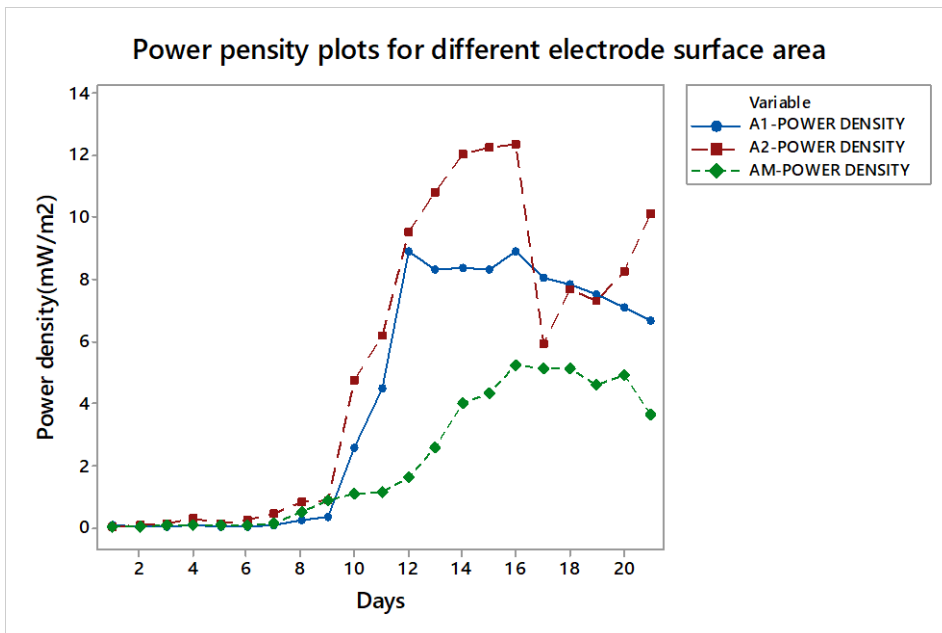


Figure 4.101: Different electrodes surface area Power density

The PD of an MFC is a reflection of unit power production per unit surface of an electrode. Figure 4.101 shows the voltage generated across various resistors and OCV. Since only internal resistance must be overcome, OCV is the highest. The cathode, anode, and electrolyte materials all contributed to the internal resistance (Fan *et al.*, 2008; Lovley *et al.*, 2006 and Kamau *et al.*, 2017).

On assessing the impact of external resistance on voltage generation of MFC, the plots of voltage in figure 4.102 were obtained. The OCV was highest in tomato at 0.593 V in tomato waste, while avocado waste generated 0.290 V OCV. Across different resistors, the voltage obtained goes through internal and external resistance and therefore, OCV voltage is higher than the voltage generated across other resistors.

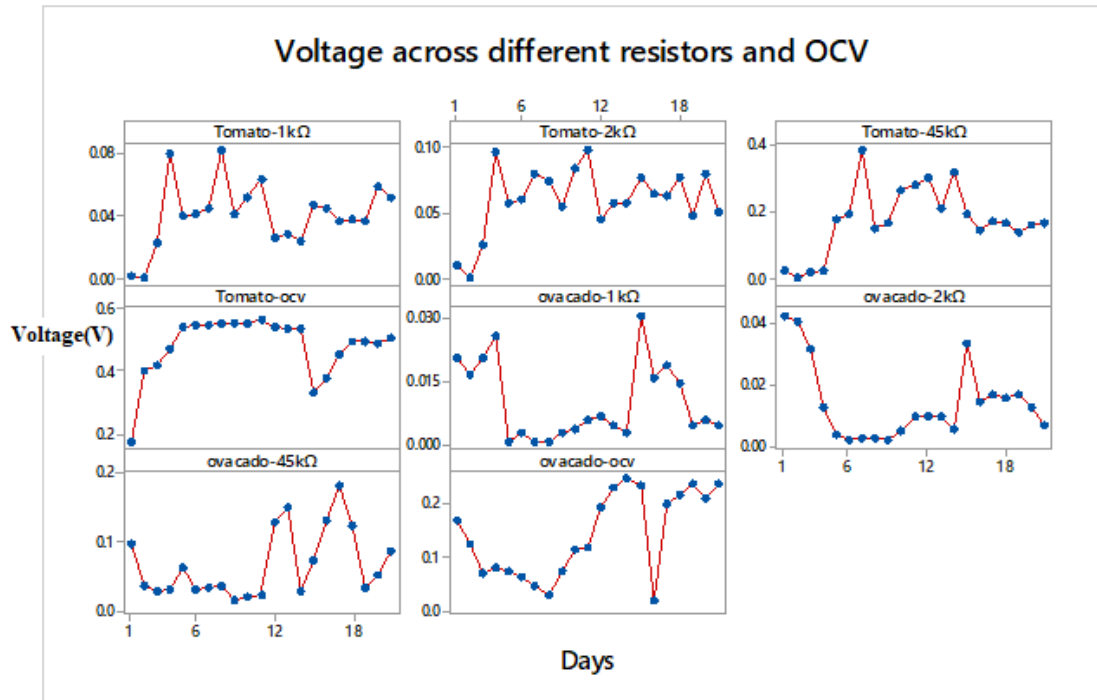


Figure 4.102: Voltage across different resistor

The maximum voltage was 0.403 V through a 45 kΩ resistor in tomato waste on day 7, according to the data. The power ranged from 0.000001 to 0.01 mW, with current densities ranging from 0.1 to 23.29 mA/m² and power densities ranging from 7.5 10⁻⁷ to 3.1036 mW/m². The high values across 45 kΩ are due to the significant amount of effort needed to overcome the high resistance. Furthermore, the results are consistent with

Ohm's law, which states that voltage is proportional to resistance. Menicucci *et al.*, (2016) previously demonstrated that voltage decreases as external resistance decreases. Other research found that as the external resistance rose from 0 - 4,000 Ω , the cell potential increased, reaching a maximum of 358 mV at a resistance of 4,000 Ω . (Ghangrekar and Shinde., 2007). Rismani-Yazdi *et al.*, (2011) found similar cathode potentials at various external resistances later on. The anode potential, on the other hand, differed depending on the external resistance used. Anode potentials were higher in MFCs with lower external resistances. This was also seen by Song *et al.*, (2010), who used a sediment microbial fuel cell (SMFC).

4.10.4 Influence of substrate proximate analysis of voltage production

In a study to assess how the proximate properties of five different fruit wastes affected the voltage and current produced by a double chamber MFC, proximate properties were analyzed using the standard procedure, and rumen fluid was used as a microbe source in the electricity generation. The moisture levels of the fruit samples ranged from 82.86 percent to 95.16 percent, with crude fat levels ranging from 0.12 percent to 0.33 percent, with avocado having the highest fat content at 9.03 percent. The banana had the highest carbohydrate content (19.24%) and the tomato waste had the lowest carbohydrate content (2.93%). The proximate properties of different fruit waste from Nairobi County are shown in Table 4.18. Mathuriya, (2014), recorded high moisture content in organic waste in a previous study with similar findings.

Table 4.18: Proximate analysis properties for different wastes

SAMPLE	% MOISTURE	% PROTEIN	% FAT	% ASH	% FIBRE	% NFE	ENERGY (Kcal/100g)
Tomato	95.16±1.23	0.57±0.01	0.12±0.02	0.46±0.02	0.76±0.04	15.08±2.31	2.93±0.01
Banana	74.30±0.09	3.05±0.05	0.51±0.02	1.67±0.05	1.24±0.04	93.66±5.62	19.24±2.31
Avocado	82.83±2.36	1.32±0.01	9.03±1.25	0.84±0.03	2.61±0.05	100.03±3.66	3.37±0.85
Mango	86.82±0.84	0.87±0.03	0.68±0.05	0.44±0.05	1.28±0.05	49.24±2.01	9.91±0.96
Melon	92.85±0.08	0.91±0.02	0.33±0.21	0.74±0.04	0.76±0.09	24.18±1.55	4.42±0.02

Tomato waste produced the highest voltage (0.701V), followed by avocado (0.584V), and watermelon (0.019V). The voltage increased in all fruits with incubation time, with some variations after day five. Current and voltage rose linearly for the majority of the fruits. Surface plots of daily voltage and current produced from various fruits and fruit mixes are shown in Figure 4.103.

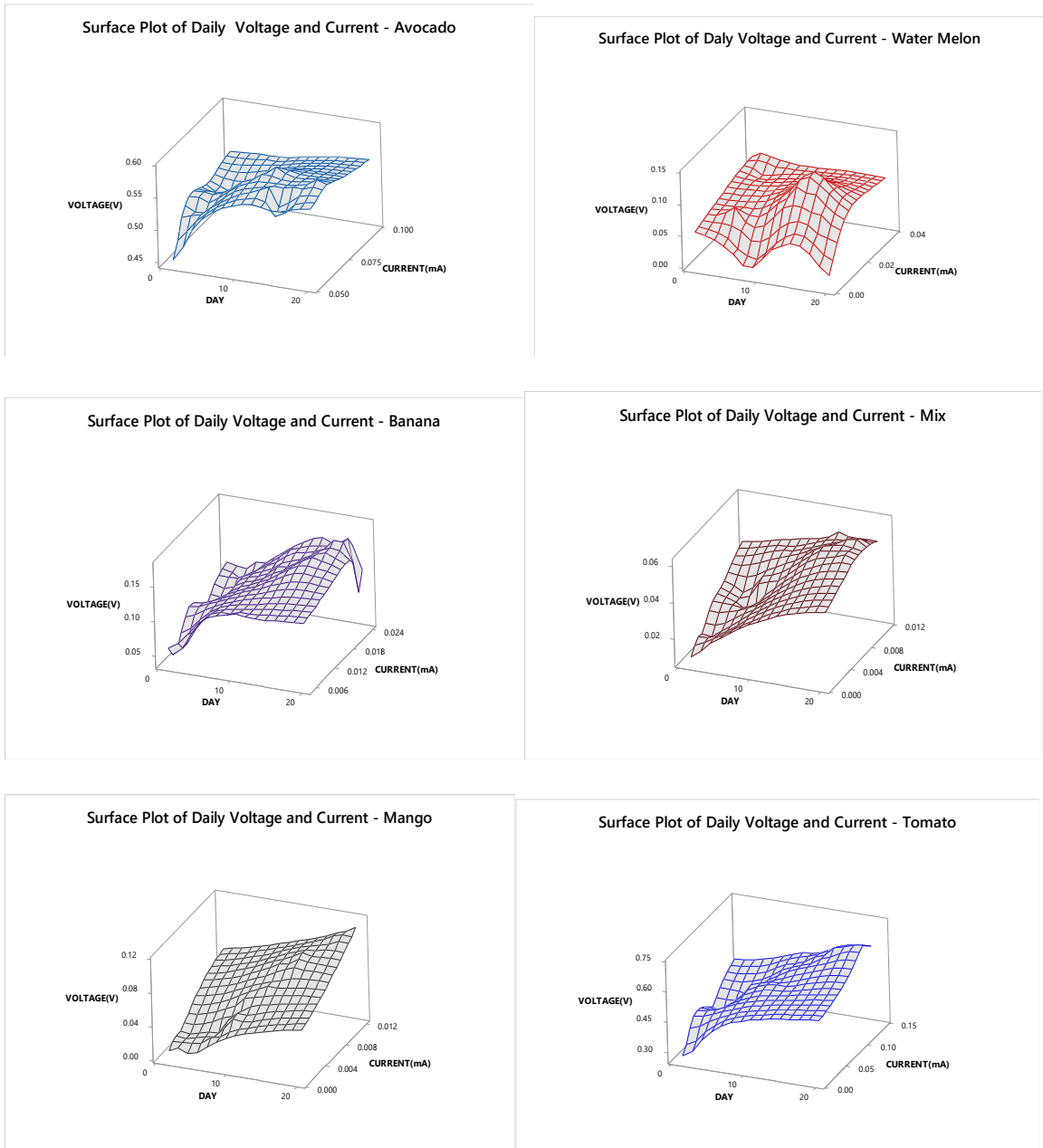


Figure 4.103: Different fruits wastes current and voltage

The results are consistent with those reported by Parkash *et al.*, 2015 on avocado fruits, which generated an initial voltage of 0.637 V and a final voltage 0.657 V. The voltage generated increases with time. A rapid increase in voltage generation occurred in the first four minutes and gradually increased. The voltage increases exponentially as time increases (Parkash *et al.*, 2015).

High moisture levels are important for the creation of more electron-mobile solutions and the transfer of electrons to the MFC's cathode (Adebule *et al.*, 2018). According to Wang *et al.*, (2009), moisture content greater than 10% increased voltage production by more than threefold. This is shown by the findings of this study, which found a voltage difference of 0.128 V between tomato and avocado due to a 12.33 percent difference in moisture content.

Similarly, the moisture disparity between a banana and a tomato resulted in an 8.9-fold voltage margin. The carbon source, which influenced the microbial population, was critical for the growth of optimal electrogenic biofilms in MFCs (Chae *et al.*, 2009; Asensio *et al.*, (2016). High carbohydrate levels resulted in high voltage, as demonstrated by the 0.126 V and 0.004 V voltages reported on day 10 for banana and watermelon, respectively. This shows that a 14.82 percent carbohydrate difference results in a 15-fold increase in voltage production. Microbial activities depended heavily on carbohydrates as a carbon source. The observed trend in terms of energy is that the higher the energy of the fruit waste, the lower the voltage produced. In figure 4.104, a pattern can be seen. This is because of the high-energy substrate necessitated a high level of microbial activity (this explained the high current recorded).

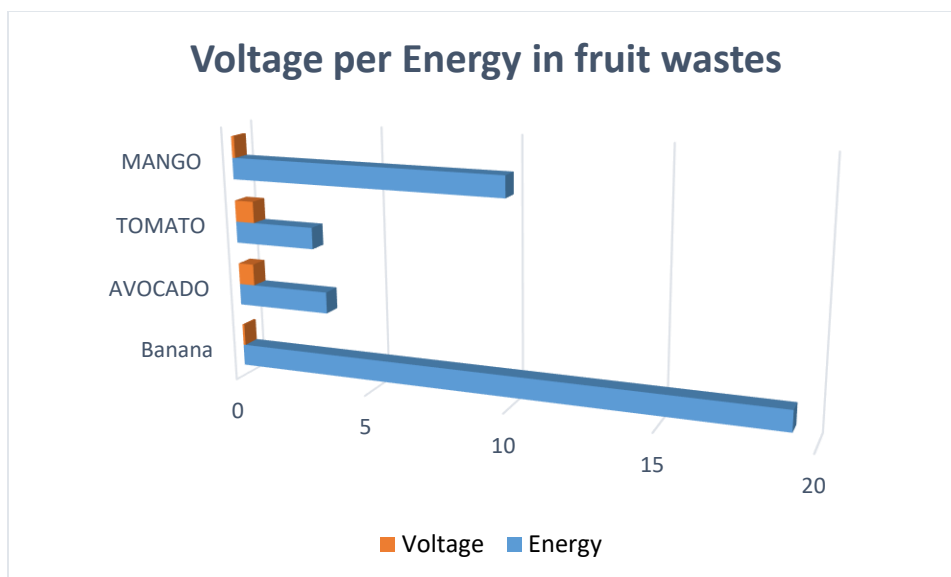


Figure 4.104: Bar graph of fruit energy levels versus voltage output

The effect of fat levels in fruit wastes had no discernible effect on the voltage produced. Fat avocados, for example, have a fat content of 9.92 percent, while tomato waste has a fat content of 0.12 percent. On day 11, the voltage difference was less than 0.022. When a substrate with double the protein levels was used, the voltage produced increased two-fold.

4.10.5 Pilot-scale study

Under ideal conditions, power densities of over 1 kW/m^3 (reactor volume) and 6.9 W/m^2 (anode area) have been achieved in laboratory research on various MFC technologies. The biggest challenge is to get these innovations out of the lab and into real-world bioenergy production systems (Logan, 2010). The voltage obtained from the co-digestion of tomato waste with rumen waste in a 4 liter pilot-scale MFC study in open circuit(OCV) and across different resistors is shown in figure 4.105. Day 1 voltage was high and then decreased up to day 4. This was explained by the fact that; the microbes need time to adapt to the anodic chamber environment before they operate at full capacity. After that, the voltage generated increased with time and was dependent on the

days' temperature. The highest OCV voltage generated was on days 13 and 16 at 0.049V and 0.047V, respectively.

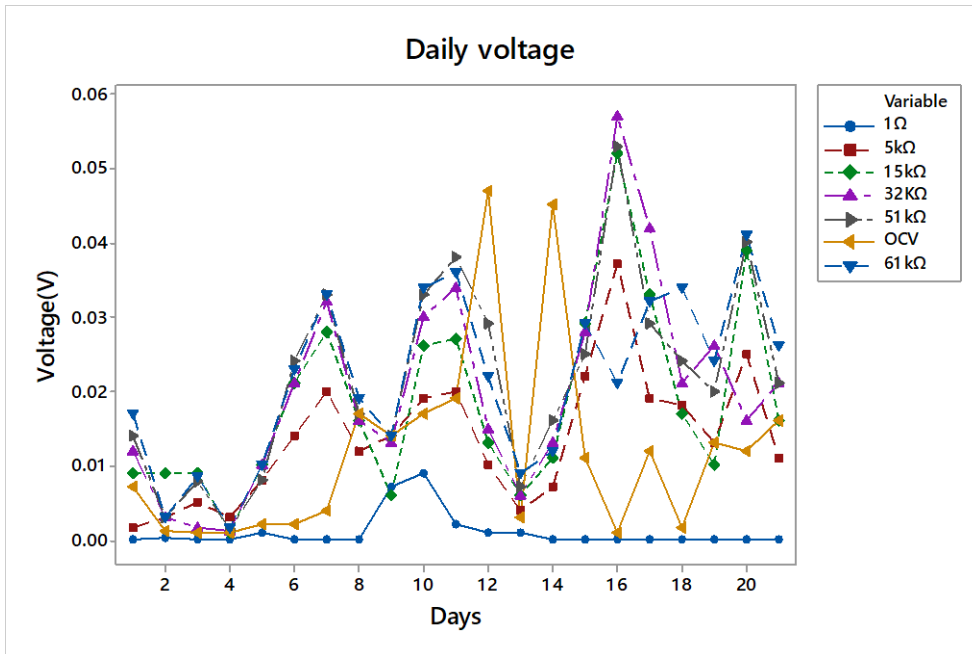


Figure 4.105: Pilot-scale voltage in OCV and across different resistors

The voltage obtained across different resistors showed compliance with Ohms law as it was observed to increase with an increase in resistance. It was observed to be lowest in 1Ω and highest in 32kΩ at 0.057V. The results obtained were consistent with those observed in reported MFC scaling up research (Goto and Yoshida, 2019; Dewan *et al.*, 2008; Hiegemann *et al.*, 2016; Tota-Maharaj and Parneet, 2015).

4.10.6 Chlorothalonil degradation studies

One of the primary application of MFC technology is the bioremediation of organic pollutants due to its green approach and high efficiency (Mbugua *et al.*, 2019). MFC technology was investigated in the bio-degradation of chlorothalonil, which is commonly used in tomato farming. Tomato wastes were doped with the pesticide residue as a co-substrate and subjected to MFC electricity generation. The tomato waste proximate parameters (Table 4.19) were analyzed, which is essential for MFC substrate studies (Rominiyi *et al.*, 2017). The moisture level was 95.16 and 4.84 % on a wet and dry basis, respectively. All the other properties were higher on a dry basis compare to a wet basis.

Table 4.19: Proximate properties of tomatoes

Properties	Wet Weight	Dry Weight
Moisture	95.16±1.23	4.84±0.06
Volatile Matter	4.38±0.03	85.63±1.09
Carbohydrates	2.93±0.02	55.42±0.56
Protein	0.57±0.01	11.89±0.69
Fat	0.12±0.01	2.57±0.02
Ash	0.46±0.02	9.53±0.32
Mineral Matter	0.51±0.03	10.48±0.25
Energy (Kcal/100g)	15.08±0.09	292.37±1.56

The energy values of tomato waste were 19 times higher on a dry basis compare to wet basis. The daily voltage in all the samples increased from day 1 to 9. There was a voltage drop that was recorded on day 10 when the pesticide solutions were introduced apart from the set where no pesticide was added. The voltage starts to increase. On day 20, the voltage reduced, which was attributed to the destabilization of anaerobic conditions during sampling. An upward trend was observed, and it formed a plateau around day 27. This was explained by the diminishing substrate levels translating to decreasing microbial activities and subsequent death of microbes. Figure 4.106 shows the voltage generated from various levels of glucose solution.

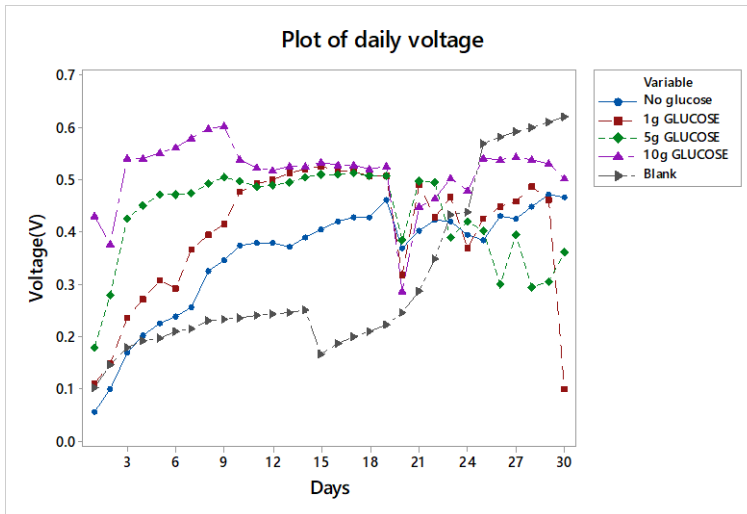


Figure 4.106: Daily voltage production from various glucose levels

The recorded voltage on sampling days were 0.603V, 0.527V and 0.502V on day 9, 19 and 30, respectively for the set containing 10g glucose in 100ppm chlorothalonil solution. Glucose served as a good substrate in the breakdown of chlorinated pesticides, as earlier observed by Huang *et al.*, (2012) in mineralization of pentachlorophenol.

The current generated from the set-ups is shown in figure 4.107. The current was lowest on the set up with blank tomatoes since it had no inoculum. In glucose solutions, the recorded current was lowest in 10g glucose solution followed by 5g and 1g, respectively.

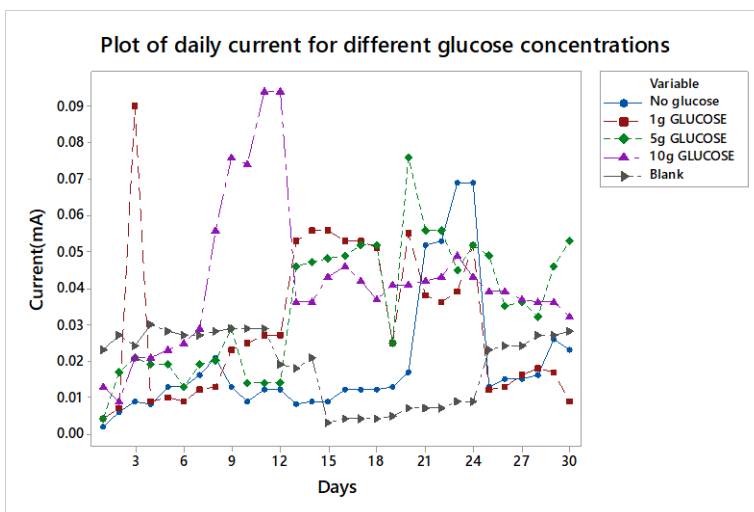


Figure 4.107: Plots of daily current for various glucose levels

From figure 4.107, the highest current was obtained from the set-up with no glucose solution. Current is the flow of electrons therefore, the microbes fed on tomatoes and pesticide molecules at a faster rate compared to the solutions containing glucose. The performance of the MFC was described by the power capacity, which was calculated by multiplying voltage and current. Daily plots for power obtained are shown in figures 4.108.

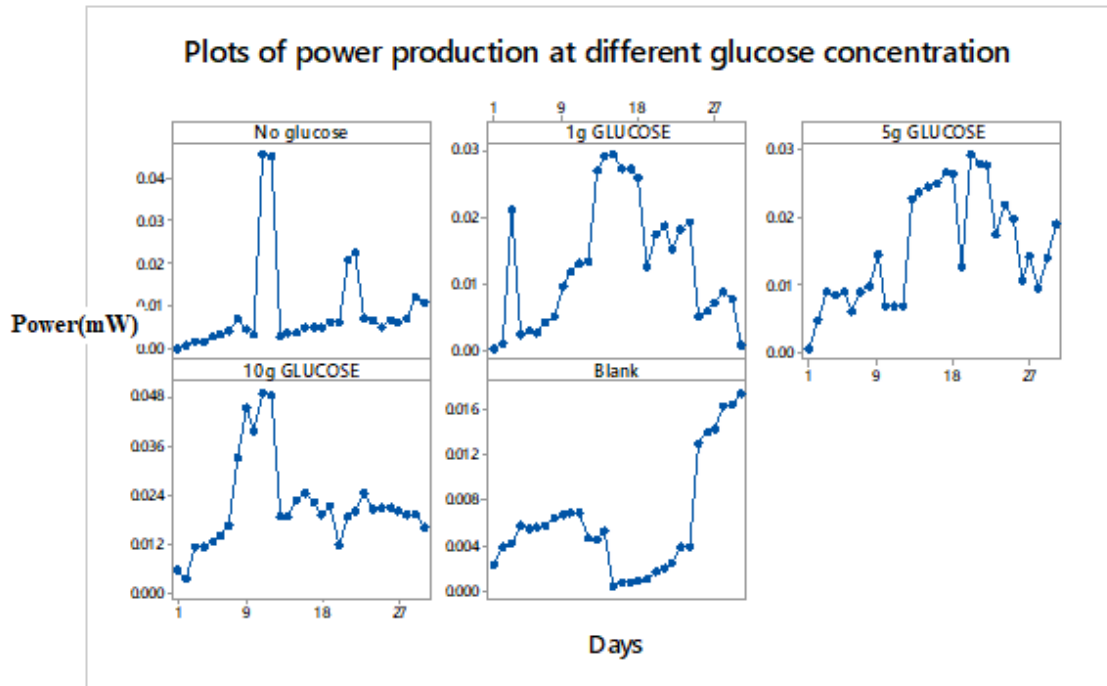


Figure 4.108: Daily power production at different glucose levels

The power obtained was in the range of 0.0056 mW to 0.0492 mW for 5g glucose in the 100ppm chlorothalonil solution. The surface plot of daily power and current density is shown in figure 4.109. Current and power density were calculated as reported by Kamau *et al.*, (2017).

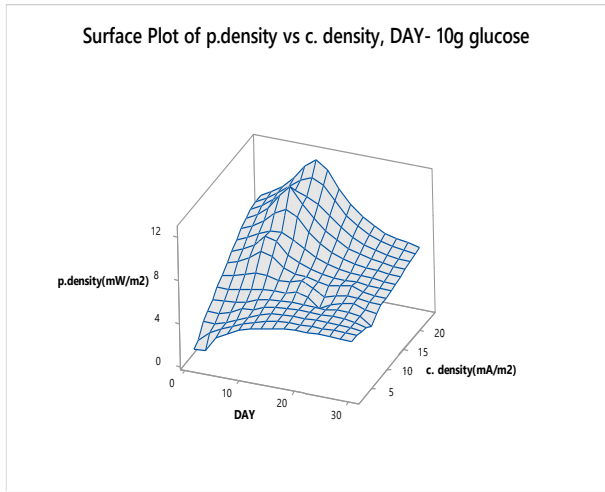
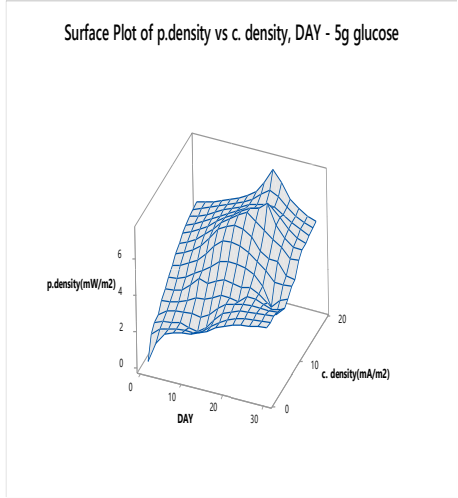
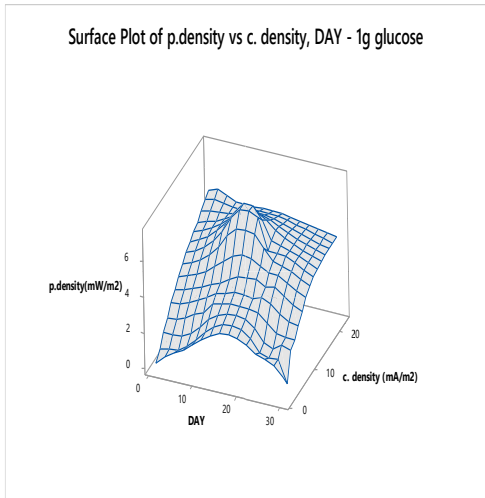
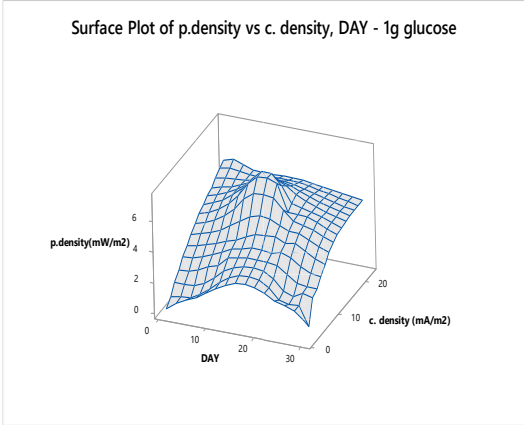
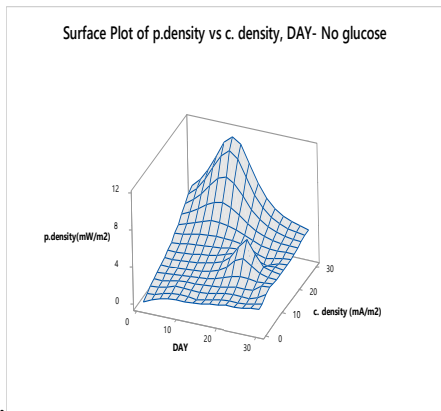


Figure 4.109: Surface plots of daily power density and current density

The percentage levels of chlorothalonil degraded is shown in figure 4.110. As expected, degradation increased with time of exposure. This was due to the fact that as time increased, microbes needed food to survive and therefore, they consumed the substrate doped with the pesticide residue. The percentage of degradation at various glucose levels is displayed by figure 4.110.

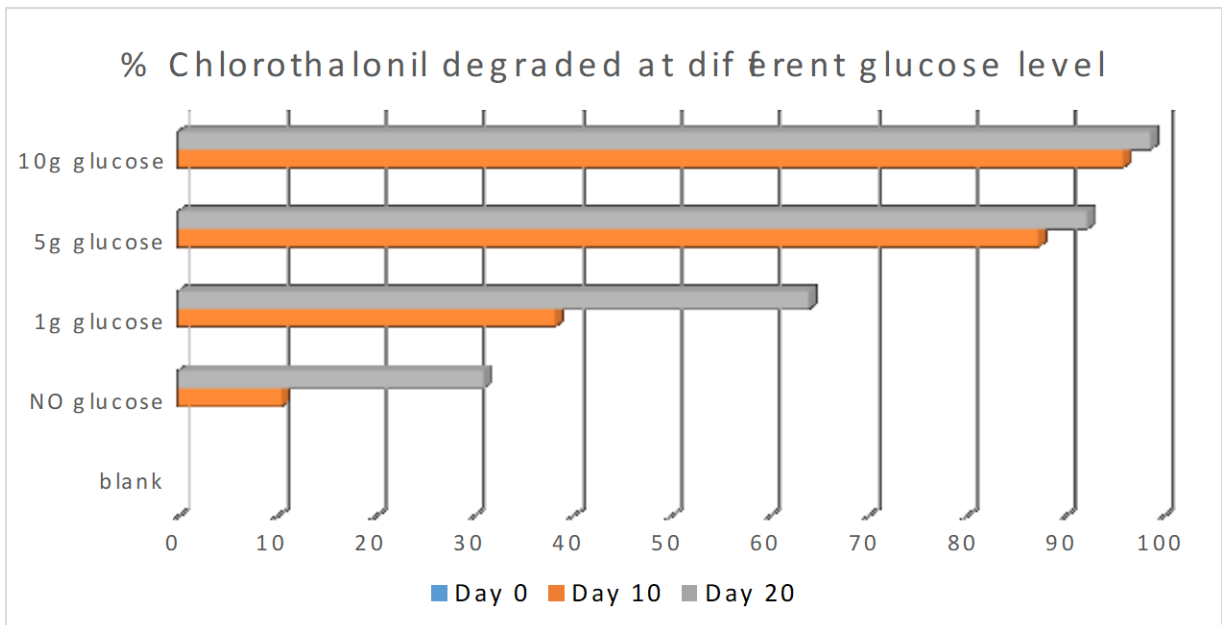


Figure 4.110: Percentage chlorothalonil degraded at different glucose levels

High degradation levels were recorded in the 10g glucose doped substrate. This was due to the increased available microbe food translating to increased consumption of residue (Mbugua *et al.*, 2017).

4.10.7 Concentration Variation

The results on the variation of concentration on microbial activities are given in figure 4.111. The voltage was highest for the 20ppm pesticide solution. In this case, as opposed to earlier observations, the addition of glucose doped solution had no significant impact on voltage. The highest voltage was recorded at 20 ppm, then 10 ppm and least in the blank

set-up. The lowest voltage was observed on day 20 due to the destabilization of the biofilm during sampling.

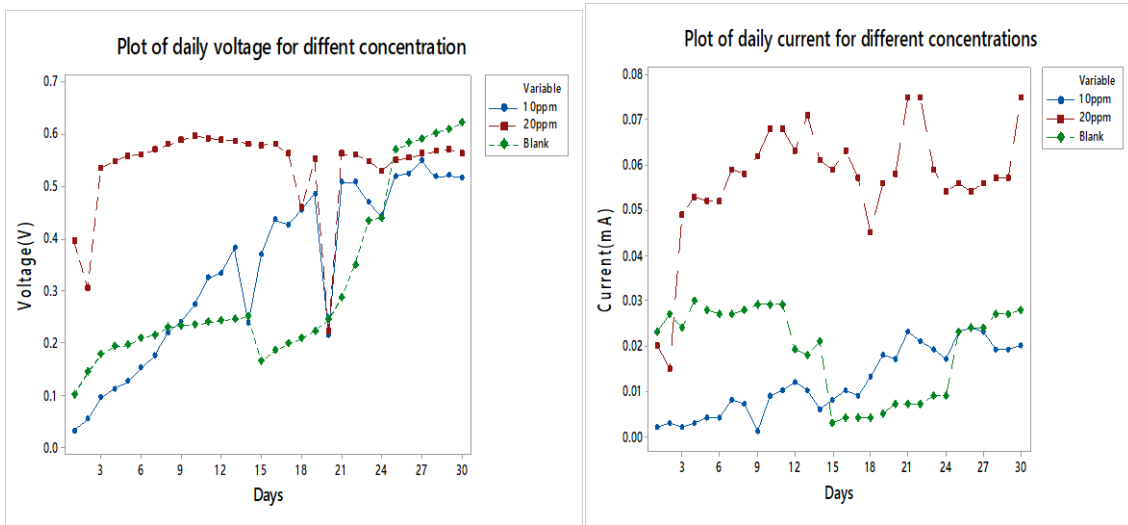


Figure 4.111: Daily voltage and current generated for varying amount of chlorothalonil. The daily current was lowest in blank set-up, 20ppm solution, and 10ppm solution, respectively, as shown in figure 4.111. Figure 4.112 showed the power obtained from different concentrations of chlorothalonil.

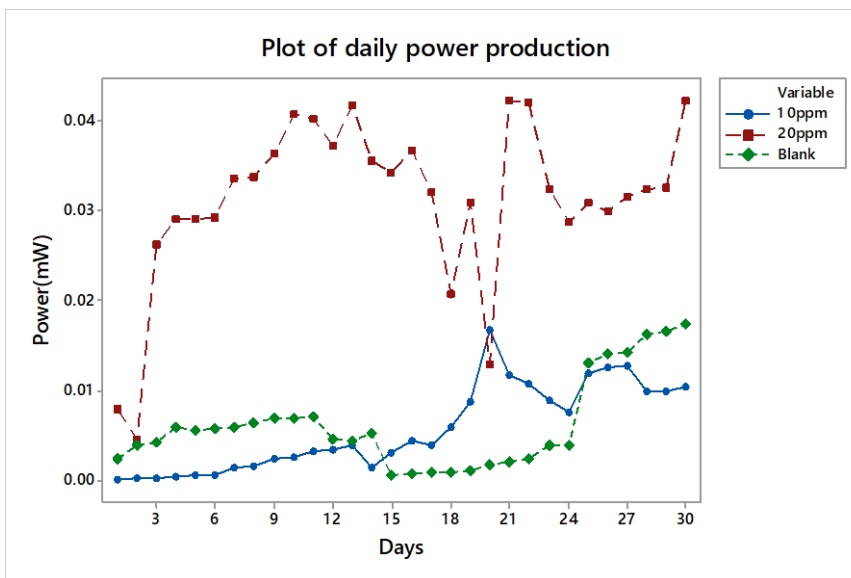


Figure 4.112: Daily power generated for a varying amount of chlorothalonil

4.11 Bio-slurry application

The effect of biogas digestate on container gardens crop production was set up on loam soil. The soil used was examined for nutrient composition and the results are tabulated in table 4.20.

Table 4.20: Loam soil properties

Profile	Properties	Profile	Properties
Soil depth cm	Top	Calcium milli-equivalent%	44.4±2.11
Soil pH-H ₂ O (1:2.5)	6.5±0.51	Magnesium me%	3.1±0.09
Elect. Cond. ms/cm	0.3±0.01	Potassium me%	1.5±0.66
Carbon %	2.7±0.32	Sodium me%	3.6±1.11
Sand %	40±3.56	Sum me%	52.6±3.44
Silt %	40±4.55	Base %	100+
Clay %	20±2.88	ESP	14.4±6.74
Texture Class	Loam	Total nitrogen %	0.25±0.08
Cat. Exch. Capacity. me%	24.8±2.67	Phosphorus ppm	44±5.00
Zinc ppm	62.9±10.22	Iron ppm	96.2±12.90
Copper ppm	1.22±0.11	me is milli-equivalent	

According to the soil analysis report (table 4.20), the soil properties were satisfactory for crops' growth. However, a recommendation is made for application of manure during land preparations. The organic green matter from the market wastes is significantly transformed into a dark fluid via anaerobic digestion within 7 days. Figure 4.113 showed the mixed market wastes and the digestate. During AD, 25-30% of the total solids was converted to biogas and bio-slurry (Gurung, 1998). The composition of bio-slurry depends upon several factors: the kind of substrate, moisture, types of feed, etc. Bio-slurry is applied as plant fertilizer directly or as compost.



(a)



(b)

Figure 4.113: A photo of (a) mixed market waste and (b) the digestate.

In figure 4.113, the greenish color shows the fresh blended waste with high total solids and volatile matter. On incubation in anaerobic digester and extraction of energy from the matter, the second picture was obtained showing black matter. This is the bio-slurry employed in crop production. The crops grown in a container garden where the application of digestate on crop production was compared with other manure applications are shown in figure 4.114. The manure was applied without any pre-treatment by taking about 1 Kg of the manure and spreading it over the soil surface on container garden.



Figure 4.114: Container gardens with (a) bio-slurry, (b) cow dung (c) dried manure and (d) blank

The impact of different manure applied in the container garden was monitored in terms of crop leaf health and appearance and well as crop height. The increase in the length of maize, beans, peas, kales, spinach and tomato were monitored after three weeks and the results are shown in figure 4.115.

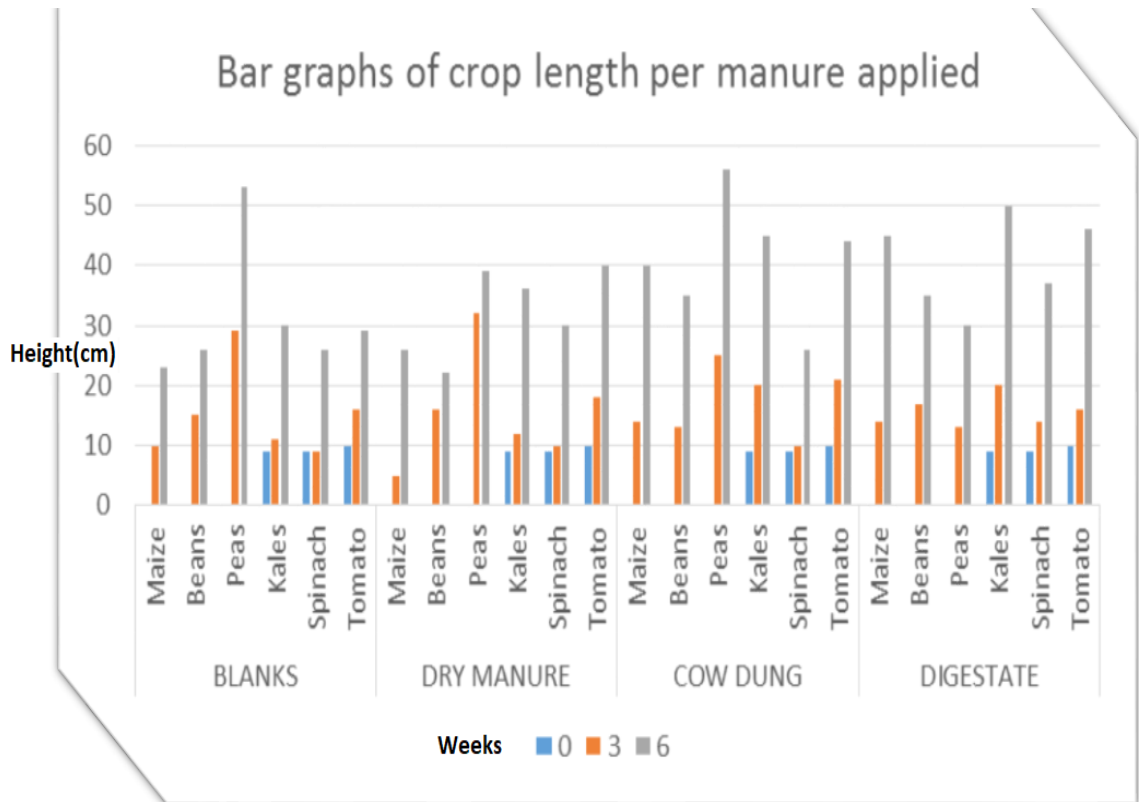


Figure 4.115: Bar graphs of crop lengths per manure applied

The increase in peas height was highest at 57cm in cow dung. From week 0-2, no increase in height was recorded in maize bean and peas as they had not germinated. The size in kales, spinach and tomato, was recorded after transplant. Overall the effects of digestate and cow dung were almost similar in terms of height change. Table 4.21 showed the observed results per manure in weeks in the three phases of crop production i.e., germination and transplanting, growth and development in terms of length and crop health and flowering and fruition stages. The monitoring was done for 6 weeks since the kales and spinach had reached the harvest time.

Table 4.21: General observation for crops with different manure

Week	Observation	Blank	Dry manure	Cow dung	Bio-slurry
0	Germination and Transplant	Germination within one week. Transplanted seedlings were well established	Germination within one week Transplanted seedlings were well established	Germination within one week. Transplanted seedlings were well established	Delayed germination within one week. Transplanted seedlings were well established
3	Length and health	An increase in length for all the crops was noted. Spinach and kales leaves were small in diameter	An increase in length for all the crops was noted. Spinach and kales leaves were wide	An increase in length for all the crops was noted. Spinach and kales leaves were wider than those of dried manure	An increase in length for all the crops was noted. Spinach and kales leaves were wider than those of dried manure
6	Flowering, fruiting	Minimal increase in length from week 3. No flowering or fruiting observed in tomato	An increase in length was observed. Flowering in both peas and tomato was observed. Kales and spinach ready for harvest	An increase in length was observed. Flowering in both peas and tomato (3 fruits) was observed. Kales and spinach ready for harvest	An increase in length was observed. Flowering in both peas, beans, and tomato (5 fruits) was observed. Kales and spinach ready for harvest

The observed growth pattern of crops in terms of size and plant health in weeks 1, 3, 6 and 9 is shown in figures 4.116, 4.117, 4.118 and 4.119, respectively. Figure 4.116,

manure was applied in the different container gardens after transplanting. In figure (4.116) set a is bio-slurry, b is cow dung, c is dry manure, and d is the blank set.



Figure 4.116: Crop production in container garden (week 1)

After 3 weeks, the kales, spinach and tomato plants had increased in height while peas, beans and maize had germinated. Leaf health and appearance is shown in figure 4.117.



Figure 4.117: Crop production in container garden (week 3)

The growth and development of the crop were observed to improve with time, as shown in figure 4.113. Better results on plant leaf appearance and health were observed to be

better in the set with the bio-slurry followed by the set with dried manure. In the blank set, the crops started dying due to the depletion of nutrients in the soil, as per figure 4.118.



Figure 4.118: Crop production in container garden (week 6)

In week 6, the kales, spinach and tomato crops were uprooted and the maize, beans and peas growth monitored. With time, the produce with dried manure and cow dung started wilting, showing depletion of nutrients in the soil.



Figure 4.119: Crop production in container garden (week 9)

In general, the impact of bio-slurry in crop farming was the best followed by dried manure due to high nutrient content as well as high composting matter. The impact of bio-slurry in the growth of avocado plant was investigated, and the increase in length is shown in figure 4.120.

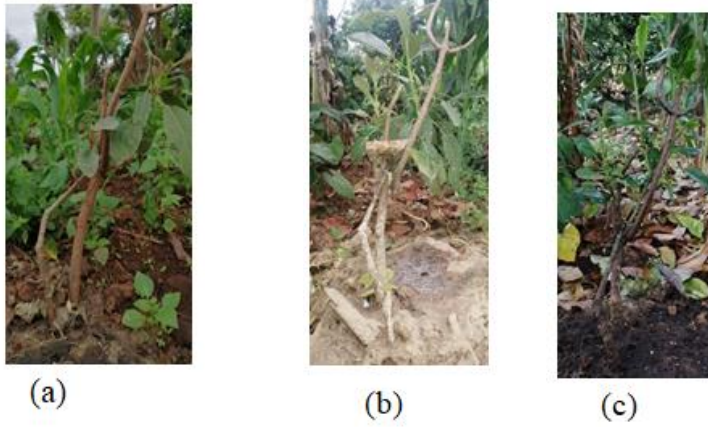


Figure 4.120: The avocado tree where digestate application was done. (a)week 3 (b) week 6 (c) week 9.

CHAPTER 5

5.1 CONCLUSIONS AND RECOMMENDATIONS

This section presents a summarized overview of the results obtained in this study as well as some recommendations and beneficiaries of this work. The fruits and vegetable wastage in Wakulima and Kangemi markets is high resulting in the accumulation of solid waste. The wastage levels depend on seasons and fruit or vegetable properties. The wastes contain high levels of proximate properties like moisture, carbohydrates, fat and proteins. Based on the results and discussion in chapter four, the following conclusions are made:

5.2 Conclusions

The cow dung and the rumen fluid contain high microbial counts making them favorable for energy recovery in AD and MFC technologies. The bacteria count from the rumen fluid and fresh cow dung observed in this research were $3.15 \pm 0.01 * 10^{10}$ cfu/mL and $1.50 \pm 0.02 * 10^{10}$ cfu/g, respectively. Rumen fluid had almost three times bacteria count compared to fresh cow dung. Further analysis of the inoculums showed that both rumen fluid and cow dung samples had; *Streptococcus spp.*, *Bacillus subtilis*, *Bacillus Cereus*, *E. coli* and *Micrococcus luteus* microbes. Further investigation showed that the volatile solids were found to be 81.69 ± 1.52 and 73.50 ± 2.20 % of the total solids while the C: N ratio was 29.62 ± 0.51 and 17.06 ± 0.50 in rumen fluid and cow dung, respectively.

The analysis of the fruit and vegetable market wastes showed that the macro and micronutrient analysis revealed that the wastes have some heavy metals at 15.20 ± 2.70 ppm lead, zinc at 176 ± 11 ppm iron at 3742 ± 235 ppm. The calcium and potassium levels in fresh wastes mixtures were in the range of 1.53 ± 0.07 % and 3.59 ± 0.22 %, respectively. The proximate analysis showed moisture content of 74.31 – 95.86% for all the wastes. Low percentages of proteins and fats were observed at 0.52 -3.49 % and 0.09 – 1.54 %, respectively.

respectively. The carbohydrate levels ranged from 1.99 ± 0.12 to 32.17 ± 2.31 % while the crude fiber in this study was in the range of 0.54 – 2.61%.

Anaerobic digestion of fruits and vegetable wastes results in biogas generation with the rate of biogas formation reported highest in day 0-3 of AD which gradually reduced in the remaining retention time of AD. The best inoculum to substrate ratios for optimum biogas generation was 1:1 cow dung to substrate and 1:1.5 substrate to rumen fluid. Co-digestion of waste reduced the retention time because the presence of cow dung or rumen fluid in waste increased the growth of micro-organism rapidly. The CH₄ contents in biogas composition were in the range 49–60% depending on the wastes and inoculum used. Temperature, pH, C: N, pretreatment and substrate composition were among the significant factors which were observed to influence biogas recovery from market wastes. The optimal temperature for bio-methanation studies reported in this study was thermophilic followed by mesophilic and psychrophilic respectively. The pH range of 6.8-7.2 was observed to be optimal for fruits and vegetable waste bio-methanation studies with frequent regulations. The best working range for C: N ratio was 19 – 30, with higher levels significantly reducing biogas production. The biochemical methane potential studies revealed that biogas formation ranged from 1000 to 3500 mL with a methane composition of 56 – 60%. The data obtained further shows that higher digestibility (74 - 96%) translated to high methane production.

The portable digester developed in this research work incorporated pH, temperature and agitation mechanisms. The digester increased biogas production six-fold in comparison to the un-agitated digester. A portable biogas safety device was designed and developed using *Arduino* micro-controller. The device alerted the user in the event of excess smoke, methane leakage and/or fire breakout via a call or SMS using the SIM900 GSM module.

The average measured level of raw biogas was 227 ± 2.69 ppm H₂S, $>20 \pm 5.90$ % CO₂ and $52-56 \pm 1.99$ % CH₄. The most efficient upgrade material was zeolite rocks with upgrade levels of 89 – 93 % methane. The total removal for zeolite was observed to be 75 % for CO₂ and 95.34 % for H₂S.

In microbial fuel cells, the microscopic and biochemical studies of the cultures confirmed the presence of *Proteus* and *Clostridium spp.* in the anodic compartment of MFC. The highest values of voltage, current and power obtained were 0.5090 V, 0.28 μ A, 0.0093 μ W, respectively while the power and current density calculated for tomato wastes ranged from 1.805 to 61.141 mW/m² and 6.772 and 98.164 mA/m², respectively. Tomato waste recorded a 0.584 V optimum voltage while avocado generated 0.248 V with an electrode S/A of $6.666 * 10^{-3}$ m².

5.3 Recommendations

In the two markets, food wastage should be minimized at all cost to improve food security in Kenya and avoid landfill in major markets in the city and other markets. Whenever this is unavoidable, methane and carbon dioxide trappers are highly recommended in both markets and slaughterhouses to trap green house gases and curb global warming. More specifically, the following recommendations are made:

1. Characterize bacteria from other markets in Kenya
2. Assess other parameters (other than proteins, carbohydrates etc) in the waste
3. Develop other upgrading and purification methods (eg use of activated carbon, bone charcoal etc)
4. Application of Internet of things in reactor designs to make them more efficient and effective.
5. Investigation of online biogas production process monitoring to detect digester failure before they can take place.
6. Assess application of other market waste in electricity generation.
7. Analyse the bio-slurry from biogas reactors and its potential application to tea, coffee and maize farming.

5.4 Recommendations for Further Work

From the results, conclusions and the recommendations obtained in this work, the following suggestions are proposed as further works to improve waste to renewable energy projects;

1. Characterization of microbes in cow dung and rument fluid to understand the anaerobic digestion process fully.
2. The influence of heavy metals and other contamination on anaerobic degradation of market wastes should be investigated.
3. Optimized studies of biogas generation from slughethouses, upgrading and subsequent packaging in cylinder for distribution.
4. Application and implementation of digester automation proposed in this study in full scale biogas digesters designs.
5. A thorough understanding of electricigens and their electron transfer mechanisms would aid in the development of more efficient methods for improving MFC efficiency and subsequent applications in electric devices.

5.5 Beneficiaries of The Work

Waste management for renewable energy generation has the potential of improving lives for Kenya citizens. This is because everyone needs energy in a waste-free environment. This work has a direct impact on the following:

1. Nairobi and Kiambu County Governments: Dagoretti and Kiamaiko slaughterhouses produce thousands of liters of rumen fluid, which is washed to Nairobi River. The fluid is rich in microbes, which can be used for waste digestion. The work is focused on collecting the fluid and using it in biogas production on a pilot-scale for both governments. These reduce the amount of money the County governments pay to NEMA for waste as well as generation of revenue from the sale of fluid. The amount of money

the County governments use on the treatment of water-borne diseases from Nairobi River will also be reduced.

2. **Farmers:** Digestion of waste anaerobically has the advantage of nutrient-rich digestate for use in agricultural land. This will significantly reduce the amount of money spent on fertilizers and increase food production. Farmers will also be provided with cheap and effective digesters as well as be trained on improved ways of cooking gas production.

3. **Forester and environmentalist:** When people embrace the new technology which will be developed in this work, deforestation will be a thing of the past. Forest cover will increase, translating to the achievement of vision 2030. This will be achieved by providing wood fuel alternatives.

4. **Mothers and women at large:** Mothers spend most of their time fetching firewood to cook for their families. Improved Biogas plants will lower the time they use to fetch fuel, thereby enhancing their lives as saved time will be used for other activities.

5. **Business and market people:** Our market in the cities are full of organic waste. This has both air and surface pollution. The use of market waste in gas production using rumen fluid will ensure a high rate of waste digestion, which will increase space for business as the wasteland will be well managed.

6. **Slaughterhouses:** Rumen fluid rich in anaerobic bacteria isolated can be used to digest cow dung from the abattoir. This means that in Kiamaiko and Dagoretti, slaughterhouse biogas plants will be constructed. Slaughterhouses can hence use the gas generated to boil water and for lighting purposes. The amount of money they pay for waste will reduce significantly as they will utilize waste for biogas production. The digestate can be sold to farmers as fertilizer, while excess gas can be sold to neighboring citizens.

7. **NGOs and institutions:** The digester design proposed in this work will incorporate heating and agitation mechanisms, which are significant causes of digester failure. Most of NGO's funded biogas production failure results from digester setbacks. The technology and innovation from this work will be shared widely with NGOs and institutions to ensure digester operation conditions and failures are addressed.

The work is essential in all aspects and has a direct impact on everyone since it touches energy and waste management, which are pillars of the Kenya Vision 2030.

5.6 References

- Abatzoglou, N. and Boivin, S. (2009). A review of biogas purification processes. *Biofuels. Bio products and Bio refining*, **3**, 42-71.
- Abdel-Hadi, M. A. and S. A. M. Abd El-Azeem. (2008). Effect of heating, mixing and digester type on biogas production from buffalo dung. *Journal of Agricultural Engineering*, **25**, 1454-1477.
- Abu Qdais H, Bani H. K, Shatnawi N. (2010). Modeling and optimization of biogas production from a waste digester using artificial neural network and genetic algorithm. *Resources. Conservation and Recycling*, **54**(6), 359- 63.
- Achmad, K. T. B., Hidayati Y. A., Fitriani D. and Imanudin O. (2011). The effect of C/N ratios of a mixture of beef cattle feces and water hyacinth (*Eichornia Crassipes*) on the quality of biogas and sludge. *Lucrari Stiintifice Journal*, **55**, 117-120.
- Adebule A.P, Aderiye B.I and Adebayo A.A. (2018). Improving Bioelectricity Generation of Microbial Fuel Cell (MFC) With Mediators Using Kitchen Waste as Substrate. *Ann Appl Microbiol Biotechnol J*, **2**(1), 1008
- Adegunloye, D.V., Adetuyi F.C., Akinyosoye F.A., Doyeni M.O. (2007). Microbial Analysis of Compost using Cow dung as Booster. *Pakistan Journal of Nutrition*, **6**(5), 506-510.
- Adekunle K.F and Okolie J.A. (2015). A Review of Biochemical Process of Anaerobic Digestion. *Advances in Bioscience and Biotechnology*, **6**, 205-212
- Adiotomre, K.O. and Ukrakpor E.F. (2015). Production of biogas from kitchen waste and cow dung. *International journal of innovative scientific & engineering technologies research*, **3**(2), 52 – 64.
- Adriano, D.C. (1986). Trace Elements in the Terrestrial Environment. Springer-Verlag, New York, Berlin, Heidelberg, Tokyo, 99.
- Adubofuor J, Amankwah E.A, Arthur B.S and Appiah F. (2010). Comparative study related to physico-chemical properties and sensory qualities of tomato juice and cocktail

juice produced from oranges, tomatoes and carrots. *African Journal of Food Science*, **4**(7), 427-433.

Adubofuor, J., Amankwah, E.A., Arthur, B.S., and Appiah, F. (2010). Comparative study related to physic-chemical properties and sensory qualities of tomato juice produced from oranges, tomatoes and carrots. *African Journal of Food Science*, **4**(7), 427-433.

African Development Fund (2014): Last mile connectivity projects report Country: Kenya. Project Appraisal Report, 1 -29.

Agarwal A., Singhmar A., Kulshrestha M., and Mittal A. K. (2005). Municipal solid waste recycling and associated markets in Delhi, India. *Resources, Conservation and Recycling*, **44**(1), 73–90.

Aguilar, F.X. (2001) How to Install a Polyethylene Biogas Plant, In Integrated Bio-Systems Network, 1–10

Ahmed W. A, Aggour M., Naciri M. (2017). Biogas Control: Methane Production Monitoring Using Arduino. *International Scholarly and Scientific Research & Innovation* **11**(2), 130-133

Ahmed, W., Aggour, M., Naciri, M. (2017). Biogas Control: Methane Production Monitoring Using Arduino. *International Journal of Biotechnology and Bioengineering*, **11**(2), 130 – 133.

Akhras G. (2000). Smart Materials and Smart Systems for the Future, *Canadian Military Journal*, **1**(3), 25-32.

Al Seadi T, Rutz D, Prassl H, Köttner M, Finsterwalder T, Volk S, Janssen R. (2008). Biogas handbook, Esbjerg: University of Southern Denmark, 1-126

Al Seadi T. and Holm Nielsen J. (2004). Utilization of waste from food and agriculture: Solid waste: Assessment, Monitoring and Remediation. *Waste management series*, **4**, 735-754.

Alberty, R. A. (2003). Thermodynamics of Biochemical Reactions, John Wiley & Sons: New York, 54-98.

- Alduchov, O.A. and Eskridge, R.E. (1996). Improved Magnus form approximation of saturation vapor pressure. *Journal of Applied Meteorology*, **35**, 601-609.
- Alegbeleye O.O, Singleton A S and Sant'Ana. (2018). Sources and contamination routes of microbial pathogens to fresh produce during field cultivation: A review, *Food Microbiology*, **73**, 177 – 208.
- Alemayehu G. and Abile T. (2014). Co-Digestion of Ethiopian Food Waste with Cow Dung for Biogas Production. *International Journal of Research (IJR)*, **1(7)**, 475-500.
- Alemu M. T. and Tesfaye S. T (2019). Production and Evaluation of Biogas from Mixed Fruits and Vegetable Wastes Collected from Arba Minch Market. *American Journal of Applied Chemistry*, **7(6)**, 185-190.
- Ali, S., Shah, T. A., Afzal, A., and Tabassum, R. (2018). Exploring lignocellulosic biomass for bio-methane potential by anaerobic digestion and its economic feasibility. *Energy & Environment*, **29(5)**, 742–751.
- Alibardi, L., Cossu, R. (2016). Effects of carbohydrate, protein and lipid content of organic waste on hydrogen production and fermentation products. *Waste Management*, **47**, 69-77.
- Al-Juhaimi, F. Y., Hamad, S. H., Al-Ahaideb, I. S., Al-Otaibi, M. M., Ghafoor, K., Abbasi, T. and Abbasi, S. A. (2014). Biogas Production through the Anaerobic Digestion of Date Palm, *BioResources*, **9** (2), 3323-3333.
- Al-Kharousi Z.S, Guizani N, Al-Sadi A.M, Al-Bulushi I.M, and Shaharoon B. (2016). Hiding in Fresh Fruits and Vegetables: Opportunistic Pathogens May Cross Geographical Barriers, *International Journal of Microbiology*, 1-14.
- Ambar P, Endang S, Rochijan, Nanung A F, Yudistira S and Mochammad F. H. (2017). Potential test on utilization of cow's rumen fluid to increase biogas production rate and methane concentration in biogas. *Asian J. Anim. Sci.*, **11**, 82-87.
- Amend, J. P. and Shock, E. L. (2001). Energetics of overall metabolic reactions of thermophilic and hyperthermophilic Archaea and Bacteria. *FEMS Microbiol. Rev.*, **25**, 175-243.

Amon T., Amon B., Kryvoruchko V., Machmüller A., Hopfner-Sixt K., Bodiroza V. An, B.X., Rodriguez, L., Sarwatt, S.V., Preston, T.R., Dolberg, F. (1997). Installation and performance of low-cost polyethylene tube biodigesters on small-scale farms. *Rev. Mond. Zootech.*, **88**, 38–47.

Amon T., Amon B., Kryvoruchko V., Zollitsch W., Mayer K., Gruber L. (2007). Biogas production from maize and dairy cattle manure—Influence of biomass composition on the methane yield, *Agriculture, Ecosystems and Environment*, **118**, 173-182.

Amon, T., Amon B., Kryvoruchko V., Machmüller, A., Hopfner-Sixt, K., Bodiroza V., Hrbek, R., Friedel J., Pötsch E., Wagentristl H. (2007). Methane production through anaerobic digestion of various energy crops grown in sustainable crop rotations. *Bioresour. Technol.*, **98**, 3204–3212.

Amsaveni M, Anurupa A, Preetha A, Malarvizhi C, Gunasekaran M. (2015). GSM based LPG leakage detection and controlling system, *the International Journal of Engineering and Science (IJES)*, 112-116.

Anand, R.C.; Singh, R. (1993). A simple technique, charcoal coating around the digester, improves biogas production in winter. *Bioresour. Technol.*, **45**, 151–152.

Angelidaki, I. and Sanders, W. (2004). Assessment of the anaerobic biodegradability of macropollutants. *Re/Views in Environmental Science & Bio/Technology*, **3**(2), 117-129.

Angelidaki, I., Ellegaard, L. & Ahring, B. K. (1999). A comprehensive model of anaerobic bioconversion of complex substrates to biogas. *Biotechnology and Bioengineering*, **63**, 363-372.

Angelidaki, I., Ellegaard, L., & Ahring, B. K. (1993). A Mathematical Model for Dynamic Simulation of Anaerobic Digestion of Complex Substrates: Focusing on Ammonia Inhibition. *Biotechnology and Bioengineering (Print)*, **42**, 159-166.

Anjan, K.K. (1988). Development and evaluation of a fixed dome plug flow anaerobic digester. *Biomass*; **16**, 225–235.

Annor J, Adzitey F, Ansah T and Ampadu O.M (2018). Effect of Rumen Content to Water Ratio in Biogas Production, *J. Appl. Sci. Environ. Manage*, **22** (8), 1257 –1262.

Anusha & Shaik M. (2012). Detection of Gas Leak and Its Location Using Wireless Sensor, 1-8.

AOAC (1990). Official Methods of Analysis: Association of Analytical Chemists (14th Edn.). USA, 22209, 20-34.

AOAC (2000). Association of Official Analytical Chemists. Official Methods of Analysis, 5th edition, AOAC, Arlington, Virginia, USA, 807 – 809.

AOAC (2005). Official methods of analysis 18th ed. Arlington, V.A Association of Official Analytical Chemist, 806-842.

Arikan, O. A., Mulbry, W., & Lansing, S. (2015). Effect of temperature on methane a. production from field-scale anaerobic digesters treating dairy manure. *Waste Management*, **43**, 108-113.

Aritra D and Mondal C. (2015). Comparative Kinetic Study of Anaerobic Treatment of Thermally Pretreated Source-Sorted Organic Market Refuse, *Journal of Engineering*, **2015**, 1-15

Ariunbaatar J., Esposito G., Yeh D. H. and Lens P. N. L. (2016). Enhanced Anaerobic Digestion of Food Waste by Supplementing Trace Elements: Role of Selenium (VI) and Iron (II). *Frontiers in Environmental Science*, **4**(8), 1-11.

Arthur G. and John H. (2006). Digestion of the Various Foods by Hydrolysis, in Textbook of Medical Physiology, edited by Anonymous 11th ed. (Elsevier Saunders, Philadelphia, PA, 808.

Asensio Y, Fernandez-Marchante, C M, Lobato J, Canizares P, Rodrigo M A. (2016). Influence of the fuel and dosage on the performance of double compartment microbial fuel cells. *Water Res*, **99**, 6-23.

Asensio, Y., Fernandez-Marchante, C.M., Lobato, J., Canizares, P. and Rodrigo, M.A. (2016). Influence of the Fuel and Dosage on the Performance of Double Compartment Microbial Fuel Cells. *Water Research*, **99**, 16-23.

- Asibey-Berko, E. & Tayie F.A.K. (1999). Proximate analysis of some underutilized Ghanaian Vegetables. *Ghana J. Sci.*, **39**, 91-92.
- Asmita V, Prabhakar S, Kayalvizh I (2018). Gas Leakage Detection and Smart Alerting and Prediction Using IoT. *International Journal of Innovative Research & Studies*, **8**(2), 294-298.
- Asquer C., Pistis A, Scano E.A. (2013). Characterization of Fruit and Vegetable Wastes as A Single Substrate for The Anaerobic Digestion, *Environmental Engineering and Management Journal*, **12**(11), 89-92.
- ASTM D(1989). Standards method of proximate analysis of coal and coke, in gaseous fuels; coal and coke section 5, 05.05, Annual book of ASTM standards, **299**(84), 3172-73
- Atkinson H. J., Giles G. R. And Desjardins J. G. (1958). Effect of Farmyard Manure On the Trace Element Content of Soils and of Plants Grown Thereon, *Plant and Soil*, **10**(1), 32-36.
- Aurora, S.P. (1983). Microbial Digestion in Ruminants. Indian Council of Agricultural Research, New Delhi, 1-9.
- B.P (2019). B.P energy Outlook 2019 Edition Report, 56-67.
- Babel S, Fukushi K, Sitanrassamee B. (2004). Effect of acid speciation on solid waste liquefaction in an anaerobic acid digester. *Water Res.*, **38**(9), 2416-22.
- Balasubramaniyam U, Zisengwe LS, Meriggi N, Buysman E. (2008). Biogas production in climates with long cold winters. Wageningen, Wageningen University, 6-67.
- Balch, W.E., Schoberth, S., Tanner, R.S., Wolfe, R.S. (1977). Acetobacterium, a new genus of hydrogen oxidizing, carbon Dioxide-Reducing, Anaerobic Bacteria. *International Journal of Systemic Bacteriology*, **27**, 355-361.
- Banks, C.J., Heaven, S., Zhang, Y. and Baier, U. (2018). Food waste digestion: Anaerobic Digestion of Food Waste for a Circular Economy. Murphy, J.D. (Ed.) IEA Bioenergy Task 37, 12.

- Bansal A.K, Kapoor S and Agrawal Mayank K (2013). The road to zero waste: anaerobic digester. *Int J Environ Sci* **3**(5), 0976–4402.
- Bard, A. J, Parsons R and Jordan, J. (1985). Eds. Standard Potentials in Aqueous Solution; Marcel Dekker: New York, 34-89.
- Bardiya, N. &Gaur, A. (1997). Effects of carbon and nitrogen ratio on rice straw biomethanation. *J. Rural Energy* **4**, 1–16.
- Baserga, U. (1998). Landwirtschaftliche Co-Vergärungs-Biogasanlagen. FAT-Berichte Nr. 512, Eidg. Forschungsanstalt für Agrarwirtschaft und Landtechnik, Tänikon, Schweiz, 1-11.
- Baserja, U. (1984). Biogas production from cowdung: Influence of time and fresh liquid manure. *Swiss-Bio Tech.*, **2**, 19-24.
- Batstone, D. J., Keller, J., Angelidaki, I., Kalyuzhnyi, S. V., Rozzi, A., Sanders, W. T. M., Siegrist, H. & Vavilin, V. A. (2002). Anaerobic Digestion Model No. 1 (ADM1), 65-77.
- Bavutti M, Guidetti L, Allesina G, Libbra A, Muscio A, Pedrazzi S. (2014). Thermal stabilization of digester of biogas plants by means of optimization of the surface radiative properties of the gasometer domes. *Energy Procedia* **45**, 1344–1353
- Beede D. N. and Bloom D. E. (1995). the economics of municipal solid waste, *The World Bank Research Observer* **10**, 113-150.
- Bernd B., Georg H. and Klaus M. (1997). Waste Management. Springer, Berlin, ISBN: 3-540-59210-5, 127-257
- Bharati S. S and Shinkar N. P. (2014). Kinetic Modeling for Anaerobic Digestion: A Review, *International Journal of Civil Engineering and Technology (IJCIET)*, **5**(2), 127-136
- Bharti S. and Maneesha S. (2015). Isolation and characterization of bacteria from cow dung of desi cow breed on different morpho-biochemical parameters in Dehradun,

Uttarakhand, India, *International journal of advances in pharmacy, biology and chemistry* **4**(2), 276-281.

Biffinger J.C, Fitzgerald L.A, Ray R. (2011). The utility of *Shewanella japonica* for microbial fuel cells. *Bioresour Technol*; **102**(1), 290-7.

Biffinger J.C, Pietron J, Bretschger O, (2008). The influence of acidity on microbial fuel cells containing *Shewanella oneidensis*. *Biosens Bioelectron*; **24**(4), 906-11.

Biffinger, Justin C. and Ringeisen, Bradley R. (2008). Engineering Microbial Fuels Cells: *Recent Patents on Biotechnology*, **2**, 150-155.

Bilitewski B, Härdtle G, Marek K, Weissbach A and Boeddicker H. (1997). Waste management. Springer-Verlag, Berlin, Heidelberg, Germany, 259 -338.

Bioactive physic-chemical properties and sensory qualities of tomato juice produced from Biogas (2007). Retrospect and prospects Georgia. Rural Energy Program, USAID, Washington, DC, 1-50.

Biswas, J., Chowdhury, R., Bhattacharya P. (2006). Kinetic studies of biogas generation using municipal waste as feed stock, *Enzyme and Microbial Technology*, **38**(3-4), 493-503.

Biswas, J., Chowdhury, R., Bhattacharya P. (2007). Mathematical modeling for the prediction of biogas generation characteristics of an anaerobic digester based on food/vegetable residues. *Biomass Bioenergy*, **31**, 80–86.

Blackburn, T.H. and Hobson, P.N. (1960). Isolation of Proteolytic Bacteria from the Sheep Rumen, *J. gen. Microbiol*, **22**, 282-289.

Bochmann, G. and Montgomery, L.F.R. (2013). Storage and pre-treatment of substrates for biogas production. In: *The Biogas Handbook: Science, Production and Applications*. Elsevier Inc., 85-103.

Bond T, Templeton M.R. (2011). History and future of domestic biogas plants in the developing world. *Energy Sustain Dev*, **15**, 347–354.

- Bouallagui H, Cheikh B. R, Marouani L, Hamdi M. (2003). Mesophilic biogas production from fruit and vegetable waste in a tubular digester. *Biores Technol*, **86**,85–89.
- Bouallagui, H.; Ben Cheikh, R.; Marouani, L.; Hamdi, M. (2003). Mesophilic biogas production from fruit and vegetable waste in a tubular digester. *Bioresour. Technol.*, **86**, 85–89.
- Boyle, W. C. (1977). Energy Recovery from Sanitary Landfills. In: *Microbial Energy Conversion*. Edited by: H. G. Schlegel & J. Barnea: 119 – 138
- Bożym M., Floozak I., Zalanowska P., Wojdalski J., Klimkiewicz M. (2015). An analysis of metal concentrations in food wastes for biogas production. *Renewable Energy*, **77**, 467-472.
- Brandli, R.C., Kupper, T., Bucheli, T.D., Zennegg, M., Huber, S., Ortelli, D., Muller, J., Schaffner, C., Iozza, S., Schmid, P., Berger, U., Edder, P., Oehme, M., Stadelmann, F.X., Tarradellas, J. (2007). Organic pollutants in Swiss compost and digestate; Part 2. polychlorinated dibenzo-p-dioxins, and -furans, dioxin-like polychlorinated biphenyls, brominated flame retardants, perfluorinated alkyl substances, pesticides, and other compounds. *J. Environ. Monit.* **9**, 465-472.
- Bruce L, Bert H, Rene R, Uwe S, Jurg K, Stefano R, Peter A, Willy V and Korneel R (2006), microbial fuel cells: methodology and technology, *environmental science & technology*, **40**(17), 5181 – 5192.
- Bryant M. P., McBride B. C., and Wolfe. R. S. (1968). Hydrogen-oxidizing methane bacteria. I. Cultivation and methanogenesis. *J. Bacteriol.* **95**, 118-1123.
- Budiyono I, Widiassa N, Johari S. and Sunarso. (2011). Study on Slaughterhouse Wastes Potency and Characteristic for Biogas Production. *Internat. J. of Waste Resources*, **1**(2), 4-7.
- Budiyono, I.N. Widiassa, Seno Johari and Sunarso. (2010). Increasing Biogas Production Rate from Cattle Manure Using Rumen Fluid as Inoculums. *International Journal of Basic & Applied Sciences* **10**, 41-47.

- Budiyono, Widiyasa, I.N., Johari, S. and Sunarso. (2014). Increasing Biogas Production Rate from Cattle Manure Using Rumen Fluid as Inoculums. *International Journal of Science and Engineering*, **6**(1), 31-38.
- Burade A And. Bhagat M.S. (2016). Generation of Biogas from Vegetable Leftovers. *International Journal of Innovative Research in Science, Engineering and Technology*, **6**(2), 2513-2521.
- Buren, A.V. (1979). A Chinese Biogas Manual; Intermediate Technology Publications: Rugby, UK, 23-78.
- Buswell A.M and Mueller H.F. (1952). Mechanism of fermentation. *Ind Eng Chem*, **44**, 2441–2460.
- Buswell, A. M. and Mueller, H. F. (1952). Mechanism of Methane Fermentation, *Industrial and Engineering Chemistry*, **44**(3), 550 – 552
- Buyuksonmez, F., Rynk, R., Hess, T.F., Bechinski, E. (2000). Occurrence, degradation and fate of pesticides during composting Part II: Occurrence and fate of pesticides in compost and composting systems. *Compost Sci. Util*, **8**, 61-81.
- Callaghan, F., Wase, D., Thayanythy, K. and Forster, C. (2002). Continuous co-digestion of cattle slurry with fruit and vegetable wastes and chicken manure. *Biomass Bioenergy*, **22**, 71–77.
- Cao Y, Mu H, Liu W, Zhang R, Guo J, Xian M and Liu H. (2019). Electricigens in the anode of microbial fuel cells: pure cultures versus mixed communities, *Microb Cell Fact*, **18**(39), 1-14
- Carmela V and Ana I. (2017). Smart gas detection system, Institute of Electrical and Electronics, 1-10
- Carneiro J.S, Nogueira R.M, Martins M.A, Valladãod. M, Pires E.M. (2018). The Oven-Drying Method for Determination of Water Content in Brazil Nut, *Bioscience Journal* **34**(3), 595-602
- Castillo E, Cristancho D, Arellano V. (2006). Study of the operational conditions for anaerobic digestion of urban solid wastes. *Waste Manage*, **26**(5), 546-56.

- Catal T, Shoutao X, Kaichang L, Hakan B, Hong L, (2008). Electricity production from polyalcohols in single-chamber microbial fuel cells. *Biosens. Bioelectron.* **24**, 855–860.
- Cavinato, C., Fatone, F., Bolzonella, D., Pavan, P. (2010). Thermophilic anaerobic co-digestion of cattle manure with agro-wastes and energy crops: Comparison of pilot and full scale experiences. *Bioresour. Technol.*, **101**, 545–550.
- Chae K J, Choi M J, Lee J W, Kim K Y, Kim, I S. (2009). Effect of different substrates on the performance, bacterial diversity, and bacterial viability in microbial fuel cells. *Bioresour. Technol*, **100**, 3518-3525.
- Chae, K. J., Jang, A., Yim, S. K., & Kim, I. S. (2008). The effects of digestion temperature and temperature shock on the biogas yields from the mesophilic anaerobic digestion of swine manure. *Bioresource Technology*, **99**, 1-6.
- Chae, K.J., Choi, M.J., Lee, J.W., Kim, K.Y. and Kim, I.S. (2009). Effect of Different Substrates on the Performance, Bacterial Diversity, and Bacterial Viability in Microbial Fuel Cells. *Bioresource Technology*, **100**, 3518-3525.
- Chandra R, Takeuchi H and Hasegawa T (2012). Methane production from lignocellulosic agricultural crop wastes: a review in context to second generation of biofuel production. *Renew Sustain Energ Rev*; **16**: 1462–1476.
- Chang, S.K.C., Zhang, Y. (2017). Protein analysis. Ch. 18, in Food Analysis, 5th ed. S.S. Nielsen (Ed.), Springer, New York, 255-386.
- Chaudhry A.S (2008). Slaughtered cattle as a source of rumen fluid to evaluate supplements for *in vitro* degradation of grass nuts and barley straw. *The Open Veterinary Science Journal*, **2**, 16 – 22.
- Chaudhuri S.K and Lovley D.R. (2003). Electricity generation by direct oxidation of glucose in mediator less microbial fuel cells. *Nat Biotechnol*, **21**, 1229–32.
- Chen H, Zheng P, Xie Z. (2014). Principle, components and performance of Shewanella fuel cell. *Environ Sci Technol*, **37**(10), 37-41.

- Chen, Y., Ke, Z., and Liang, Y. (2019). Influence of moisture content of solid-state NaOH pretreatment and co-digestion on methane production in the semi-dry anaerobic digestion of rose stalk. *BioRes*, **14**(2), 4210-4223.
- Chenamani S. (2018). Analysis of Abattoir Waste for Biogas Production in Kumasi Ghana. *Energy Resources Assessment*, 50 – 65.
- Chinwendu S, Chibueze U and Esihe Tochukwu E. (2013). Anaerobic Digester Considerations of Animal Waste. *American Journal of Biochemistry*, **3**(4), 93-96
- Chudoba P, Chevalier J.J, Chang J and Capdeville B. (1991). Effect of anaerobic stabilization of activated sludge on its production under batch conditions at various S(o)/X(o) ratios. *Water Sci Technol*, **23**, 917–926
- Chynoweth D.P, Turick C.E, Owens J.M, Jerger D.E and Peck M.W. (1993). Biochemical methane potential of biomass and waste feedstocks. *Biomass Bioenergy* **5**, 95–111.
- Chynoweth, D.P., Owens, J.M., Legrand, R. (2001). Renewable methane from anaerobic digestion of biomass. *Renew. Energy*, **22**,1–8.
- Converti I, Del Borghi A, Zilli M, Arni S, Del Borghi M. (1999). Anaerobic digestion of the vegetable fraction of municipal refuses: Mesophilic versus Thermophilic conditions. *Bioprocess Biosyst. Eng.*, **21**(4), 371-6.
- Cook E. J., (1986). Anaerobic sludge digestion: Manual of practice Alexandria VA: Water pollution control federation. *Task force on Sludge stabilization*, **16**. 158-165.
- Cu T. T. T., Pham H. C., Le T. H., Nguyen V. C, Le X. A, Nguyen X. T, and Sommer S. G. (2012). Manure management practices on biogas and non-biogas pig farms in developing countries - using livestock farms in Vietnam as an example. *J. Clean. Prod.* **27**, 64-71.
- Cuellar A.D, Webber M.E. (2008). Cow power: the energy and emissions benefits of converting manure to biogas. *Environ Res Lett*, **3**(3), 1748–9326

- Cuetos M.J, Fernandez C., Gomez X, Moran A. (2011). Anaerobic co-digestion of swine manure with energy crop residues. *Biotechnol Bioprocess Eng*, **16**, 1044–1052
- Culhane T. H. (2013). Biogas Digester, Tamera - Peace Research Center, 123-126.
- Cun-fang Liu, (2008). Prediction of Methane Yield at Optimum pH for Anaerobic digestion of Organic Fraction of Municipal Solid Waste. *Bioresource Technology*, **99** (4), 882-888
- Dahiya, A.K. and Vasudevan P. (1985). Biogas plant slurry as an alternative to chemical fertilizers. In: *Biomass* **9**, 67 – 74.
- Damisa, D., Ameh, J. B. and Umoh, V. J. (2008). Effect of chemical pretreatment of some lignocellulosic wastes on the recovery of cellulose from aspergillus niger AH3 mutant. *African Journal of Biotechnology*, **7**(14), 2444-2450.
- Daniyan, I. A., Daniyan, O. L., Abiona, O. H., Mpofo, K. (2019). Development and Optimization of a Smart System for the Production of Biogas using Poultry and Pig Dung. *Procedia Manufacturing*, **35**, 1190–1195.
- Das A. and Mondal C. (2016). Biogas Production from Co-digestion of Substrates: A Review. *International Research Journal of Environment Science*, **5**(1), 49-57
- Debnath, G., Jain, M.C., Kumar, S., Sarkar K., and Sinha S.K. (1996). Methane emissions from rice fields amended with biogas slurry and farm yard manure. *climate change*, **33**, 97-109.
- Deepanraj B, Sivasubramanian V, Jayaraj S. (2015). Experimental and kinetic study on anaerobic digestion of food waste: The effect of total solids and pH. *Journal of Renewable and Sustainable Energy*, **7**, 063-104.
- Demirel, B. and Scherer, P. (2008). The Roles of Acetotrophic and Hydrogenotrophic Methanogens during Anaerobic Conversion of Biomass to Methane: A Review. *Reviews on Environmental Science and Biotechnology*, **7**, 173-190.
- Deressa L, Libsu S, Chavan R. B., Manaye D, Dabassa A. (2015). Production of Biogas from Fruit and Vegetable Wastes Mixed with Different Wastes. *Environment and Ecology Research*, **3**(3), 65-71

- Devlin D.C, Esteves S.R.R, Dinsdale R.M, Guwy A.J. (2011). The effect of acid pretreatment on the anaerobic digestion and dewatering of waste activated sludge. *Bioresource Technology*, **102**, 4076-4082.
- Dewan A., Beyenal H. and Lewandowski Z. (2008). Scaling up microbial fuel cells. *Environ. Sci. Technol*, **42**(20),7643–7648.
- Dhont J and Berghe V.E. (2003). Analytical Techniques in Aquaculture Research, 1-36
- Dieter D. and Angelika S. (2008). Biogas from Waste and Renewable Resources; an Introduction: 42 - 430.
- Dioha I. J., Ikeme C.H., Nafi’u T., Soba N. I. and Yusuf M.B.S, (2013). Effect of Carbon to Nitrogen Ratio On Biogas Production. *International Research Journal of Natural Sciences*, **1**(3), 1 -10.
- Dioha I. J., Ikeme C.H., Nafi’u T., Soba N. I. and Yusuf M.B.S. (2013). Effect of Carbon to Nitrogen Ratio On Biogas Production, *International Research Journal of Natural Sciences*, **1**(3), 1 -10.
- Divyang R.S, Hemant J. N and Pradeep A. (2016). Purification of Biogas using Chemical Scrubbing and Application of Purified Biogas as Fuel for Automotive Engines. *Research Journal of Recent Sciences*, **5**, 1-6.
- Doan J. (2009). Biogas projects in Australia: commercial applications and preliminary project risk assessment. 1–5.
- Dobre P, Nicolae F and Matei F. (2014). Main factors affecting biogas production - an overview. *Romanian Biotechnological Letters*,**19** (3), 9283-9296.
- Dobre, P., Farcaș, N., Găgeanu I. (2009). The influence of temperature on the organic substratum in the production of biogas. - *Lucrări Științifice INMATEH*, NR. 27, București.
- Dokulilová, T., Koutny, T., & Vitez, T. (2018). Effect of Zinc and Copper on Anaerobic Stabilization of Sewage Sludge. *Acta Universitatis Agriculturae et Silviculturae Mendelianae Brunensis*, **66**, 357-363.

- EAP. (2014). A Guide to Air Quality and Your Health, U.S. Environmental Protection Agency Office of Air Quality Planning and Standards Outreach and Information Division Research Triangle Park, NC, 1-232.
- EAP_a. (2015). Air Quality Guide for Ozone, Office of Air Quality and Radiation (6301A) EPA-456/F-15-006, 143-150.
- EAP_b. (2015). Air Quality Guide for Particle Pollution, Office of Air Quality and Radiation (6301A) EPA-456/F-15-005, 136.
- Ejigu, F. (2010). Bio slurry in Ethiopia: What it is and How to Use It. NBPE & ISD. Addis Ababa, 1-20.
- El-Mashad, H.M. & Zhang, R. (2010). Biogas production from co-digestion of dairy manure and food waste. *Bioresour. Technol.*, **101**, 4021–4028.
- EnDev (2012). Dynamic market for cooking devices in Kenya. Energizing Development, Germany. Ministry of Energy, Kenya, 1-23.
- Energy technology developments beyond 2020 for the transition to a decarbonized European energy system by 2050. (2013). European Commission, Brussels, 45-50
- Eskicioglu C, Kennedy K. J and Droste R L. (2007). Enhancement of batch waste activated sludge digestion by microwave pretreatment. *Water Environment Research.*, **79**, 2304-2317.
- Eskicioglu C, Kennedy K.J, Droste R. L. (2007). Enhancement of batch waste activated sludge digestion by microwave pretreatment. *Water Environ Res*, **79**(11), 2304-17
- European Parliament (2017). Report on initiative on resource efficiency: reducing food waste, improving food safety (2016/2223(INI)), 28 April 2017.
- Ezekoye V.A and Ezekoye B.A. (2009). Characterization and storage of biogas produced from the anaerobic digestion of cowdung, spent grains/cow dung and cassava peels/rice husk, *The Pacific Journal of Science and Technology*, **10**(2), 898-904

- Ezekoye, V.A.; Okeke, C.E. (2006). Design, construction, and performance evaluation of plastic biodigester and the storage of biogas. *Pac. J. Sci. Technol.*, **7**, 176–184.
- Falohun A.S., Oke A.O., Abolaji B.M. (2016). Dangerous Gas Detection using an Integrated Circuit and MQ-9. *International Journal of Computer Applications*, **135** (7), 30-34.
- Fan, Y. Z., Sharbrough E. (2008). Quantification of the Internal Resistance Distribution of Microbial Fuel Cells." *Environmental Science & Technology*, **42** (21), 8101-8107.
- FAO. (1986). Food analysis general techniques, additives, contaminants and composition, Manuals of Food Quality Control, Food and Nutrition Paper 14/7.
- FAO. (2011). Global Food Losses and Food Waste: Extent, Causes and Prevention; 1-26.
- FAO. (2012). Towards the Future we want: End Hunger and Make the Transition to Sustainable Agricultural and Food Systems, Food and Agriculture Organization of the United Nations Rome, 17-25.
- FAOSTAT. (2019). Tomato production in 2018, Crops/Regions/World list/Production Quantity (pick lists)"*UN Food and Agriculture Organization, Corporate Statistical Database (FAOSTAT)*. Retrieved 18 June 2020, 34-91.
- Fapetu S, Keshavarz T, Clements M, Kyazze G. (2016). Contribution of direct electron transfer mechanisms to overall electron transfer in microbial fuel cells utilizing *Shewanella oneidensis* as biocatalyst. *Biotechnol Lett*, **38**(9), 1465-73.
- Faridullah F, Pervaiz A, Irshad M, Alam A, Mahmood Q and Ashraf M. (2014). Trace elements characterization in fresh and composted livestock manures. *The Journal of Hydrology* **1**, 1–6.
- Ferrer I., Garfí, M. Uggetti, E., Ferrer-Martí L., Calderon, A., Velo E. (2011). Biogas production in low-cost household digesters at the Peruvian Andes. *Biomass Bioenergy*, **35**, 1668–1674.

- Ferrer, I., Gamiz, M., Almeida, M., Ruiz, A. (2009). Pilot project of biogas production from pig manure and urine mixture at ambient temperature in Ventanilla (Lima, Peru). *Waste Manag. (Oxf.)*, **29**, 168–173.
- Ferry, J.G., Smith, P.H., Wolfe, R.S. (1974). Methanospirillum, a New Genus of Methanogenic Bacteria, and Characterization of *Methanospirillum hungatii sp.nov.* *International Journal of Systematic Bacteriology*, **24**, 465-469.
- Forst C. (2002). Technologies demonstrated at echo: horizontal biogas digester, 1-4.
- Forster-Carneiro T, Perez M, Romero L.I. (2008). Anaerobic digestion of municipal solid wastes: Dry thermophilic performance, *Bioresource Technology*, **99**, 8180-8184
- Frazier, W.C., and Westhoff, D.C. (1995). Food Microbiology. 4th ed. New Delhi: Tata McGraw-Hill publishing Company Limited, 384-96.
- Frey J, Pell A, Barthiaume R, Lapierre H, Lee S, Ha J, Mendell J & Angert E. (2009). Comparative studies of microbial populations in the rumen, duodenum, ileum and faeces of lactating dairy cows. *Appl Environ Microbiol*, **75**, 2598-2602.
- Gagandeep K, Yadwinder.S.B. and. Kothari, D.P. (2017). Isolation and Identification of Bacteria's from Cattle Dung used in Microbial Fuel Cells to Generate Bioelectricity. *International Refereed Journal of Reviews and Research*, **5**(6), 2348 – 2001.
- Gagandeep K. (2017). Isolation and Identification of Bacteria's from Cattle Dung used in Microbial Fuel Cells to Generate Bioelectricity. *International Refereed Journal of Reviews and Research*, **5**(6), 1-18
- Gammaa A.M. O, Hajo E. E and Amro B. H. (2015). Effect of cow rumen fluid concentration on biogas production from goat manure. *Sudanese Journal of Agricultural Sciences*, **2**, 1 – 7.
- Garba B., Atiku A.T. and Aliyu M. (1998). Proceedings of the World Renewable Energy Congress V. 20-25 September 1998, Florence, Italy, Part III, (Edited by A.A.M. Sayigh).

- Garfí, M., Ferrer-Martí, L., Perez, I., Flotats, X., Ferrer I. (2011). Codigestion of cow and guinea pig manure in low-cost tubular digesters at high altitude. *Ecol. Eng.*, **37**, 2066–2070.
- Garfí, M., Gelman, P., Comas, J., Carrasco, W., Ferrer, I. (2011). Agricultural reuse of the digestate from low-cost tubular digesters in rural Andean communities. *Waste Manag. (Oxf.)*, **31**, 2584–2589.
- Gelegenis, J., Georgakakis, D., Angelidaki, I., Mavris, V. (2007). Optimization of biogas production by co-digesting whey with diluted poultry manure. *Renew. Energy*, **32**, 2147–2160.
- Gene F. P. (1986). Fundamentals of anaerobic, *Environmental Engineering*, **112**: 867-920.
- Gerardi, M.H. (2003). The microbiology of anaerobic digesters., Canada: John Wiley & Sons, Inc, 59-117
- Gerardi, M.H. (2003). The Microbiology of Anaerobic Digesters; John Wiley & Sons, Inc.: Hoboken, NJ, USA, 59-117.
- Ghangrekar M.M, Shinde V.B. (2007). Performance of membrane-less microbial fuel cell treating wastewater and effect of electrode distance and area on electricity production. *Bioresour Technol* **98**(15), 2879–2885
- Ghatak M. D. and Mahanta P. (2014). Comparison of kinetic models for biogas production rate from sawdust. *International Journal of Research in Engineering and Technology*, **3**(7), 248–254.
- Ghoreyshi A.A., Jafary T., Najafpour G.D., Haghparast F. (2011). Effect of type and concentration of substrate on power generation in a dual chambered microbial fuel cell. *World Renewable Energy Congress*, 1174-1181.
- Gil, A., Siles, A.J., Serrano, A., Chica, A., Martín, M. (2018). Effect of variation in the C/[N+P] ratio on anaerobic digestion. *Environ. Prog. Sustain. Energy*, **38**, 228–236.

- Gislason, E.A., Craig, N.C. (2005). Cementing the foundations of thermodynamics: comparison of system-based and surroundings-based definitions of work and heat. *J. Chem. Thermodynamics* **37**, 954-966.
- Githiomi J.M., Oduor N.M. (2012). Strategies for Sustainable Wood Fuel Production in Kenya. *International Journal of Applied Technology*, **2**, 103-110.
- González I. and Calderon A.J. (2018). Measurement System Based on Arduino for Biogas Sensing: Development Considerations and Laboratory Scale Approach, *International Journal on Advances in Systems and Measurements*, **11**(1 & 2), 93-99
- Gopinath, L.R., Merlin Christy P., Mahesh K., Bhuvaneshwari R., Divya D. (2014). Identification and Evaluation of Effective Bacterial Consortia for Efficient Biogas Production, *IOSR Journal of Environmental Science, Toxicology and Food Technology (IOSR-JESTFT)*, **8**(3), 80-86.
- Gorby Y.A, Yanina S., McLean J.S. (2006). Electrically conductive bacterial nanowires produced by *Shewanella oneidensis* strain MR-1 and other microorganisms. *Proc Natl Acad Sci USA*, **103**(30), 11358-63.
- Goto, Y. and Yoshida, N. (2019). Scaling up Microbial Fuel Cells for Treating Swine Wastewater. *Water*, **11**, 1803.
- Graunke, R. (2007). Converting Food Waste to Biogas: Sustainable Gator Dining. *Sustainability*, **1**(6), 391-394
- Griffin, M.E., McMahon, K.D., Mackie, R.I., Raskin, L. (1998). Methanogenic population dynamics during start-up of anaerobic digesters treating municipal solid waste and biosolids. *Biotechnol. Bioeng.*, **57**, 342–355.
- Groot, L. and A. Bogdanski. (2013). Bioslurry Brown Gold? A review of scientific literature on the co-product of biogas production. *Environment and Natural Resources Series*. FAO, Rome, Italy:32.
- GTZ. (2007). Eastern Africa Resource Base: GTZ Online Regional Energy Resource Base: Regional and Country Specific Energy Resource Database: IV - Energy Policy: 1-36.

- GTZ. (2009). Bernard Mutiso Osawa, Country Chapter: Kenya. In Renewable Energies in East Africa Regional Report, 56-78
- Guarino G., Carotenuto C., Di Cristofaro F., Papa S., Morrone B., Minale M., (2016). Does the c/n ration really affect the biomethane yield? A three years' investigation of buffalo manure digestion. *Chemical Engineering Transactions*, **49**, 463-468
- Gurung, B. (1998). Training programme on proper use of slurry for the technical staff of SNV/BSP. A training manual, 1-25
- Gustavsson, J., Cederberg, C., Sonesson, U. and Van Otterdijk, R., Meybeck, (2011). A Global Food Losses and Food Waste. Food and Agricultural Organization of the United Nations, 76.
- Gustavsson, J., Cederberg, C., Sonesson, U., Otterdijk, R.V. and Meybeck, A. (2011). Global food losses and food waste: extent, causes and prevention, 20-65
- Hagegard K. (2009). Small-scale biogas by Lake Victoria. Analyzing and implementing the biogas technology for cooking in rural African households, 13-25
- Hamad, M.A., Abdel Dayem, A.M., El Halwagi, M.M. (1981). Evaluation of the performance of two rural biogas units of Indian and Chinese design. *Energy Agric.*, **1**, 235–250.
- Han T.H, Cho M.H and Lee J. (2014). Indole oxidation enhances electricity production in an E. coli-catalyzed microbial fuel cell. *Biotechnol Bioproc E*, **19**, 126-31.
- Hansen K.H, Angelidaki I, Ahring B.K. (1998). Anaerobic digestion of swine manure: Inhibition by ammonia. *Water Res*, **32**, 5–12.
- Hiegemann H., Herzer D., Nettmann E., Lubken M., Schulte P., Schmelz K.G., Gredigk-Hoffmann S., Wichern M. (2016). An integrated 45 L pilot microbial fuel cell system at a full-scale wastewater treatment plant, *Bioresour. Technol.*, **218**, 115-122.
- Hoboken, N. J. (2005). Impedance spectroscopy: theory, experiment, and applications. New York, 13-19.

- Hobson, P. N., Bousfield, S. & Summers, R. (1981). Methane production from agricultural and domestic wastes. Applied Science Publishers Ltd, London, 181-217.
- Hoerz T, Kramer P, Klingler B, Kellner C, Wittur T, Klopotek FV, Krieg A, Euler H. (2008). Biogas digest, vol II. Biogas—application and product development. Inf Advisory Serv Approp Technol, 1-81.
- Holm – Nielsen, J.B., Seadi, J. A., and Oleskowicz – Popiel, P. (2009). The future of anaerobic digestion and biogas utilization. In: *Bioresource Technology* **100**, 5478 – 5484.
- Hossain, M.E., Jahangir A., M., Hakim, M.A., Amanullah, A.S.M. & Ahsanullah, A.S.M. Hossain, M.E., JahangirAlam, M., Hakim, M.A., Amanullah, A.S.M., and Ahsanullah, A.S.M. (2010). An assessment of physicochemical properties of some tomato genotypes and varieties grown at Rangpur. *Bangladesh Research Publications Journal*, **4**(3), 235-243
- Hrbek R., Friedel J., Pötsch, E., Wagentristsl, H., Schreiner, M., Zollitsch, W., Pötsch, Istok J.D. (2013). Push-pull tests for site characterization. In: Lecture notes in earth system sciences, **444**. Springer, Berlin, 1-56
- Huang, L., Gan, L., Wang, N., Quan, X., Logan, B. E., & Chen, G. (2012). Mineralization of pentachlorophenol with enhanced degradation and power generation from air cathode microbial fuel cells. *Biotechnology and Bioengineering*, **109**(9), 2211-2221.
- Ieropoulos I. A., Greenman J., Melhuish C. and Hart J., (2006). Comparative study of three types of microbial fuel cell, *Enzyme Microb Tech*, **37**, 238–245.
- ISAT/GTZ (1999). Biogas Digest Volume II. Biogas - Application and Product Development, In-formation and Advisory Service on Appropriate Technology (ISAT), Deutsche Ge-sellschaft für Technische Zusammenarbeit (GTZ), 1-81
- Isong, E.U., S.A.R. Adewusi, E.U. Nkanga, E.E. Umoh and E.E. Offiong. (1999). Nutritional and phytochemical studies of three varieties of *Gnetum africanum* (afang). *Food Chem.* **64**, 489-493.
- Jash, T. and Ghosh, D.N. (1990). Studies on residence time distribution in cylindrical and rectangular biogas digesters. *Energy*, **15**, 987–991.

- Javid H, Najeeb U. R., Abdul L., Muhammad H., Murtaza H., Zabta K. S. (2010). Proximate and essential nutrients evaluation of selected vegetables species from kohat region, pakistan, *Pak. J. Bot.*, **42**(4), 2847-2855
- Jayaraj S., Deepanraj B. and Sivasubramanian V. (2014). Study On the Effect of pH On Biogas Production from Food Waste by Anaerobic Digestion, the 9th International Green Energy Conference, 799-805.
- Jeptoo, A., Aguyoh, J. N. and Saidi, M. (2012). Improving Carrot Yield and Quality through the Use of Bio-slurry Manure. *Sustainable Agriculture Research* **2**(1), 1-6
- Jha A. K., Li J., Zhang L., Ban Q., and Jin Y. (2013). Comparison between Wet and Dry Anaerobic Digestions of Cow Dung under Mesophilic and Thermophilic Conditions, *Advances in Water Resource and Protection.*, **1**(2), 28-38
- Jia J, Tang Y, Liu B, Wu D, Ren N, Xing D. (2013). Electricity generation from food wastes and microbial community structure in microbial fuel cells. *Bioresour. technology*, **144**, 94–99.
- Jiang, Y. B., Zhong W.H, Deng H, Han C. (2016). Characterization of Electricity Generated by Soil in Microbial Fuel Cells and the Isolation of Soil Source Exo-electrogenic Bacteria. *Frontiers of Microbiology*, **7**, 1776.
- Joanna M. L and Barbano D. M. (1999). Kjeldahl Nitrogen Analysis as a Reference Method for Protein Determination in Dairy Products. *Journal of AOAC International*, **82**(6), 1389-1402.
- Kalambe S, Sapkal RS, Sapkal V.S. (2012). Low pressure separation technique of biogas into CH₄ and CO₂ employing PDMS membrane. *IJAET* **3**(1), 311–315
- Kalia, A. and Gupta R. P. (2006). Fruit Microbiology, in Handbook of Fruits and Fruit Processing, Y.H. Hui, Editor. 2006, Blackwell Publishing: Iowa, U.S.A., 4.
- Kalia, A.K.; Kanwar, S.S. (1998). Long-term evaluation of a fixed dome Janata biogas plant in hilly conditions. *Bioresour. Technol.*, **65**, 61–63.

- Kamau J. M, Mbui D. N, Mwaniki J. M, Mwaura F. B. (2020). Lab scale biogas production from market wastes and Dagoretti slaughterhouse waste in Kenya. *International Journal of Energy and Environmental Research*, **8** (1),12-21.
- Kamau J.M, Mbui D.N, Mwaniki J.M, Mwaura F.B, Kamau G.N. (2017). Microbial Fuel Cells: Influence of External Resistors on Power, Current and Power Density. *J Thermodyn Catal* **8**, 182.
- Kamau J.M, Mbui D.N, Mwaniki J.M, Mwaura F.B. (2017). Cow Dung to Kilo Watt using Double Chamber Microbial Fuel Cell. *Engineering and Technology*, **3**(5), 1-15
- Kamau J.M, Mbui D.N, Mwaniki J.M, Mwaura F.B. (2019). Application of microbial fuel cells in the degradation of 2,4,5,6-tetrachloroisophthalonitrile (chlorothalonil). *Journal of Bioscience and Biotechnology Discovery*, **4**(2), 28-35.
- Kamau, J. M., Mbui, D. N., Mwaniki J. M., & Mwaura, F. B. (2020). Proximate analysis of fruits and vegetables wastes from Nairobi County, Kenya. *Research Journal of Food Science and Nutrition*, **5**(1), 9-15.
- Kamm, B., Gruber, P. R., Kamm, M. (2006). Bio-refineries – *Industrial Processes and Products Status Quo and Future Directions*,1-40
- Kamra N.D., (2005). Rumen microbial ecosystem, *Current Science*, **89**(1), 124-135
- Kanat, G. and Saral, A. (2009). Estimation of Biogas Production Rate in a Thermophilic UASB Reactor Using Artificial Neural Networks. *Environmental Modeling & Assessment*, **14**, 607-614.
- Kartikey, G., Aneja K.R., Rana, D. (2016). Current Status of Cow as a Bioresource for sustainable development, *Bioresources. Bioprocessing*, **3**(28), 1-11
- Katami T., Yasuhara A., and Shibamoto T. (2004). Formation of dioxins from incineration of foods found in domestic garbage. *Environmental Science and Technology*, **38**(4), 1062– 1065.

- Katare S. and Rahi D.C. (2016). Biogas Purification & Enrichment Through Stepped Scrubbing. *International Journal of Engineering Sciences & Research Technology*, **5**(7),795-780
- Keenan, P.J., Isa, J., Switzenbaum, M.S. (1993). Inorganic solids development in a pilot-scale anaerobic reactor treating municipal solid waste landfill leachate. *Water Environ. Res.* **65**, 181–188.
- Khanzada, S.K., Shaikh W., Sofia S., Kazi T.G., Ghani K.U., Kabir A. and Sheerazi T.H. (2008). Chemical constituents of Tamarindus indica L. medicinal plant in Sindh. *Pak. J. Bot.*, **40**(6), 2553-2559.
- Kim B.H, Kim H.J, Hyun M.S. (1999). Direct electrode reaction of Fe (III)-reducing bacterium, *Shewanella putrefaciens*. *J Microbiol Biotechnol*; **9**(2), 127-31.
- Kim, J. K., Oh B. R, Chun Y. N. and Kim S. W., (2006). Effects of temperature and hydraulic retention time on anaerobic digestion of food waste. *Journal of Bioscience and Bioengineering* **102**, 328-323.
- Kiyasudeen S.K, Ibrahim M. K and Ismail S.A. (2015). Characterization of Fresh Cattle Wastes Using Proximate, Microbial and Spectroscopic Principles. *American-Eurasian J. Agric. & Environ. Sci.*, **15** (8), 1700-1709
- Kjeldahl, J. (1883). Neue Methode zur Bestimmung des Stickstoffs in organischen Körpern, *Z. Anal. Chem.* **22**, 366-382
- Kleerebezem, R. and Van L., M. (2006). Critical analysis of some concepts proposed in ADM1. *Water Science and Technology*, **54**, 51-57.
- Kleinert M, Barth T (2008) Phenols from lignin. *Chem Eng Technol* **31**, 736–745
- Kong, X., Du, J., Ye, X., Xi, Y., Jin, H., Zhang M. and Guo D. (2018). Enhanced Methane Production from Wheat Straw with the Assistance of Lignocellulolytic Microbial Consortium TC-5. *Bioresour. Technol.*, **263**, 33–39.
- Kossmann W., Pönitz U., Habermehl S., Hoerz T., Krämer P., Klingler B., Kellner C., Wittur T., von Klopotek F., Krieg A. and Euler H. (2000). Biogas Digest Volume I – IV. German Agency for Technical Cooperation (GTZ). Eschborn. Germany, 1-46.

Kumar G.A, Rajasekhar K, Satyanarayana B.V.V., Murthy K.S, (2012). Implementation of Real Time Detection of Gas leakage in Industries using ARM7 & ZigBee, 1-4.

Kumar K. N. and Goel S. (2009). Characterization of Municipal Solid Waste (MSW) and a proposed management plan for Kharagpur, West Bengal, India, *Resources, Conservation and Recycling*, **53**(3), 166–174.

Kumar K.G, Kamal R.A and Rana D. (2016). Current status of cow dung as a bioresource for Sustainable Development. *Bioresource and Bioprocessing*, **3**(28),1-11.

Kumar S., Bhattacharyya J. K., Vaidya A. N., Chakrabarti T., Devotta S., and Akolkar A. B. (2009). Assessment of the status of municipal solid waste management in metro cities, state capitals, class I cities, and class II towns in India: an insight, *Waste Management*, **29**(2), 883–895.

Kumar S., Joshi R., Dhar H., Verma S., and Kumar M. (2017). Improving methane yield and quality via co-digestion of cow dung mixed with food waste. *Bioresour. Technol.*, **251**, 259–263.

Kumar S., Mondal A. N., Gaikwad S. A., Devotta S. and Singh R.N. (2004). Qualitative assessment of methane emission inventory from municipal solid waste disposal sites: a case study. *Atmospheric Environment*, **38**(29), 4921–4929.

Kunwar P., Sandeep K. K., Monika Y., Nidhi P., Aakash C. and Vivekanand V. (2017). Food Waste to Energy: An Overview of Sustainable Approaches for Food Waste Management and Nutrient Recycling, *BioMed Research International*, **2**, 1-19

Kuria J, Maringa M. (2008). Developing simple procedures for selecting, sizing, scheduling of materials and costing of small bio-gas units. *Spring* **3**, 9–40

Laichena, J.K. and Wafula, J.C. (1997). Biogas technology for rural households in Kenya. *OPEC Rev.* **21**, 223–244.

Lansing, S., Martin, J.F., Botero, R., Nogueira da Silva, T., and da Silva, E.D. (2010). Wastewater transformations and fertilizer value when co-digesting differing ratios of

swine manure and used cooking grease in low-cost digesters. *Biomass and bioenergy* **34**, 1711 – 1720.

Lansing, S., Martin, J.F., Botero, R.B., da Silva, T.N., da Silva, E.D. (2010). Methane production in low-cost, unheated, plug-flow digesters treating swine manure and used cooking grease. *Bioresour. Technol.*, **101**, 4362–4370.

Lansing, S., Martin, J.F., Botero, R.B., Nogueira da Silva, T., Dias da Silva, E. (2010). Wastewater transformations and fertilizer value when co-digesting differing ratios of swine manure and used cooking grease in low-cost digesters. *Biomass Bioenergy* **34**, 1711–1720.

Lazor M, Hutnan M, Sedlacek S, Koles N, and Spalkova V. (2010). Anaerobic co-digestion of poultry manure and waste kitchen oil. In 37th International conference of SSCHE May, 24–28.

Lee, Y., Nagamany N. (2011). Electricity production in membrane-less MFC fed with livestock organic solid waste. *Bio-resource technology*, **102**(10), 5831–5835.

Lehtomäki, A., Huttunen, S., Rintala, J. (2007). Laboratory investigations on co-digestion of energy crops and crop residues with cow manure for methane production: Effect of crop to manure ratio. *Resour. Conserv. Recycl.*, **51**, 591–609

Lesteur M, Bellon M.V, Gonzalez C. (2010). Alternative methods for determining anaerobic biodegradability: a review. *Process Biochem*; **45**, 431–440

Leta T, Solomon L, Chavan, R, Kabtamu D & Anbessa D. (2015). Production of Biogas from Fruit and Vegetable Wastes Mixed with Different Wastes. *Environment and Ecology Research*, **3**, 65-71.

Levi, K.L.; Dorothy, M. (2009). Assessment of the effect of mixing pig and cow dung on biogas yield. *Agric. Eng. Int. CIGR J.* **11**, 1–7.

Li D.L, Xu M.Y and Sun G.P. (2008). Electricity generated by *Shewanella* decolorationis s12 in microbial fuel cell. *Microbiology*; **35**, 777-81.

- Li Y., Sun Y.M, Kong X.Y. (2009). Progress in research of electrigenes in microbial fuel cell. *Microbiology*, **36**, 1404-9.
- Li, R., Chen, S., Li, X., Saifullah Lar, J., He, Y., Zhu, B. (2009). Anaerobic codigestion of kitchen waste with cattle manure for biogas production. *Energy Fuels*, **2** (23), 2225–2228.
- Li-ping F. and Song X. (2016). Overview on Electricigenes for Microbial Fuel Cell, the Open. *Biotechnology Journal*, **10**, 398-406.
- Liu J, Yong YC, Song H. (2012). Activation enhancement of citric acid cycle to promote bioelectrocatalytic activity of arcA knockout Escherichia coli toward high-performance microbial fuel cell. *ACS Catal*; **2**, 1749-52.
- Liu L, Xiao Y, Wu Y. (2014). Electron transfer mediators in microbial electrochemical systems. *Prog Chem*; **26**(11), 1859-66.
- Liu M, Shao J, Zhou B. (2010). Progress in research of microbial electricigenic respiration. *Chin J Appl Environ Biol*, **16**(3), 445-52.
- Liu, G. Q., Zhang, R. H., El-Mashad, H. M., Dong, R. J. (2009). Effect of feed to inoculum ratios on biogas yields of food and green wastes. *Bioresour. Technol.*, **100**, 5103–5108.
- Liu, H., Ramnarayanan, R., Logan, B. E. (2004). Production of electricity during wastewater treatment using a single chamber microbial fuel cell. *Environ. Sci. Technol.*, **38**, 2281-2285.
- Liu, J.H., Zhang, M.L., Zhang, R.Y., Zhu, W.Y., Mao, S.Y. (2016). Comparative studies of the composition of bacterial microbiota associated with the ruminal content, ruminal epithelium and in the faeces of lactating dairy cows. *Microb. Biotechnol.*, **9**, 257–268.
- Liu, W.K., Yang, Q.C., and Du, L. (2009). Soilless cultivation for high-quality vegetables with biogas manure in China: Feasibility and benefit analysis. In: *Renewable Agriculture and Food Systems*: **24**(4), 300–307.

- Llabres L. P. and Mata A. J. (1987). Kinetic study of the anaerobic digestion of straw-pig manure mixtures, *Biomass* **14**, 129 – 142
- Llabrés-Luengo, P., Mata-Alvarez, J. (1988). Influence of temperature, buffer, composition and straw particle length on the anaerobic digestion of wheat straw-pig manure mixtures. *Resour. Conserv. Recycl.* **1**, 27–37.
- Lo H.M, Kurniawan T.A., Sillanp M.E.T. (2010). Modeling biogas production from organic fraction of MSW co-digested with MSWI ashes in anaerobic bioreactors. *Bioresource Technology*, **101**(16), 6329–6335.
- Logan B.E, Regan J.M. (2006) Electricity-producing bacterial communities in microbial fuel cells. *Trends Microbiol*; **14**(12), 512-8.
- Logan B.E. Hamelers B, Rozendal R. (2006). Microbial fuel cells: methodology and technology. *Environ Sci Technol*; **40**(17), 5181-92.
- Logan, B.E. (2010). Scaling up microbial fuel cells and other bio-electro-chemical systems, *Appl. Microbiol. Biotechnol.*, **85**, 1666–1671.
- Logan, Bruce E. (2008). Microbial Fuel Cells. New York: Wiley-Interscience,
- Logan. B, Huang L. (2007). Electricity generation and treatment of paper recycling wastewater using a microbial fuel cell. *Appl. Microbiol. Biotechnol*, **80**, 349–355.
- Lopes, W.S., Leite V.D. and Prasad S. (2004). Influence of inoculums on performance of anaerobic reactors for treating municipal solid waste. *Bioresource Technology*, **94**, 261-266.
- Lovley D.R. (2006). Bug juice: harvesting electricity with microorganisms. *Nature Reviews Microbiology* **4**, 497-508.
- Luo H, Guangli L, Renduo Z, Song J (2008). Phenol degradation in microbial fuel cells. *Chem. Eng. J.*, **147**, 259–264.
- Lybbert, T. and Sumner D. (2010). Agricultural Technologies for Climate Change Mitigation and Adaptation in Developing Countries: Policy Options for Innovation and Technology Diffusion, ICTSD–IPC Platform on Climate Change, Agriculture and Trade, Issue Brief No.6, International Centre for Trade and Sustainable Development, Geneva,

Switzerland and International Food & Agricultural Trade Policy Council, Washington DC, USA, 1-32.

Lycopene Content of Some Tomato Cultivars Obtained from Kano State, *Nigeria*
Ma H., Wang Q., Qian D., Gong L., and Zhang W. (2009). The utilization of acid-tolerant bacteria on ethanol production from kitchen garbage,” *Renewable Energy*, **34**(6), 1466–1470.

Majeed A and Malik S.R. (2018). Enhancement of Biogas Production by Co-Digestion of Fruit and Vegetable Waste with Cow Dung and Kinetic Modeling. *International Research Journal of Engineering and Technology (IRJET)*, **5**(12), 1238-1246.

Makhura E.P, Muzenda E, and Tumeletso L. (2020). Effect of co-digestion of food waste and cow dung on biogas yield, *E3S Web of Conferences* **181**, 01005.

Malvankar N.S, Lovley D.R (2014). Microbial nanowires for bioenergy applications. *Curr Opin Biotechnol*, **27**, 88-95.

Mancini, G., Papirio, S., Lens, P.N.L., Esposito, G. (2018). Increased biogas production from wheat straw by chemical pretreatments. *Renew. Energy* **119**, 608 – 614.

Manichandana K, Simrah U, Harshavardhini B, Anisha D, Ramana M. B V, and shor C.K (2018). Gas Leakage Detection and Smart Alerting System *Global Journal of Engineering Science and Researches*; 24 - 30

Marcato, C.E., Mohta, R. M Revel, J.C., Pouech, P., Hafidi, M., and Guiresse, M. (2009). Impact of anaerobic digestion on organic matter quality in pig slurry. IN: *International Biodeterioration & Biodegradation* **63**, 260 – 266.

Martí-Herrero, J. (2011). Reduced hydraulic retention times in low-cost tubular digesters: Two issues. *Biomass Bioenergy*, **35**, 4481–4484.

Masih S.A, Devasahayam M, Zimik M. (2012). Optimization of power generation in a dual chambered aerated membrane microbial fuel cell with *E. coli* as biocatalyst. *J Sci Ind Res (India)*; **71**(9), 621-6.

- Mata A. J., Viturtia A., Llabres L. P. and Cecchi F. (1993), Kinetic and performance study of batch twophase anaerobic digestion of fruit and vegetable wastes, *Biomass and bioenergy*, **5**(6), 481 – 488.
- Mata-Alvarez, J. (2003). Bio-methanization of the Organic Fraction of Municipal Solid Wastes; IWA Publishing: London, UK, 1-20.
- Mata-Alvarez, J., Macé, S., Llabrés, P. (2000). Anaerobic digestion of organic solid wastes. An overview of research achievements and perspectives. *Bioresour. Technol.*, **74**, 3–16.
- Matheri. (2016). The Role of Trace Elements on Anaerobic Co-digestion in Biogas Production, Proceedings of the World Congress on Engineering 2016 Vol II WCE 2016, June 29 - July 1, 2016, London, U.K, 5-29
- Mathuriya A.S. (2014). Eco-Affectionate Face of Microbial Fuel Cells. Critical Reviews in *Environmental Science and Technology*, **44**, 97-153.
- Mathuriya, A.S. and Sharma, V.N. (2009). Bioelectricity Production from Various Wastewaters through Microbial Fuel Cell Technology. *Journal Biochemical of Technology*, **1**, 133-137.
- Mbugua, J., Mbui, D., Mwaniki, J., Mwaura, F. and Sheriff, S. (2020). Influence of Substrate Proximate Properties on Voltage Production in Microbial Fuel Cells. *Journal of Sustainable Bioenergy Systems*, **10**, 43-51.
- Mehlich, A. (1953). Determination of P, Ca, Mg, K, Na, and NH₄. North Carolina Soil Test Division (Mimeo 1953), 23-89.
- Melikoglu M., Lin C. S. K., and Webb C. (2013). Analyzing global food waste problem: pinpointing the facts and estimating the energy content. *Central European Journal of Engineering*, **3**(2): 157–164.
- Melikoglu, M., Lin, C.S.K. and Webb, C. (2013). Analyzing global food waste problem: pinpointing the facts and estimating the energy content. *cent.eur.j.eng*, **3**, 157–164

- Menicucci J, Beyenal H, Marsili E, Veluchamy RA, Demir G, Lewandowski Z. (2006). Procedure for determining maximum sustainable power generated by microbial fuel cell. *Environ Sci Technol* **40**, 1062–1068
- Micoli, L., Bagnasco, G., & Turco, M. (2014). H₂S removal from biogas for fueling MCFCs: New adsorbing materials. *International Journal of Hydrogen Energy*, **34**, 1783–1787
- Misra, U.; Singh, S.; Singh, A.; Pandey, G.N. (1992). A new temperature controlled digester for anaerobic digestion for biogas production. *Energy Convers. Manag.*, **33**, 983–986.
- Mohammad, N. (1991). Biogas plants construction technology for rural areas. *Bioresour. Technol.* **35**, 283–289.
- Monlau, F., Aemig, Q., Barakat, A., Steyer, J.P., Carrère, H. (2013). Application of optimized alkaline pretreatment forenhancing the anaerobic digestion of different sunflower stalks varieties, *Environ. Technol.*, **34**, 2155–2162
- Moreau, R. A., Liu, K. S., Winkler-Moser, J. K., and Singh, V. (2011). Changes in Lipid Composition During Dry Grind Ethanol Processing of Corn. *J. Am. Oil Chem. Soc.*, **3**, 435-442.
- Mostajir B, Floe'h EL, Mas S, Pete R, Parin D, Nouguiet J, Fouilland E, Vidussi F (2013). A new transportable floating mesocosm platform with autonomous sensors for real-time data acquisition and transmission for studying the pelagic food web functioning. *Limnology and oceanography: methods*, **11**(7), 394-409
- Moulik, T.K., Srivastava, U.K., Shingi, P.M. (1978). Bio-Gas System in India: A Socio-Economic Evaluation; Centre for Management in Agriculture, Indian Institute of Management: Ahmedabad, India., 5-7
- Mozgawa, W., Jastrzebski, W., & Handke, M. (2005). Vibration Spectra of D4R and D6R Structural Units. *Journal of Molecular Structures*. 663-670, 744-747.
- Mucharam, I.S., Pariatmoko, and de Groot, R. (2012). Turn waste into Benefit: Credit Access to Dairy Farmers in East Java, Indonesia for Biogas Units. A partnership of

Nestlé Indonesia and Hivos. In: Company- Community Partnerships for Health in Indonesia. Case Study, 23 – 45.

Mujawar H., Bachuwar D., and Kasbe S. (2015)., Design and development of LPG gas leakage detection and controlling system, *Avishkar-Solapur University Research Journal*, **4**,1-7

Muralidharan, V. S. (1997). Warburg impedance - Basics revisited. *Anti-Corrosion*.

Murto M., Björnsson L., Mattiasson B. (2004). Impact of food industrial waste on anaerobic co-digestion of sewage sludge and pig manure. *J. Environ. Manag.*, **70**, 101–107.

Musisi N, Allman J., S. Geiger S, Chamberlin J. and Headey D. D. (2014). Land Pressures, the Evolution of Farming *Systems*, and Development Strategies in Africa: A Synthesis', *Food Policy*, **48**, 56

Mwaniki J. M., Kali A.M, Mbugua J.K., Kamau G.N. (2016). A New Variant of the Hydraulic Stirring Mechanism for Pilot Scale Wet Thermophilic Anaerobic Digester. *Journal of Kenya Chemical Society*, **9**(1), 135-155

Na Li, Fenglin, Y., Huining, X., Jian, Z. & Qingwei, P. (2018). Effect of Feedstock Concentration on Biogas Production by Inoculating Rumen Microorganisms in Biomass Solid Waste. *Applied Biochemistry and Biotechnology*. **184**,1219–1231

Naegele HJ, Lemmer A, Oechsner H, Jungbluth T. (2012). Electric energy consumption of the full scale research biogas plant “unterer lindenhof”: results of longterm and full detail measurements. *Energies* **5**, 5198–5214.

Nallamothe R.B, Teferra A, & Rao B.V. (2013). Biogas Purification, Compression and Bottling, *G.J. E.D.T.*, **2**(6), 34-38.

Nand, K. (1994). Production of methane from green peas shells in floating dome digesters, *Indian Food Industry.*, **3**, 23-24.

NAS. (1977). Methane Generation from Human, Animal and Agricultural Waste; National Academy of Sciences: Washington, DC, USA, 25-57

Nene (1999). Utilizing Traditional Knowledge in Agriculture, Traditional Knowledge of India and Sri Lanka, 32-38.

Neves L, Oliveira R, Alves M. (2003). Influence of inoculum activity on the biomethanization of a kitchen waste under different waste/inoculum ratios. *Process Biochem.* (Oxford, U. K.), **39**(12), 2019- 2024.

Neves L. and. Oliveira R. R. (2009). Co-digestion of cow manure, food waste and intermittent input of fat. *Bioresource Technology*, **100**(6), 1957-1962.

Newman, J. S. (1973). *Electrochemical Systems*; Prentice Hall: Englewood Cliffs, NJ,

Ni C, Chen BY, Wu YX, (2014). Feasibility study of simultaneous bioelectricity generation and reductive decolorization using *Shewanella xiamenensis* BC01 in dual-chamber microbial fuel cells. *J Xiamen Univ*; **53**, 404-12.

Nielfa A, Cano R and Fdz-Polanco M. (2015). Theoretical methane production generated by the co-digestion of organic fraction municipal solid waste and biological sludge. *Biotechnol Reports*, **5**, 14–21.

Nielsen, S.S. (2010). Food analysis. In S. Suzanne Nielsen (Ed.), (4th ed.). New York Dordrecht Heidelberg London: Springer, 85-177

Niessen J, Uwe S, Fritz S. (2004). exploiting complex carbohydrates for microbial electricity generation – a bacterial fuel cell operating on starch. *Electrochem. Commun.*, **6**, 955–958.

Oghenero W. O, Ejiroghene K. O, Patrick O. E. (2016). Analysis of the Effect of Carbon/Nitrogen (C/N) Ratio on the Performance of Biogas Yields for Non-Uniform Multiple Feed Stock Availability and Composition in Nigeria. *International Journal of Innovative Science, Engineering & Technology*, **3**(5), 119-126

Oko-Ibom, G. O., and Asiegbu, J. E. (2007). Aspects of tomato fruit quality as influenced by cultivar and scheme of fertilizer application. *Journal of Agriculture, Food, Environment and Extension*. **6**(1), 1-11.

Olah, G. A., Goepfert, A., Prakash, G. K. S. (2006). Beyond Oil and Gas: *The Methanol Economy*, Wiley-VCH, Weinheim, 2636-2639

- Ononogbo C., Nwifo, O.C., Nwaji G.N., Okoronkwo C.A. and Igbokwe, J. O. (2016) effective mixing, parametric and operational consideration in the construction of a floating drum biogas plant, *International Journal for Research in Mechanical & Civil Engineering*, **2**(2), 1-10
- Osman A.M, Elhasan E.H and Hassan A.B. (2015). Effect of cow rumen fluid concentration on biogas production from goat manure, *Sudanese Journal of Agricultural Sciences*, **2**,1-7
- Ostrem, K. & Themelis, Nickolas J. (2004). Greening Waste: Anaerobic Digestion Fortreating the Organic Fraction of Municipal Solid Wastes, 1-59
- Ozbayram E.G, Orhan I, Bahar I, Hauke H and Sabine K. (2018). Comparison of Rumen and Manure Microbiomes and Implications for the Inoculation of Anaerobic Digesters. *Microorganisms*, **6**(1), 1-10
- PAC (2010). Practical Action Consulting Bioenergy and Poverty in Kenya: Attitudes, Actors and Activities. PISCES Working Paper, Nairobi, Kenya, 18-34
- Pages Diaz, J., Pereda R I., Lundin, M. and Sarvari Horvath, I. (2011) Co-Digestion of Different Waste Mixtures from Agro-Industrial Activities: Kinetic Evaluation and Synergetic Effects. *Bioresource Technology*, **102**, 10834- 10840
- Palmisano, A.C. and Barlaz, Morton A., (1996). Microbiology of solid waste.
- Pao, S. and P.D (1997). Petracek Shelf life extension of peeled oranges by citric acid treatment. *Food Microbiol.*, **14**, 485-491.
- Papagiannakis, R. G. and Hountalas, D.T. (2004). Combustion and exhaust emissions characteristics of a dual fuel compression ignition engine operated with pilot diesel fuel and natural gas. *Energ. Convers. Manage*, **45**, 2971-2987.
- Parajuli P (2011) Biogas measurement techniques and the associated errors. M.Sc. Thesis University of Jyvaskyla, Finland, 23 - 34
- Park D. H. and Zeikus J. (2000). Electricity generation in microbial fuel cells using neutral red as an electronophore, *Applied and Environmental Microbiology*, **66** (4) 1292-1297

- Park, D. H., Laivenieks, M., Guettler, M. V., Jain, M. K. and Zeikus, J. G. (1999). Microbial utilization of electrically reduced neutral red as the sole electron donor for growth and metabolite production. *Appl. Environ. Microbiol.*, **65**, 2912-2917.
- Park, D. H., Zeikus, J. G. (2003). Improved fuel cell and electrode designs for producing electricity from microbial degradation. *Biotechnol. Bioeng.*, **81**, 348-355.
- Park, H. S., Kim, B. H., Kim, H. S., Kim, H. J., Kim, G. T., Kim, M. (2001). A novel electrochemically active and Fe(III)-reducing bacterium phylogenetically related to *Clostridium butyricum* isolated from a microbial fuel cell. *Anaerobe* **7**, 297–306.
- Parkash, A., Aziz, S., Abro, M., Soomro, S.A., & Kousar, A. (2015). Design and Fabrication of Microbial Fuel Cell Using Cow Manure for Power Generation, *Sci.Int.(Lahore)*,**27**(5),4235-423.
- Peces, M., Astals, S., Mata-Alvarez, J. (2005). Effect of Moisture on Pretreatment Efficiency for Anaerobic Digestion of Lignocellulosic Substrates, *Waste Manag.*, **46**, 189–196.
- Pereira, J. A., Oliveira, I., Sousa, A., Ferreira, I. C., Bento, A., Estevinho, L. (2008). Bioactive properties and chemical composition of six walnuts (*Juglans regia*L.) cultivars. *Food Chem Toxicol* **46**, 2103-2111.
- Persson J, Mårten W, Stephen O (2008) Handbook for Kjeldahl Digestion: 11- 42
- Pertiwinigrum A, Susilowati E, Rochijan, Fitriyanto N.A, Soeherman Y and Fahmi H. M. (2017). Potential Test on Utilization of Cow’s Rumen Fluid to Increase Biogas Production Rate and Methane Concentration in Biogas. *Asian Journal of Animal Sciences*, **11**, 82-87.
- Pham, C. H., Triolo, J. M., Cu, T. T., Pedersen, L., & Sommer, S. G. (2013). Validation and recommendation of methods to measure biogas production potential of animal manure. *Asian-Australasian journal of animal sciences*, **26**(6), 864–873
- Philip S. (2014). Savage Research Group: Energy, University of Michigan. physiochemical attributes of processing and non-processing tomato cultivar.

- Pohland, F.G. and Ghosh S. (1971). Developments in anaerobic stabilization of organic wastes - the two-phase concept. *Environ. Lett.*, **1**, 255-256.
- Potter, M. C. (1911). Electrical Effects Accompanying the Decomposition of Organic Compounds, **84**(571), 260-276.
- Poulsen, T.G. and Adelard, L (2016), Improving biogas quality and methane yield via co-digestion of agricultural and urban biomass wastes. *Waste Manag.* **54**, 118–125.
- Pratiksha P. and Gireesh B. K. (2012). Isolation and Identification of Methanogenic Bacteria from Cowdung, *International Journal of Current Research*, **4**(7), 028-031
- Pratima K. C and Bhakta B. A. (2015). Production of Biogas from Slaughterhouse Waste in Lalitpur Sub-Metropolitan City, Proceedings of IOE Graduate Conference. 143–149.
- Pugalenth, M., Vadivel, V., Gurumoorthi, P. & Janardhannan, K. (2004). Comparative nutritional evaluation of little known legumes, *Tamarindus indica*, *Erythrina indica* and *Sesbania bispinosa*. *Tro. Subtro. Agroecosyst.*, **4**, 107-123.
- Rabaey, K., Boon, N., Siciliano, S. D., Verhaege, M., Verstraete, W. (2004). Biofuel cells select for microbial consortia that self-mediate electron transfer. *Appl. Environ. Microbiol.*, **70**, 5373- 5382.
- Rabaey, K., Verstraete, W. (2005). Microbial fuel cells: novel biotechnology for energy generation. *Trends Biotechnol.*, **23**, 291 - 298
- Rahman M.S, Saha S.K, Khan M.R.H, Habiba U, Hossen S.M. (2013). Present situation of renewable energy in Bangladesh: Renewable energy resources existing in Bangladesh., 10
- Rajendran K, Aslanzadeh S, Taherzadeh M.J (2012). Household biogas Digesters, *Energies*, **5**(8), 2911–2942
- Ralph, M. & Dong, G.J. (2010). Environmental Microbiology Second, A JOHN WILEY & SONS, INC., PUBLICATION., 281-301
- Ramana, K.V., Singh, L. (2000) Microbial degradation of organic wastes at low temperatures. *Def. Sci. J. Newdelhi*, **50**, 382–390.

- Rao, M. S., Singh, S. P. (2004). Bioenergy conversion studies of organic fraction of MSW: kinetic studies and gas yield–organic loading relationships for process optimisation. *Bio-resource Technology* **95** (2), 173- 185.
- Raposo F, Borja R, Rincón B and Jiménez A.M. (2008). Assessment of process control parameters in the biochemical methane potential of sunflower oil cake. *Biomass Bioenergy* **32**, 1235–1244.
- Raposo F, Fernández CV, De la Rubia M. (2011). Biochemical methane potential (BMP) of solid organic substrates: evaluation of anaerobic biodegradability using data from an international interlaboratory study. *Journal of Chemical Technology and Biotechnology*, **86**(8), 1088-1098.
- Raveendran S, Ashok P, Parameswaran B. (2015). Pretreatment of Biomass, Chapter 4 – Alkaline Treatment, 51-60.
- Rea, J. (2014), Thesis: Kinetic Modeling and Experimentation of Anaerobic Digestion., Massachusetts Institute of Technology: USA. 1 -58.
- Reece, J. B., Urry, L. A., Cain, M. L. 1., Wasserman, S. A., Minorsky, P. V., Jackson, R., and Campbell, N. A. (2014). *Campbell biology* (Tenth edition.). Boston: Pearson.89-90
- Reza A, Ali S, Alibakhsh K, Hossein H and Majid A. T. (2016). The role of biogas to sustainable development (aspects environmental, security and economic), *Journal of Chemical and Pharmaceutical Research*, **8**(4), 112-118
- Rishabh A, Naman G, Vinay B, Maharishi V. (2018). Gas Leakage Detection System, DIT University, Dehradun, India, 34-67
- Rismani-Yazdi H, Christy A, Carver S.M, Yu Z, Dehority B.A, Tuovinen O.H. (2011). Effect of external resistance on bacterial diversity and metabolism in cellulose-fed microbial fuel cells. *Bioresour Technol*, **102**, 278–283
- Rodriguez, L. and Preston, T. (2001). Biodigester Installation Manual; Food & Agriculture Organization: Roma, Italia., 67.
- Rominyi, O. L., Fapetu O.P, Owolabi J.O and Adaramola B.A. (2017). Determination of energy content of the municipal solid waste of Ado-Ekiti metropolis, Southwest, Nigeria. *Current journal of applied science and technology*, **23**(1), 1-11.

- Rozej, A., Montusiewicz, A. and Lebiocka, M. (2008). No Title. *Archives of Env. Protection*, **34**(3), 299-304.
- Rozzi A, Remigi E. (2004). Methods of assessing microbial activity and inhibition under anaerobic conditions: a literature review. *Rev Environ Sci Biotechnol*, **3**, 93–115
- Rusin, J., Chamradova, K., & Grycova, B. (2017). The influence of biomass agitation on biogas and methane production using the high-solids thermophilic anaerobic digestion. *Green Processing and Synthesis*, **6**(3), 273-279.
- Rzepka P, Jasso-Salcedo A.B, Janicevs A, Vasiliev P, Hedin N. (2019). Upgrading raw biogas Symposium into biomethane with structured sized zeolite [NaK]-A adsorbents in a PVSA unit, *Energy Procedia*, **158**, 6715–6722
- Sabran F. H and Saharuddin R. S. (2019). Measurement of Level Content of Methane in Household Waste Based on *Arduino* and Gas Sensor, *Journal of Physics Conference Series*, **1244**(1), 1-5.
- Sadaka, S.S. and Engler, C.R (2003) Effect of initial total solids om composting of raw manure with biogas recovery. *Compost Sci. and Utilization*, **11**(4), 361-369.
- Safley, L.M., Jr. (1992) Westerman, P.W. Performance of a low temperature lagoon digester. *Bioresour. Technol.* **41**, 167–175.
- Sager, M. (2007), Trace and nutrient elements in manure, dung and compost samples in Austria, *Soil Biol. Biochem.***39**, 1383–1390
- Salihua A and Alama Z. (2015). Upgrading Strategies for Effective Utilization of Biogas, *Environmental Progress & Sustainable Energy*, **34**(5), 1512-1519.
- Sambrook, J., Fritsch, E. F. and Maniatis, T. (1989). *Molecular Cloning: A Laboratory Manual*, Cold Spring Harbor, NY: Cold Spring Harbor Laboratory Press, 345 - 455
- Sanders, W. T. M., Veeken, A. H. M., Zeeman, G. and Van Lier, J. B. (2003). Analysis and optimization of the anaerobic digestion of the organic fraction of municipal solid waste. Mata-Alvarez, J. (ed.) *Bio-methanization of the organic fraction of municipal solid wastes*. London: IWA Publishing, 65

Sarker, S.; Møller, H.B (2013). Boosting biogas yield of anaerobic digesters by utilizing concentrated molasses from 2nd generation bioethanol plant. *Int. J. Energy Environ.* **4**, 199–210.

Sarker, S.and Møller, H.B (2014). Regulating feeding and increasing methane yield from co-digestion of C 5 molasses and cattle manure. *Energy Convers. Manag.* **84**, 7–12.

Sawant A, Heyde, N.V, Straley, B.A, Donaldson, S.C, Love, B.C, Kanabel, S.J, Jayaroo B.M; (2007). Antimicrobial Resistant Enteric Bacteria from Dairy Cattle. *Applied Environmental Microbiology* **73**, 156-163.

Sadi T.A, Rutz D, Prassl H (2013) Chapter 1 overview of biogas technology. In: The complete biogas handbook. 2nd edn., 10-14

Sean C., Gavin C. and Vincent O., (2006). Psychrophilic and Mesophilic Anaerobic Digestion of Brewery Effluent. A Comparative Study, *Water Research* **40** (13).

Semenec L., Franks A.E. (2014). The microbiology of microbial electrolysis cells. *Microbiol Aust*; **11**, 201-6.

Serge, W. (2012). Etude De La Valeur Agronomique Du Compost a Base D'effluent De Biodigesteur. Ministere de L'Agriculture de L'Hydraulique. Secretariat General. Centre Agricole Polyvalent de Matourkou (CAP-M). Burkina Faso, 262-268.

Shah, N. (1997). The role of bio-energy utilization in sustainable development. *Int. J. Glob. Energy Issues*, **9**, 365–381.

Shalini S., Sushil K, Jain M.C., Dinesh K. (2001). Increased biogas production using microbial stimulants, *Bioresource Technology*, **78**(3), 313-6

Sharma A. and Kar S.K. (2015). Energy Sustainability through Green Energy, *Green Energy and Technology*, 1-9

Shi J., Xu F., Wang Z., Stiverson J. A., Yu Z., and Li Y. (2014). Effects of microbial and non-microbial factors of liquid anaerobic digestion effluent as inoculum on solid-state anaerobic digestion of corn Stover, *Bioresour. Technol.*, **157**, 188–196.

- Shian, S.-T., Chang, M.-C., Ye, Y.-T.; Chang, W. (1979). The construction of simple biogas digesters in the province of Szechwan, China. *Agric. Wastes*, **1**, 247–258.
- Shital I, Priyanka R, Aishwarya G, Nayakwadi V.N (2018), Gas Leakage Detection and Smart Alerting System Using IOT, *International Journal of Innovative Research & Studies*, **8**(2), 291 -298.
- Shiv K., Harash, D.K. and Ghireesh B.K (2012). A Study on Electrical Generation from Cow Dung Using Microbial Fuel Cells, *Journal of biochem technology* **3**(4), 442- 447.
- Shunchang Y, Yikan L, Na W, Yingxiu Z, Spyros S, Pratap P. (2019). Low-cost, Arduino-based, portable device for measurement of methane composition in biogas, *Renewable Energy*, **138**, 224-229
- Shunchang Y., Yikan L., Na W., Yingxiu Z, Spyros S., Pratap P. (2019). Low-Cost, Arduino-Based, Portable Device for Measurement of methane composition in biogas. *Renewable Energy*, **138**, 224 - 229
- Shyam, M.; Sharma, P.K. (1994). Solid-state anaerobic digestion of cattle dung and agro-residues in small-capacity field digesters. *Bioresour. Technol.*, **48**, 203–207.
- Sibisi, N.T., Green, J.M. (2005). A floating dome biogas digester: Perceptions of energizing a rural school in Maphephetheni, Kwazulu-Natal. *J. Energy S. Afr.* **16**, 45–52.
- Simon L. (1999). Biogas upgrading and utilization, IEA Bio-energy, Energy from biological conversion of organic waste SNV Domestic Biogas (2011) **4**, 3-16
- Singh, D., Singh, K.K., Bansal, N.K. (1985). Heat loss reduction from the gas holder/fixed gas dome of a community-size biogas plant. *Int. J. Energy Res.*, **9**, 417–430.
- Singh, K.P., Suman, A., Singh, P.N., and Srivastava, T.K. (2007). Improving quality of sugarcane-growing soils by organic amendments under subtropical climatic conditions of India. In: *Biol Fertil Soils*, **44**, 367–376.
- Singh, L., Maurya, M., Ram, M.S. and Alam, S. (1993). Biogas production from night soil: Effects of loading and temperature. *Bioresour. Technol.*, **45**, 59–61.

- Singh, L., Maurya, M.S., Ramana, K.V. and Alam, S.I. (1995). Production of biogas from night soil at psychrophilic temperature. *Bioresour. Technol.*, **53**, 147–149.
- Singh, N. and Gupta, R.K. (1990). Community biogas plants in India. *Biol. Wastes*, **32**, 149–153.
- SNV. (2011). Technology and Mass- Dissemination Experiences from Asia. Biogas compact course PPRE- Oldenburg University, 8 - 85
- Soetaert W, Vandamme E. J (2008) Biofuels. John Wiley & Sons Ltd., Great Britain, 1–8
- Song T. S, Yan Z. S, Zhao Z. W, Jiang H. L (2010). Removal of organic matter in freshwater sediment by microbial fuel cells at various external resistances. *J Chem Technol Biotechnol*, **85**, 1489–1493
- Spears J.W (2003). Trace Mineral Bioavailability in Ruminants, *The Journal of Nutrition*, **133**, 1506 –1509
- Speece, R.E. (1996). Anaerobic Technology for Industrial Wastewaters. *Archae Press*, USA, ISBN:0-9650226-0-9, 43
- Stauffer B. D, Hirschenhofer H., Klett J, G., and Engleman R., (2004). Fuel Cell Handbook, 7th edition., 332
- Subramanian, S.K. (1977). Bio-Gas Systems in Asia; Management Development Institute: Newdelhi, India, **11**.
- Sunil M. P, Ashik N, Vidyasagar B, Vinay S. (2013). Smart Biogas Plant, *International Journal of Innovative Technology and Exploring Engineering (IJITEE)*, **3**(3); 62 – 66.
- Suruchi D, Ankita M, Ajinkya J, Sonali P and Rushikesh B. (2016). Biogas Monitoring System for Measuring Volume using Microcontroller & GSM. *International Journal of Current Engineering and Technology*, **6**(5), 1553-1557
- Symons, G.E. and Buswell, A.M. (1933). The methane fermentation of carbohydrates. *J. Am. Chem. Soc.* **55**, 2028-2036.

- Taherdanak M, Zilouei H, Karimi K. (2016). The influence of dilute sulfuric acid pretreatment on biogas production from wheat plant, *International Journal of Green Energy*, **13**(11), 1129-1134.
- Takashima M., Speece R.E., and Parkin G.F (1990). Mineral requirements for methane fermentation. *Critical Reviews in Environmental Science and Technology*, **19**(5), 465-479.
- Talaro, P. K. (2009). *Foundation in Microbiology*, San Francisco: Pearson Benjamin, 51-124.
- Talyan V., Dahiya R. P., and Sreekrishnan T. R., (2008). State of municipal solid waste management in Delhi, the capital of India. *Waste Management*, **28**(7), 1276–1287.
- Tekin A.R and Dalgıç A.C. (2000). Biogas production from olive pomace, *Resources Conservation and Recycling* **30**(4), 301-313
- Tender L., Gray S., Groveman E., Lowy D., Kauffma P., Melhado R., Tyce R., Flynn D., Petrecca R., and Dobarro J. (2008). The first demonstration of a microbial fuel cell as a viable power supply: Powering a meteorological buoy, *J. Power Source*, **179**, 571–575.
- Tewelde, S., Eyalarasan, K., Radhamani, R., Karthikeyan, K. (2012). Biogas production from co-digestion of brewery wastes [BW] and cattle dung [CD]. *Int. J. Latest Trends Agric. Food Sci.*, **2**, 90-93.
- Thauer, R. K., Jungermann, K., Decker, K. (1977). Energy conservation in chemotrophic anaerobic bacteria. *Bacteriol. Rev.*, **41**, 100-180.
- The German-Dutch-Norwegian Partnership - Energizing development (EnDev) (2012) - Up scaling Proposal, 1-26
- Thomas K, Thomas D. B, Rahel C. Br, Didier O, Patrick E. (2008). Dissipation of pesticides during composting and anaerobic digestion of source-separated organic waste in full-scale plants. *Bioresource Technology*, 215-220
- Tira H. S., Padang Y. A., Mirmanto, and Hendriono (2015). *Appl. Mechanics and Materials*, **777**, 443–448.

- Tira H.S, Yesung A. P., Salman M. W., Made W., Raden D. A. (2018). The Utilization of Corn Cob and Zeolite as Adsorbents for Hydrogen Sulfide and Carbon Dioxide Removal from Biogas, *International Journal of Mechanical Engineering and Technology (Ijmet)*, **9**(9), 545–551.
- Tota-Maharaj K and Parneet P (2015). Performance of pilot-scale microbial fuel cells treating wastewater with associated bioenergy production in the Caribbean, *Int J Energy Environ Eng* **6**, 213–22.
- Tran, T. S. and Simard R. R (1993) Mehlich III-Extractable Elements. In: M. R. Carter, Ed. *Soil Sampling and Methods of Analysis*, 43-49.
- Trisakti, B., Irvan, Zahara, I., Taslim, & Turmuzi, M. (2017). Effect of agitation on methanogenesis stage of two-stage anaerobic digestion of palm oil mill effluent (POME) into biogas, *AIP Conference Proceedings* **1840**(1), 1-9
- U.S. Energy Information Administration. (2017). Annual Energy Outlook 2017with projections to 2050, 7 - 34
- U.S. Energy Information Administration. (2019). Annual Energy Outlook 2017with projections to 2050, 18 - 25
- Ukpebor J. and Ukpebor E. (2016) application of QUECHERS method for multi-residue pesticides determination in lettuce and apple using gas chromatography-mass spectrometry, *Nigerian Journal of Technology (NIJOTECH)*, **35**(3), 544 – 549
- Ullah, M., Sen, R., Hasan, K., Isalm, B., and Khan, S. (2008). Bio-slurry management and its effect on soil fertility and crop production, Project report, 23- 50
- United Nations Asian and Pacific Centre for Agricultural Engineering and Machinery Beijing (APCAEM) (2007); Recent Developments in Biogas Technology for Poverty Reduction and Sustainable Development 21-34.
- US Department of Energy. (2014). Anaerobic Digestion Basics, 2014.,1-6
- USEPA. (2008). Terms of Environment: Glossary, Abbreviations and Acronyms, United States Environmental Protection Agency (EPA), 1-70.

- Valerio P, Francesco P, Guerriero E, Bencini A & Drigo S. (2016). Biogas cleaning and upgrading with natural zeolites from tuffs. *Environmental Technology*, **37**(11,) 1418-1427
- Valero, D., Montes, A.J., Rico, J.L., Rico, C. (2016). Influence of headspace pressure on methane production in Biochemical Methane Potential (BMP) tests. *Waste Manage.* **48**, 193–198.
- Vavilin Va, Fernandez B, Palatsi J, Flotats X. (2008). Hydrolysis kinetics in anaerobic degradation of particulate organic material: An overview. *Waste Manage*; **28** (6), 939 - 51.
- VDI 4630. (2006). Fermentation of Organic Materials. Characterization of the Substrates, Sampling, Collection of Material Data, Fermentation Tests. VDI-Handbuch Energietechnik, 36-89
- Veeken A, Kalyuzhnyi S, Scharff H, Hamelers B. (2000). Effect of pH and Hydrolysis of Organic Solid Waste. *J Enviro Eng.*, **10**, 76-81.
- Velázquez-Martí B, Meneses-Quelal O.W, Gaibor-Chavez J and Niño-Ruiz Z. (2018). Review of Mathematical Models for the Anaerobic Digestion Process, Anaerobic Digestion, IntechOpen: London, UK, 1–20.
- Verma, S. (2002). Anaerobic Digestion of Biodegradable Organics in Municipal Solid Wastes. Department of Earth & Environmental Engineering (Henry Krumb School of Mines) Fu Foundation School of Engineering & Applied Science Columbia University, 67 - 76
- Vesilind, P.A. (Ed). (1998). Wastewater Treatment Plant Design (4th Edition). London, UK and Alexandria, VA, USA: IWA Publishing and the Water Environment Federation.,50
- Vijayanand C. and Singaravelu M. (2016), Refinery Technologies in Upgradation of Crude Biogas to Biomethane, *Advances in Life Sciences*, **5**(3), 715-724.
- Vilajeliu-Pons A, Bañeras L, Puig S. (2016). External resistances applied to mfc affect core microbiome and swine manure treatment efficiencies. *PLoS One*; **11**(10), 1640 -44.

- Vintila, T., Neo, S., Vintila, C. (2012). Biogas Production Potential from Waste in Timis County, Scientific Papers: *Animal Science and Biotechnologies*, **45** (1), 366-373
- Vintiloiu, A., Lemmer, A., Oechsner, H., Jungbluth, T. (2012). Mineral substances and macronutrients in the anaerobic conversion of biomass: An impact evaluation. *Eng. Life Sci.*, **12**, 287–294.
- Viswanath, P., Perma, S., Sumithra, D. and Nand, K. (1991). Anaerobic digestion of fruit and vegetable processing wastes for biogas production, *Bioresource Technology*, **40**, 43-48.
- Voelegi Y. and Lohri, C. (2009). Research on anaerobic digestion of organic solid waste at household level in Dar es Salaam, Tanzania; Bachelor Thesis at ZHAW (Zurich University of Applied Sciences) in collaboration with Eawag (Swiss Federal Institute of Aquatic Science and Technology), 54 - 67
- Vögeli, Y, Lohri C, Gallardo A, Diener S, Zurbrügg C (2014). Anaerobic Digestion of Bio-waste in Developing Countries - Practical Information and Case Studies. Swiss Federal Institute of aquatic science and technology(EAWAG) Dubendorf, Switzerland, 2014, 14-75.
- Wall D. M, O’Kiely P and Murphy J.D. (2013). The potential for bio-methane from grass and slurry to satisfy renewable energy targets. *Bioresour Technol*; **149**, 425–431.
- Walla, C. and Schneeberger, W. (2008). The optimal size for biogas plants. *Biomass Bioenergy* **32**, 551-557
- Wang X, Tang J, Cui J, Liu Q, Giesy J.P, Hecker M. (2014) Synergy of Electricity Generation and Waste Disposal in Solid State Microbial Fuel Cell (MFC) of Cow Manure Composting. *International Journal of Electrochemical Science*, **9**, 3144-3157.
- Wang X, Yujie F, Nanqi R, Heming W, He L, Nan L, Qingliang Z. (2008). Accelerated start-up of two-chambered microbial fuel cells: effect of positive poised potential. *Electrochem. Acta*, **54**, 1109–1114.
- Wang, X., Tang, J., Cui, J., Liu, Q., Giesy, J.P. and Hecker, M. (2009). Synergy of Electricity Generation and Waste Disposal in Solid State Microbial Fuel Cell (MFC) of

- Cow Manure Composting. *International Journal of Electrochemical Science*, **9**, 3144-3157.
- Warnars L and Oppenoorth H. (2014). Bioslurry: A Supreme Fertiliser, a study on bioslurry results and uses, 8 – 53.
- Warnars, P. (2012). From Biomass to Biogas: Present Day Status & Future Requirements. Master Thesis International Development Studies. Utrecht University, 50
- Weinrich, S., Schäfer, F., Bochmann, G., Liebetrau, J., (2018). Value of batch tests for biogas potential analysis; method comparison and challenges of substrate and efficiency evaluation of biogas plants. Murphy, J.D. (Ed.) IEA Bioenergy Task **37**, 10
- Wlodzimier, M., Magdalena, K., & Kataryzana, B. (2011). FT-IR of zeolites from different structural groups. *Chemik*, **65** (7), 667-674.
- World Bank Group (1998). Pollution prevention and abatement handbook toward cleaner production / The World Bank Group in collaboration with UNEP and UNIDO, 2-59.
- Wrighton K.C, Thrash J.C, Melnyk R.A. (2011). Evidence for direct electron transfer by a gram-positive bacterium isolated from a microbial fuel, *Applied and Environmental Microbiology* **77**(21), 7633-9
- Xavier, S. and Nand, K (1990). A preliminary study on biogas production from cowdung using fixed-bed digesters. *Biol. Wastes*, **34**,161–165.
- Xie H. (2012). *Shewanella haliotis* Z4 and *Enterococcus faecalis* in: Z5 and their characteristics of electricity generation (in China). Changsha, China: South China University of Technology, 45.
- Xue, L., Liu G., Parfitt J., Liu X., Van Herpen E., Stenmarck Å., O’connor C., Östergren K. and Cheng, S. (2017). Missing food, missing data? A critical review of global food losses and food waste data. *Environmental Science & Technology*, **51**(12), 6618- 6633.
- Yang, G., Zhang, P., Zhang, G., Wang, Y., Yang, A. (2015). Degradation properties of protein and carbohydrate during sludge anaerobic digestion, *Bioresource Technology*, **192**, 126-130.

- Yangyang L, Yiyang J, Aiduan B, Hailong L, Jinhui L. (2017). Effects of organic composition on mesophilic anaerobic digestion of food waste, *Bioresource Technology*, **244**, 213-224
- Yasin, M., Wasim, M. (2011). Anaerobic Digestion of buffalo dung, sheep waste and poultry litter for Biogas Production. *Journal of Agricultural Research* **49** (1), 73-82.
- Yen, H.W. and Brune, D.E. (2007) Anaerobic co-digestion of algal sludge and waste paper to produce methane. *Bioresour. Technol.*, **98**, 130–134.
- Zennaki B.Z, Zadi A., Lamini H., Aubinear M. and Boulif M. (1996). Methane Fermentation of cattle manure: Effects of HRT, temperature and substrate concentration. *Tropicul. Tural.*, **14**, 134-140.
- Zhang E, Cai Y, Luo Y, Piao Z. (2014). Riboflavin-shuttled extracellular electron transfer from *Enterococcus faecalis* to electrodes in microbial fuel cells. *Can J Microbiol*; **60**(11), 753-9.
- Zhang G, Zhao Q, Jiao Y, Wang K, Lee DJ, Ren (2011). Biocathode Microbial Fuel Cell for Efficient Electricity Recovery from Dairy Manure, *Biosensors and Bioelectronics*, **31**(1), 537-543.
- Zhang T, Cui C, Chen S. (2008). The direct electrocatalysis of *Escherichia coli* through electroactivated excretion in microbial fuel cell. *Electrochem Commun*; **10**, 293-7.
- Zhang Y, Zhao Q, Li W. (2014). Research advances in microbial electron transfer of bio-electrochemical system. *Dev Energy Sci*; **2**(4), 39-46.
- Zhang, D. (1989). An analysis of domestic biogas storage installations in China. *Biomass* **20**, 61–67.
- Zhao G, Ma F, Wei L, Chua H, Chang C, Zhang X. (2012). Electricity generation from cattle dung using MFC technology during anaerobic acidogenesis and the development of microbial populations, *waste management*, **32**(9), 1651–1658.

Zhou Y. L., Zhang Z. Y., Nakamoto T., Li Y., Yang Y. N., Utsumi M., Sugiura N. (2011). Influence of substrate-to-inoculum ratio on the batch anaerobic digestion of bean curd refuse-okara under mesophilic conditions. *Biomass Bioenergy*, **35**, 3251–3256.

Internet References

Ahmad S. (2018). How to use MAX6675 Thermocouple k type sensor with Arduino, retrieved from https://robojax.com/learn/arduino/?vid=robojax_MAX6675_thermocouple on march 13th, 2021

Caballero C.D. (2017). How to use a PH probe and sensor, retrieved from <https://www.botshop.co.za/how-to-use-a-ph-probe-and-sensor/> on 27th May, 2020 at 05.24AM

EU Parliament. (2016). European Parliament resolution of 16 May 2017 on initiative on resource efficiency: reducing food waste, improving food safety (2016/2223(INI). Available <http://www.europarl.europa.eu/sides/getDoc.do?type=TA&language=EN&reference=P8-TA-2017-0207>, last accessed March, 10th, 2021.

Fahad E. (2020). Flame Sensor Arduino, Fire Sensor Arduino, Circuit diagram & programming retrieved from <https://www.electronicclinic.com/flame-sensor-arduino-fire-sensor-arduino-circuit-diagram-programming/> on march 13th, 2021

Fahad E. (2020). K Type Thermocouple, MAX6675, and Arduino based Temperature Monitoring retrieved from <https://www.electronicclinic.com/k-type-thermocouple-max6675-and-arduino-based-temperature-monitoring/> on march 13th, 2021

FAO (1996). Biogas technology: A training manual for extension. Support for Development of national Biogas Programme (FAO/TCP/NEP/4451-T). Nepal. Retrieved from: www.fao.org/docrep/008/ae897e/ae897e00.htm . on February, 2021.

Fitzgerald S. (2013). Arduino motors retrieved from <http://www.arduino.cc/en/Tutorial/Sweep> on March 2021.

- Geiger O. (2010). Earth bag biogas plant. <http://www.naturalbuildingblog.com/earthbag-biogas-plant/> access on 20.11.2020 at 11.32AM
- Hafner, S.D., Richards B.K., Astals, S., Holliger, C., Koch, K., Weinrich, S. (2019). Calculation of Methane Production from Gravimetric Measurements. Standard BMP Methods Document 203, Version 1.0. Available online: <https://www.dbfz.de/en/BMP> (accessed on 19 November 2020).
- JRC. (2017). Food waste Accounting: Methodologies, challenges and opportunities, JRC Technical Report. Available http://publications.jrc.ec.europa.eu/repository/bitstream/JRC109202/jrc_technical_report_food_waste_rev_2_online_final.pdf , last accessed Oct 2020.
- Justin M. (2012). Microbial Fuel Cells: Generating Power from Waste, retrieved from <https://illuminate.usc.edu/microbial-fuel-cells-generating-power-from-waste/> on April, 2021
- Karve A.D. (2007), Compact biogas plant, a low cost digester for biogas from waste starch. <http://www.arti-india.org.>, 1-98
- Kumar S. (2018). Interfacing Flame Sensor with Arduino to Build a Fire Alarm System retrieved from <https://circuitdigest.com/microcontroller-projects/arduino-flame-sensor-interfacing>, on march 13th, 2021
- Mukherjee A. (2016). Smoke Detection using MQ-2 Gas Sensor retrieved from <https://create.arduino.cc/projecthub/Aritro/smoke-detection-using-mq-2-gas-sensor-79c54a> on march 13th, 2021
- Riyaz J. (2019). How to Connect MQ2 Gas Sensor to Arduino retrieved from <https://create.arduino.cc/projecthub/Junezriyaz/how-to-connect-mq2-gas-sensor-to-arduino-f6a456>, on march 13th, 2021
- Sajidas A (2019): Biotech digester designs (<http://www.biotechindia.org/Inventions.aspx>
- Shunchang Y, Spyros S, and Pratap P. (2020). Inexpensive, Arduino-based device for on-line, automatic, real-time measurement of methane composition and biogas flowrate from anaerobic digesters, 1- 11. retrieved from <https://www.authorea.com/users/362442/article/483597> - Inexpensive, Arduino-based

device for on-line, automatic, real-time measurement of methane composition and biogas flowrate from anaerobic digesters

SNV. (2013). On: [http://www.snvworld.org/en/publications/ bio-slurry-management-and-its-effect-on-soil-fertility-and-crop-](http://www.snvworld.org/en/publications/bio-slurry-management-and-its-effect-on-soil-fertility-and-crop-production) production accessed on march 10th 2021

Suryateja (2018) Arduino Modules - Flame Sensor retrieved from <https://create.arduino.cc/projecthub/SURYATEJA/arduino-modules-flame-sensor-6322fb>, on march 13th, 2021

Zafar S (2020), [Biogas from Slaughterhouse Wastes](https://www.bioenergyconsult.com/biogas-from-slaughterhouse-wastes), Slaughterhouse Waste Management retrieved from <https://www.bioenergyconsult.com/biogas-from-slaughterhouse-wastes> on April 16, 2021.

5.7 APPENDICES

5.7.1 Appendix A: NACOSTI Research Permit

CONDITIONS

1. The License is valid for the proposed research, research site specified period.
2. Both the Licence and any rights thereunder are non-transferable.
3. Upon request of the Commission, the Licensee shall submit a progress report.
4. The Licensee shall report to the County Director of Education and County Governor in the area of research before commencement of the research.
5. Excavation, filming and collection of specimens are subject to further permissions from relevant Government agencies.
6. This Licence does not give authority to transfer research materials.
7. The Licensee shall submit two (2) hard copies and upload a soft copy of their final report.
8. The Commission reserves the right to modify the conditions of this Licence including its cancellation without prior notice.



REPUBLIC OF KENYA



National Commission for Science,
Technology and Innovation

RESEARCH CLEARANCE
PERMIT

Serial No.A **18362**

CONDITIONS: see back page

**THIS IS TO CERTIFY THAT:
MR. MBUGUA JAMES KAMAU
of UNIVERSITY OF NAIROBI, 18-902
KIKUYU, has been permitted to conduct
research in Kiambu , Nairobi Counties**

**Permit No : NACOSTI/P/18/8019/21510
Date Of Issue : 24th April,2018
Fee Received :Ksh 2000**

**on the topic: OPTIMIZATION AND
DESIGN OF AN EFFECTIVE ANAEROBIC
DIGESTER FOR BIOGAS PRODUCTION
USING VEGETABLE WASTES FROM
KENYAN MARKETS**

**for the period ending:
23rd April,2019**



**Applicant's
Signature**

**Director General
National Commission for Science,
Technology & Innovation**

5.7.2 Appendix B: Macro and micro nutrient composition in market wastes

Concentrations are as stated in the Unit of concentration column

Digested and Fresh Fruits and Vegetables XRF report

Element	Digested Fruits & Vegetables	Fresh Fruits & Vegetables	Unit of concentration
Potassium (K)	5.91 ± 0.34	3.59 ± 0.22	%
Calcium (Ca)	1.74 ± 0.15	1.53 ± 0.07	%
Titanium (Ti)	102 ± 14	268 ± 28	ppm
Manganese (Mn)	251 ± 22	280 ± 24	ppm
Iron (Fe)	2520 ± 240	3742 ± 235	ppm
Zinc (Zn)	295 ± 15	176 ± 11	ppm
Bromine (Br)	48.3 ± 3.1	34.4 ± 2.6	ppm
Rubidium (Rb)	54.8 ± 2.7	35.4 ± 2.8	ppm
Strontium (Sr)	137 ± 9	101 ± 8	ppm
Zirconium (Zr)	80.8 ± 6.3	68.3 ± 3.2	ppm
Niobium (Nb)	13.4 ± 1.7	15.2 ± 2.7	ppm
Lead (Pb)	<10	15.1 ± 3.6	ppm

5.7.3 Appendix C: The 60 Liters' Digester Description

The measurement details of the fabricated 60liters digester are described and illustrated in figure A.1.



Figure 5.1: Schematic of the 60 L digester.

The 60 L digester is made up of a 60 L plastic drum with an air tight cover supported by a metallic seal for air tight sealing. On the inner side of the seal is a rubber seal. The inlet is made with a 33cm 3' pipe attached to the drum with a 3' 90⁰ elbow while the outlet pie is made of a 3' 90⁰ elbow which is 36 cm from the bottom of the digester and 26 cm from the inlet pipe. A gas outlet pipe is made using ½' pipe fitted with a gate valve for gas outlet control. To increase gas outlet pressure, a narrower pipe is attached after the gate valve.

The warm water circulation pipe is ½' plastic pipe coiled inside the digester and exit the reactor via the outlet waste pipe. Water flows through the pipe at 2 liters per minute with the initial startup taking 2 hours too achieve the required temperature. Digester insulation with a blanket was done to prevent heat loss.

The stirrer is made up of a 64.5 cm metallic bar with 3 16 cm long spiral rods placed at 15cm intervals from the bottom of the stirrer. A hand handle is placed at the upper end of the stirrer to facilitate manual agitation.

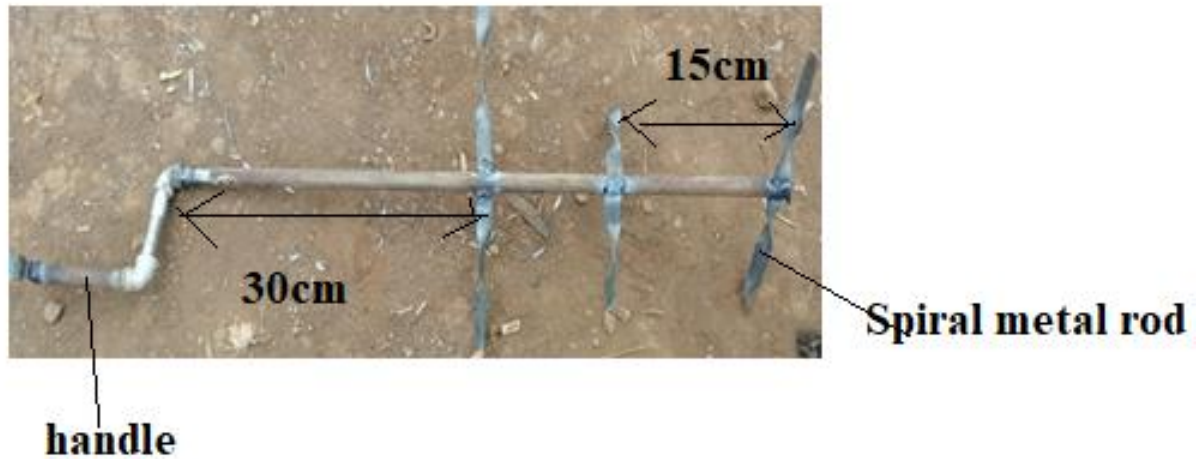


Figure 5.2: A schematic of the metallic stirrer

5.7.4 Appendix D: The 120 Liters' Digester Description

The measurements and the connections of various parts of the 120l digesters is shown in figure 5.3. The digester was made from a 120 l plastic drum with an air tight cover supported by a metallic seal for air tight sealing. On the inner side of the seal is a rubber seal. The inlet is made 17cm from the drum base with a 4' 90⁰ elbow while the outlet pie is made of a 4' 90⁰ elbow which is 47cm from the bottom of the digester and 34cm from the inlet pipe. A gas outlet pipe is made using ½' pipe fitted with a ball cork for gas outlet control. A ½' male adapter is attached at the tip of the ½' PPR pipe and a brass end cap attached to connect the gas to a gas pipe. To increase gas outlet pressure, a narrower pipe is attached after the gate valve.

The warm water circulation pipe is ½' plastic pipe coiled inside the digester and exit the reactor via the outlet waste pipe. Water flows through the pipe at 2 liters per minute with the initial startup taking 4 hours to achieve the required temperature. Digester insulation with a blanket was done to prevent heat loss.

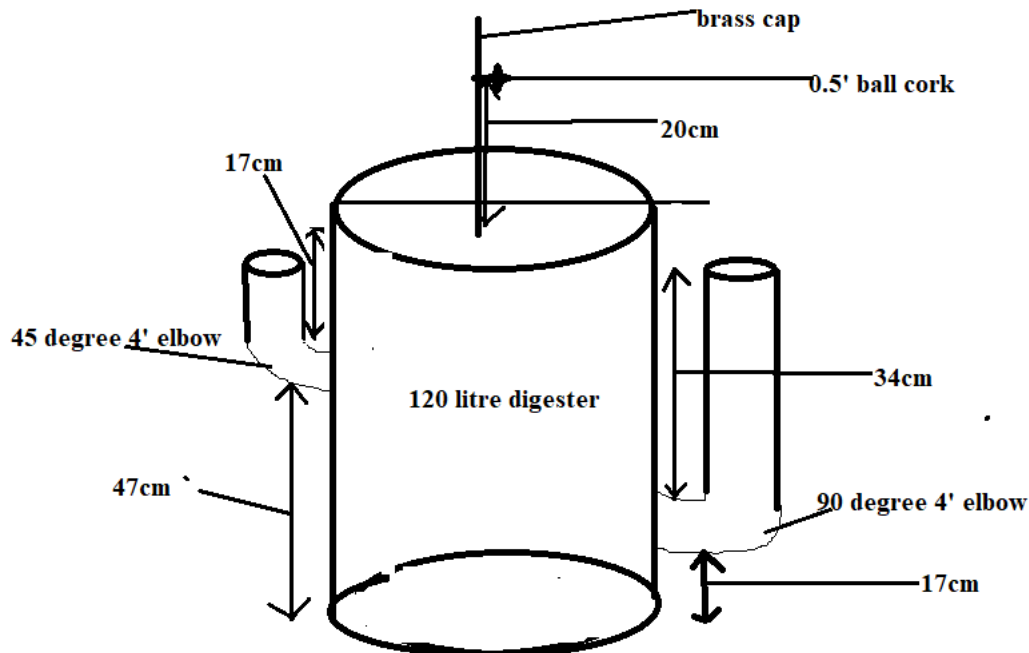


Figure 5.3: Schematic of the 60 l digester

The stirrer is made with a $\frac{3}{4}$ ' plastic pipe with a vehicle air fan with five propelling parts attached at the end of the pipe. On the other end of the pipe, a 12v 300rpm gear dc motor with high torque and low noise. The motor is attached to an external power source for agitation purposes. The stirrer is shown in figure 5.4.

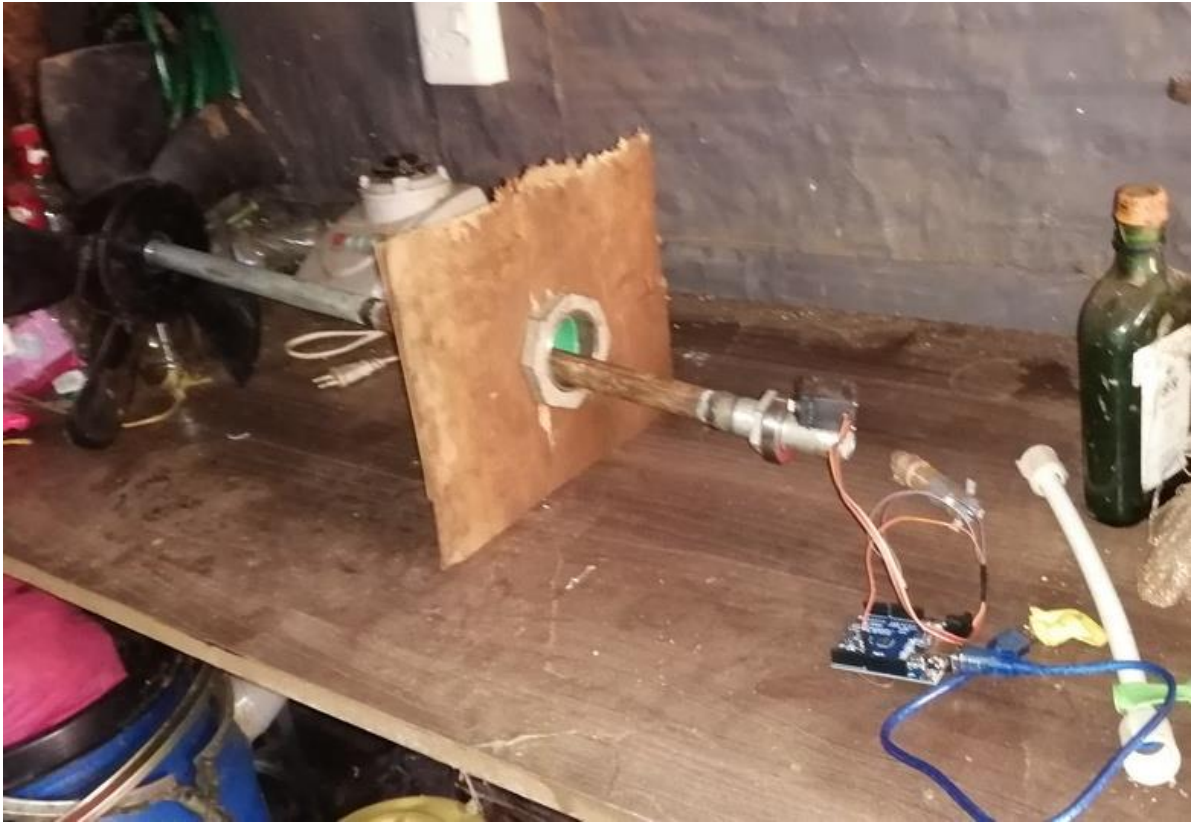


Figure 5.4: A schematic of the agitator

The following steps were followed in fabrication of the plastic digester



Figure 5.5: Fabrication of plastic drum digester steps

5.7.5 Appendix E: The 1450 Liters' Ferro-cement Digester Description

A 1450l Ferro cement digester was constructed as per the schematics shown in figure 5.6 as described in the methodology section.

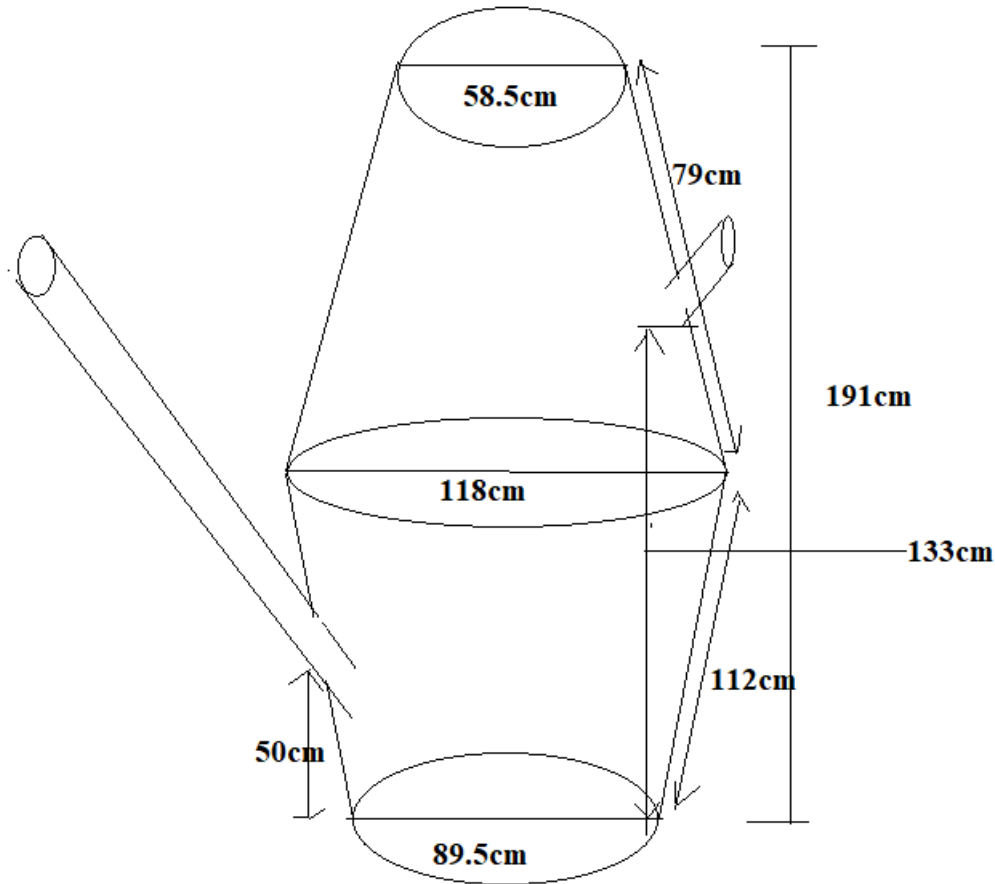


Figure 5.6: A schematic of the 1400 liters Ferro-cement digester

The inlet pipe composed of a 45° elbow fitted with a 4' waste pipe and made 50cm from the base of the tank. The outlet pipe was fixed 133cm from the base using a 45° 4' elbow. The gas outlet is made up of a ½' PPR pipe fitted with a ball cork and a LPG gas pipe via a brass gas nozzle.

A 600cm ¾' warm water pipe is coiled in the tank for warm water circulation. The water is allowed to flow at 5 liters per minute.

The stirrer is made up of 188 cm non-corrosive metal rod fitted with 18 cm twisted metal bars spaced at 20 cm intervals. A manual handle is placed at the end of the stirrer for manual stirring. The agitator enters the tank at 45° through the outlet pipe. The stirrer is shown in figure 5.7.

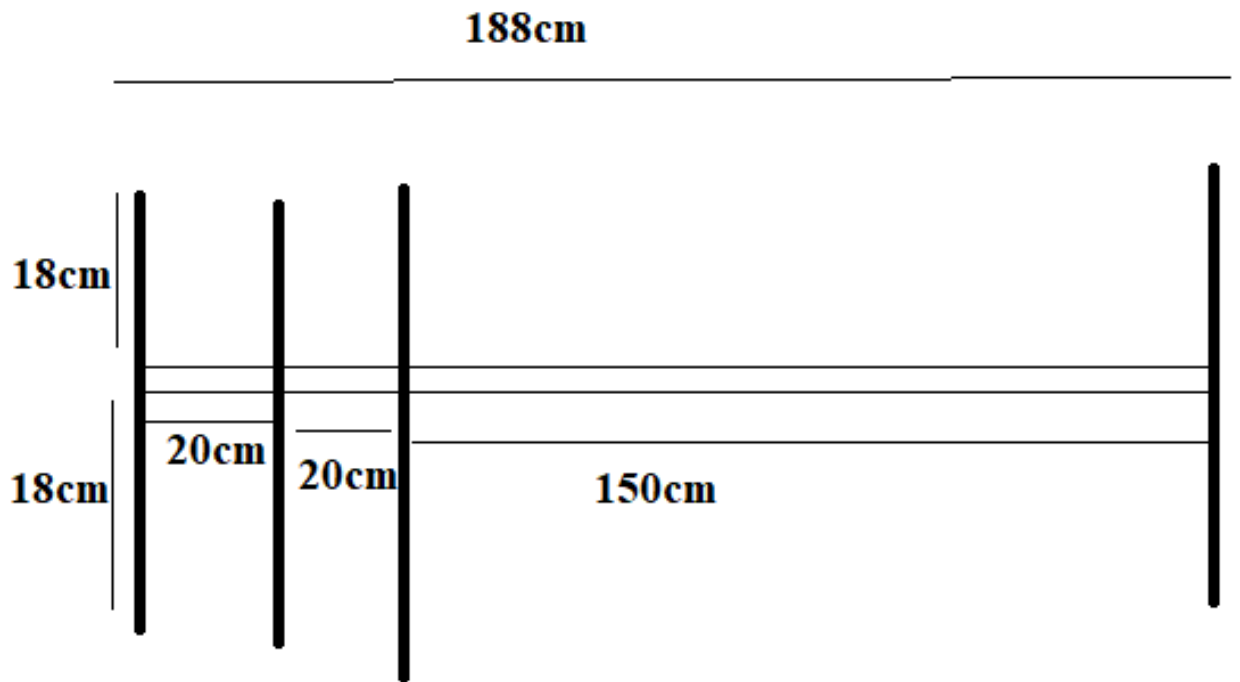


Figure 5.7: A schematic of the manual stirrer

The steps shown in figure 5.8 were used to fabricate the ferro-cement reactor



Figure 5.8: The steps followed in fabrication of Ferro-cement reactor

The steps followed in fabrication of the 14 m³ are shown in figure 5.10 while the operation of both ferro-cement and the 14 m³ is described in figure 5.11.



Figure 5.10: The steps followed in fabrication of 14 m³ reactor



Figure 5.11: Picture demonstration of how to use biogas digesters

5.7.7 Appendix G: Digester Temperature regulation

```
#include "max6675.h"
#include "Wire.h"
#include "LiquidCrystal_I2C.h"
#include <SoftwareSerial.h>
SoftwareSerial mySerial (9, 10);
LiquidCrystal_I2C lcd(0x27,16,2);
int soPin = 3;// SO=Serial Out
int csPin = 4;// CS = chip select CS pin
int sckPin = 5;// SCK = Serial Clock pin
char call;
MAX6675 thermocouple(sckPin, csPin, soPin);
void setup() {
    // put your setup code here, to run once:
    Serial.begin(9600);
    lcd.begin();// initializ the LCD1602
    lcd.backlight();// turn the backlight ON for the LCD
    lcd.print("Digester Temperature");
    lcd.setCursor(0,1);
    lcd.print("Thermocouple");
    mySerial.begin(9600); // Setting the baud rate of GSM Module
    pinMode(7, OUTPUT);
    delay(3000);
}
void loop() {
    // put your main code here, to run repeatedly:
    Serial.print("C = ");
```

```

Serial.println(thermocouple.readCelsius());
lcd.clear();// clear previous values from screen
  lcd.setCursor(0,0);// set cursor at character 0, line 0
  lcd.print("Temperature");
  lcd.setCursor(0,1);// set cursor at character 0, line 1
  lcd.print(thermocouple.readCelsius());
  lcd.setCursor(5,1);// set cursor at character 9, line 1
  lcd.print((char)223);
  lcd.setCursor(6,1);// set cursor at character 9, line 1
  lcd.print("C");
delay(200);
  if(thermocouple.readCelsius(<30){
mySerial.println("ATD+254724305124;");// ATDxxxxxxxxxx;
  Serial.println("Digester Temperature is low,circulate warm water "); // print response
over serial port
  delay(1000);
} else if(thermocouple.readCelsius(>30)
{
  mySerial.println("ATD+254724305124;");// ATDxxxxxxxxxx;
  Serial.println("Digester Temperature is high, circulate cold water "); // print response
over serial port
  delay(1000);
} else
{
  Serial.println("Digester Temperature is okey");
}
delay(2000);
}

```

5.7.8 Appendix H: pH monitoring and regulation

```
#include "Adafruit_GFX.h"
#include "LiquidCrystal_I2C.h"
#include "Wire.h"
#include "SoftwareSerial.h"

#define SensorPin A1 // the pH meter Analog output is connected with the Arduino's
Analog

SoftwareSerial mySerial(9, 10);
LiquidCrystal_I2C lcd(0x27,16,2);
unsigned long int Value; //Store the value of the sensor feedback
int buf[1];
char msg;
void setup()
{
  Serial.begin(9600);
  Serial.println("Ready"); //Test the serial monitor
  lcd.begin();// initializ the LCD1602
  lcd.backlight();// turn the backlight ON for the LCD
  lcd.print("pH VALUE");
  lcd.setCursor(0,1);
  lcd.print("pH");
  mySerial.begin(9600); // Setting the baud rate of GSM Module
  Serial.println("GSM SIM900A BEGIN");
  delay(300);
}
void loop()
{
```

```

Serial.print("pH = ");
buf[1]=analogRead(SensorPin);
Value=0;
float pHValue=(float)Value*5.0/1024/6; //convert the analog into millivolt
pHValue=3.5*pHValue;           //convert the millivolt into pH value
Serial.print("  pH:");
lcd.print("  pH:");
Serial.print(pHValue,2);
Serial.println(" ");
mySerial.println("pH: ");// The SMS text you want to send
delay(100);
lcd.clear();// clear previous values from screen
lcd.setCursor(0,0);// set cursor at character 0, line 0
lcd.print("pHValue");
lcd.setCursor(0,1);// set cursor at character 0, line 1
lcd.print(analogRead(SensorPin));
lcd.setCursor(5,1);// set cursor at character 9, line 1
lcd.print((char)223);
lcd.setCursor(6,1);// set cursor at character 9, line 1
lcd.print("pH:");
delay(100);
  if(analogRead(SensorPin) < 6.5)
  {
    mySerial.println("AT+CMGF=1"); //Sets the GSM Module in Text Mode
    delay(1000); // Delay of 1000 milli seconds or 1 second
    mySerial.println("AT+CMGS=\"+25xxxxxxxxx\"\\r"); // Replace x with mobile
number
    delay(1000);
  }

```

```

mySerial.println("Add NaOH");// The SMS text you want to send
delay(100);
mySerial.println((char)26);// ASCII code of CTRL+Z
delay(1000);
mySerial.println("AT+CNMI=2,2,0,0,0");// AT Command to receive a live SMS
delay(1000);
Serial.print("Add NaOH");
lcd.print("Add NaOH");
}
else if(analogRead(SensorPin) > 7.2)
{
mySerial.println("Add HCL");// The SMS text you want to send
Serial.print("Add HCL");
lcd.print("Add HCL");
}
else if(6.6<analogRead(SensorPin)<7.1)
{
lcd.print("pH is OK");
}
else
{
lcd.print("Raise or lower the pH");
}
delay(1000);
}

```

5.7.9 Appendix I: Biogas leaks, smoke and fire detection code

// This is a program detects the methane in biogas, lpg leakage from the cylinder, CO and smoke in the kitchen and alerts the user via a phone call. In addition, it raises an alarm in event of fire.

// The code and the idea was designed and developed by James Kamau Mbugua as part of PhD project work.

```
#include "MQ2.h"
```

```
#include "LiquidCrystal_I2C.h"
```

```
#include "Wire.h"
```

```
#include "SoftwareSerial.h"
```

```
SoftwareSerial mySerial(9, 10);
```

```
LiquidCrystal_I2C lcd(0x27,16,2);
```

```
int redLed = 12;
```

```
int greenLed = 11;
```

```
int buzzer = 8;
```

```
int pin = A0;
```

```
int lpg,co, smoke;
```

```
// threshold value
```

```
int sensorThres = 200;
```

```
int sensor1Thres = 40;
```

```
char call;
```

```
int flame_sensor = 2;
```

```
int flame_detected;
```

```
int no_flame;
```

```
MQ2 mq2(pin);
```

```
void setup() {
```

```
  lcd.begin();// initializ the LCD1602
```

```
  lcd.backlight();// turn the backlight ON for the LCD
```

```

mq2.begin();
Serial.begin(9600);
lcd.setCursor(0,1);
lcd.print("pin ");
mySerial.begin(9600); // Setting the baud rate of GSM Module
Serial.println("GSM SIM900A BEGIN");
delay(300);
pinMode(redLed, OUTPUT);
pinMode(greenLed, OUTPUT);
pinMode(buzzer, OUTPUT);
pinMode(pin, INPUT);
pinMode(flame_sensor, INPUT);
}

void loop() {
  //co = values[1];
  co = mq2.readCO();
  //smoke = values[2];
  smoke = mq2.readSmoke();
  //lpg = values[0];
  lpg = mq2.readLPG();
  Serial.print("Pin: ");
  delay(100);
  lcd.setCursor(0,0);
  lcd.print("LPG:");
  lcd.print(lpg);
  lcd.print(" CO:");
  lcd.print(co);
  lcd.setCursor(0,1);

```



```

lcd.print("SMOKE:");
lcd.print(smoke);
lcd.print(" PPM");
delay(1000);
flame_detected = digitalRead(flame_sensor);
if (flame_detected == 1)
{
    Serial.println("fire detected, extinguish it");
    lcd.setCursor(5,1);
    lcd.print("FLAME DETECTED:");
    lcd.print(flame_detected);
    digitalWrite(buzzer, HIGH);
    mySerial.println("ATD+254724305124;"); // ATDxxxxxxxxxx;
    Serial.println("Calling "); // print response over serial port
    delay(1000);
}
else
{
    Serial.println("No flame detected. stay cool");
    lcd.setCursor(6,1);
    lcd.print("No_Flame:");
    lcd.print(no_flame);
    digitalWrite(buzzer, LOW);
    delay(100);
    Serial.println("No call");
}
// Checks if it has reached the threshold value
if(lpg > sensorThres)

```

```

{
  mySerial.println("ATD+254735345517;"); // ATDxxxxxxxxxx;
  Serial.println("Calling "); // print response over serial port
  delay(1000);
  digitalWrite(redLed, HIGH);
  digitalWrite(greenLed, LOW);
  tone(buzzer, 1000, 200);
  Serial.println("lpg leakage detected, take caution");
}
  else if(smoke > sensor1Thres)
  {
    mySerial.println("ATD+254735345517;"); // ATDxxxxxxxxxx;
    Serial.println("Calling "); // print response over serial port
    Serial.println("smoke level exceeded, go out");
    delay(1000);
    digitalWrite(redLed, HIGH);
    digitalWrite(greenLed, LOW);
    tone(buzzer, 1000, 200);
  }else
{
  Serial.println("No call");
  digitalWrite(redLed, LOW);
  digitalWrite(greenLed, HIGH);
  noTone(buzzer);
}
delay(1000);
}

```

5.7.10 Appendix J: 14m³ and 1.45m³ Biogas Digesters Costing

14M3 BIOGAS TANK BUDGET				
NO	ITEM	Quantity	TOTAL	
1	Concrete blocks molder	1 piece	7900	
2	Sand	15 tonnes	15000	
3	Cement	20 bags	12000	
4	Waterproof	4liters	4000	
5	wire mesh	2meters	300	
6	J8 metallic bar	3pieces	1800	
7	Polythene paper	10meters	1000	
	Sub-Total		42000	42000
	Labour			
1	Digging of 14m3 hole	300/ft	12000	
2	Concrete blocks making	1200blocks	9000	
3	Digester building	2 weeks	45000	
	Sub-Total		66000	66000
	GRAND TOTAL			108000
6m3 FERRO-CEMENT DIGESTER				
1	Chicke wire	50meters	3500	
2	J6 mettalic molding bars	10 pieces	6000	
3	Waterproof	2 liters	2000	
4	Binding wires	5kg	650	
5	Ballast	1 tonne	2500	
6	Sand	7 tonnes	7500	
	Sub-Total		22150	22150
	Labour			
1	Digging of 6m3 hole	300/ft	6000	
2	Framework fabrication	1	3500	
3	Tank building	3 days	12000	
	Sub-Total		21500	21500
	Grand Total			43650

5.7.11 Appendix K: OBA macro-nutrient biogas prediction

SAMPLE	% PROTEIN	% FAT	% ASH	% CARB.	OBA BIOGAS(I)	% CH ₄	EQUATION
Kales	21.68	3.22	18.45	31.12	0.335	52.7	$C_{9.5}H_{15.4}O_{5.2}NNa_{1.3}Cl_{1.3} + 4.8H_2O \rightarrow 5.0CH_4 + 3.5CO_2 + NH_4^{++HCO_3^-}$
Cabbage	16.12	0.96	9.7	57.71	0.356	51	$C_{17.8}H_{28.9}O_{12.1}N_{1.1}NaCl + 6.4H_2O \rightarrow 9.0CH_4 + 7.6CO_2 + 1.1NH_4^{++1.1HCO_3^-}$
Pumkin Leaves	25.99	2.12	23.86	28.54	0.311	52.2	$C_{8.0}H_{12.9}O_{4.2}NNa_{1.4}Cl_{1.37} + 4.4H_2O \rightarrow 4.2CH_4 + 2.8CO_2 + NH_4^{++HCO_3^-}$
<i>Cucumis ficifolia</i>	26.11	2.46	17.52	29.46	0.341	52.4	$C_{8.2}H_{13.2}O_{4.3}NNa_{1.0}Cl_{1.0} + 4.5H_2O \rightarrow 4.3CH_4 + 2.9CO_2 + NH_4^{++HCO_3^-}$
Pigweed	22.98	1.83	25.26	20.39	0.288	52.4	$C_{7.3}H_{11.7}O_{3.6}NNa_{1.7}Cl_{1.7} + 4.3H_2O \rightarrow 3.8CH_4 + 2.5CO_2 + NH_4^{++HCO_3^-}$
<i>Eracastrum arabicum</i>	26.57	1.85	18.76	26.38	0.33	52.2	$C_{7.6}H_{12.2}O_{3.9}NNa_{1.1}Cl_{1.1} + 4.4H_2O \rightarrow 4.0CH_4 + 6CO_2 + NH_4^{++HCO_3^-}$
Coriander	33.01	1.19	24.3	19.56	0.31	52.1	$C_{6.1}H_{9.7}O_{2.8}NNa_{1.1}Cl_{1.1} + 4.0H_2O \rightarrow 3.2CH_4 + 1.9CO_2 + NH_4^{++HCO_3^-}$
African Nightshade	22.69	2.23	16.67	23.45	0.333	52.5	$C_{7.9}H_{12.7}O_{4.0}NNa_{1.1}Cl_{1.1} + 4.5H_2O \rightarrow 4.2CH_4 + 2.8CO_2 + NH_4^{++HCO_3^-}$
Spinach	22.8	2.52	25.67	28.54	0.32	52.5	$C_{8.7}H_{13.9}O_{4.6}NNa_{1.7}Cl_{1.7} + 4.6H_2O \rightarrow 4.6CH_4 + 3.1CO_2 + NH_4^{++HCO_3^-}$
Comfrey	21.71	1.98	23.13	24.37	0.299	52.3	$C_{8.1}H_{13.1}O_{4.3}NNa_{1.6}Cl_{1.6} + 4.5H_2O \rightarrow 4.3CH_4 + 2.9CO_2 + NH_4^{++HCO_3^-}$
Tomato	11.89	2.57	9.53	55.42	0.361	51.6	$C_{20.1}H_{33.5}O_{13.9}NNa_{1.2}Cl_{1.2} + 6.7H_2O \rightarrow 10.5CH_4 + 8.8CO_2 + NH_4^{++HCO_3^-}$
Potato	8.73	3.34	5.02	62.51	0.383	51.8	$C_{34.1}H_{56.5}O_{24.1}N_{1.2}NaCl + 9.9H_2O \rightarrow 17.6CH_4 + 15.3CO_2 + 1.2NH_4^{++1.2HCO_3^-}$
Sweet Potato	4.42	4.07	2.81	46.76	0.4	52.6	$C_{45.6}H_{76.3}O_{31.8}N_{1.1}NaCl + 12.5H_2O \rightarrow 23.9CH_4 + 20.6CO_2 + 1.1NH_4^{++1.1HCO_3^-}$
Pawpaw	6.36	3.15	4.65	62.9	0.381	51.7	$C_{38.8}H_{64.5}O_{28.1}NNa_{1.1}Cl_{1.1} + 10.3H_2O \rightarrow 20.3CH_4 + 17.7CO_2 + NH_4^{++HCO_3^-}$
Banana	11.89	1.97	6.53	49.06	0.371	51.5	$C_{22.2}H_{36.6}O_{15.1}N_{1.2}NaCl + 7.7H_2O \rightarrow 11.5CH_4 + 9.6CO_2 + 1.2NH_4^{++1.2HCO_3^-}$
Avocado	7.69	52.64	4.92	2.36	0.776	68.1	$C_{45.4}H_{81.5}O_{6.4}N_{1.0}NaCl + 23.7H_2O \rightarrow 30.9CH_4 + 13.5CO_2 + 1.0NH_4^{++1.0HCO_3^-}$
Courgette	22.92	5.48	15.58	36.5	0.368	53.4	$C_{10.5}H_{17.1}O_{5.6}NNa_{1.0}Cl_{1.0} + 5.1H_2O \rightarrow 5.6CH_4 + 3.9CO_2 + NH_4^{++HCO_3^-}$
Cucumber	12.65	5.19	11.14	48.13	0.372	53	$C_{18.6}H_{30.8}NNa_{1.3}Cl_{1.3} + 6.8H_2O \rightarrow 9.9CH_4 + 7.8CO_2 + NH_4^{++HCO_3^-}$
Mango	6.61	5.23	3.33	61.91	0.402	52.5	$C_{51.4}H_{85.8}O_{35.7}N_{1.3}NaCl + 14.4H_2O \rightarrow 27CH_4 + 23.1CO_2 + 1.3NH_4^{++1.3HCO_3^-}$
Water Melon	12.72	4.63	10.49	49.34	0.372	52.7	$C_{18.6}H_{30.8}O_{11.9}NNa_{1.2}Cl_{1.2} + 6.7H_2O \rightarrow 9.8CH_4 + 7.8CO_2 + NH_4^{++HCO_3^-}$
Market Waste	17.28	5.43	13.87	32.22	0.367	53.8	$C_{11.80}H_{19.38}O_{6.41}NNa_{1.2}Cl_{1.2} + 5.50H_2O \rightarrow 6.34CH_4 + 4.45CO_2 + NH_4^{++HCO_3^-}$

